

Genome-wide association study of lipidomes of *Arabidopsis thaliana* accessions identifies genes affecting lipid metabolism under unstressed and stressed conditions

by

Yu Song

B.S., Ocean University of China, 2014

M.S., Ocean University of China, 2017

AN ABSTRACT OF A DISSERTATION

submitted in partial fulfillment of the requirements for the degree

DOCTOR OF PHILOSOPHY

Department of Biochemistry and Molecular Biophysics
College of Arts and Sciences

KANSAS STATE UNIVERSITY
Manhattan, Kansas

2022

Abstract

In unfavorable conditions, plants make adjustments of metabolic pathways to adapt to the environment. As essential components of plant cells, lipids respond to environmental stresses in a variety of ways, including maintaining membrane structure and signaling. The model plant *Arabidopsis thaliana* is widely distributed in Eurasia and its natural accessions have tremendous genetic and phenotypic diversity, which enables genome-wide association study (GWAS) to identify candidate genes affecting lipid metabolism under stressed and unstressed conditions.

A lipidomics approach was established, allowing quantitative analysis of 358 lipid analytes in *Arabidopsis* leaf tissues. The lipidomics approach was applied to *Arabidopsis* accession Columbia-0 (Col-0) to investigate lipid changes in leaf tissues under cold and mechanical-wounding stresses. In cold, the most prominent variation in leaf tissue of Col-0 was the large accumulation of triacylglycerols (TAGs) and major phospholipids containing very long chain fatty acids (VLCFAs). The highly unsaturated 54C-TAG species showed large induction after -2 °C treatment, while the less unsaturated 50C- and 52C-TAGs accumulated during cold acclimation and declined at -2 °C. Mechanical wounding treatment resulted in large variations in the leaf lipid profile with the greatest change being the accumulation of lipids with oxidized fatty acyl chains.

Application of the lipidomics approach to natural accessions of *Arabidopsis* grown under unstressed condition or subjected to cold or mechanical wounding showed that large variations exist in *Arabidopsis* leaf lipidomes. Among the candidate genes identified from GWAS under cold stress are genes, including *FAD2*, *FAD7*, *LOH2*, *KCS9*, and *FABI*, known to be involved in fatty acyl desaturation, fatty acyl elongation, and sphingolipid synthesis. A strong correlation between certain components of the cold-induced lipidome and freezing tolerance was observed

in the investigated *Arabidopsis* accessions, suggesting potential roles for specific lipids and associated genes in plant freezing tolerance. Two genomic regions, found only under wounding stress, are strongly associated with large numbers of esterified oxophytodienoic acid (OPDA) and esterified dinor-oxophytodienoic acid (dnOPDA) lipids, as well as with free OPDA. One of these regions contains three genes, AT3G25760 (*AOC1*), AT3G25770 (*AOC2*), and AT3G25780 (*AOC3*), while the other region contains one gene, AT4G15440 (*HPL1*). Haplotype analysis of gene expression level demonstrated that a SNP, associated with oxidized lipid level, in the upstream region of *HPL1* is also associated with expression of *HPL1* upon wounding. Additional lipidomic analysis on T-DNA insertion and overexpression mutants suggested that *AOC1*, *AOC2*, and *AOC3* all play positive effects on production of esterified OPDA and dnOPDA lipids in *Arabidopsis* leaves under wounding stress.

This work utilizes GWAS to analyze and interpret complex lipidomics data in *Arabidopsis*, leading to advances in understanding plant lipid metabolism and stress responses. The list of candidate genes related to lipid metabolism during plant stress responses provides a resource for future engineering of plants with altered levels of lipids that improve stress tolerance.

Genome-wide association study of lipidomes of *Arabidopsis thaliana* accessions identifies genes affecting lipid metabolism under unstressed and stressed conditions

by

Yu Song

B.S., Ocean University of China, 2014

M.S., Ocean University of China, 2017

A DISSERTATION

submitted in partial fulfillment of the requirements for the degree

DOCTOR OF PHILOSOPHY

Department of Biochemistry and Molecular Biophysics
College of Arts and Sciences

KANSAS STATE UNIVERSITY
Manhattan, Kansas

2022

Approved by:

Major Professor
Ruth Welti

Copyright

© Yu Song 2022

Abstract

In unfavorable conditions, plants make adjustments of metabolic pathways to adapt to the environment. As essential components of plant cells, lipids respond to environmental stresses in a variety of ways, including maintaining membrane structure and signaling. The model plant *Arabidopsis thaliana* is widely distributed in Eurasia and its natural accessions have tremendous genetic and phenotypic diversity, which enables genome-wide association study (GWAS) to identify candidate genes affecting lipid metabolism under stressed and unstressed conditions.

A lipidomics approach was established, allowing quantitative analysis of 358 lipid analytes in *Arabidopsis* leaf tissues. The lipidomics approach was applied to *Arabidopsis* accession Columbia-0 (Col-0) to investigate lipid changes in leaf tissues under cold and mechanical-wounding stresses. In cold, the most prominent variation in leaf tissue of Col-0 was the large accumulation of triacylglycerols (TAGs) and major phospholipids containing very long chain fatty acids (VLCFAs). The highly unsaturated 54C-TAG species showed large induction after -2 °C treatment, while the less unsaturated 50C- and 52C-TAGs accumulated during cold acclimation and declined at -2 °C. Mechanical wounding treatment resulted in large variations in the leaf lipid profile with the greatest change being the accumulation of lipids with oxidized fatty acyl chains.

Application of the lipidomics approach to natural accessions of *Arabidopsis* grown under unstressed condition or subjected to cold or mechanical wounding showed that large variations exist in *Arabidopsis* leaf lipidomes. Among the candidate genes identified from GWAS under cold stress are genes, including *FAD2*, *FAD7*, *LOH2*, *KCS9*, and *FABI*, known to be involved in fatty acyl desaturation, fatty acyl elongation, and sphingolipid synthesis. A strong correlation between certain components of the cold-induced lipidome and freezing tolerance was observed

in the investigated *Arabidopsis* accessions, suggesting potential roles for specific lipids and associated genes in plant freezing tolerance. Two genomic regions, found only under wounding stress, are strongly associated with large numbers of esterified oxophytodienoic acid (OPDA) and esterified dinor-oxophytodienoic acid (dnOPDA) lipids, as well as with free OPDA. One of these regions contains three genes, AT3G25760 (*AOC1*), AT3G25770 (*AOC2*), and AT3G25780 (*AOC3*), while the other region contains one gene, AT4G15440 (*HPL1*). Haplotype analysis of gene expression level demonstrated that a SNP, associated with oxidized lipid level, in the upstream region of *HPL1* is also associated with expression of *HPL1* upon wounding. Additional lipidomic analysis on T-DNA insertion and overexpression mutants suggested that *AOC1*, *AOC2*, and *AOC3* all play positive effects on production of esterified OPDA and dnOPDA lipids in *Arabidopsis* leaves under wounding stress.

This work utilizes GWAS to analyze and interpret complex lipidomics data in *Arabidopsis*, leading to advances in understanding plant lipid metabolism and stress responses. The list of candidate genes related to lipid metabolism during plant stress responses provides a resource for future engineering of plants with altered levels of lipids that improve stress tolerance.

Table of Contents

List of Abbreviations	xiii
List of Figures	xv
List of Tables	xviii
Acknowledgements.....	xix
Dedication	xxi
Chapter 1 - Introduction.....	1
Rationale of studying lipid metabolism in plants under unfavorable conditions	1
Arabidopsis and 1001 Genomes Project.....	2
Low temperature stress and wounding stress in plants.....	3
Plant molecular responses to low temperature and wounding.....	4
Lipid metabolism under low temperature stress and wounding stress	5
Desaturation	5
Elongation	6
Hydrolysis	7
Oxidation.....	8
Acylation.....	9
Galactosylation	11
Association mapping to identify genetic loci responsible for phenotypic traits.....	12
Lipidomics in plant science	14
Lipid extraction.....	14
Mass spectrometry analysis	15
Data processing.....	15
Data analysis	16
Application of lipidomics in plant science	17
Hypotheses.....	18
Outline of dissertation.....	18
Figures	21
References.....	25

Chapter 2 - Development of a direct-infusion lipidomics approach to identify lipid changes in Arabidopsis leaf tissues in response to various stresses	35
Introduction.....	35
Materials and Methods.....	38
Plant materials and growth conditions	38
Super-cold treatment	38
Mechanical wounding treatment.....	39
Lipid extraction	39
Mass spectrometry analysis	40
Data processing and normalization	42
Statistical analysis	43
Results.....	43
MS analysis of lipids in leaf tissues of Arabidopsis	43
Variations in leaf lipid profile of Arabidopsis in response to super-cold stress	45
Variations in leaf lipid profile of Arabidopsis in response to wounding stress	48
Discussion.....	50
Figures	59
Tables.....	65
References.....	68
Chapter 3 - GWAS on lipidomes of <i>Arabidopsis thaliana</i> reveals the potential regulators for lipid remodeling under cold stress	74
Introduction.....	74
Materials and Methods.....	77
Plant materials and growth conditions	77
Lipidomic analysis of Arabidopsis accessions	78
Data processing and normalization	78
Freezing tolerance assays.....	79
Genome-wide association study	79
Gene expression analysis (RT-qPCR)	81
Statistical analysis	82
Results.....	82

Super-cold treatment induced significant changes of lipid profiles among 360 <i>Arabidopsis</i> natural accessions.....	82
Accumulation of TAG in leaves is a major change in lipid profile under low temperature.	83
Polar glycerolipid remodeling is a distinct signature under low temperature.....	84
The relative abundance of some lipid species is highly correlated with freezing tolerance.	84
GWAS study on lipidomics data revealed candidate genes related to lipid metabolism.....	86
Variation in <i>FAD2</i> regulates ω -6 desaturation in leaf phospholipids under cold stress	87
Variation in <i>FAD7</i> regulates ω -3 desaturation in leaf galactolipids under cold stress	89
Variation in <i>LOH2</i> and <i>KCS9</i> regulate GlcCer biosynthesis and fatty acyl elongation under cold stress.....	90
Variation in other lipid related genes regulate lipid metabolism under cold stress	92
SNPs in <i>FAD2</i> determine the expression level of the gene	93
Discussion.....	94
Figures	104
Tables.....	116
References.....	117
Chapter 4 - Genome wide association in <i>Arabidopsis thaliana</i> accessions, under control conditions and after wounding, identifies genetic variation related to lipid levels and reveals two genes affecting the production of oxophytodienoic acid and related lipids	
Introduction.....	124
Materials and Methods.....	127
Plant materials and growth conditions	127
Lipidomic analysis of 360 <i>Arabidopsis</i> accessions.....	127
Data processing and normalization	128
Analysis and quantification of JA, JA-Ile, and OPDA	128
Data as percentages	129
Lipid data analysis	130
Genome-wide association study (GWAS).....	130
Gene expression analysis (RT-qPCR)	131
Results.....	132

Natural variation of the leaf lipid composition occurs in <i>Arabidopsis thaliana</i> under control and wounding conditions	132
Wounding induced overall changes of lipid composition in 360 <i>Arabidopsis</i> accessions .	133
GWAS study on lipidomics data revealed candidate genes related to lipid metabolism....	135
Chromosomal regions identified in both control and wounding conditions suggest natural variation in several genes related to lipid metabolism.....	137
Natural variation in allene oxide cyclase-encoding genes and HYDROPEROXIDE LYASE 1 regulates lipid oxidation in leaves during wounding	139
SNPs in or near <i>AOC2</i> and <i>HPL1</i> are associated with the expression levels of the genes .	143
Discussion.....	145
Figures	152
Tables.....	159
References.....	162
Chapter 5 - Functional characterization of AOCs on esterified (dn)OPDA production in	
<i>Arabidopsis</i> under wounding stress	169
Introduction.....	169
Materials and Methods.....	171
Plant materials and growth conditions	171
Cloning of coding sequence of <i>Arabidopsis AOC1, AOC2, AOC3</i>	172
Overexpression vector construction and transformation	172
Wounding treatment and leaf harvesting	173
Quantitative RT-PCR analysis of AOC expression in mutant lines	173
Lipid extraction and MS analysis.....	174
Data processing and lipid profile analysis	174
Statistical analysis.....	174
Results.....	175
Overexpression of <i>AOC1/2/3</i> in leaf tissues of wild-type <i>Arabidopsis</i> (Col-0)	175
The relative amounts of esterified OPDA and dnOPDA are affected by the expression level of <i>AOC1</i> and <i>AOC2</i>	175
Knockout of <i>AOC1</i> and <i>AOC3</i> led to complete or partial loss of ability to generate esterified OPDA and dnOPDA under wounding	176

Discussion.....	178
Figures	180
Tables.....	184
References.....	186
Chapter 6 - Conclusions and future directions.....	189
Conclusions.....	189
Future directions	193
References.....	195
Appendix A - Copyright Permissions	199
Appendix B - Chapter 3 Supplemental Figures	200
Appendix C - Chapter 4 Supplemental Figures	203

List of Abbreviations

acDGDG	Acylated digalactosyldiacylglycerol
acMGDG	Acylated monogalactosyldiacylglycerol
acPG	Acylated phosphatidylglycerol
AGAP1	Acylated Galactolipid Associated Phospholipase 1
ANOVA	Analysis of variance
AOC1	Allene Oxide Cyclase 1
AOC2	Allene Oxide Cyclase 2
AOC3	Allene Oxide Cyclase 3
AOS	Allene Oxide Synthase
APCI	Atmospheric pressure chemical ionization
ASG	Acyl steryl glycosides
CDS	Coding sequence
DAG	Diacylglycerol
DGAT	Diacylglycerol acyltransferase
DGDG	Digalactosyldiacylglycerol
DGMG	Digalactosylmonoacylglycerol
dnOPDA	Dinor-oxophytodienoic acid
EOT	Epoxy-octadecanoic acid
ER	Endoplasmic reticulum
ESI	Electrospray ionization
FAB1	Fatty Acid Biosynthesis 1
FAD	Fatty Acid Desaturase
GlcCer	Glycosylceramide
GWAS	Genome-wide association study
HPL1	Hydroperoxide Lyase 1
IS	Internal standard
JA	Jasmonic acid
KCS	3-Ketoacyl-CoA Synthase
LC-MS	Liquid chromatography-mass spectrometry
LD	Linkage disequilibrium
LOH2	Longevity Assurance Gene1 Homolog 2
LOX	Lipoxygenase
LPC	Lysophosphatidylcholine
LPE	Lysophosphatidylethanolamine
LPL	Lysophospholipid
MALDI	Matrix assisted laser desorption ionization
MGDG	Monogalactosyldiacylglycerol
MGMG	Monogalactosylmonoacylglycerol
MRM	Multiple reaction monitoring
OPDA	Oxophytodienoic acid
PA	Phosphatidic acid
PC	Phosphatidylcholine
PCA	Principal component analysis
PDAT	Phospholipid:Diacylglycerol Acyltransferase

PE	Phosphatidylethanolamine
PG	Phosphatidylglycerol
PI	Phosphatidylinositol
PLA	Phospholipase A
PLB	Phospholipase B
PLC	Phospholipase C
PLD	Phospholipase D
PS	Phosphatidylserine
QC	Quality control
QTL	Quantitative trait locus
SE	Steryl ester
SFR2	SENSITIVE TO FREEZING 2
SG	Steryl glucoside
SNP	Single nucleotide polymorphism
SQDG	Sulfoquinovosyldiacylglycerol
TA	Trienoic fatty acids
TAG	Triacylglycerol
TeGDG	Tetra-galactosyldiacylglycerol
TrGDG	Tri-galactosyldiacylglycerol
UTR	Untranslated region
VLCFA	Very long chain fatty acid

List of Figures

Figure 1-1. Collection sites for the 1135 accessions in 1001 Genomes Project.....	21
Figure 1-2. Lipid modifications in response to mechanical wounding and low temperature stress in Arabidopsis leaves	22
Figure 1-3. General workflow of plant lipidomics	24
Figure 2-1. Plant appearance before cold acclimation, after acclimation, after super-cold treatment, and after postfreezing recovery.....	59
Figure 2-2. Stress treatment experimental design.....	60
Figure 2-3. Heatmap of autoscaled lipid levels in unstressed, cold acclimated, and super-cold- treated samples.....	61
Figure 2-4. Changes in TAG and DAG profiles in leaf tissues of Col-0 under various stresses..	62
Figure 2-5. Changes in PC and PE profiles in leaf tissues of Col-0 under various stresses	63
Figure 2-6. Significantly changed lipid analytes after mechanical wounding treatment.....	64
Figure 3-1. Changes in the relative contents of 32 lipid classes in leaf tissues among the 360 investigated Arabidopsis accessions in unstressed and super-cold treated group	104
Figure 3-2. Heatmap of autoscaled lipid levels in unstressed (control) and super-cold treated leaves in 360 accessions.....	105
Figure 3-3. Changes in the relative contents of 11 DAG, TAG species in leaf tissues in the 360 investigated Arabidopsis accessions in standard condition (control) and after super-cold treatment	106
Figure 3-4. Changes in the relative contents of 28 PC species in leaf tissues among the 360 investigated Arabidopsis accessions in unstressed and super-cold treated group	107
Figure 3-5. The relative level of PC (18:1/18:3) is associated with the SNP in the 5' UTR intron of <i>FAD2</i>	108
Figure 3-6. Correlation heatmaps of correlations of relative contents of individual PC and PE species with freezing tolerance, latitude, and some local temperature variables.....	109
Figure 3-7. The relative level of MGDG (18:2/18:3) is associated with missense SNP in <i>FAD7</i>	110
Figure 3-8. Correlation heatmaps of correlations of relative contents of individual MGDG species with freezing tolerance, latitude, and some local temperature variables.....	111

Figure 3-9. The relative level of GlcCer (d18:1-h16:0) is associated with the SNP in 3' UTR of <i>LOH2</i>	112
Figure 3-10. The relative level of GlcCer (t18:1-h22:0) is associated with missense SNP of <i>KCS9</i>	113
Figure 3-11. Correlation heatmaps of correlations of relative contents of individual GlcCer species with freezing tolerance, latitude, and some local temperature variables.....	114
Figure 3-12. Relationship between <i>FAD2</i> expression level and the relative content of two PC species	115
Figure 4-1. Changes in the relative contents of 32 lipid classes and 14 esterified (dn)OPDA species in leaf tissues in the 360 investigated Arabidopsis accessions before and 45 min after wounding treatment	152
Figure 4-2. Significant SNPs and candidate genes identified from GWAS	153
Figure 4-3. GWAS mapping (Manhattan plot) and haplotype analysis for lipid species identified in unstressed population of Arabidopsis	154
Figure 4-4. The relative level of acMGDG (18:4-O/34:8-2O) (Arabidopside E) is associated with the SNPs in non-coding sequence of <i>AOC2</i> and <i>HPL1</i>	155
Figure 4-5. The relative level of free OPDA is associated with the SNPs in non-coding sequence of <i>AOC2</i> and <i>HPL1</i>	156
Figure 4-6. Association between SNPs, gene expression level, and Arabidopside E level.....	157
Figure 4-7. Proposed model of free and esterified (dn)OPDA biosynthesis in Arabidopsis leaves under mechanical wounding stress	158
Figure 5-1. Gene expression analysis of wounded leaves of wild-type and T1 generation <i>AOC1/2/3</i> overexpression lines.....	180
Figure 5-2. Analysis of arabidopside E in wounded leaves of wild-type and T1 generation <i>AOC1/2/3</i> overexpression lines.....	180
Figure 5-3. Relationship between <i>AOC2</i> expression level and Arabidopside E level in WT and T1 generation <i>AOC2</i> overexpression plants	181
Figure 5-4. Comparison of lipid profiles between WT and SALK_073059 (<i>aoc1</i>)	182
Figure 5-5. Analysis of oxidized lipid classes in wounded leaves of wild-type and T-DNA insertion lines of <i>AOC1/2/3</i>	183

Figure 5-6. Analysis of Arabidopside E in wounded leaves of wild-type and T-DNA insertion
lines of *AOCI/2/3* 183

List of Tables

Table 2-1. Internal standards employed in lipid profiling	65
Table 2-2. Lipid name abbreviations	66
Table 3-1. Summary statistics of variation and heritability for 32 lipid classes in 360 accessions of Arabidopsis after super-cold treatment.....	116
Table 4-1. Summary statistics of variation and heritability for 32 lipid classes in 360 accessions of Arabidopsis before and after wounding.....	159
Table 4-2. Lipid species showing strong associations with genomic region W-144 and region W-201.....	160
Table 4-3. Single nucleotide polymorphisms (SNPs) in non-coding regions of <i>AOCs</i> and <i>HPL1</i> are associated with arabidopside E under wounding stress	161
Table 5-1. Primers used for genotyping.....	184
Table 5-2. Primers used for gene cloning	184
Table 5-3. Primers used for RT-qPCR.....	185

Acknowledgements

I would like to express my deepest appreciation to my major professor, Dr. Ruth Welti for her support, suggestions, encouragement, and guidance during the past five years. Dr. Welti not only provided me with knowledge and expertise in plant science including lipidomics, experiment design, and paper writing, but taught me many precious experiences which are valuable for my career and the rest of my life. I would like to thank my committee members, Dr. Mark Ungerer for his help in plant freezing experiments, Dr. Kathrin Schrick for her advice and help in qPCR, and Dr. Timothy Durrett for his teaching, help, and suggestions in plant molecular biology, and the past member of my committee, Dr. Geoffrey Morris, for his knowledge on plant genetics and association studies. And I appreciate Dr. Zifei Liu for serving as chair for my doctoral defense.

I am also grateful to my current and previous lab members. I appreciate Mary Roth and Pamela Tamura for maintaining instruments and maintaining a fantastic laboratory. Specifically, I thank Pam for lipid extraction of a huge amount of leaf samples in Chapters 3 and 4. I thank Mary for teaching me everything about lipidomics and setting up acquisition methods in 6500+. I also want to thank Libin Yao, who helped me for FA analysis in Arabidopsis leaves. I would like to thank PhD students in my lab, Zolian Zoong Lwe and Pallikonda Arachchige Dona Bashanee Vinusha Wickramasinghe. Zolian helped me a lot for gene expression analysis and Vinusha always gave me help and good advice for my study. I want to thank previous undergraduate students working in my lab, Daniel Hemphill and Abdulrahman Naeem, who did freezing tolerance measurements for 679 Arabidopsis accessions in Chapter 3. I want to thank previous lab members Dr. Hieu Vu and Dr. Sunitha Shiva, who established the initial MRM list for my

lipidomics method in Chapter 2. I want to thank Madeline Colter for her contribution in wound-induced lipidomics and GWAS.

I want to extend my thanks to my collaborators and researchers who provided assistance in my projects. I would like to thank Dr. Abraham Koo and Dr. Athen Kimberlin at University of Missouri for measuring free OPDA in Chapter 4. I also want to thank the PhD students in Dr. Durrett lab, Nicholas Neumann and Linah Alkotami, for helping with gene cloning, plasmid construction, and *Agrobacterium*-mediated transformation.

I want to thank the Johnson Cancer Research Center for summer stipend support and United States Department of Agriculture National Institute of Food and Agriculture, Hatch/Multi-State project 1013013 for funding my research project.

I am really grateful to have a group of friends in Manhattan and I want to thank Taihao Yang, Ye Zou, Xin Xu, Yao Yan, Mian Huang, and Miao Li for their company and support during the past 5 years.

At last, I want to thank my parents. They give me unconditional love, most trust, continuous support and encouragement throughout my life. I am proud of having the best parents in the world. I truly appreciate my girlfriend Xiaoxu Wang, who is always understanding, supportive, and gives me power to have gone so far. Coming across with her is my greatest fortune.

Dedication

I dedicate this dissertation to my parents, Chun Song and Rongcheng Sun, for their unconditional love and support in the past 31 years.

Chapter 1 - Introduction

Rationale of studying lipid metabolism in plants under unfavorable conditions

Plants are exposed to a wide range of adverse environmental conditions and their growth and development are affected by many factors including biotic and abiotic stressors. These stresses include extreme temperature, high salinity, drought, flooding, nutrient deficiency, heavy metal, bacterial and fungal infection, harmful insects, and grazing herbivores. A great loss of annual crop yield is caused by low temperature and natural wounding damages so development of more cold- and wounding-tolerant crop varieties can expand cultivated lands and increase food production. In unfavorable conditions, plants can make adjustments of metabolic pathways to adapt to the changing environment in a process called acclimation.

In plants, lipids function in a variety of ways. They are essential components of cells and organelles by acting as a hydrophobic barrier for the membrane (Karnovsky et al., 1982; van Meer et al., 2008). In addition, lipids function as a compact energy source for seed germination and plant development (Nakamura et al., 2014). Furthermore, they act as signaling molecules to regulate plant growth and development (Kim, 2020; Li-Beisson et al., 2013). In recent years, emerging evidence reveals the potential roles of glycerolipid remodeling in plant stress responses. One of the key biological roles is to adjust membrane physiochemical properties to optimize its functions with respect to unfavorable conditions (Moellering & Benning, 2011; Nakamura, 2013). Another important role is to remove oxidized or damaged acyl chains, sequester cytotoxic fatty acids and release signaling lipids and in stress responses (Hermansson et al., 2011; Nakamura, 2013; Vu et al., 2014a). To date, thousands of genes and their encoded enzymes for lipid biosynthesis have been identified but most of them remain to be characterized

in *Arabidopsis thaliana* (Li-Beisson et al., 2013). Some enzymes are activated only in specific stresses and may function in lipid remodeling of membranes or in cell signaling cascades to make plants more stress tolerant (Cook et al., 2021; Hou et al., 2016; Okazaki & Saito, 2014). An extensive amount of work needs to be done to determine the plant biochemical and genetic basis of lipid metabolism in unfavorable environments.

Arabidopsis and 1001 Genomes Project

Arabidopsis thaliana is one of the best-known flowering plants and the most popular model organism in plant science especially in the field of genetics and molecular biology. *Arabidopsis* possesses many important features that include small size, short life cycle, and prolific seed production through self-pollination, which make it well-suited for laboratory experiments. Moreover, its small, diploid, well-sequenced genome have made it the premier model for plant biology in the past 30 years (Koornneef & Meinke, 2010).

Arabidopsis has a wide geographical distribution from North Africa to the Arctic Circle and natural accessions show tremendous genetic and phenotypic diversity making them valuable resources for association mapping. The 1001 Genomes Project was launched in 2008 describing whole-genome sequence variations in 1001 accessions of *Arabidopsis* (Weigel & Mott, 2009). Until 2016, a more detailed map of variation acquired from 1135 high-quality re-sequenced natural accessions was published (Alonso-Blanco et al., 2016), which enables genome-wide association study (GWAS) on various phenotypes. The world-wide distribution of the 1135 accessions in 1001 Genomes Project is shown in Figure 1-1.

All the important features of *Arabidopsis thaliana* described above make it an excellent plant material in nature science to investigate lipid metabolism under stresses and study mechanism of plant stress tolerance.

Low temperature stress and wounding stress in plants

In this dissertation, I mainly focus on two stresses: low temperature (cold) and mechanical wounding. These two stresses have great significance in agriculture, and are relatively simple to manipulate in laboratory so that they can be applied reproducibly to a large number of *Arabidopsis* natural accessions.

Low temperature is a major abiotic stress in plants. Different from freezing stress, which causes cellular damages due to osmotic dehydration triggered by extracellular ice crystallization (Steponkus, 1984; Uemura et al., 1995), the mechanism of injury under cold is a direct effect of the low temperature. Cold stress can result in poor germination, stunted seedlings, yellowing of leaves, withering, and reduced tillering in many plant species such as maize (*Zea mays*) and soybean (*Glycine max*) with obvious signs of injury upon exposure to temperatures below 10 °C (Yadav, 2010). At the cellular level, cold temperature affects membrane rigidification and reduces stability and activities of enzymes, leading to membrane damage and impaired photosynthesis. *Arabidopsis* is a freezing-tolerant plant species: after the exposure to low but non-freezing temperatures for a period of one day or more (cold acclimation), the freezing tolerance of the Columbia-0 accession is greatly enhanced with the lethal freezing temperature dropping from -2 to -8 °C (Gilmour et al., 1988; Uemura et al., 1995).

Mechanical wounding can be performed using a hemostat or needle in the laboratory to imitate plant wounding in nature, where tissue damage is caused by chewing insects, large herbivores, or severe weather, such as wind and hail. Wounding not only causes ruptured cells and nutrient loss but opens the gate for pathogen infection at the wounding site. Plants have evolved constitutive and induced defense mechanisms to respond to wounding to hinder further pathogen infection (Savatin et al., 2014).

Plant molecular responses to low temperature and wounding

Under low temperature conditions, plants exhibit various molecular responses, including production of small signaling molecules, biosynthesis of cold associated and inducible proteins, and adjustment of membrane composition (Heidarvand & Amiri, 2010). Small molecules, including calcium, reactive oxygen species, and nitric oxide, are involved in cellular processes such as regulation of gene expression and hormone signaling activation, leading to upregulation of antioxidant enzyme activities and osmoprotectant accumulation, which help plants survive cold stress (Yuan et al., 2018; Zheng et al., 2021). Some proteins, e.g., dehydrins and antifreeze proteins, are induced during cold acclimation and enable plants to survive in freezing conditions (Gupta & Deswal, 2014; Kosová et al., 2007). Antifreeze proteins bind to and inhibit the growth of ice crystals that are formed in the apoplast during subzero temperatures due to their high ice recrystallization inhibition activities and low thermal hysteresis. Dehydrins are hydrophilic, reliably thermostable, and disordered proteins which can protect plant cells from dehydration injury caused by freezing. Another strategy for plant survival at low temperatures is modulation of membrane composition, including lipid remodeling of the plasma and chloroplast membranes (Cook et al., 2021; Uemura et al., 2006).

Plants have evolved constitutive and induced defense mechanisms to respond to wounding and reduce further microbes infection (Savatin et al., 2014). The constitutive mechanism includes strengthened physical barriers (biosynthesis of cuticle or lignin) and release of toxic metabolites for insects and herbivores. In the induced defense mechanism upon wounding, endogenous molecules are released from the wounding site to function as damage-associated molecular patterns, which are involved in plant immune system against pathogen infection.

Lipid metabolism under low temperature stress and wounding stress

During cold acclimation, plants utilize various adaptive responses to cope with low temperature including changes in lipid composition, which functions in maintaining membrane structure, in signaling, or both. Previous studies have demonstrated that various lipid modifications, such as fatty acid desaturation (Gao et al., 2020; Hugly & Somerville, 1992; Iba, 2002; Miquel et al., 1993; Routaboul et al., 2000; Upchurch, 2008; Wolter et al., 1992), phospholipid hydrolysis (Li et al., 2008; Welte et al., 2002), head group acylation (Degenkolbe et al., 2012; Nilsson et al., 2015; Tan et al., 2018; Vu et al., 2014a; Vu et al., 2012), and head group galactosylation (Fourrier et al., 2008; Moellering et al., 2010; Roston et al., 2014) occur during cold or freezing stress to modulate plant damage (Figure 1-2B). Wounding also causes global changes in metabolome including many lipid compounds, produced by glycerolipid hydrolysis (Narvaez-Vasquez et al., 1999; Vu et al., 2015; Vu et al., 2014c; Yang et al., 2012; Zien et al., 2001), fatty acid oxidation (Buseman et al., 2006; Ibrahim et al., 2011; Vu et al., 2014a; Vu et al., 2014c; Vu et al., 2012), head-group acylation (Ibrahim et al., 2011; Nilsson et al., 2015; Vu et al., 2014a; Vu, Shiva et al., 2014c; Vu et al., 2012), galactolipid galactosylation (Vu et al., 2015; Vu et al., 2014c), and sterol glycosylation (Vu et al., 2015; Vu et al., 2014c) (shown in Figure 1-2A). Some lipid changes are unique to specific stresses, and many lipid modifications are common features in both cold and wounding stress.

Desaturation

It is well accepted that plant membrane fluidity is mediated by fatty acid desaturation in response to low temperature and several fatty acid desaturases are known to be responsible for fatty acid desaturation in different cellular locations and organs (Upchurch, 2008). In chloroplast membranes, levels of highly saturated phosphatidylglycerol (PG) are related to the low-

temperature adaptability of plants (Gao et al., 2020; Iba, 2002; Wolter et al., 1992), while high level of polyunsaturated PG, monogalactosyldiacylglycerol (MGDG), and Digalactosyldiacylglycerol (DGDG) have been shown to contribute to low temperature survival (Hugly & Somerville, 1992). Fatty acid desaturases 5 and 6, (FAD5, FAD6) are involved in fatty acid desaturation in the chloroplast during cold stress. Fatty acid desaturation also occurs in extra-chloroplast membranes and fatty acid desaturase 2 (FAD2) plays an essential role in accumulating polyunsaturated phospholipids during cold stress (Miquel et al., 1993). Increasing trienoic fatty acids (TA) in chloroplast membranes enhances low temperature tolerance in plants, and fatty acid desaturases 7 and 8 (FAD7/8) are important enzymes for TA biosynthesis in chloroplast (Iba, 2002; Routaboul et al., 2000). Upon wounding, there is an increase in fatty acid unsaturation level of membrane lipids, especially for fully desaturated phosphatidylcholine (PC) and phosphatidic acid (PA) (34:6 and 36:6 species) (Vu et al., 2015; Vu et al., 2014c). The fluid state of plasma membrane or chloroplast membrane is a structural asset for their normal functions and low temperature results in the transition from a fluid state to a rigid gel phase. Plants can increase the fatty acyl unsaturation level in membrane lipids to enhance membrane fluidity and stabilization under cold (Chen & Thelen, 2013; Harayama & Riezman, 2018; Miquel et al., 1993).

Elongation

In *Arabidopsis*, there are 21 members in 3-ketoacyl-CoA synthase (KCS) family, and most of them have been characterized as involved in very long chain fatty acid (VLCFA) biosynthesis (Joubès et al., 2008). Although the effects of fatty acid desaturation on cold tolerance are well studied, less is known about the role of fatty acid elongation in response to cold and wounding. It was recently discovered that the VLCFA content in sphingolipids was

increased in response to cold (Resemann et al., 2021). Another recent study revealed that overexpression of *KCS1* in *Arabidopsis* increased VLCFAs content and chilling tolerance (Chen et al., 2020). *KCS2* and *KCS20* are involved in production of suberin precursors and monomers and the expression of *KCS2* was induced by wounding treatment (Franke et al., 2009). Upon wounding, suberin was deposited to seal novel aboveground surfaces caused by mechanical wounding (Schreiber et al., 2005). VLCFAs are specifically present in several membrane lipids and essential for membrane homeostasis under various stresses, VLCFAs are enriched in PC, PE, and PS, where they play a role in membrane domain organization and interleaflet coupling (Batsale et al., 2021).

Hydrolysis

Phospholipases are enzymes that hydrolyze phospholipids into fatty acids and other lipophilic substrates. Phospholipase in the plant kingdom consist of phospholipases A, B, C, and D (PLA, PLB, PLC, and PLD). PLAs cleave the *sn*-1 or *sn*-2 fatty acyl chain from the glycerol backbone, producing lysophospholipids, while PLDs hydrolyze the head-group phosphoester linkage producing PA (Chen et al., 2011). In *Arabidopsis*, freezing induced a dramatic degradation of phospholipids along with a large accumulation of PA, which is catalyzed by PLD α 1 (Li et al., 2008; Welti et al., 2002). PLA-catalyzed phospholipid hydrolysis was also observed during freezing, but to a lesser extent compared with PLD catalyzed reaction. After wounding, PA was produced from phospholipid hydrolysis due to the action of PLD α 1 (Vu et al., 2015; Vu et al., 2014c; Zien et al., 2001). Besides PA, lysophosphatidylcholine (LPC) and lysophosphatidylethanolamine (LPE) were increased in *Arabidopsis* leaves upon wounding (Vu et al., 2015; Vu, Shiva, Roth, et al., 2014). These may be formed from PC and phosphatidylethanolamine (PE) hydrolysis catalyzed by PLA2s (Narvaez-Vasquez et al., 1999;

Yang et al., 2012). PA, LPLs, and free fatty acid generated after phospholipid hydrolysis are signaling molecules which can bind to proteins to regulate their activity and localization, or can influence the membrane recruitment of proteins, or participate in phytohormone signaling pathways, thus, affect plant responses in various stresses (Hou et al., 2016; Okazaki & Saito, 2014).

Oxidation

Free oxylipins and esterified oxylipins have been structurally identified in various plant species and are associated with different stresses like freezing and wounding (Genva et al., 2019; Savchenko et al., 2014). In *Arabidopsis*, oxylipins are synthesized enzymatically from unsaturated fatty acids through the lipoxygenase (LOX) pathway (Porta & Rocha-Sosa, 2002). As the major oxylipins produced under various stresses and precursors of jasmonic acid (JA), oxophytodienoic acid (OPDA) and dinor-oxophytodienoic acid (dnOPDA) are synthesized via the allene oxide synthase (AOS) branch of oxylipin metabolism (Griffiths, 2015). Over the years, more and more esterified *Arabidopsis* oxylipins such as OPDA/dnOPDA-containing galactolipids have been structurally characterized, but the biosynthetic pathway of esterified oxylipins remains unclear (Andersson et al., 2006; Hisamatsu et al., 2003, 2005; Nilsson et al., 2014; Stelmach et al., 2001; Vu et al., 2012). Under freezing stress, *Arabidopsis* accumulated very low amounts of esterified oxylipins; only MGDG (18:4-O/16:4-O) was significantly increased. Different from freezing stress, wounding treatment induced a drastic accumulation of OPDA- and dnOPDA-containing galactolipids in *Arabidopsis*, and this accumulation represents one of the major changes in the lipid profile (Buseman et al., 2006; Ibrahim et al., 2011; Vu et al., 2014a; Vu et al., 2014c; Vu et al., 2012). JA and OPDA both function as signaling molecules and induce the expression of overlapping but distinct sets of genes which can regulate plant

defenses under stresses. JA signaling is to some extent dependent on the key transcriptional activator MYC2/JIN1, which is regulated by COI1-dependent degradation of JAZ repressors while OPDA has been found to induce a set of largely COI1-independent genes (Chini et al., 2007; Santner & Estelle, 2007; Taki et al., 2005).

Acylation

Head group-acylated chloroplast lipids were discovered in the 1960s (Heinz, 1967), and more efforts and progress have been made during the past 15 years to characterize and quantify different head group-acylated lipids including acylated MGDG (acMGDG), acylated DGDG (acDGDG), and acylated PG (acPG) (Andersson et al., 2006; Kourtchenko et al., 2007; Nilsson et al., 2015; Vu et al., 2014a). In Arabidopsis, acylated galactolipid associated phospholipase 1 (AGAP1) has been shown to be responsible for formation of head group-acylated chloroplast lipids (Nilsson et al., 2015). T-DNA insertion mutant lines, *agap1-1* and *agap1-2*, both failed to accumulate ac-MGDG, acPG and acDGDG, under freezing stress. Both wounding and freeze-thaw treatments can increase the level of acylated chloroplast lipids in many plant species, especially in Arabidopsis leaves. When Arabidopsis is wounded, lipid oxidation is prominent in acylated chloroplast lipids with ox-acMGDG, ox-acDGDG, and ox-acPG rapidly produced (Vu et al., 2014a; Vu et al., 2014c; Vu et al., 2012). Non-oxidized acMGDGs are also induced upon wounding but with different kinetics, i.e., a slower rate of formation compared to ox-acMGDG (Vu et al., 2014a; Vu et al., 2014c). Sub-lethal freezing of Arabidopsis induces a different accumulation pattern of acMGDGs, leading to elevated non-oxidized acMGDG during and immediately after freezing, while most ox-acMGDG species were unchanged (Vu et al., 2014a; Vu et al., 2022; Vu et al., 2012). Despite ample evidence that acylated galactolipids accumulate

in response to biotic and abiotic stresses, the biological functions of head group-acylated chloroplast lipids remain elusive.

Triacylglycerol (TAG) biosynthesis is an acylation process occurring on the endoplasmic reticulum (ER) via the Kennedy pathway in which acyl-CoA is sequentially acylated into the *sn*-1- and *sn*-2-positions of glycerol 3-phosphate to synthesize PA; the final step is *sn*-3 acylation of diacylglycerol (DAG) catalyzed by diacylglycerol acyltransferase (DGAT) (Xu & Shanklin, 2016). An alternative route of acylation of DAG into TAG is catalyzed by phospholipid:diacylglycerol acyltransferase (PDAT) using PC as an acyl donor (Dahlqvist et al., 2000). When *Arabidopsis* was subjected to low temperature, there was an obvious accumulation of TAGs, especially of highly unsaturated TAG species (Degenkolbe et al., 2012). The *dgat1* mutant in *Arabidopsis* exhibited higher sensitivity upon freezing exposure while overexpression of *DGAT1* increased freezing tolerance in *Arabidopsis* (Arisz et al., 2018; Tan et al., 2018). Transgenic experiments showed that *Arabidopsis* depleted of *PDAT1* are more susceptible to cold exposure, while *PDAT1* overexpression plants had more cold resilience compared to wild-type plants (Demski et al., 2020). All the evidence above reveals that acylation of storage lipids in vegetative tissues is an important process of plant in response to low temperature stress. Environmental stress causes degradation of membrane lipids, leading to accumulation of toxic lipid intermediates (free FA, DAG), TAG functions as a pool to sequester these toxic compounds and prevent cellular damages under unfavorable conditions (Fan et al., 2013; Lippold et al., 2012).

Acyl steryl glycosides (ASG) is another class of acylated lipids existing in plasma membrane. Although steryl glycoside acyltransferase activity has been measured in a variety of plant tissues, no genes encoding steryl glycoside acyltransferases have yet been characterized in

plant kingdom. In 21-day old *Arabidopsis*, ASGs were largely increased after a 10-day cold acclimation at 6 °C, while in summer oat and winter rye it was found that ASG level was higher in the less freeze-resistant summer oat compared to winter rye (Tarazona et al., 2015; Uemura & Steponkus, 1994). A remarkable increase of ASGs was also observed in *Arabidopsis* leaves after mechanical wounding treatment (Vu et al., 2014c). Although some studies correlate changes in ASG with specific responses to different types of stress, the biological basis underlying the role of ASG in plant stress is just starting to be uncovered.

Galactosylation

Lipid galactosylation was first observed in *Arabidopsis* under freezing stress. SENSITIVE TO FREEZING 2 (SFR2) has been characterized as responsible for biosynthesis of tri- and tetra-galactosyldiacylglycerol (TrGDG and TeGDG) by the processive addition of galactose moieties from MGDG (Moellering et al., 2010; Roston et al., 2014), and SFR2 played a critical role in plant freezing tolerance (Fourrier et al., 2008; Moellering et al., 2010). More recently, lipid galactosylation has been discovered as occurring in *Arabidopsis* under wounding stress, when TrGDG and TeGDG were found to be significantly increased, suggesting SFR2 pathway is also induced in response to wounding, although to a lesser extent than under freezing stress (Vu et al., 2015; Vu et al., 2014c). Galactolipids including MGDG, DGDG, TrGDG, and TeGDG are important components in chloroplast membrane, MGDG has a cone-shape due to its small head group while DGDG and polygalactolipids TrGDG and TeGDG have cylinder-shape because of a larger head group. It is known that MGDG, DGDG, TrGDG, and TeGDG are readily interconvertible, plants can regulate galactolipid composition to enhance membrane stability under different stresses (Moellering et al., 2010; Torres-Franklin et al., 2007; Zhang et al., 2019). The conversion from MGDG to DGDG and to polygalactolipids stabilizes chloroplast

membranes by increasing the ratio of bilayer-forming to non-bilayer-forming galactolipids during freezing (Moellering et al., 2010).

Association mapping to identify genetic loci responsible for phenotypic traits

For phenotypes or traits that vary continuously, biologist use quantitative genetics to characterize the genetic basis of traits. Quantitative trait locus (QTL) is a region of genome which is associated with a quantitative phenotype, and analysis of QTLs connects quantitative and molecular genetics. The most popular approaches to dissect the genetic architecture of quantitative traits are QTL mapping and association mapping. QTL mapping, also called linkage mapping, was initiated in the 1980's (Lander & Botstein, 1989) and has been widely applied in plant breeding since then. It is usually performed in a constructed bi-parental population derived from a known pedigree. However, the power of QTL mapping and accuracy of QTL detection are limited to the genetic diversity of the investigated population. Genome wide association study (GWAS) overcomes the shortcomings of QTL mapping as it uses genetic variation from a large natural population (Cortes et al., 2021). It can now be successfully applied in Arabidopsis due to the establishment of 1001 Genomes Project, in which genomes of 1135 natural accessions were sequenced with over 10 million biallelic single nucleotide polymorphisms (SNPs) identified along the whole genome (Weigel & Mott, 2009). There are many factors influencing the power of GWAS including sample size, quality of genotype data, genetic heterogeneity, and confounding genetic background (Korte & Farlow, 2013). Increasing sample size and selecting geographically distant accessions can maximize the genetic variability within the population. The older 250 K SNPs data originally available for Arabidopsis only constituted a small proportion of the SNPs within the population, leaving many causal variants for specific phenotypes undetected. In 2006, the full genome sequences of 1135 accessions of Arabidopsis were published, providing

many more SNPs for GWAS (Koch, 2016). Despite this, the linkage disequilibrium (LD) structure, especially the long-range LD between SNPs, still presents difficulties in distinguishing causative variants from linked neutral markers (Kim et al., 2007).

During the past two decades, GWAS becomes an increasingly powerful tool to address the genetic architecture of complex traits in plants especially in model plant *Arabidopsis*. GWAS has been used to identify genes associated with morphological, physiological, and molecular traits in *Arabidopsis*. Atwell et al., (2010) performed GWAS on 107 phenotypes and identified many excellent candidate genes for follow-up experiments. With the development of high-throughput phenotyping methods such as metabolomics, metabolic genome-wide association study (mGWAS) shows great power to detect genetic determinants for variation in plant metabolism. Most mGWAS studies were done in *Arabidopsis* and investigated metabolites, including primary metabolites and secondary metabolites (Angelovici et al., 2017; Strauch et al., 2015). Additionally, GWAS has been applied in *Arabidopsis* to identify genes associated with lipid synthesis and composition. Branham performed GWAS analysis on the fatty acid composition of seed oil of 391 wild *Arabidopsis* accessions and identified 19 regions of interest associated with the seed oil composition (Branham et al., 2016). Recently, Menard utilized GWAS to dissect the genetic control of fatty acid desaturation in developing seeds and found that ω -6 desaturation is largely controlled by *cis*-acting sequence variants in *FAD2* (Menard et al., 2017).

Although a huge number of GWA studies have performed to look for the genetic basis of various phenotypes in different plant species and many GWAS analysis tools been developed, there is no common platform where different studies on various plant species are well cataloged (Gupta et al., 2019). In 2012, an interactive web-based tool called GWAPP was launched for

GWAS analysis in Arabidopsis (Seren et al., 2012). By using an efficient linear mixed (LM) model, the mapping is performed rapidly with genome-wide scans for ~206,000 SNPs and 1386 individuals completed in minutes. More recently, a new interactive web application called GWA-Portal was developed which is the successor of the GWAPP (Seren, 2018). Compared with GWAPP, GWA-Portal provides additional genotype datasets (Swedish genome, 1001 genomes, Imputed full sequence) with more SNPs and an accelerated linear mixed model (AMM) which does account for population structure.

Lipidomics in plant science

In the latter part of the twentieth century, mass spectrometry was employed to elucidate the chemical structures of plant lipids, and gas chromatography-mass spectrometry was used for analysis of simple lipids from plants. Quantitative analysis of a wide range of complex plant lipids by mass spectrometry, or plant “lipidomics”, began in the early 2000s in our laboratory (Welti et al., 2002; Welti & Wang, 2004). Lipidomics has increased the ease and speed of lipid analysis for plant scientists, and mass spectrometry has enabled the discovery of numerous new plant lipids. Many hundreds of papers utilizing plant lipid profiling using mass spectrometry have been published. Plant lipidomics involves many aspects including lipid extraction, lipid analysis using MS, and data processing. Figure 1-3 is a general workflow of plant lipidomics.

Lipid extraction

The Folch method (Folch et al., 1957) and the Bligh and Dyer method (Bligh & Dyer, 1959) are two of the most accepted lipid extraction methods for biological samples. For plant tissues, Ryu and Wang developed an efficient approach for various plant tissues by incorporating hot isopropanol to inhibit lipolytic enzymes into a modification of the Bligh and Dyer extraction method (Ryu & Wang, 1998). Recently, a modified method for plant leaf lipid extraction was

developed by Shiva et al. (2018) in our laboratory; this single-extraction method is efficient, less laborious, and suitable for large-scale lipidomics applications using leaves of various plant species.

Mass spectrometry analysis

With the development of MS technologies, ionization sources and different mass analyzers have been used for lipidomics (Jurowski et al., 2017; Li et al., 2014; Wang et al., 2019). Ion sources consist of electrospray ionization (ESI), atmospheric pressure chemical ionization (APCI), atmospheric, matrix assisted laser desorption ionization (MALDI), desorption ionization (DESI), and direct analysis in real time (DART). Among these ion sources, ESI is predominantly used in plant lipidomics. Mass analyzers include quadrupole, ion trap, time of flight, Fourier transform, and Orbitrap. Lipidomics methods can be divided into two different categories: direct-infusion MS methods and liquid chromatography-mass spectrometry (LC-MS) methods. Direct-infusion MS methods have been widely used in plant lipidomics during the past 20 years due to their relative simplicity, high sample throughput, and cost-effectiveness. Vu, Shiva, et al. (Shiva et al., 2013; Vu et al., 2014b) developed a direct infusion method using electrospray ionization (ESI) triple quadrupole mass spectrometry to analyze plant phospholipids and glycolipids by a series of precursor and neutral loss scans. More recently, Song updated and extended the analysis by employing multiple reaction monitoring (MRM) to measure a greater number of analytes in a shorter time (Song et al., 2020), this MS method will be described in Chapter 1.

Data processing

Processing of lipidomics data is a big challenge for plant scientists due to the complexity and quantity of raw data and limited internal standards (IS) for the plant lipidome. Lipid data

analysis is a two-step process: the first step is raw data processing, and the second step is statistical analysis. For raw data processing of lipidomics, many commercial software have been developed such as LipidSearch (ThermoFisher), LipidView(SCIEX), Lipidizer Platform (SCIEX), and SimLipid (PREMIER Biosoft); these software are usually expensive and only work with raw files from particular manufacturers (Shulaev & Chapman, 2017). However, a number of open-source lipid analysis software options are available to plant scientists for lipid identification and quantification from the direct-infusion MS experiments. LipidomeDB Data Calculation Environment (DCE) was created to process lipidomics data obtained by direct infusion using precursor or neutral loss scanning (Zhou et al., 2011). It provides multiple functions including targeting the peaks of interest in spectral lists, performing isotopic deconvolution, and calculating the amounts of lipid compared to internal standards. A recent update of LipidomeDB DCE extends its functionality to process data acquired in direct-infusion MRM mode, allowing more accurate quantification of a targeted list of lipid compounds in animal and plant samples (Fruehan et al., 2018). To assure consistency of data for each analyte throughout long periods of mass spectral data acquisition, a data correction strategy utilizing quality control samples (QC), based on work by Dunn et al. (2011), can be employed after the quantification step. Normalization to QC values can increase the analytical precision of lipid quantification.

Data analysis

The most commonly used statistical methods for lipidomics data are divided into two categories: unsupervised statistical approaches and supervised statistical approaches.

Unsupervised statistical methods include principal component analysis (PCA), hierarchical clustering, and self-organizing maps, while supervised statistical methods include analysis of

variance (ANOVA), partial least squares (PLS), k-nearest neighbors, and discriminant function analysis (DFA). MetaboAnalyst is a freely accessible, easy-to-use web server for metabolomic data analysis (Xia et al., 2009). Different kinds of input data including MS peak lists, compound/concentration data can be uploaded into MetaboAnalyst for data processing, data normalization, statistical analysis. MetaboAnalyst has been successfully applied in lipidomics data analysis using statistical approaches such as fold change analysis, t-tests, PCA, PLS-DA, and hierarchical clustering (Wang et al., 2019; Xia et al., 2009; Xia & Wishart, 2016).

Application of lipidomics in plant science

The application of lipidomics using mass spectrometry has greatly advanced the progress of plant science in the past 20 years (Kehelpannala et al., 2021; Shulaev & Chapman, 2017; Tenenboim et al., 2016). First, lipidomics provides a comprehensive and detailed view of lipids in metabolic pathways and participating in regulatory mechanism in plants. Metabolic engineering of crops requires clear understanding of plant metabolic networks and their regulation. Second, lipidomics is widely used to study lipid metabolism in plant development and stress responses. Lipidomic, genetic, and biochemical studies are often integrated to help us get a better understanding of the functions of lipids in plants. Additionally, mass spectrometry is a powerful tool for detecting novel lipid compounds which are often present at very low abundance in plant tissues. The specific functions of novel lipids also can be uncovered with the help of well-designed lipidomics experiments, typically in concert with analysis of genetically variant plants. Furthermore, lipidomics is being employed in large-scale screening experiments on some plant species because of its high-throughput feature. Natural variation in lipids within a mapping population detected by lipidomics is an excellent resource for QTL mapping or GWA

mapping, and novel genes that are associated with lipid metabolism under unstressed or stressed conditions can be identified for further characterization.

Hypotheses

Lipid metabolism in response to various stresses and the function of specific lipids and lipid-related genes remain to be determined. The motivation of this thesis is to address lipid changes and corresponding pathways under cold and mechanical wounding stress conditions. The two major tools utilized in this research are lipidomics and GWAS, which are integrated to provide new insights into the biosynthesis of lipids and their involvement in plant defense mechanisms. The hypotheses tested are:

(1) Natural variation of lipidomes of plants under unstressed and stressed conditions exists in a large group of *Arabidopsis thaliana* accessions chosen from the 1001 Genomes Project. Some genetic variants identified by GWAS are key determinants of gene expression and enzyme activity as well as the level of lipid products.

(2) The levels of certain induced or repressed lipid species among natural accessions under cold are correlated with freezing tolerance, indicating their positive or negative roles in plant freezing tolerance.

(3) Natural genomic variation in *AOCs* and *HPLI*, two candidate genes detected in the GWAS of plants subjected to wounding, regulates the production of free and esterified oxylipins in the jasmonate pathway by a fine-tuned mechanism.

Outline of dissertation

This dissertation utilizes lipidomics to investigate variation in leaf lipidomes among hundreds of *Arabidopsis* natural accessions in unstressed or stressed conditions. GWAS on

lipidomes reveals candidate genes which regulate both lipid metabolism and plant stress responses.

Chapter 2 describes a modified lipidomic approach to identify stress-induced changes in leaf lipid profile of Arabidopsis. It includes super-cold (cold stress) and mechanical wounding treatment used in this research, an optimized lipid extraction method for plant leaf tissues, direct-infusion MRM scanning operated in SCIEX Triple Quad 6500+, and data processing and normalization using MultiQuant 3.0 and LipidomeDB DCE. In this work, the lipidomic approach is modified from previous methods and establishes an excellent platform for high-throughput analysis of various lipid phenotypes in plant leaf tissues. A lipidomics study carried out during the methods development showed that cold and mechanical wounding stresses resulted in distinct patterns of stress-induced lipid composition and revealed possible roles for specific lipids and their biosynthetic pathways in plant stress responses.

Chapter 3 describes a comparative analysis of leaf lipidomes among 679 natural Arabidopsis accessions using the lipidomics platform established in Chapter 2 and characterizes the response of the leaf lipidome of the accessions to low temperature. After a “super-cold” treatment (3-day cold acclimation at 4 °C followed by -2 °C for 16 h), most of the investigated lipid species were significantly changed, with the most obvious inductions being in TAGs and VLCFA-containing membrane lipids. GWAS on individual lipid species suggested that lipid remodeling under cold stress is in part controlled by natural sequence variants in specific lipid-related genes, including *FAD2*, *FAD7*, *LOH2*, *KCS9*, and *FABI*. The relative abundance of several lipid species was significantly correlated with the freezing tolerance of the measured accessions, providing evidence for the role of specific lipid species and genes in plant freezing tolerance.

Chapter 4 describes a comparative analysis of leaf lipidomes among 360 natural *Arabidopsis* accessions and characterizes the response of the leaf lipidome to mechanical wounding. Upon wounding, there was large production of esterified oxylipins in most investigated accessions, and great variation existed in oxidized lipidomes among the accessions. GWAS on individual lipid species suggested that production of most esterified OPDA and esterified dnOPDA species after wounding was in part controlled by natural sequence variants in two genomic regions containing *AOC1/2/3* and *HPL1* respectively. Haplotype analysis showed that the relative abundances of oxylipins and oxylipin-containing lipids were correlated with sequence variation in non-coding regions in or near *AOC1/2/3* and upstream region of *HPL1*. Analysis of gene expression showed that sequence variant in upstream region significantly influenced *HPL1* level and HPL1 inhibited esterified (dn)OPDA production upon wounding in *Arabidopsis*.

Chapter 5 describes the functional characterization of *AOC1/2/3* in biosynthesis of esterified (dn)OPDA under mechanical wounding stress. There was positive correlation between *AOC2* expression and the relative contents of esterified (dn)OPDA in WT and T1 overexpression lines of *AOC2* demonstrating that *AOC2* can promote esterified (dn)OPDA production upon wounding. Comparative analysis of leaf lipidomes between WT and T-DNA insertion lines *aoc1* and *aoc3* showed that *AOC1* is indispensable for the biosynthesis of esterified (dn)OPDA and knockout of *AOC3* led to a partial loss of the ability to generate esterified (dn)OPDA under wounding.

Chapter 6 summarizes the major results and conclusions for each chapter. Future perspectives and feasible experiments are also proposed.

Figures



Figure 1-1. Collection sites for the 1135 accessions in 1001 Genomes Project

The geographic information (longitude, latitude) related to the site of collection of each accession was obtained from 1001 Genomes Project database

(<https://1001genomes.org/accessions.html>). The map was constructed in Google Maps.

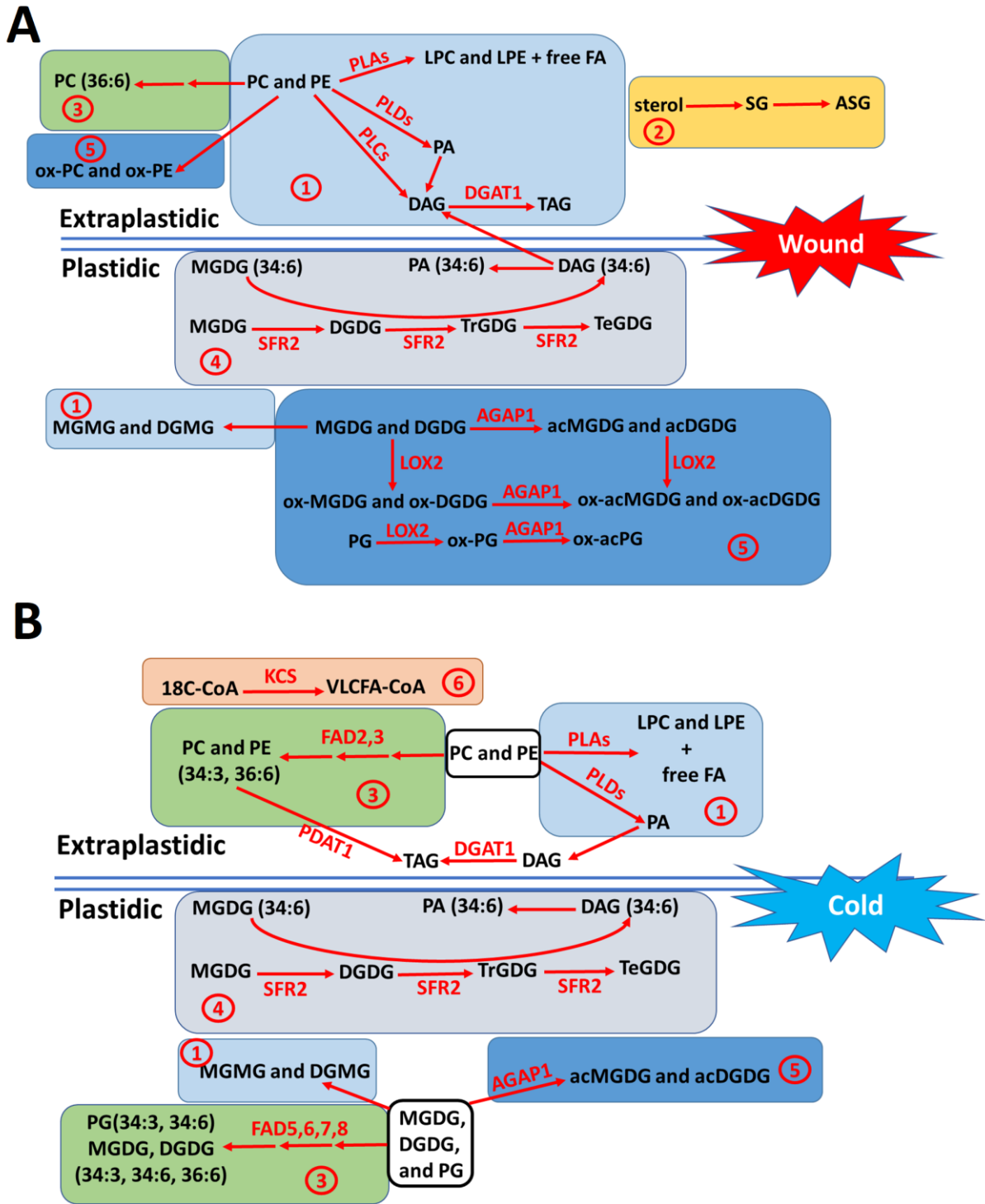


Figure 1-2. Lipid modifications in response to mechanical wounding and low temperature stress in Arabidopsis leaves

Red arrows indicate induced lipid pathways under mechanical wounding stress (A) and low temperature (including cold and freezing) stress (B). Black text indicates lipids and red text indicates enzymes. Panel A is adapted from Vu et al. (Figure 2, 2015), panel B is a summary based on previous research (Arisz et al., 2018; Chen et al., 2020; Degenkolbe et al., 2012; Fourier et al., 2008; Gao et al., 2020; Hugly & Somerville, 1992; Iba, 2002; Miquel et al., 1993; Moellering et al., 2010; Nilsson et al., 2015; Resemann et al., 2021; Roston et al., 2014; Tan et al., 2018; Upchurch, 2008; Vu et al., 2014a; Vu et al., 2012; Welte et al., 2002; Wolter et al., 1992). Numbers represent different kinds of lipid modifications: (1) membrane lipid hydrolysis; (2) sterol glycosylation and acylation; (3) membrane lipid desaturation; (4) galactolipid galactosylation; (5) oxidation and head-group acylation of membrane lipids; (6) fatty acyl elongation.

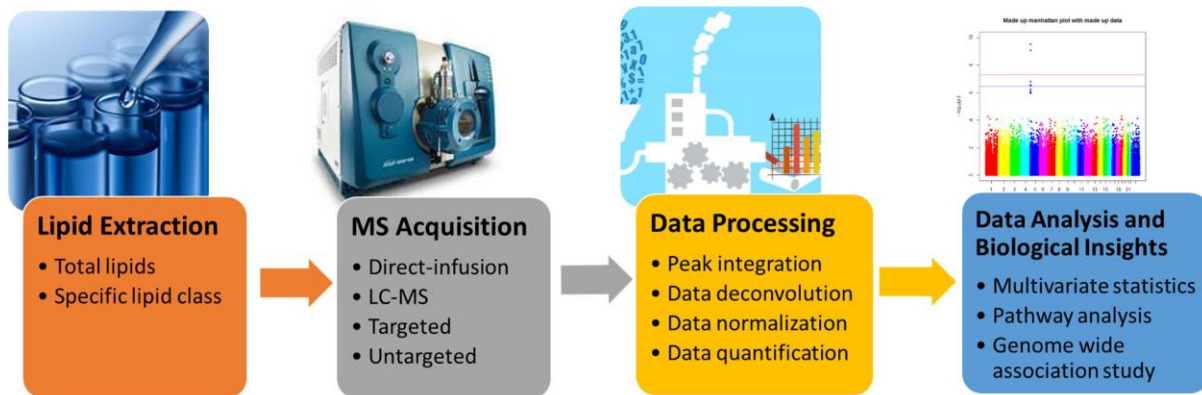


Figure 1-3. General workflow of plant lipidomics

Generally, lipidomics analysis involves lipid extraction, MS analysis, data processing, and data analysis (biological interpretation). Lipid extraction methods can be tailored towards specific groups of lipids or total lipids. MS methods can be categorized into direct-infusion without LC and LC-MS, or they can be divided into targeted and untargeted with/without a priori knowledge about sample composition. Data processing usually includes signal integration, isotope deconvolution, data correction, and data normalization. There are various ways to analyze lipidomics data, e.g. multivariate statistical analysis, pathway analysis, GWAS.

References

- Alonso-Blanco, C., Andrade, J., Becker, C., Bemm, F., Bergelson, J., Borgwardt, K. M., Cao, J., Chae, E., Dezwaan, T. M., Ding, W., Ecker, J. R., Exposito-Alonso, M., Farlow, A., Fitz, J., Gan, X., Grimm, D. G., Hancock, A. M., Henz, S. R., Holm, S., ... Zhou, X. (2016). 1,135 Genomes Reveal the Global Pattern of Polymorphism in *Arabidopsis thaliana*. *Cell*, *166*, 481–491.
- Andersson, M. X., Hamberg, M., Kourtchenko, O., Brunnström, A., McPhail, K. L., Gerwick, W. H., Göbel, C., Feussner, I., & Ellerström, M. (2006). Oxylinin profiling of the hypersensitive response in *Arabidopsis thaliana*. Formation of a novel oxo-phytodienoic acid-containing galactolipid, arabidopside E. *The Journal of Biological Chemistry*, *281*, 31528–31537.
- Angelovici, R., Batushansky, A., Deason, N., Gonzalez-Jorge, S., Gore, M. A., Fait, A., & DellaPenna, D. (2017). Network-Guided GWAS Improves Identification of Genes Affecting Free Amino Acids. *Plant Physiology*, *173*, 872–886.
- Arisz, S. A., Heo, J.-Y., Koevoets, I. T., Zhao, T., van Egmond, P., Meyer, A. J., Zeng, W., Niu, X., Wang, B., Mitchell-Olds, T., Schranz, M. E., & Testerink, C. (2018). DIACYLGLYCEROL ACYLTRANSFERASE1 Contributes to Freezing Tolerance. *Plant Physiology*, *177*, 1410–1424.
- Atwell, S., Huang, Y. S., Vilhjálmsson, B. J., Willems, G., Horton, M., Li, Y., Meng, D., Platt, A., Tarone, A. M., Hu, T. T., Jiang, R., Muliylati, N. W., Zhang, X., Amer, M. A., Baxter, I., Brachi, B., Chory, J., Dean, C., Debieu, M., ... Nordborg, M. (2010). Genome-wide association study of 107 phenotypes in *Arabidopsis thaliana* inbred lines. *Nature*, *465*, 627–631.
- Batsale, M., Bahammou, D., Fouillen, L., Mongrand, S., Joubès, J., & Domergue, F. (2021). Biosynthesis and Functions of Very-Long-Chain Fatty Acids in the Responses of Plants to Abiotic and Biotic Stresses. *Cells*, *10*, 1284.
- Bligh, E. G., & Dyer, W. J. (1959). A rapid method of total lipid extraction and purification. *Canadian Journal of Biochemistry and Physiology*, *37*, 911–917.
- Branham, S. E., Wright, S. J., Reba, A., & Linder, C. R. (2016). Genome-Wide Association Study of *Arabidopsis thaliana* Identifies Determinants of Natural Variation in Seed Oil Composition. *The Journal of Heredity*, *107*, 248–256.
- Buseman, C. M., Tamura, P., Sparks, A. A., Baughman, E. J., Maatta, S., Zhao, J., Roth, M. R., Esch, S. W., Shah, J., Williams, T. D., & Welti, R. (2006). Wounding stimulates the accumulation of glycerolipids containing oxophytodienoic acid and dinor-oxophytodienoic acid in *Arabidopsis* leaves. *Plant Physiology*, *142*, 28–39.
- Chen, G., Snyder, C. L., Greer, M. S., & Weselake, R. J. (2011). Biology and Biochemistry of Plant Phospholipases. *Critical Reviews in Plant Sciences*, *30*, 239–258.

- Chen, L., Hu, W., Mishra, N., Wei, J., Lu, H., Hou, Y., Qiu, X., Yu, S., Wang, C., Zhang, H., Cai, Y., Sun, C., & Shen, G. (2020). AKR2A interacts with KCS1 to improve VLCFAs contents and chilling tolerance of *Arabidopsis thaliana*. *The Plant Journal: For Cell and Molecular Biology*, *103*, 1575–1589.
- Chen, M., & Thelen, J. J. (2013). ACYL-LIPID DESATURASE2 Is Required for Chilling and Freezing Tolerance in *Arabidopsis*. *The Plant Cell*, *25*, 1430–1444.
- Chini, A., Fonseca, S., Fernández, G., Adie, B., Chico, J. M., Lorenzo, O., García-Casado, G., López-Vidriero, I., Lozano, F. M., Ponce, M. R., Micol, J. L., & Solano, R. (2007). The JAZ family of repressors is the missing link in jasmonate signalling. *Nature*, *448*, 666–671.
- Cook, R., Lupette, J., & Benning, C. (2021). The Role of Chloroplast Membrane Lipid Metabolism in Plant Environmental Responses. *Cells*, *10*, 706.
- Dahlgvist, A., Ståhl, U., Lenman, M., Banas, A., Lee, M., Sandager, L., Ronne, H., & Stymne, S. (2000). Phospholipid:diacylglycerol acyltransferase: An enzyme that catalyzes the acyl-CoA-independent formation of triacylglycerol in yeast and plants. *Proceedings of the National Academy of Sciences*, *97*, 6487–6492.
- Degenkolbe, T., Giavalisco, P., Zuther, E., Seiwert, B., Hinch, D. K., & Willmitzer, L. (2012). Differential remodeling of the lipidome during cold acclimation in natural accessions of *Arabidopsis thaliana*. *The Plant Journal: For Cell and Molecular Biology*, *72*, 972–982.
- Demski, K., Łosiewska, A., Jasieniecka-Gazarkiewicz, K., Klińska, S., & Banaś, A. (2020). Phospholipid:Diacylglycerol Acyltransferase1 Overexpression Delays Senescence and Enhances Post-heat and Cold Exposure Fitness. *Frontiers in Plant Science*, *11*, 611897.
- Dunn, W. B., Broadhurst, D., Begley, P., Zelena, E., Francis-McIntyre, S., Anderson, N., Brown, M., Knowles, J. D., Halsall, A., Haselden, J. N., Nicholls, A. W., Wilson, I. D., Kell, D. B., Goodacre, R., & Human Serum Metabolome (HUSERMET) Consortium. (2011). Procedures for large-scale metabolic profiling of serum and plasma using gas chromatography and liquid chromatography coupled to mass spectrometry. *Nature Protocols*, *6*, 1060–1083.
- Fan, J., Yan, C., & Xu, C. (2013). Phospholipid:diacylglycerol acyltransferase-mediated triacylglycerol biosynthesis is crucial for protection against fatty acid-induced cell death in growing tissues of *Arabidopsis*. *The Plant Journal*, *76*, 930–942.
- Folch, J., Lees, M., & Sloane Stanley, G. H. (1957). A simple method for the isolation and purification of total lipides from animal tissues. *The Journal of Biological Chemistry*, *226*, 497–509.
- Fourrier, N., Bédard, J., Lopez-Juez, E., Barbrook, A., Bowyer, J., Jarvis, P., Warren, G., & Thorlby, G. (2008). A role for SENSITIVE TO FREEZING2 in protecting chloroplasts against freeze-induced damage in *Arabidopsis*. *The Plant Journal: For Cell and Molecular Biology*, *55*, 734–745.

- Franke, R., Höfer, R., Briesen, I., Emsermann, M., Efremova, N., Yephremov, A., & Schreiber, L. (2009). The DAISY gene from *Arabidopsis* encodes a fatty acid elongase condensing enzyme involved in the biosynthesis of aliphatic suberin in roots and the chalazal-micropyle region of seeds. *The Plant Journal: For Cell and Molecular Biology*, *57*, 80–95.
- Fruehan, C., Johnson, D., & Welti, R. (2018). LipidomeDB Data Calculation Environment Has Been Updated to Process Direct-Infusion Multiple Reaction Monitoring Data. *Lipids*, *53*, 1019–1020.
- Gao, J., Lunn, D., Wallis, J. G., & Browse, J. (2020). Phosphatidylglycerol Composition Is Central to Chilling Damage in the *Arabidopsis* *fab1* Mutant. *Plant Physiology*, *184*, 1717–1730.
- Genva, M., Obounou Akong, F., Andersson, M. X., Deleu, M., Lins, L., & Fauconnier, M.-L. (2019). New insights into the biosynthesis of esterified oxylipins and their involvement in plant defense and developmental mechanisms. *Phytochemistry Reviews*, *18*, 343–358.
- Gilmour, S. J., Hajela, R. K., & Thomashow, M. F. (1988). Cold Acclimation in *Arabidopsis thaliana*. *Plant Physiology*, *87*, 745–750.
- Griffiths, G. (2015). Biosynthesis and analysis of plant oxylipins. *Free Radical Research*, *49*, 565–582.
- Gupta, P. K., Kulwal, P. L., & Jaiswal, V. (2019). Association mapping in plants in the post-GWAS genomics era. *Advances in Genetics*, *104*, 75–154.
- Gupta, R., & Deswal, R. (2014). Antifreeze proteins enable plants to survive in freezing conditions. *Journal of Biosciences*, *39*, 931–944.
- Harayama, T., & Riezman, H. (2018). Understanding the diversity of membrane lipid composition. *Nature Reviews. Molecular Cell Biology*, *19*, 281–296.
- Heidarvand, L., & Maali Amiri, R. (2010). What happens in plant molecular responses to cold stress? *Acta Physiologiae Plantarum*, *32*, 419–431.
- Heinz, E. (1967). [Acylgalactosyldiglyceride from leaf homogenates]. *Biochimica Et Biophysica Acta*, *144*, 321–332.
- Hermansson, M., Hokynar, K., & Somerharju, P. (2011). Mechanisms of glycerophospholipid homeostasis in mammalian cells. *Progress in Lipid Research*, *50*, 240–257.
- Hisamatsu, Y., Goto, N., Hasegawa, K., & Shigemori, H. (2003). Arabidopsides A and B, two new oxylipins from *Arabidopsis thaliana*. *Tetrahedron Letters*, *44*, 5553–5556.
- Hisamatsu, Y., Goto, N., Sekiguchi, M., Hasegawa, K., & Shigemori, H. (2005). Oxylipins Arabidopsides C and D from *Arabidopsis thaliana*. *Journal of Natural Products*, *68*, 600–603.

- Hou, Q., Ufer, G., & Bartels, D. (2016). Lipid signalling in plant responses to abiotic stress: Lipid signalling in plant responses to abiotic stress. *Plant, Cell & Environment*, *39*, 1029–1048.
- Hugly, S., & Somerville, C. (1992). A role for membrane lipid polyunsaturation in chloroplast biogenesis at low temperature. *Plant Physiology*, *99*, 197–202.
- Iba, K. (2002). Acclimative response to temperature stress in higher plants: Approaches of gene engineering for temperature tolerance. *Annual Review of Plant Biology*, *53*, 225–245.
- Ibrahim, A., Schütz, A.-L., Galano, J.-M., Herrfurth, C., Feussner, K., Durand, T., Brodhun, F., & Feussner, I. (2011). The Alphabet of Galactolipids in *Arabidopsis thaliana*. *Frontiers in Plant Science*, *2*, 95.
- Joubès, J., Raffaele, S., Bourdenx, B., Garcia, C., Laroche-Traineau, J., Moreau, P., Domergue, F., & Lessire, R. (2008). The VLCFA elongase gene family in *Arabidopsis thaliana*: Phylogenetic analysis, 3D modelling and expression profiling. *Plant Molecular Biology*, *67*, 547–566.
- Jurowski, K., Kochan, K., Walczak, J., Barańska, M., Piekoszewski, W., & Buszewski, B. (2017). Analytical Techniques in Lipidomics: State of the Art. *Critical Reviews in Analytical Chemistry*, *47*, 418–437.
- Karnovsky, M. J., Kleinfeld, A. M., Hoover, R. L., & Klausner, R. D. (1982). The concept of lipid domains in membranes. *The Journal of Cell Biology*, *94*, 1–6.
- Kehelpannala, C., Rupasinghe, T., Hennessy, T., Bradley, D., Ebert, B., & Roessner, U. (2021). The state of the art in plant lipidomics. *Molecular Omics*, *17*, 894–910.
- Kim, H. U. (2020). Lipid Metabolism in Plants. *Plants (Basel, Switzerland)*, *9*, E871.
- Kim, S., Plagnol, V., Hu, T. T., Toomajian, C., Clark, R. M., Ossowski, S., Ecker, J. R., Weigel, D., & Nordborg, M. (2007). Recombination and linkage disequilibrium in *Arabidopsis thaliana*. *Nature Genetics*, *39*, 1151–1155.
- Koch, L. (2016). 1001 genomes and epigenomes. *Nature Reviews Genetics*, *17*, 503–503.
- Koornneef, M., & Meinke, D. (2010). The development of *Arabidopsis* as a model plant. *The Plant Journal: For Cell and Molecular Biology*, *61*, 909–921.
- Korte, A., & Farlow, A. (2013). The advantages and limitations of trait analysis with GWAS: A review. *Plant Methods*, *9*, 29.
- Kosová, K., Vítámvás, P., & Prášil, I. T. (2007). The role of dehydrins in plant response to cold. *Biologia Plantarum*, *51*, 601–617.
- Kourtchenko, O., Andersson, M. X., Hamberg, M., Brunnström, A., Göbel, C., McPhail, K. L., Gerwick, W. H., Feussner, I., & Ellerström, M. (2007). Oxo-phytodienoic acid-

- containing galactolipids in Arabidopsis: Jasmonate signaling dependence. *Plant Physiology*, *145*, 1658–1669.
- Lander, E. S., & Botstein, D. (1989). Mapping mendelian factors underlying quantitative traits using RFLP linkage maps. *Genetics*, *121*, 185–199.
- Li, M., Yang, L., Bai, Y., & Liu, H. (2014). Analytical Methods in Lipidomics and Their Applications. *Analytical Chemistry*, *86*, 161–175.
- Li, W., Wang, R., Li, M., Li, L., Wang, C., Welti, R., & Wang, X. (2008). Differential degradation of extraplastidic and plastidic lipids during freezing and post-freezing recovery in Arabidopsis thaliana. *The Journal of Biological Chemistry*, *283*, 461–468.
- Li-Beisson, Y., Shorrosh, B., Beisson, F., Andersson, M. X., Arondel, V., Bates, P. D., Baud, S., Bird, D., Debono, A., Durrett, T. P., Franke, R. B., Graham, I. A., Katayama, K., Kelly, A. A., Larson, T., Markham, J. E., Miquel, M., Molina, I., Nishida, I., ... Ohlrogge, J. (2013). Acyl-lipid metabolism. *The Arabidopsis Book*, *11*, e0161.
- Lippold, F., vom Dorp, K., Abraham, M., Hölzl, G., Wewer, V., Yilmaz, J. L., Lager, I., Montandon, C., Besagni, C., Kessler, F., Stymne, S., & Dörmann, P. (2012). Fatty acid phytol ester synthesis in chloroplasts of Arabidopsis. *The Plant Cell*, *24*, 2001–2014.
- Menard, G. N., Moreno, J. M., Bryant, F. M., Munoz-Azcarate, O., Kelly, A. A., Hassani-Pak, K., Kurup, S., & Eastmond, P. J. (2017). Genome Wide Analysis of Fatty Acid Desaturation and Its Response to Temperature. *Plant Physiology*, *173*, 1594–1605.
- Miquel, M., James, D., Dooner, H., & Browse, J. (1993). Arabidopsis requires polyunsaturated lipids for low-temperature survival. *Proceedings of the National Academy of Sciences of the United States of America*, *90*, 6208–6212.
- Moellering, E. R., & Benning, C. (2011). Galactoglycerolipid metabolism under stress: A time for remodeling. *Trends in Plant Science*, *16*, 98–107.
- Moellering, E. R., Muthan, B., & Benning, C. (2010). Freezing tolerance in plants requires lipid remodeling at the outer chloroplast membrane. *Science (New York, N.Y.)*, *330*, 226–228.
- Nakamura, M. T., Yudell, B. E., & Loor, J. J. (2014). Regulation of energy metabolism by long-chain fatty acids. *Progress in Lipid Research*, *53*, 124–144.
- Nakamura, Y. (2013). Phosphate starvation and membrane lipid remodeling in seed plants. *Progress in Lipid Research*, *52*, 43–50.
- Narvaez-Vasquez, Florin-Christensen, & Ryan. (1999). Positional specificity of a phospholipase A activity induced by wounding, systemin, and oligosaccharide elicitors in tomato leaves. *The Plant Cell*, *11*, 2249–2260.
- Nilsson, A. K., Johansson, O. N., Fahlberg, P., Kommuri, M., Töpel, M., Bodin, L. J., Sikora, P., Modarres, M., Ekengren, S., Nguyen, C. T., Farmer, E. E., Olsson, O., Ellerström, M., &

- Andersson, M. X. (2015). Acylated monogalactosyl diacylglycerol: Prevalence in the plant kingdom and identification of an enzyme catalyzing galactolipid head group acylation in *Arabidopsis thaliana*. *The Plant Journal: For Cell and Molecular Biology*, *84*, 1152–1166.
- Nilsson, A. K., Johansson, O. N., Fahlberg, P., Steinhart, F., Gustavsson, M. B., Ellerström, M., & Andersson, M. X. (2014). Formation of oxidized phosphatidylinositol and 12-oxo-phytodienoic acid containing acylated phosphatidylglycerol during the hypersensitive response in *Arabidopsis*. *Phytochemistry*, *101*, 65–75.
- Okazaki, Y., & Saito, K. (2014). Roles of lipids as signaling molecules and mitigators during stress response in plants. *The Plant Journal*, *79*, 584–596.
- Porta, H., & Rocha-Sosa, M. (2002). Plant lipoxygenases. Physiological and molecular features. *Plant Physiology*, *130*, 15–21.
- Resemann, H. C., Herrfurth, C., Feussner, K., Hornung, E., Ostendorf, A. K., Gömann, J., Mittag, J., van Gessel, N., Vries, J. de, Ludwig-Müller, J., Markham, J., Reski, R., & Feussner, I. (2021). Convergence of sphingolipid desaturation across over 500 million years of plant evolution. *Nature Plants*, *7*, 219–232.
- Roston, R. L., Wang, K., Kuhn, L. A., & Benning, C. (2014). Structural determinants allowing transferase activity in SENSITIVE TO FREEZING 2, classified as a family I glycosyl hydrolase. *The Journal of Biological Chemistry*, *289*, 26089–26106.
- Routaboul, J. M., Fischer, S. F., & Browse, J. (2000). Trienoic fatty acids are required to maintain chloroplast function at low temperatures. *Plant Physiology*, *124*, 1697–1705.
- Ryu, S. B., & Wang, X. (1998). Increase in free linolenic and linoleic acids associated with phospholipase D-mediated hydrolysis of phospholipids in wounded castor bean leaves. *Biochimica Et Biophysica Acta*, *1393*, 193–202.
- Santner, A., & Estelle, M. (2007). The JAZ proteins link jasmonate perception with transcriptional changes. *The Plant Cell*, *19*, 3839–3842.
- Savatin, D. V., Gramegna, G., Modesti, V., & Cervone, F. (2014). Wounding in the plant tissue: The defense of a dangerous passage. *Frontiers in Plant Science*, *5*, 470.
- Savchenko, T. V., Zastrijnaja, O. M., & Klimov, V. V. (2014). Oxylipins and plant abiotic stress resistance. *Biochemistry. Biokhimiia*, *79*, 362–375.
- Schreiber, L., Franke, R., & Hartmann, K. (2005). Wax and suberin development of native and wound periderm of potato (*Solanum tuberosum* L.) and its relation to peridermal transpiration. *Planta*, *220*, 520–530.
- Seren, Ü. (2018). GWA-Portal: Genome-Wide Association Studies Made Easy. *Methods in Molecular Biology (Clifton, N.J.)*, *1761*, 303–319.

- Seren, Ü., Vilhjálmsson, B. J., Horton, M. W., Meng, D., Forai, P., Huang, Y. S., Long, Q., Segura, V., & Nordborg, M. (2012). GWAPP: A web application for genome-wide association mapping in Arabidopsis. *The Plant Cell*, *24*, 4793–4805.
- Shiva, S., Enniful, R., Roth, M. R., Tamura, P., Jagadish, K., & Welti, R. (2018). An efficient modified method for plant leaf lipid extraction results in improved recovery of phosphatidic acid. *Plant Methods*, *14*, 14.
- Shiva, S., Vu, H. S., Roth, M. R., Zhou, Z., Marepally, S. R., Nune, D. S., Lushington, G. H., Visvanathan, M., & Welti, R. (2013). Lipidomic analysis of plant membrane lipids by direct infusion tandem mass spectrometry. *Methods in Molecular Biology (Clifton, N.J.)*, *1009*, 79–91.
- Shulaev, V., & Chapman, K. D. (2017). Plant lipidomics at the crossroads: From technology to biology driven science. *Biochimica Et Biophysica Acta. Molecular and Cell Biology of Lipids*, *1862*, 786–791.
- Song, Y., Vu, H. S., Shiva, S., Fruehan, C., Roth, M. R., Tamura, P., & Welti, R. (2020). A Lipidomic Approach to Identify Cold-Induced Changes in Arabidopsis Membrane Lipid Composition. *Methods in Molecular Biology (Clifton, N.J.)*, *2156*, 187–202.
- Stelmach, B. A., Müller, A., Hennig, P., Gebhardt, S., Schubert-Zsilavec, M., & Weiler, E. W. (2001). A novel class of oxylipins, sn1-O-(12-oxophytodienoyl)-sn2-O-(hexadecatrienoyl)-monogalactosyl Diglyceride, from Arabidopsis thaliana. *The Journal of Biological Chemistry*, *276*, 12832–12838.
- Steponkus, P. L. (1984). Role of the Plasma Membrane in Freezing Injury and Cold Acclimation. *Annual Review of Plant Physiology*, *35*, 543–584.
- Strauch, R. C., Svedin, E., Dilkes, B., Chapple, C., & Li, X. (2015). Discovery of a novel amino acid racemase through exploration of natural variation in Arabidopsis thaliana. *Proceedings of the National Academy of Sciences of the United States of America*, *112*, 11726–11731.
- Taki, N., Sasaki-Sekimoto, Y., Obayashi, T., Kikuta, A., Kobayashi, K., Ainai, T., Yagi, K., Sakurai, N., Suzuki, H., Masuda, T., Takamiya, K.-I., Shibata, D., Kobayashi, Y., & Ohta, H. (2005). 12-oxo-phytodienoic acid triggers expression of a distinct set of genes and plays a role in wound-induced gene expression in Arabidopsis. *Plant Physiology*, *139*, 1268–1283.
- Tan, W.-J., Yang, Y.-C., Zhou, Y., Huang, L.-P., Xu, L., Chen, Q.-F., Yu, L.-J., & Xiao, S. (2018). DIACYLGLYCEROL ACYLTRANSFERASE and DIACYLGLYCEROL KINASE Modulate Triacylglycerol and Phosphatidic Acid Production in the Plant Response to Freezing Stress. *Plant Physiology*, *177*, 1303–1318.
- Tarazona, P., Feussner, K., & Feussner, I. (2015). An enhanced plant lipidomics method based on multiplexed liquid chromatography-mass spectrometry reveals additional insights into

- cold- and drought-induced membrane remodeling. *The Plant Journal: For Cell and Molecular Biology*, *84*, 621–633.
- Tenenboim, H., Burgos, A., Willmitzer, L., & Brotman, Y. (2016). Using lipidomics for expanding the knowledge on lipid metabolism in plants. *Biochimie*, *130*, 91–96.
- Tibbs Cortes, L., Zhang, Z., & Yu, J. (2021). Status and prospects of genome-wide association studies in plants. *The Plant Genome*, *14*, e20077.
- Torres-Franklin, M.-L., Gigon, A., de Melo, D. F., Zuily-Fodil, Y., & Pham-Thi, A.-T. (2007). Drought stress and rehydration affect the balance between MGDG and DGDG synthesis in cowpea leaves. *Physiologia Plantarum*, *131*, 201–210.
- Uemura, M., Joseph, R. A., & Steponkus, P. L. (1995). Cold Acclimation of *Arabidopsis thaliana* (Effect on Plasma Membrane Lipid Composition and Freeze-Induced Lesions). *Plant Physiology*, *109*, 15–30.
- Uemura, M., & Steponkus, P. L. (1994). A Contrast of the Plasma Membrane Lipid Composition of Oat and Rye Leaves in Relation to Freezing Tolerance. *Plant Physiology*, *104*, 479–496.
- Uemura, Matsuo, Tominaga, Y., Nakagawara, C., Shigematsu, S., Minami, A., & Kawamura, Y. (2006). Responses of the plasma membrane to low temperatures. *Physiologia Plantarum*, *126*, 81–89.
- Upchurch, R. G. (2008). Fatty acid unsaturation, mobilization, and regulation in the response of plants to stress. *Biotechnology Letters*, *30*, 967–977.
- van Meer, G., Voelker, D. R., & Feigenson, G. W. (2008). Membrane lipids: Where they are and how they behave. *Nature Reviews. Molecular Cell Biology*, *9*, 112–124.
- Vu, H. S., Roston, R., Shiva, S., Hur, M., Wurtele, E. S., Wang, X., Shah, J., & Welti, R. (2015). Modifications of membrane lipids in response to wounding of *Arabidopsis thaliana* leaves. *Plant Signaling & Behavior*, *10*, e1056422.
- Vu, H. S., Roth, M. R., Tamura, P., Samarakoon, T., Shiva, S., Honey, S., Lowe, K., Schmelz, E. A., Williams, T. D., & Welti, R. (2014a). Head-group acylation of monogalactosyldiacylglycerol is a common stress response, and the acyl-galactose acyl composition varies with the plant species and applied stress. *Physiologia Plantarum*, *150*, 517–528.
- Vu, H. S., Shiva, S., Hall, A. S., & Welti, R. (2014b). A lipidomic approach to identify cold-induced changes in *Arabidopsis* membrane lipid composition. *Methods in Molecular Biology (Clifton, N.J.)*, *1166*, 199–215.
- Vu, H. S., Shiva, S., Roth, M. R., Tamura, P., Zheng, L., Li, M., Sarowar, S., Honey, S., McEllhiney, D., Hinkes, P., Seib, L., Williams, T. D., Gadbury, G., Wang, X., Shah, J., & Welti, R. (2014c). Lipid changes after leaf wounding in *Arabidopsis thaliana*: Expanded

- lipidomic data form the basis for lipid co-occurrence analysis. *The Plant Journal: For Cell and Molecular Biology*, 80, 728–743.
- Vu, H. S., Shiva, S., Samarakoon, T., Li, M., Sarowar, S., Roth, M. R., Tamura, P., Honey, S., Lowe, K., Porras, H., Prakash, N., Roach, C. A., Stuke, M., Wang, X., Shah, J., Gadbury, G., Wang, H., & Welti, R. (2022). Specific Changes in Arabidopsis thaliana Rosette Lipids during Freezing Can Be Associated with Freezing Tolerance. *Metabolites*, 12, 385.
- Vu, H. S., Tamura, P., Galeva, N. A., Chaturvedi, R., Roth, M. R., Williams, T. D., Wang, X., Shah, J., & Welti, R. (2012). Direct infusion mass spectrometry of oxylipin-containing Arabidopsis membrane lipids reveals varied patterns in different stress responses. *Plant Physiology*, 158, 324–339.
- Wang, J., Wang, C., & Han, X. (2019). Tutorial on lipidomics. *Analytica Chimica Acta*, 1061, 28–41.
- Weigel, D., & Mott, R. (2009). The 1001 genomes project for Arabidopsis thaliana. *Genome Biology*, 10, 107.
- Welti, R., Li, W., Li, M., Sang, Y., Biesiada, H., Zhou, H.-E., Rajashekar, C. B., Williams, T. D., & Wang, X. (2002). Profiling membrane lipids in plant stress responses. Role of phospholipase D alpha in freezing-induced lipid changes in Arabidopsis. *The Journal of Biological Chemistry*, 277, 31994–32002.
- Welti, R., & Wang, X. (2004). Lipid species profiling: A high-throughput approach to identify lipid compositional changes and determine the function of genes involved in lipid metabolism and signaling. *Current Opinion in Plant Biology*, 7, 337–344.
- Wolter, F. P., Schmidt, R., & Heinz, E. (1992). Chilling sensitivity of Arabidopsis thaliana with genetically engineered membrane lipids. *The EMBO Journal*, 11, 4685–4692.
- Xia, J., Psychogios, N., Young, N., & Wishart, D. S. (2009). MetaboAnalyst: A web server for metabolomic data analysis and interpretation. *Nucleic Acids Research*, 37, W652–660.
- Xia, J., & Wishart, D. S. (2016). Using MetaboAnalyst 3.0 for Comprehensive Metabolomics Data Analysis. *Current Protocols in Bioinformatics*, 55. <https://doi.org/10.1002/cpbi.11>
- Xu, C., & Shanklin, J. (2016). Triacylglycerol Metabolism, Function, and Accumulation in Plant Vegetative Tissues. *Annual Review of Plant Biology*, 67, 179–206.
- Yadav, S. K. (2010). Cold stress tolerance mechanisms in plants. A review. *Agronomy for Sustainable Development*, 30, 515–527.
- Yang, W.-Y., Zheng, Y., Bahn, S. C., Pan, X.-Q., Li, M.-Y., Vu, H. S., Roth, M. R., Scheu, B., Welti, R., Hong, Y.-Y., & Wang, X.-M. (2012). The patatin-containing phospholipase A pPLAII α modulates oxylipin formation and water loss in Arabidopsis thaliana. *Molecular Plant*, 5, 452–460.

- Yuan, P., Yang, T., & Poovaiah, B. W. (2018). Calcium Signaling-Mediated Plant Response to Cold Stress. *International Journal of Molecular Sciences*, *19*, E3896.
- Zhang, X., Xu, Y., & Huang, B. (2019). Lipidomic reprogramming associated with drought stress priming-enhanced heat tolerance in tall fescue (*Festuca arundinacea*): Lipidomic profiling for drought-induced heat tolerance. *Plant, Cell & Environment*, *42*, 947–958.
- Zheng, S., Su, M., Wang, L., Zhang, T., Wang, J., Xie, H., Wu, X., Haq, S. I. U., & Qiu, Q.-S. (2021). Small signaling molecules in plant response to cold stress. *Journal of Plant Physiology*, *266*, 153534.
- Zhou, Z., Marepally, S. R., Nune, D. S., Pallakollu, P., Ragan, G., Roth, M. R., Wang, L., Lushington, G. H., Visvanathan, M., & Welti, R. (2011). LipidomeDB data calculation environment: Online processing of direct-infusion mass spectral data for lipid profiles. *Lipids*, *46*, 879–884.
- Zien, C. A., Wang, C., Wang, X., & Welti, R. (2001). In vivo substrates and the contribution of the common phospholipase D, PLD α , to wound-induced metabolism of lipids in Arabidopsis. *Biochimica Et Biophysica Acta*, *1530*, 236–248.

Chapter 2 - Development of a direct-infusion lipidomics approach to identify lipid changes in Arabidopsis leaf tissues in response to various stresses

Part of this chapter has been published as a method chapter in book.

Song, Y., Vu, H. S., Shiva, S., Fruehan, C., Roth, M. R., Tamura, P., & Welte, R. (2020).

A Lipidomic Approach to Identify Cold-Induced Changes in Arabidopsis Membrane Lipid Composition. *Methods in Molecular Biology (Clifton, N.J.)*, 2156, 187–202.

Introduction

Abiotic stresses, including cold temperature and wounding, cause massive losses of crop yield. The development of more stress-tolerant crop species requires better understanding of the biochemistry and genetics behind plant response to stress. The cellular damage caused by cold, but above-freezing temperatures, is a “direct temperature effect”, and is increased incrementally in response to decreases in temperature, in contrast to the sharp increase in damage that occurs when the temperature is decreased to the point of freezing (Yadav, 2010). *Arabidopsis thaliana* is a cold-tolerant plant species, which can enhance its freezing tolerance after cold acclimation (Gilmour et al., 1988; Uemura et al., 1995). Mechanical wounding treatment imitates plant wounding stress in nature, where tissue damage is caused by chewing insects, large herbivores, or severe weather like wind and hail. Plants have evolved a number of defense mechanisms to respond to cold and wounding, and lipid remodeling is one of the major molecular responses. Previous studies showed that cold and mechanical wounding both caused global changes in lipidome of Arabidopsis (Barrero-Sicilia et al., 2017; Burgos et al., 2011; Buseman et al., 2006;

Chen et al., 2020; Degenkolbe et al., 2012; Ibrahim et al., 2011; Nilsson et al., 2012; Tarazona et al., 2015; Vu et al., 2014a; Vu et al., 2014c; Vu et al., 2012; Welti et al., 2002; Zheng et al., 2016). Lipid changes include modifications of various lipids, such as glycerolipid hydrolysis, fatty acid oxidation, head-group acylation, galactolipid galactosylation, and sterol glucosylation.

In the past, analysis of lipids was hampered by the poor sensitivity, resolution, and arduousness of “traditional” analytical technology. Mass spectrometry-based lipidomics offers many advantages in monitoring cold- and wounding-induced lipid changes. Large numbers of lipid molecular species can be analyzed in a relatively short time, with higher sensitivity and resolution than traditional methods. Lipid extracts from cold- or wounding-treated plants can be introduced to a mass spectrometer by direct infusion (Vu et al., 2014c; Vu et al., 2012; Zheng et al., 2016) or by liquid chromatography (Burgos et al., 2011; Degenkolbe et al., 2012; Ibrahim et al., 2011; Nilsson et al., 2012; Tarazona et al., 2015), and both approaches have been utilized in *Arabidopsis* stress studies. Vu, Shiva, and coworkers (Shiva et al., 2013; Vu et al., 2014b) established a comprehensive lipidomic approach including lipid extraction, mass spectral analysis, and data processing. They developed a direct infusion method using electrospray ionization (ESI) triple quadrupole mass spectrometry to analyze plant phospholipids and glycolipids by a series of precursor and neutral loss scans. The method was optimized and applied to detect changes in levels of phospholipids, galactolipids, and others, including oxidized and head group-acylated monogalactosyldiacylglycerols (acMGDGs), under freezing and wounding stress (Vu et al., 2014a; Vu et al., 2012). A direct-infusion MS method with multiple reaction monitoring (MRM) was employed to measure 264 lipid analytes extracted from leaves of *Arabidopsis* subjected to mechanical wounding, providing higher sensitivity and precision for lipid quantification (Vu et al., 2014c). Ryu and Wang (1998) developed an effective approach for

various plant tissues by incorporating hot isopropanol to inhibit lipolytic enzymes and the final solvent proportions were similar to the Bligh and Dyer extraction solvent, and this extraction method is widely applied in plant lipidomics studies in the past 20 years. Recently, a modified method for plant leaf lipid extraction was developed by Shiva (Shiva et al., 2018); this single-step extraction method is efficient, less laborious, and suitable for large-scale lipidomics applications using leaves of various plant species. In 2011, an online data processing tool called LipidomeDB Data Calculation Environment (DCE) was created to process lipidomics data obtained by direct infusion using precursor or neutral loss scanning (Zhou et al., 2011). It provides multiple functions including targeting the peaks of interest in spectral lists, performing isotopic deconvolution, and calculating the amounts of lipid compared to internal standards. A recent update of LipidomeDB DCE extends its functionality to process data acquired in direct-infusion MRM mode, allowing more accurate quantification of a targeted list of lipid compounds in animal and plant samples (Fruehan et al., 2018).

In this chapter, we update and extend the lipidomics approach by using the single-extraction protocol and employing a new MRM list to measure a greater number of analytes (358 lipid molecular species) in a shorter time (8 min) (Song et al., 2020). The direct-infusion MRM method measures selected phospholipids, galactolipids, other glycerolipids, sphingolipids, and sterol derivatives, with diacyl lipids designated by lipid class and both fatty acids at the levels of acyl carbons:double bonds. The intensities of peaks in each sample are compared to those of added internal standards. For lipid data analysis, we use the commercial software MultiQuant 3.0 and the online software LipidomeDB DCE for high-throughput data processing. To assure consistency of data for each analyte throughout long periods of mass spectral data acquisition, a data correction strategy utilizing quality control samples (QC), based on work by Dunn (2011), is

employed in this lipidomic approach (Vu et al., 2014c). Finally, the lipidomic approach was validated in *Arabidopsis* under two stresses (cold stress and mechanical wounding stress) with hundreds of lipid species accurately quantified in extracts of *Arabidopsis* leaves. Cold and wounding result stress-induced lipid profiles exhibiting different patterns.

Materials and Methods

Plant materials and growth conditions

Arabidopsis thaliana accession Columbia-0 (Col-0) seeds were sown in each well in 72-well plug trays (International Greenhouse Company, Danville, IL, USA) filled with loosely packed, Pro-Mix “PGX” soil (Hummert International, Springfield, MO, USA) saturated with 0.01% 20-20-20 fertilizer (Hummert International, Springfield, MO, USA). Trays were put in refrigerator or cold room at 4 °C for 3 days for stratification of seeds and then moved into a growth chamber under a 14/10 h light/dark cycle at 21 °C with 60% humidity. Light intensity was maintained at 90 $\mu\text{mol}/\text{m}^2/\text{s}$ with cool white fluorescent lights. Trays were covered with propagation domes for the first 9 days to maintain high humidity. Trays were watered once every four days. On day 12 after sowing, plants were thinned to one plant per well. On day 20, trays were fertilized again with 0.01% 20-20-20 fertilizer.

Super-cold treatment

For the cold treatment, on day 26, plants were transferred into a cold room with the desired temperature (4 °C) for cold acclimation. The light intensity and day-night cycle in the cold room were set to match the ongoing growing conditions (90 $\mu\text{mol}/\text{m}^2/\text{s}$, 14/10 h light/dark). Plants were acclimated in the cold room for 3 days. On day 29, leaf #5 was harvested from cold-acclimated plants as samples for lipid extraction. Before moving into the freezing chamber, plants in soil were saturated with water prior to adding ice chips. The temperature inside the

freezing chamber was gradually decreased from the cold acclimation point (4 °C) to -2 °C in 1 h and held at -2 °C overnight (16 h, e.g., from 5:00 pm to 9:00 am of next day). After the super-cold treatment, on day 30, plants were moved into a growth chamber at 21 °C for 1 h for postfreezing recovery. As shown in Figure 2-1, plants didn't show an obvious change in appearance during cold acclimation, after the super-cold (-2 °C for 16 h) treatment, or after postfreezing recovery from super-cold treatment. Leaf #5 was cut after postfreezing recovery as plant tissues for lipid extraction in cold group. Leaf numbers were determined as described by Telfer et al. (1997).

Mechanical wounding treatment

For the mechanical wounding treatment, on day 26, a hemostat was used to wound leaf #5 of each plant twice across the mid-vein, about 6 mm apart. After 45 min, leaf #5 of plant in the wounding group was cut for lipid extraction, while leaf #5 from control plants was also harvested for extraction.

All stress conditions are described in Figure 2-2.

Lipid extraction

The harvested leaf tissues were directly dropped into an 8-mL vial containing 1.5 mL of isopropanol with 0.01% BHT preheated on the heating block to 75 °C. Leaf tissue was fully submerged in hot isopropanol and the temperature was maintained at 75 °C for 15 min. After cooling down to room temperature, 4.5 mL of extraction solvent, chloroform–methanol–water (40:55:5, v/v/v), was added into the vial containing leaf tissues. The vials were shaken on an orbital shaker at 100 rpm for 24 h. After being shaken, the extracted leaf tissue was transferred into a new vial using forceps. The leaf tissue in this vial was dried first in a fume hood and then in an oven at 105 °C overnight. The dried leaf tissues were weighed using an AX26 DeltaRange

microbalance (Mettler-Toledo, Greifensee, Switzerland). The original vial, containing the extracted lipids, was stored at -20 °C.

Mass spectrometry analysis

For each analytical sample, 20 µL of internal standard mix (composition is summarized in Table 2-1) was added to a 2-mL amber glass vial. A volume of lipid extract equivalent to 0.085 mg dry tissue mass was added to the to the 2-mL amber glass vial containing IS mix, and the vial was placed in the vacuum concentrator (CentriVap, Labconco Corp., Kansas City, MO) to evaporate the solvent. Finally, 300 µL of MS solvent, chloroform–methanol–300 mM ammonium acetate in water (30:66.5:3.5, v/v/v), was added to the vial to dissolve the IS mix and extracted lipids.

For “standards-only” samples, 20 µL of internal standard mix was added to a 2-mL amber glass vial and evaporated using the nitrogen gas stream evaporator, 300 µL of MS solvent was added to make the IS sample.

QC samples were prepared by pooling 1 mL of lipid extract (of the original 6 mL) from each sample from different treatments to make a QC stock solution. The concentration of the QC stock solution was calculated in terms of the amount of dry leaf mass of sample used to make the combined extract per volume. To make a solution for 100 QC samples, 2 mL of IS mix and a volume of the QC pool equivalent to 8.5 mg of dry leaf mass were combined. Solvent in the QC pool was evaporated using a nitrogen evaporator with water bath set at 40 °C. 30 mL MS solvent was added to redissolve the IS mix and extracted lipids in the QC pool, and 300 µL of QC mixture was transferred into each of 100 2-mL amber glass vials to make 100 working QC samples. Each working QC sample contained the same amount of lipid extract (0.085 mg dry leaf mass equivalent), internal standard mix (20 µL), and MS solvent (300 µL) as each analytical

sample. The working QC samples were labeled and stored at -80 °C and brought to room temperature 1 h before sample injection into MS.

Analytical samples, IS samples, and QC samples for MS analysis were arranged in a VT54 rack as shown in Table S2-1.

Data was acquired in a SCIEX TripleQuad 6500+ mass spectrometer (Sciex, Framingham, MA, USA) equipped with an ESI source operating in direct infusion mode. 75 μL of each sample vial was injected into a LC pump LC-30AD (Shimadzu, Japan) with an autosampler CTC PAL HTC-xt (LEAP). Three sections of PEEKsil tubing (1/32" OD \times 50 μm ID \times 5 cm, 1/32" OD \times 50 μm ID \times 15 cm, 1/32" OD \times 50 μm ID \times 50 cm; IDEX Health & Science, USA) was used to infuse the samples into the mass spectrometer. The pump gradient was 7 min with solvents and flow rates as follows: from 0 to 3 min, methanol at 25 $\mu\text{L}/\text{min}$; from 3 to 5 min, methanol at 70 $\mu\text{L}/\text{min}$; from 5 to 5.6 min, methanol–acetic acid (9:1, v/v) at 70 $\mu\text{L}/\text{min}$; from 5.6 to 7 min, methanol at 25 $\mu\text{L}/\text{min}$. The MS acquired data from 0 to 5 min. Each sample was infused once, and both positive and negative MRM scanning were performed on the same infusion. Positive MRM mode contained 121 transitions and negative MRM mode contained 237 transitions, 27 cycles were performed during the acquisition time. Parameters for each MRM transition, including intact ion m/z (quadrupole 1 or Q1), fragment m/z (second analyzer, that is, quadrupole 3 or Q3), collision energy (CE), and dwell time are listed in Table S2-2. Sample acquisition begins after a 15-s delay. In positive mode, the ion spray voltage is 5500 V, the curtain gas, 35 psi; the source temperature, 100 °C; the ion source gas (GAS1), 45 psi; the ion source gas (GAS2), 45 psi; the declustering potential, 100 V; and the entrance potential, 10 V. In negative mode, the ion spray voltage is -4500 V, the curtain gas, 35 psi; the

source temperature, 100 °C; GAS1, 45 psi; GAS2, 45 psi; the declustering potential, −100 V; and the entrance potential, −10 V.

Data processing and normalization

For raw data from the SCIEX 6500+ mass spectrometer, the software MultiQuant 3.0 (Sciex, Framingham, MA, USA) was used to process and export MRM data (combined and averaged over the infusion) from Analyst to Excel. A quantitation method was established based on a QC sample, which is likely to contain all the analytes of interest. For MRM data acquired by direct infusion, the “Summation” integration algorithm was used and the retention time(s) and summation window(s) were adjusted so that the entire time (5 min) that you would like to sum is covered in all samples. This quantification method was applied to process all the samples. Finally, a text file that can be opened in Excel was exported.

The exported MS data were inserted into an Excel template for MRM data processing at LipidomeDB DCE (<http://lipidome.bcf.ku.edu:8080/Lipidomics/> (Fruehan et al., 2018)). After data calculation in LipidomeDB DCE, the MS data were isotopically deconvoluted and normalized to the internal standards. An output Excel file was generated which included the calculated lipid level of each analyte.

For data normalization, the background intensity in the spectrum of each lipid analyte was first removed by subtracting the average of the appropriate internal standard samples from that tray. An adaptation of the method of Dunn (2011) was used to reduce the variability caused by instability of the instrument and assure the consistency of the data throughout the entire acquisition period (Vu et al., 2014c). The detailed normalization process was described by Song et al. (2020).

The amounts of lipid analyzed per dry mass were calculated by dividing the output of the calculated amounts by 0.085 mg dry tissue mass. The absolute content was in “normalized intensity per extracted dry mass,” where a value of 1 equals the same intensity as 1 nmol of the relevant internal standard(s). The percentage of total normalized signal was calculated by multiplying each value times 100 and dividing by the sum of the normalized analyte values for that sample.

Statistical analysis

Auto-scaling, two-sample t-test, and analysis of variance (ANOVA) with Tukey’s post hoc tests were performed based on absolute content of individual lipid species before and after stress treatment, and the heat maps were produced using utilities at the MetaboAnalyst website (<https://www.metaboanalyst.ca/MetaboAnalyst/home.xhtml>).

Results

MS analysis of lipids in leaf tissues of Arabidopsis

The direct-infusion ESI-MS method with MRM scanning established using the Sciex 6500+ triple quadrupole mass spectrometer provided high resolution and sensitivity for analysis of a wide range of lipid analytes. Each lipid analyte in the MRM list is defined by its mode of analysis (positive or negative) and corresponding adduct, an intact ion formula and mass (m/z), a fragment ion formula and mass (m/z), a collision energy (CE), a lipid name indicating its unique structure, and an arbitrary “lipid number” corresponding the species detected by a particular set of parameters used in MS analysis. Abbreviations used in lipid annotations are summarized in Table 2-2. Each analyte in the MRM list has been annotated based on previous and current MS data acquired by triple quadrupole (QQQ) MS and quadrupole time-of-flight (QTOF) MS analysis. References for molecular species identification are indicated in Table S2-2. MS settings

for each MRM transition including intact ion mass (Q1), fragment ion mass (Q3), CE, and dwell time are also listed in Table S2-2. Some lipid annotations are ambiguous and one MRM transition may correspond to multiple annotations, because direct-infusion MRM mode is unable to differentiate compounds and fragments with the same nominal m/z s. The most likely annotations and alternative annotations detected by the MRM mode are listed in Table S2-2. Compared with the previous direct-infusion method utilizing MRM mode in the triple–quadrupole MS (Vu et al., 2014c), the updated MRM list built in TripleQuad 6500+ MS allows more lipid analytes detecting in negative mode to better characterize the individual acyls on the diacyl species. In addition, the MRM list includes more TAG and DAG species providing more information on storage lipid metabolism in Arabidopsis leaf tissues.

The direct-infusion ESI-MS method, PEEKsil tubing is used to infuse the samples into mass spectrometer to reduce the retention of all lipid compounds in the loop and/or tubing; this reduces carryover between infusions, compared to the regular Peek tubing. Using PEEKsil tubing, most lipid analytes are eluted into the mass spectrometer within 4 min. In the previous MS method (Vu et al., 2014c), separate infusions were made for acquisition in the negative and positive modes and the infusion of each sample took 35 min. Thus, the newly established method has a shorter infusion period with 5-min infusion and 2-min washing. Both positive and negative scanning are operated during the same infusion period, which is possible due to the fast equilibration of the Sciex 6500+ when switching between polarities, in comparison to that on the Water Xevo TQS, which was used previously (Vu et al., 2014c). Twenty-seven cycles of the MRM list are acquired within 5 min. Using the “Summation” integration algorithm, the MRM transition intensity for each lipid analyte is summed throughout the entire acquisition time (5 min). Overall, the infusion and data acquisition method in the current protocol is faster than

previous direct-infusion method, making it preferable for high-throughput analysis of lipid extracts.

To detect lipid changes under different stresses, the goal of the quantification is to compare levels of each lipid analyte in different plant samples, so the consistency the quantification for each lipid analyte throughout long periods of data acquisition is more important than accuracy of absolute level. After data normalization, using an adapted method of Dunn (Dunn et al., 2011; Vu et al., 2014c), the intra-day variability caused by instability of the instrument was significantly reduced. Normalization to QC values increased the analytical precision, as indicated by a decrease in the average coefficient of variation for all lipid analytes from 11.7% before normalization to 10.7% after intra-day correction (Table S2-3).

In total, of the 358 MRM transitions quantified in the updated method, 295 of these lipid analytes met the criteria of the coefficient of variation in the (identical) QC samples less than 30%. Of these, 286 represent unique analytes, whereas 9 represent the same lipid measured with different instrument parameters. All the 286 unique lipid analytes will be further analyzed to investigate the lipid changes in leaf tissues of Col-0 under cold and wounding stresses. Of the 286 lipid analytes, quantification results are presented as three forms: (i) normalized absolute content (normalized mass spectral intensity per mg of dry leaf mass) in Table S2-4; (ii) relative content in percent composition (% of total content) in Table S2-5.

Variations in leaf lipid profile of Arabidopsis in response to super-cold stress

After the cold acclimation or super-cold treatment, overall changes in leaf lipid profile in Col-0 were observed. Of the 286 unique lipid analytes, 196 were significantly different in at least one of the three pairwise comparisons by ANOVA shown in Table S2-6 ($P < 0.01$ after correction for FDR). Tukey's post-hoc test indicates that 155 lipid species were significantly

different in comparisons between both ‘Cold acclimation’ vs ‘Control’ and ‘Super-cold stress, 1 h recovery’ vs ‘Control’ (Table S2-8). The three pairwise comparisons of lipid classes/subclasses by ANOVA were also included in Table S2-6; most lipid classes and sub-classes also were significantly different in at least one of the three pairwise comparisons. The autoscaled lipid levels of individual samples are displayed as a heat map in Figure 2-3. Variation in lipid levels was not only observed in samples subjected to the same treatment, as well as among treatments (control, cold acclimated, and super-cold-treated plants).

Three-day cold acclimation and super-cold treatment after cold acclimation induced similar changes for most lipids in leaves of Col-0, with the most significant changes in lipid levels between cold acclimation and super-cold treatment being increases in DAG (205%, 141%), TAG (416%, 851%), steryl ester (SE) (506%, 484%), LPC (131%, 133%), and LPE (167%, 157%). Decreases in MGDG (30%, 25%), Glycosylceramide (GlcCer) (30%, 23%), PC (14%, 10%), phosphatidylserine (PS) (38%, 31%), ASG (42%, 49%), and TrGDG (35%, 42%) were also observed. Additionally, in response to super-cold stress and cold acclimation, as compared to the control treatment, there is a reduction of lipids with oxidized fatty acyl chains, including ox-acDGDG, ox-DGDG, ox-MGDG, ox-SQDG, ox-PG, ox-PC, and ox-PE.

Among the changes in leaf lipid profile in response to cold acclimation or super-cold stress, the most prominent variation is the large accumulation of storage lipids, especially TAG. In the TAG profile during cold acclimation (Figure 2-4a), most TAG species were greatly induced except for two prokaryotic TAG species containing 34:6 (i.e., 18:3/16:3) moieties which were not significantly changed. After super-cold treatment, there was an overall increase of TAG species except for TAG(16:0/34:6) and TAG(16:0/34:1) compared to standard condition. Some highly unsaturated 54C-TAG species such as TAG(18:2/36:4), TAG(18:1/36:6),

TAG(18:2/36:5), TAG(18:3/36:5), and TAG(18:3/36:6) showed further induction after super-cold treatment at -2 °C compared to their contents after cold acclimation, while less-unsaturated 50C- and 52C-TAG species such as TAG(16:0/34:1), TAG(16:0/34:2), TAG(16:0/34:3), TAG(18:2/34:1), and TAG(18:2/34:2) significantly reduced compared to their levels after cold acclimation.

As shown in Figure 2-4b, an overall increase in the level of DAGs was observed during cold acclimation, the only species which was unchanged after cold acclimation is DAG(18:3/16:3). After super-cold treatment, the absolute contents of most DAG species were obviously reduced compared to their levels after cold acclimation but significantly higher than standard condition. Interestingly, most DAG species showed similar pattern with less unsaturated 50C- and 52C-TAG species including TAG(16:0/34:2), TAG(16:0/34:3), and TAG(18:2/34:1) during cold acclimation and after mild-freezing treatment with strong positive correlation (Pearson's $r > 0.9$, Table S2-8). Another highly correlated cluster in correlation matrix contains highly unsaturated 54C-TAG species including TAG(18:2/36:4), TAG(18:1/36:6), TAG(18:2/36:5), TAG(18:3/36:5), and TAG(18:3/36:6). Under different cold stress at 4 °C or -2 °C, less unsaturated 50C- and 52C-TAGs and highly unsaturated 54C-TAGs seem to be synthesized through different metabolic pathways.

Of the 196 significantly changed lipid analytes after cold acclimation or super-cold treatment, one of the most dramatic changes was fatty acid remodeling of polar glycerolipids. Under cold stress, glycerolipid remodeling occurred in plant cell with a significant increase of acyl chain length and acyl desaturation level. As shown in Figure 2-5, 32C-/34C-/36C-PC and 32C-/34C-PE species were significantly reduced while 40C-PC, 38C-PE, 40C-PE, and 42C-PE species containing VLCFA were increased after the cold acclimation or super-cold treatment. At

the same time, levels of most PC and PE species with at least one saturated FA (16:0, 18:0, or 20:0) were decreased, while levels of highly unsaturated PE species containing 18:3 were increased in response to cold.

Variations in leaf lipid profile of *Arabidopsis* in response to wounding stress

At 45 min after the mechanical wounding treatment, a change in overall leaf lipid profile in Col-0 was observed. The autoscaled lipid levels of individual samples are displayed as a heat map in Figure 2-6a, the variation in lipid levels was not only observed in samples subjected to the same treatment, but also among treatments (control and wounded plants). Of the 286 unique lipid analytes, 232 were significantly different between control group and wounded group by the two-sample t-test ($P < 0.01$ after correction for FDR) with the majority being increased in level (161 lipid analytes increased and 71 analytes reduced in level after wounding), as shown in Table S2-7. A volcano plot was generated from MetaboAnalyst with $P < 0.01$ and a fold change > 1.0 (Figure 2-6b). Comparison results in lipid classes/subclasses before and after wounding treatment were also included in Table S2-7.

Mechanical wounding treatment resulted in large changes in the leaf lipid profile of Col-0 with the greatest changes in the level of lipids with oxidized fatty acyl chains. The accumulation of oxidized lipids mainly occurred in chloroplasts, especially for ox-DGDG (8.5-fold), ox-DGMG (32.3-fold), ox-MGDG (25.4-fold), ox-MGMG (52.7-fold), ox-PG (6.8-fold), and ox-SQDG (4.3-fold). Simultaneously, the precursors of these lipid classes, DGDG, MGDG, PG, and SQDG with normal fatty acyl chains showed obvious reduction. Lipid oxidation was also observed in extra-plastidic lipids, including ox-ASG with a 2.6-fold increase, ox-PC with 79%, and ox-PE with a 16% increase at 45 min after wounding treatment. Head-group acylation of lipids is another remarkable change in leaf lipid composition in response to wounding stress.

There were 7.3-fold and 48.7-fold increases in the level of acMGDG with normal fatty acyl chains and acMGDG with at least one oxidized fatty acyl chains at 45 min after wounding treatment. acDGDG with oxidized fatty acyl chains (ox-acDGDG) and ASG with unoxidized fatty acyl chains showed 20% and 73% increase respectively. Another obvious change in lipid composition is the large production of PA with a 6.9-fold increase along with decreases of the major phospholipids PC and PE (by 25% and 21%) after wounding treatment. Other lipid classes with increased levels in response to wounding include lysophospholipids (5.8-fold increase in LPC and LPE), SG (84% increase), monogalactosylmonoacylglycerol (MGMG) (46% increase), DAG (52% increase), and TAG (2.5-fold increase). Other lipid classes showing decreases after wounding included phosphatidylinositol (PI) (15% decrease) and PS (26% decrease).

Of the 232 significantly changed lipid analytes under wounding stress, most of these lipid species were increased in amount, with the most prominent change being the massive accumulation of lipids with oxidized fatty acyl chains (ox-lipids). The induced lipid analytes include 1 ox-acDGDG species, 48 ox-acMGDG species, 9 ox-DGDG species, 2 ox-DGMG species, 21 ox-MGDG species, 1 ox-MGMG species, 7 ox-PG species, 5 ox-PC species, 4 ox-PE species, 1 ox-SQDG species, and 3 ox-ASG species (Table S2-7). However, the increase of ox-lipids is not uniformly distributed across oxidized lipid classes or among lipid species within the same lipid class. In wounded leaf tissues of Col-0, the most increased lipid analytes were fully oxidized acMGDG, MGDG, and DGDG species with at least two OPDA/dnOPDA, such as acMGDG(18:4-O/34:8-2O) (387-fold increase), acMGDG(18:4-O/36:8-2O) (426-fold increase), MGDG(18:4-O/16:4-O) (2212-fold increase), MGDG(18:4-O/18:4-O) (1636-fold increase), and DGDG(18:4-O/18:4-O) (193-fold increase). In contrast, partially oxidized lipid species with one OPDA or dnOPDA were only slightly induced in level. In the TAG profile after wounding, most

TAG species were slightly or significantly increased, and the most increased species is TAG(18:3/34:6), which showed a 26-fold increase at 45 min after wounding treatment. In the wounding induced DAG profile, there were significant increases of several DAG species with DAG(18:3/16:3) being the most increased. Interestingly, among the induced PA species, PA(18:3/16:3) was increased the most with a 17-fold change in response to wounding. Our data on TAG(18:3/34:6), DAG(18:3/16:3), PA(18:3/16:3) fits with previous discoveries on the induced SFR2 pathway under wounding (Vu et al., 2015).

Discussion

Compared to previous freezing treatment using a lower freezing temperature at $-8\text{ }^{\circ}\text{C}$, which caused visible damage to seedlings to both cold-acclimated and non-acclimated plants (Vu et al., 2022), the freezing temperature at $-2\text{ }^{\circ}\text{C}$ used in this study didn't cause any visible damage to Col-0 in appearance. In Figure 2-1, plants appeared to be very similar before and after cold acclimation and freezing treatment, indicating that $-2\text{ }^{\circ}\text{C}$ does not cause serious damage to acclimated Arabidopsis; therefore, we call it “super cold” or “super-cold treatment”. Previous studies showed that cold temperature of $4\text{ }^{\circ}\text{C}$ induced only minor changes in the leaf lipid profile of Arabidopsis with accumulation of TAGs, DGDGs, PCs, PEs, and decrease of GlcCer, ASG, as well as remodeling of fatty acyl composition in polar membrane lipids (Barrero-Sicilia et al., 2017; Burgos et al., 2011; Chen et al., 2020; Degenkolbe et al., 2012; Hugly & Somerville, 1992; Li et al., 2015; Tarazona et al., 2015; Welti et al., 2002; Zheng et al., 2016). The measured lipid profile after 1 h recovery after $-2\text{ }^{\circ}\text{C}$ was similar to the measured lipid profile after cold acclimation in this study, and similar lipid changes detected under cold in previous studies, but changes under cold treatment are very different from the lipid variation under a colder freezing temperature $-8\text{ }^{\circ}\text{C}$. Therefore, the induced lipids during both cold acclimation and under super-

cold stress are hypothesized to be adaptive and also beneficial to plant survival in a more severe freezing environment, as previously demonstrated for changes occurring at 4 °C (Chen & Thelen, 2013; Zuther et al., 2018).

The comparative analysis of leaf lipid profiles in unstressed, cold acclimated, and super-cold treated Col-0 plants showed that the most prominent change under cold stress is the large accumulation of TAGs. In our study, the increase of TAG content was not uniformly distributed among different species. Levels of TAG species, other than the two prokaryotic species TAG(16:0/34:6) and TAG(18:3/34:6), were all significantly increased during cold acclimation. In addition to the accumulation of TAGs, we also observed an obvious induction of DAGs under cold stress. All DAG species were significantly upregulated under cold except for DAG(18:3/16:3) which was decreased after the super-cold treatment. TAGs are synthesized through the main pathway from *de novo* synthesized DAG or PC. In our study, the most induced DAG species during cold acclimation were DAG(18:1/18:1), DAG(16:0/18:1), DAG(18:0/18:1), DAG(18:1/18:2), and DAG(18:1/18:3) which is consistent with the most increased TAG species TAG(18:2/34:1), TAG(16:0/34:3), and TAG(18:3/34:2). Additionally, these DAG and TAG species were significantly decreased after super-cold treatment and highly correlated with each other in unstressed, cold-acclimated, and super-cold treated plants. Tan et al. found that the conversion of DAG to TAG by *DGAT1* is critical for freezing tolerance of Arabidopsis (Tan et al., 2018). Therefore, we hypothesize that the induced less unsaturated 50C- and 52C-TAGs during cold acclimation derive from the *de novo* biosynthetic pathway catalyzed by *DGAT1*. Some highly unsaturated 54C-TAG species including TAG(18:2/36:4), TAG(18:1/36:6), TAG(18:2/36:5), TAG(18:3/36:5), and TAG(18:3/36:6) showed different patterns with less unsaturated 50C- and 52C-TAGs. They showed further induction after super-cold treatment at -2

°C and highly correlated with each other along the entire cold treatment. Transgenic experiments showed that *Arabidopsis* depleted of *PDAT1* are more susceptible to cold exposure, while *PDAT1* overexpression plants obtained more cold resilience (Demski et al., 2020). All the evidence above suggests that the accumulation of highly unsaturated 54C-TAGs under super-cold stress -2 °C might be derived from 36C-DAG through an alternative pathway which is catalyzed by PDAT1. Previous findings suggested that plants can maintain cell membrane stability and fluidity by converting DAG to TAG in response to freezing (Chen et al., 2015). Environmental stress causes degradation of membrane lipids, leading to accumulation of toxic lipid intermediates (free FA, DAG), TAG functions as a pool to sequester these toxic compounds and prevent cellular damages under unfavorable conditions (Fan et al., 2013; Lippold et al., 2012). It is possible the accumulation of TAG during cold acclimation or -2 °C treatment helps *Arabidopsis* reduce damage caused by toxic free FA.

Plants respond to low temperature by modulating membrane lipid composition. The membrane properties under cold temperature depend on both lipid class composition and fatty acyl composition (acyl chain length and acyl desaturation level) in glycerolipids. In this study, there was a slight increase in the content of DGDG and an obvious reduction of MGDG during the cold acclimation or after the super-cold treatment in Col-0. DGDG shows high propensity for maintenance of bilayer structure of chloroplast membranes while MGDG can form non-bilayer structures under some conditions (Popova & Hinch, 2003; Takahashi et al., 2013). The increased ratio of DGDG/MGDG has been reported before (Degenkolbe et al., 2012; Zheng et al., 2016) in cold-acclimated *Arabidopsis*. We hypothesize that increased proportion of bilayer membrane lipids, e.g. DGDG, in the chloroplast membrane can enhance plant cold or freezing tolerance. In the present study, the two major phospholipid classes PC and PE displayed drastic

changes in their fatty acyl composition during cold acclimation or after the super-cold stress with increased acyl chain length and acyl desaturation level. Most PE species containing 18:3-FA were increased while most PC and PE species containing one saturated FA (16:0, 18:0, or 20:0) were decreased. It is well demonstrated that the increase of FA desaturation level under cold stress makes plants more freezing tolerant (Chen & Thelen, 2013; Hugly & Somerville, 1992; Matos et al., 2007). Another remarkable change in FA composition of PC, PE, and PG is the elongation of fatty acyl chains. In response to cold stress, levels of most 32C and 34C PC, PE, and PG species with at least one 16C fatty acid chain declined while levels of 40C PC, 38C, 40C, and 42C PE species containing one VLCFA as well as 36C PG species were increased. Recently, very long-chain fatty acids VLCFAs have been reported to contribute to plant chilling tolerance. Overexpression of *KCSI* in *Arabidopsis* enhanced VLCFAs contents and chilling tolerance (Chen et al., 2020). Studies on *fab1* mutants indicated that high levels of high-melting-point (HMP)-PG (PG(16:0/16:0)) caused deficient photosynthesis and eventual death of plants under chilling stress (Gao et al., 2020). The fluid state of plasma membrane or chloroplast membrane is a structural asset for their normal functions and low temperature results in the transition from a fluid state to a rigid gel phase (Chen & Thelen, 2013; Harayama & Riezman, 2018; Miquel et al., 1993). The increased acyl chain length and acyl chain desaturation level of major phospholipids in plasma membrane and chloroplast membrane contribute to the ability of *Arabidopsis* to adjust membrane fluidity in response to low temperature.

Sphingolipids and sterols are essential components of plasma membrane. They are not uniformly distributed within the plasma membrane and often segregate to form microdomains or lipid rafts which function in signal transduction and membrane trafficking (Cacas et al., 2012). In Col-0, there was an overall reduction in the contents of four GlcCer species during the cold

acclimation or after the super-cold treatment, which is consistent with previous observation on GlcCer during cold acclimation (Degenkolbe et al., 2012; Tarazona et al., 2015). Arabidopsis mutants deficient in sphingoid long-chain base $\Delta 8$ desaturase became more cold-sensitive with impaired growth and survival under low temperature, indicating the role of specific GlcCer species (d18:1 $\Delta 8$ *cis/trans* and t18:1 $\Delta 8$ *cis*) for cold tolerance (Chen et al., 2012). The decrease of GlcCer is hypothesized contribute to a greater hydration of the plasma membrane that could, in turn, increase membrane stability during cold stress. Sphingolipids are reported to function as signaling molecules in cold response, particularly ceramides, long chain base (LCB), and their phosphorylated forms (Ali et al., 2018; Huby et al., 2020). Little is known about the function of GlcCer in plant stress responses, we cannot assign specific roles to these molecules for freezing tolerance.

Our lipidomics study revealed a significant reduction in the total content of ASG and SG, along with an obvious induction in the content of SE during cold acclimation. After the super-cold treatment, ASG went down while SG and SE went up. The changes in sterol profiles in the cold are inconsistent with previous publications showing that in 21-day old Arabidopsis, ASGs largely increased after a 10-day cold acclimation at 6 °C (Tarazona et al., 2015). Uemura et al. explored lipid profiles and freezing tolerance in summer oat and winter rye and found that ASG level was higher in the less freeze-resistant summer oat compared to winter rye, so they hypothesized that ASG leads to poorer outcome in freezing tolerance due to its propensity to form hexagonal phase structure (Uemura & Steponkus, 1994). These discoveries are consistent with our lipidomics results on ASG profiles from leaves of plants under cold acclimated or super-cold treatment, indicating ASG might be negatively correlated with plant freezing tolerance.

Upon mechanical wounding, the major change in leaf lipid profile in Col-0 is the large production of plastidic lipids with oxidized fatty acyl chains. The rapid accumulation of esterified oxylipins has been well reported in previous lipidomics study on wounded Arabidopsis (Buseman et al., 2006; Ibrahim et al., 2011; Vu et al., 2014a; Vu et al., 2014b; Vu et al., 2012). It is known that mechanical wounding can induce the oxylipin biosynthetic pathway, generating esterified, as well as free, oxylipin compounds, which have direct functions such as antifungal and antibacterial activities or indirect functions like modulation of gene expression (Genva et al., 2019). In the oxidized lipid profile at 45 min after wounding treatment, the most induced lipid species were fully oxidized lipids with at least two OPDA or dnOPDA chains esterified in glycerolipids. A previous time-course wounding experiment showed that fully oxidized species were formed most quickly and other galactolipid species with a mixture of oxidized and normal chains were formed more slowly (levels were higher at 6 h after wounding) (Buseman et al., 2006; Vu et al., 2014c; Vu et al., 2012). Therefore, it was hypothesized that there is a preference for multiple oxidations of acyl chains on a single molecule, leading to the huge and rapid production of fully oxidized galactolipid species after wounding treatment. Esterified OPDA or dnOPDA have indirect or direct functions in plant wounding response. They might act as a pool of free OPDA or dnOPDA that could be released when necessary, the released OPDA could be used as a substrate for JA production, which is an essential hormone in defense mechanisms (Chini et al., 2007; Santner & Estelle, 2007). Moreover, they *in vitro* studies showed that some esterified OPDA such as arabidopside A, E, G have antifungal and antibacterial activities (Andersson et al., 2006; Kourtchenko et al., 2007; Pedras & To, 2017). The accumulation of arabidopsides can help Arabidopsis prevent microbe infection in wounding site, reducing further damages after wounding.

In addition to fatty acid oxidation, head-group acylation is another major process changing the leaf lipid profile under wounding stress. The total content of acMGDGs increased 42-fold at 45 min after wounding treatment in Col-0, indicating many fatty acyl chains are transferred to the 6-position on the galactose of MGDG. Nilsson and coworkers discovered that Acylated Galactolipid Associated Phospholipase 1 (AGAP1) is responsible for formation of head group-acylated lipids in the chloroplast including acMGDG, acDGDG, and acPG (Nilsson et al., 2015). Still, the biological functions of AGAP1 and head group-acylated chloroplast lipids remain elusive.

Wounding stress caused membrane lipid remodeling, the most significant changes were phospholipid hydrolytic reactions producing PA and lysophospholipids (LPLs). There were significant increases of LPC, LPE, as well as PA at 45 min after wounding in Col-0, which is in agreement with earlier lipidomics studies on Arabidopsis leaves (Vu et al., 2015; Vu et al., 2014c). Phospholipase A (PLA) and phospholipase D (PLD) have been shown to be responsible for the production of lyso-phospholipids and PA under wounding stress, respectively (Yang et al., 2012; Zien et al., 2001). PA, LPLs, and free fatty acid generated after phospholipid hydrolysis are signaling molecules which can bind to proteins to regulate their activity and localization, or can influence the membrane recruitment of proteins, or participate in phytohormone signaling pathways, thus, affect plant responses upon wounding (Hou et al., 2016; Kim & Wang, 2020; Okazaki & Saito, 2014). The induction of PAs and LPLs in Col-0 suggests phospholipid hydrolysis might be a defense process in Arabidopsis under wounding stress.

Following wounding, TAG(18:3/34:6) was the most induced species in TAG profile. The large production of TAG(18:3/34:6) was consistent with the massive accumulation of DAG(18:3/16:3) and PA(18:3/16:3), which were the most induced species in the DAG and PA

profile, respectively. It is known that the activated SFR2 enhances the processive galactosylation of galactolipids, producing TrGDG and DAG, which can be converted into TAG by an acyltransferase (Moellering et al., 2010; Roston et al., 2014) or converted to PA by a DAG kinase (Muthan et al., 2013). The co-occurrence of TAG(18:3/34:6), DAG(18:3/16:3), and PA(18:3/16:3) in our lipidomics data support the hypothesis that wounding stress activates the SFR2 pathway, possibly leading to better performance of plants in response to wounding.

Sterol lipid remodeling was observed in Col-0 with a significant increase of SGs and ASGs after wounding, which is consistent with a previous lipidomics study (Vu et al., 2015; Vu et al., 2014c). The biosynthetic pathway of conjugated sterol has been characterized in Arabidopsis in which SG and ASG are synthesized through a pathway with reactions catalyzed by UDP-glucose:sterol glycosyltransferase (SGT) and steryl glycoside acyltransferase (SGAT) (Stucky et al., 2015). With regard to SG and ASG, transgenic Arabidopsis plants overexpressing *SGT* displayed increased salt, heat, cold tolerance, and enhanced resistance against the insect *Spodoptera litura* (Mishra et al., 2013; Saema et al., 2016). The increase of SG, ASG may affect biophysical properties and biological functions of cell membranes, enhancing plant resistance to pathogen or insect infection in the wounding site. The biological basis underlying the role of SG and ASG in plant stress is just starting to be uncovered.

In conclusion, we established a lipidomics approach using the MRM mode on an electrospray ionization triple quadrupole mass spectrometer (Sciex 6500+), quantifying a wide range of lipid analytes. The optimized approach includes an efficient, less laborious single-extraction method, MS data acquisition in a direct-infusion MRM mode, and high-throughput data processing utilizing MultiQuant and LipidomeDB DCE. The lipidomics approach is rapid, accurate, and highly replicated, providing large amounts of information about lipid dynamics in

plant leaf tissues under various stresses. This approach was validated in Arabidopsis accession Col-0 under cold stress and mechanical wounding stress with hundreds of lipid species (358 analytes) accurately quantified in extracts of leaves. The lipidomics study showed the cold and mechanical wounding stresses resulted in different patterns of stress-induced lipids and revealed possible roles of specific lipids and their biosynthetic pathways in plant stress responses.

Figures

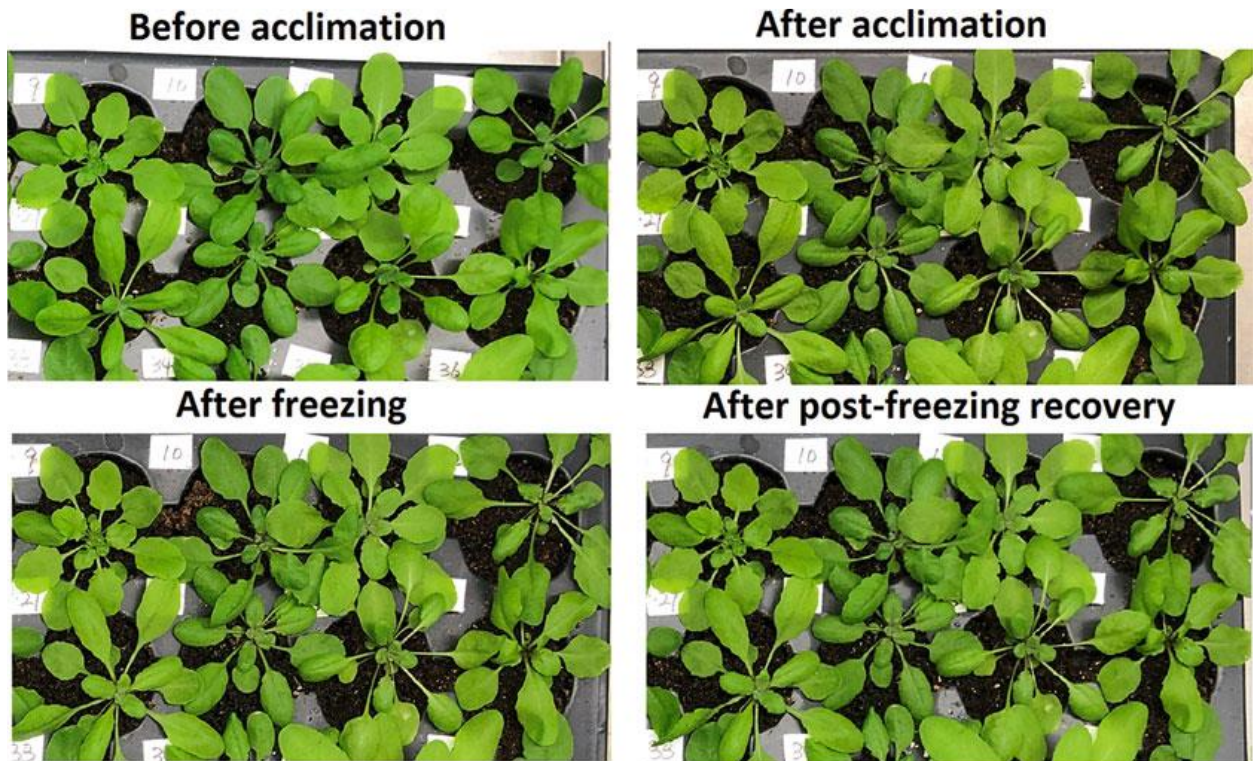


Figure 2-1. Plant appearance before cold acclimation, after acclimation, after super-cold treatment, and after postfreezing recovery

Photographs depict the same Col-0 plants at different time points: untreated (before cold acclimation) grown at 21 °C, after 3-day cold acclimation at 4 °C, after 16 h super-cold treatment at -2 °C, and after 1 h post-freezing recovery at 21 °C.

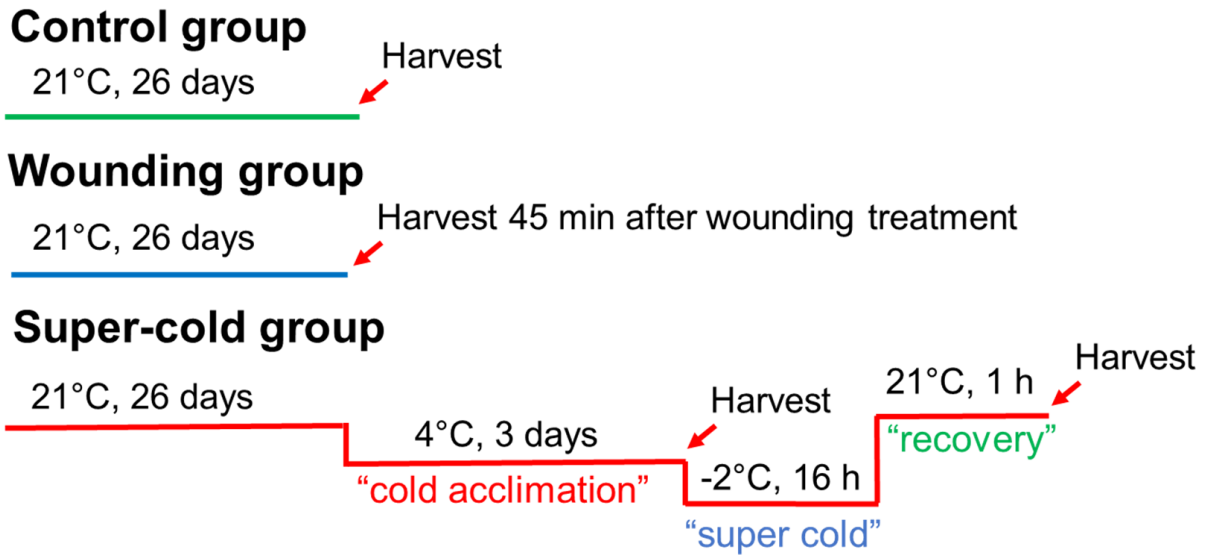


Figure 2-2. Stress treatment experimental design

Plants entered the stress treatment protocols on day 26. Lines of different colors represent different stress treatments (green: unstressed plants; blue: wounded plants; red: cold-treated plants). The red arrows indicate the time points for leaf harvesting. The harvested leaves are plant samples for lipid extraction in four groups: control group (no treatment on day 26); wounding group (45 min after mechanical wounding on day 26); cold acclimation group (26 days at 21 °C, 3 days at 4 °C); and super-cold group (26 days at 21 °C, 3 days at 4 °C, 16 h at -2 °C, 1 h at 21 °C).

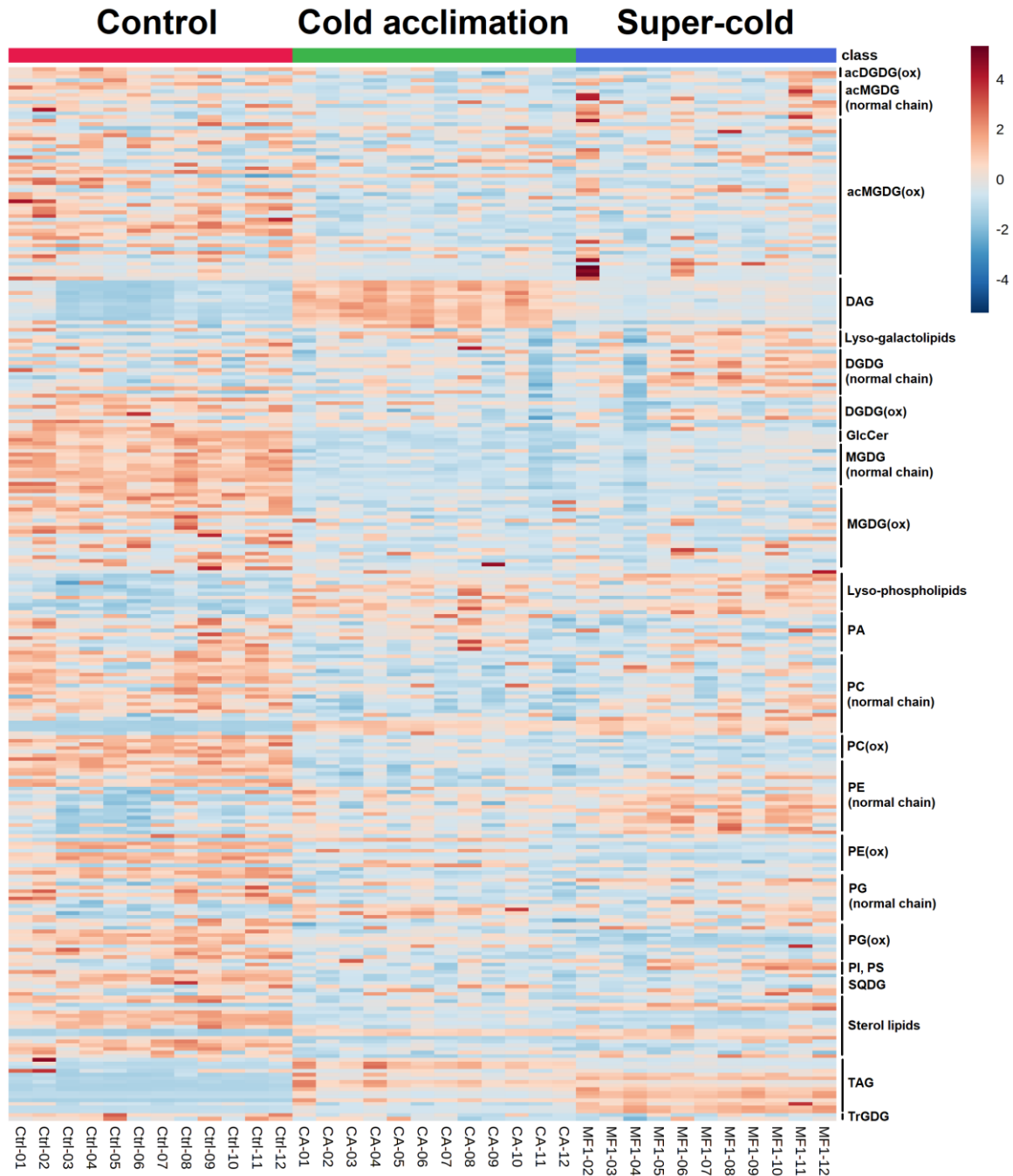


Figure 2-3. Heatmap of autoscaled lipid levels in unstressed, cold acclimated, and super-cold-treated samples

Note: 286 analytes are shown in 36 samples. Each sample represents one plant under control (unstressed) (n = 12), cold acclimation (n=12), or super-cold treatment (n = 12).

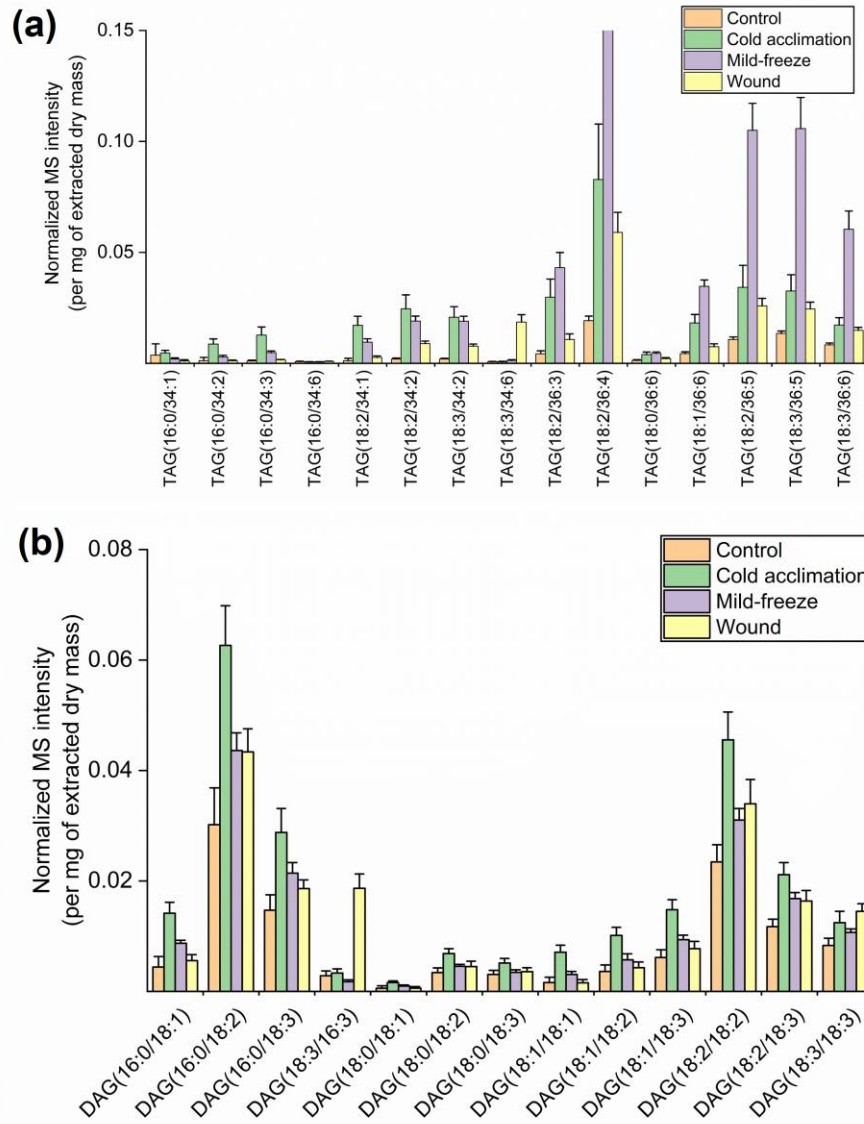


Figure 2-4. Changes in TAG and DAG profiles in leaf tissues of Col-0 under various stresses

Absolute contents (normalized MS intensity per mg dry mass) of individual TAG (a) and DAG (b) species in Col-0 under standard condition (control), after cold acclimation (4 °C), after super-cold (mild-freeze) treatment (-2 °C), and 45 min after mechanical wounding treatment.

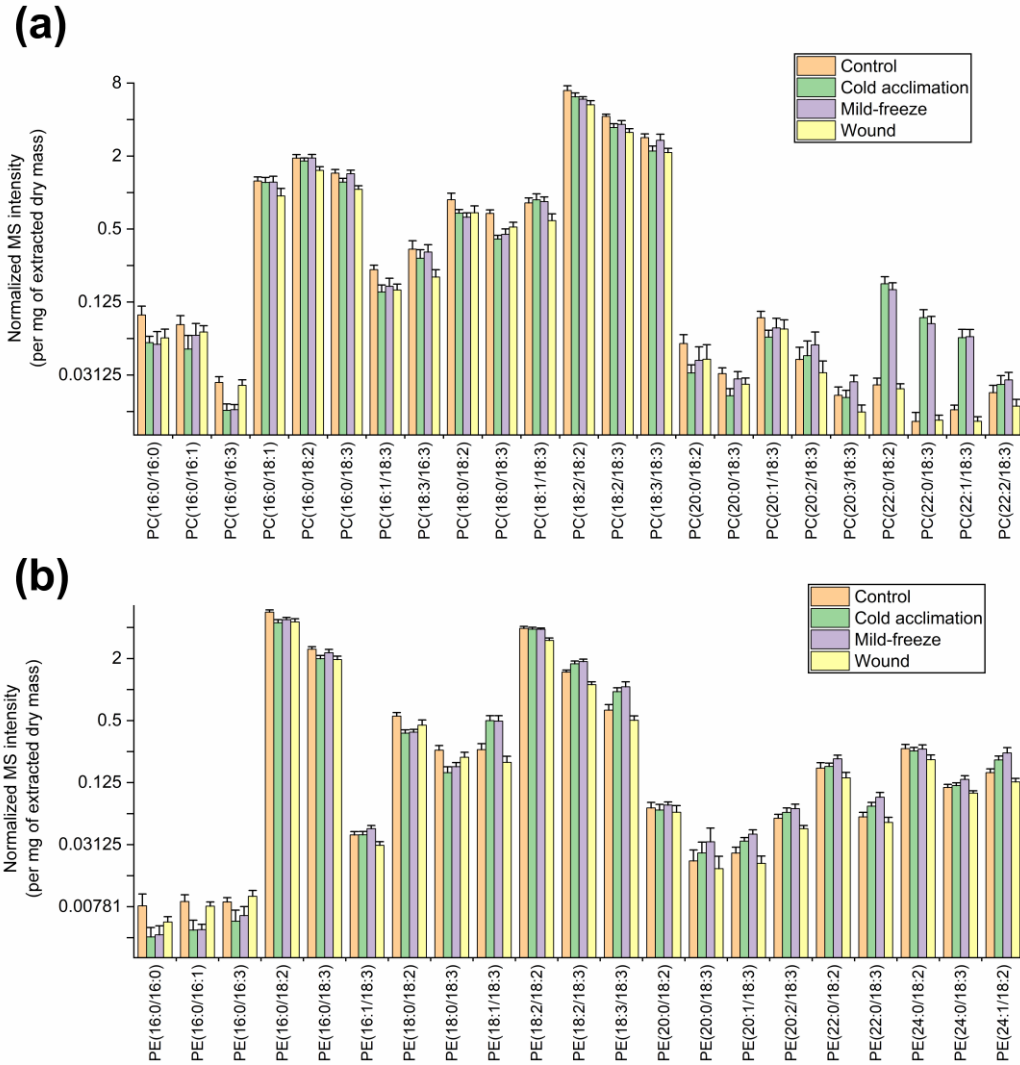


Figure 2-5. Changes in PC and PE profiles in leaf tissues of Col-0 under various stresses

Absolute contents (normalized MS intensity per mg dry mass) of individual PC (a) and PE (b) species in Col-0 under standard condition (control), after cold acclimation (4 °C), after super-cold (mild-freeze) treatment (-2 °C), and 45 min after mechanical wounding treatment.

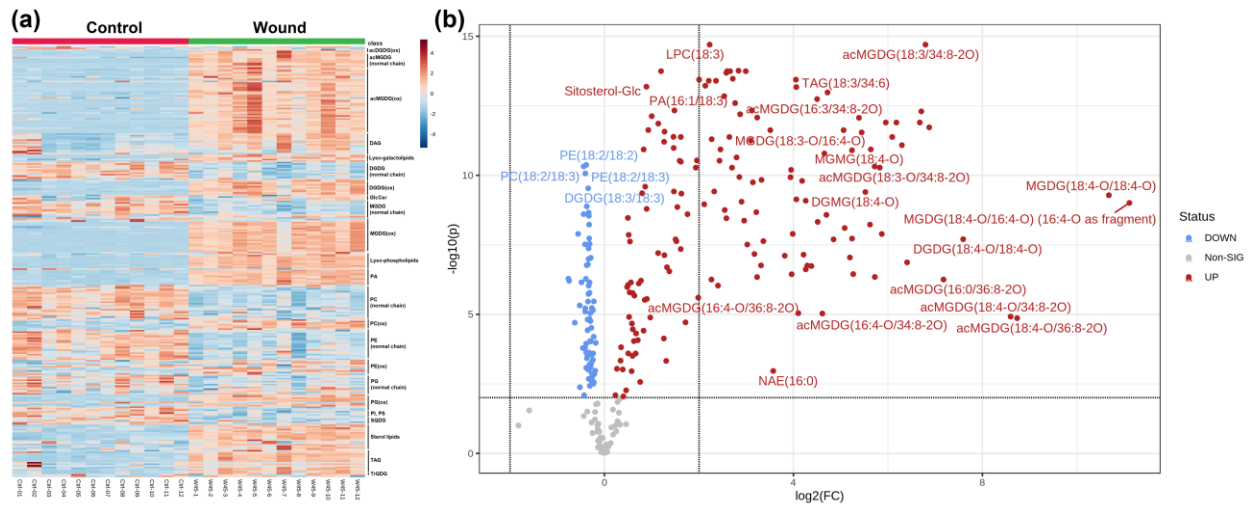


Figure 2-6. Significantly changed lipid analytes after mechanical wounding treatment

(a) Volcano plot of 286 lipid analytes of controls ($n = 12$) and wounded plants ($n = 12$), revealing 161 lipid species upregulated and 71 downregulated with a p -value < 0.01 and a fold change > 1.0 . X-axis corresponds to $\log_2(\text{fold change})$ and y-axis to $-\log_{10}(p\text{-value})$. (b) Heatmap of autoscaled lipid levels in unstressed and wounded samples. Note: 287 analytes are shown in 24 samples. Each sample represents one plant under control (unstressed) or mechanical wounding treatment ($n = 12$ for each).

Tables

Table 2-1. Internal standards employed in lipid profiling

Internal standards with individual acyl chains specified	Amount added (nmol) per 0.085 mg dry mass of leaf tissue
DGDG(16:0/18:0)	0.177
DGDG(18:0/18:0)	0.524
LPA(14:0)	0.1
LPA(18:0)	0.1
LPC(13:0)	0.2
LPC(19:0)	0.2
LPE(14:0)	0.1
LPE(18:0)	0.1
LPG(14:0)	0.1
LPG(18:0)	0.1
MGDG(16:0/18:0)	0.556
MGDG(18:0/18:0)	0.469
PA(14:0/14:0)	0.1
PA(20:0/20:0) (diphytanoyl)	0.1
PC(12:0/12:0)	0.2
PC(24:1/24:1)	0.2
PE(12:0/12:0)	0.1
PE(20:0/20:0) (diphytanoyl)	0.1
PG(14:0/14:0)	0.1
PG(20:0/20:0) (diphytanoyl)	0.1
PI(16:0/18:0)	0.096
PI(18:0/18:0)	0.096
PS(14:0/14:0)	0.067
PS(20:0/20:0) (diphytanoyl)	0.067
TAG(51:3)	0.052

Table 2-2. Lipid name abbreviations

Lipid class and subclass	Example abbreviation	Abbreviation explanation
Monoacyl glycerophospholipids		Acyl carbons: acyl carbon–carbon double bonds
Digalactosylmonoacylglycerol	DGMG(18:3)	
Lysophosphatidic acid	LPA(18:0)	
Lysophosphatidylcholine	LPC(18:3)	
Lysophosphatidylethanolamine	LPE(18:3)	
Lysophosphatidylinositol	LPI(18:3)	
Monogalactosylmonoacylglycerol	MGMG(18:3)	
Polar diacyl glycerophospholipids		Acyl carbons: carbon–carbon double bonds for one acyl chain/acyl carbons: carbon–carbon double bonds for the other acyl chain)
Acylated digalactosyldiacylglycerol	acDGDG(18:4-O/34:8-2O)	Head-group acyl carbons: head-group acyl carbon–carbon double bonds/total sn-1,2 acyl carbons: total sn-1,2 carbon–carbon double bonds
Acylated monogalactosyldiacylglycerol	acMGDG(18:4-O/34:8-2O)	Acyl carbons: carbon–carbon double bonds for one acyl chain/total acyl carbons: total carbon–carbon double bonds for the other two acyl chains combined
Acylated phosphatidylglycerol	acPG(16:1/36:8-2O)	
Phosphatidic acid	PA(18:3/18:3)	
Phosphatidylcholine	PC(18:3/18:3)	
Phosphatidylethanolamine	PE(18:3/18:3)	
Phosphatidylglycerol	PG(18:3/16:1)	
Phosphatidylinositol	PI(16:0/18:3)	
Phosphatidylserine	PS(16:0/18:3)	
Digalactosyldiacylglycerol	DGDG(18:3/16:3)	
<i>N</i> -acyl phosphatidylethanolamine	NAPE(18:3/36:6)	Head-group acyl carbons: carbon–carbon double bonds for one acyl chain/total acyl carbons: total carbon–carbon double bonds for the other two acyl chains combined

Monogalactosyldiacylglycerol	MGDG(18:3/16:3)	
Sulfoquinovosyldiacylglycerol	SQDG(16:0/18:3)	
Trigalactosyldiacylglycerol	TrGDG(18:3/16:3)	
Neutral glycerolipids		
Diacylglycerol	DAG(18:3/18:3)	Acyl carbons: carbon–carbon double bonds for one acyl chain/acyl carbons: carbon–carbon double bonds for the other acyl chain)
Triacylglycerol	TAG(18:3/36:6)	Acyl carbons: carbon–carbon double bonds for one acyl chain/total acyl carbons: total carbon–carbon double bonds for the other two acyl chains combined
Sphingolipids		
Glucosylceramide	GlcCer(34:1)-2	Carbons: carbon–carbon double bonds of sphingoid base + fatty amide)-number of hydroxyl groups in base plus acyl chain
Sterol conjugates		
Acylated sterol glucoside	Sitosterol-Glc(18:3)	
Sterol ester	Sitosterol(18:3)	
Sterol glucoside	Sitosterol-Glc	
Fatty amides		
<i>N</i> -acyl ethanolamine	NAE(16:0)	Acyl carbons: acyl carbon–carbon double bonds

Double bonds can also indicate double bond equivalents, such as rings. ‘Extra’ oxygen atoms in acyl chains are indicated by a ‘-O’; for example, oxophytodienoic acid is 18:4-O to indicate four double bond equivalents and one ‘extra’ oxygen atom.

Note: sn-1 and sn-2 positions of acyl chains on the glycerol were not determined.

References

- Ali, U., Li, H., Wang, X., & Guo, L. (2018). Emerging Roles of Sphingolipid Signaling in Plant Response to Biotic and Abiotic Stresses. *Molecular Plant*, *11*, 1328–1343.
- Andersson, M. X., Hamberg, M., Kourtchenko, O., Brunnström, A., McPhail, K. L., Gerwick, W. H., Göbel, C., Feussner, I., & Ellerström, M. (2006). Oxylipin profiling of the hypersensitive response in *Arabidopsis thaliana*. Formation of a novel oxo-phytodienoic acid-containing galactolipid, arabidopside E. *The Journal of Biological Chemistry*, *281*, 31528–31537.
- Barrero-Sicilia, C., Silvestre, S., Haslam, R. P., & Michaelson, L. V. (2017). Lipid remodelling: Unravelling the response to cold stress in *Arabidopsis* and its extremophile relative *Eutrema salsugineum*. *Plant Science: An International Journal of Experimental Plant Biology*, *263*, 194–200.
- Burgos, A., Szymanski, J., Seiwert, B., Degenkolbe, T., Hannah, M. A., Giavalisco, P., & Willmitzer, L. (2011). Analysis of short-term changes in the *Arabidopsis thaliana* glycerolipidome in response to temperature and light. *The Plant Journal: For Cell and Molecular Biology*, *66*, 656–668.
- Buseman, C. M., Tamura, P., Sparks, A. A., Baughman, E. J., Maatta, S., Zhao, J., Roth, M. R., Esch, S. W., Shah, J., Williams, T. D., & Welti, R. (2006). Wounding stimulates the accumulation of glycerolipids containing oxophytodienoic acid and dinor-oxophytodienoic acid in *Arabidopsis* leaves. *Plant Physiology*, *142*, 28–39.
- Cacas, J.-L., Furt, F., Le Guédard, M., Schmitter, J.-M., Buré, C., Gerbeau-Pissot, P., Moreau, P., Bessoule, J.-J., Simon-Plas, F., & Mongrand, S. (2012). Lipids of plant membrane rafts. *Progress in Lipid Research*, *51*, 272–299.
- Chen, L., Hu, W., Mishra, N., Wei, J., Lu, H., Hou, Y., Qiu, X., Yu, S., Wang, C., Zhang, H., Cai, Y., Sun, C., & Shen, G. (2020). AKR2A interacts with KCS1 to improve VLCFAs contents and chilling tolerance of *Arabidopsis thaliana*. *The Plant Journal: For Cell and Molecular Biology*, *103*, 1575–1589.
- Chen, Ming, Markham, J. E., & Cahoon, E. B. (2012). Sphingolipid $\Delta 8$ unsaturation is important for glucosylceramide biosynthesis and low-temperature performance in *Arabidopsis*. *The Plant Journal: For Cell and Molecular Biology*, *69*, 769–781.
- Chen, Mingjie, & Thelen, J. J. (2013). ACYL-LIPID DESATURASE2 is required for chilling and freezing tolerance in *Arabidopsis*. *The Plant Cell*, *25*, 1430–1444.
- Chen, Q.-F., Xu, L., Tan, W.-J., Chen, L., Qi, H., Xie, L.-J., Chen, M.-X., Liu, B.-Y., Yu, L.-J., Yao, N., Zhang, J.-H., Shu, W., & Xiao, S. (2015). Disruption of the *Arabidopsis* Defense Regulator Genes SAG101, EDS1, and PAD4 Confers Enhanced Freezing Tolerance. *Molecular Plant*, *8*, 1536–1549.

- Chini, A., Fonseca, S., Fernández, G., Adie, B., Chico, J. M., Lorenzo, O., García-Casado, G., López-Vidriero, I., Lozano, F. M., Ponce, M. R., Micol, J. L., & Solano, R. (2007). The JAZ family of repressors is the missing link in jasmonate signalling. *Nature*, *448*, 666–671.
- Degenkolbe, T., Giavalisco, P., Zuther, E., Seiwert, B., Hinch, D. K., & Willmitzer, L. (2012). Differential remodeling of the lipidome during cold acclimation in natural accessions of *Arabidopsis thaliana*. *The Plant Journal: For Cell and Molecular Biology*, *72*, 972–982.
- Demski, K., Łosiewska, A., Jasieniecka-Gazarkiewicz, K., Klińska, S., & Banaś, A. (2020). Phospholipid:Diacylglycerol Acyltransferase1 Overexpression Delays Senescence and Enhances Post-heat and Cold Exposure Fitness. *Frontiers in Plant Science*, *11*, 611897.
- Dunn, W. B., Broadhurst, D., Begley, P., Zelena, E., Francis-McIntyre, S., Anderson, N., Brown, M., Knowles, J. D., Halsall, A., Haselden, J. N., Nicholls, A. W., Wilson, I. D., Kell, D. B., Goodacre, R., & Human Serum Metabolome (HUSERMET) Consortium. (2011). Procedures for large-scale metabolic profiling of serum and plasma using gas chromatography and liquid chromatography coupled to mass spectrometry. *Nature Protocols*, *6*, 1060–1083.
- Fan, J., Yan, C., & Xu, C. (2013). Phospholipid:diacylglycerol acyltransferase-mediated triacylglycerol biosynthesis is crucial for protection against fatty acid-induced cell death in growing tissues of *Arabidopsis*. *The Plant Journal*, *76*, 930–942.
- Fruehan, C., Johnson, D., & Welti, R. (2018). LipidomeDB Data Calculation Environment Has Been Updated to Process Direct-Infusion Multiple Reaction Monitoring Data. *Lipids*, *53*, 1019–1020.
- Gao, J., Lunn, D., Wallis, J. G., & Browse, J. (2020). Phosphatidylglycerol Composition Is Central to Chilling Damage in the *Arabidopsis fab1* Mutant. *Plant Physiology*, *184*, 1717–1730.
- Genva, M., Obounou Akong, F., Andersson, M. X., Deleu, M., Lins, L., & Fauconnier, M.-L. (2019). New insights into the biosynthesis of esterified oxylipins and their involvement in plant defense and developmental mechanisms. *Phytochemistry Reviews*, *18*, 343–358.
- Gilmour, S. J., Hajela, R. K., & Thomashow, M. F. (1988). Cold Acclimation in *Arabidopsis thaliana*. *Plant Physiology*, *87*, 745–750.
- Harayama, T., & Riezman, H. (2018). Understanding the diversity of membrane lipid composition. *Nature Reviews. Molecular Cell Biology*, *19*, 281–296.
- Hou, Q., Ufer, G., & Bartels, D. (2016). Lipid signalling in plant responses to abiotic stress: Lipid signalling in plant responses to abiotic stress. *Plant, Cell & Environment*, *39*, 1029–1048.

- Huby, E., Napier, J. A., Baillieul, F., Michaelson, L. V., & Dhondt - Cordelier, S. (2020). Sphingolipids: Towards an integrated view of metabolism during the plant stress response. *New Phytologist*, 225, 659 – 670.
- Hugly, S., & Somerville, C. (1992). A role for membrane lipid polyunsaturation in chloroplast biogenesis at low temperature. *Plant Physiology*, 99, 197–202.
- Ibrahim, A., Schütz, A.-L., Galano, J.-M., Herrfurth, C., Feussner, K., Durand, T., Brodhun, F., & Feussner, I. (2011). The Alphabet of Galactolipids in *Arabidopsis thaliana*. *Frontiers in Plant Science*, 2, 95.
- Kim, S.-C., & Wang, X. (2020). Phosphatidic acid: An emerging versatile class of cellular mediators. *Essays in Biochemistry*, 64, 533–546.
- Kourtchenko, O., Andersson, M. X., Hamberg, M., Brunnström, A., Göbel, C., McPhail, K. L., Gerwick, W. H., Feussner, I., & Ellerström, M. (2007). Oxo-phytodienoic acid-containing galactolipids in *Arabidopsis*: Jasmonate signaling dependence. *Plant Physiology*, 145, 1658–1669.
- Li, Q., Zheng, Q., Shen, W., Cram, D., Fowler, D. B., Wei, Y., & Zou, J. (2015). Understanding the Biochemical Basis of Temperature-Induced Lipid Pathway Adjustments in Plants. *The Plant Cell*, 27, 86–103.
- Lippold, F., vom Dorp, K., Abraham, M., Hölzl, G., Wewer, V., Yilmaz, J. L., Lager, I., Montandon, C., Besagni, C., Kessler, F., Stymne, S., & Dörmann, P. (2012). Fatty acid phytyl ester synthesis in chloroplasts of *Arabidopsis*. *The Plant Cell*, 24, 2001–2014.
- Matos, A. R., Hourton-Cabassa, C., Çiçek, D., Rezé, N., Arrabaça, J. D., Zachowski, A., & Moreau, F. (2007). Alternative oxidase involvement in cold stress response of *Arabidopsis thaliana* fad2 and FAD3+ cell suspensions altered in membrane lipid composition. *Plant & Cell Physiology*, 48, 856–865.
- Miquel, M., James, D., Dooner, H., & Browse, J. (1993). *Arabidopsis* requires polyunsaturated lipids for low-temperature survival. *Proceedings of the National Academy of Sciences of the United States of America*, 90, 6208–6212.
- Mishra, M. K., Chaturvedi, P., Singh, R., Singh, G., Sharma, L. K., Pandey, V., Kumari, N., & Misra, P. (2013). Overexpression of WsSGTL1 gene of *Withania somnifera* enhances salt tolerance, heat tolerance and cold acclimation ability in transgenic *Arabidopsis* plants. *PLoS One*, 8, e63064.
- Moellering, E. R., Muthan, B., & Benning, C. (2010). Freezing Tolerance in Plants Requires Lipid Remodeling at the Outer Chloroplast Membrane. *Science*, 330, 226–228.
- Muthan, B., Roston, R. L., Froehlich, J. E., & Benning, C. (2013). Probing *Arabidopsis* chloroplast diacylglycerol pools by selectively targeting bacterial diacylglycerol kinase to suborganelle membranes. *Plant Physiology*, 163, 61–74.

- Nilsson, A. K., Fahlberg, P., Ellerström, M., & Andersson, M. X. (2012). Oxo-phytodienoic acid (OPDA) is formed on fatty acids esterified to galactolipids after tissue disruption in *Arabidopsis thaliana*. *FEBS Letters*, *586*, 2483–2487.
- Nilsson, A. K., Johansson, O. N., Fahlberg, P., Kommuri, M., Töpel, M., Bodin, L. J., Sikora, P., Modarres, M., Ekengren, S., Nguyen, C. T., Farmer, E. E., Olsson, O., Ellerström, M., & Andersson, M. X. (2015). Acylated monogalactosyl diacylglycerol: Prevalence in the plant kingdom and identification of an enzyme catalyzing galactolipid head group acylation in *Arabidopsis thaliana*. *The Plant Journal: For Cell and Molecular Biology*, *84*, 1152–1166.
- Okazaki, Y., & Saito, K. (2014). Roles of lipids as signaling molecules and mitigators during stress response in plants. *The Plant Journal*, *79*, 584–596.
- Pedras, M. S. C., & To, Q. H. (2017). Defense and signalling metabolites of the crucifer *Erucastrum canariense*: Synchronized abiotic induction of phytoalexins and galactoxylinins. *Phytochemistry*, *139*, 18–24.
- Popova, A. V., & Hinch, D. K. (2003). Intermolecular interactions in dry and rehydrated pure and mixed bilayers of phosphatidylcholine and digalactosyldiacylglycerol: A Fourier transform infrared spectroscopy study. *Biophysical Journal*, *85*, 1682–1690.
- Roston, R. L., Wang, K., Kuhn, L. A., & Benning, C. (2014). Structural Determinants Allowing Transferase Activity in SENSITIVE TO FREEZING 2, Classified as a Family I Glycosyl Hydrolase. *Journal of Biological Chemistry*, *289*, 26089–26106.
- Ryu, S. B., & Wang, X. (1998). Increase in free linolenic and linoleic acids associated with phospholipase D-mediated hydrolysis of phospholipids in wounded castor bean leaves. *Biochimica Et Biophysica Acta*, *1393*, 193–202.
- Saema, S., Rahman, L. U., Singh, R., Niranjana, A., Ahmad, I. Z., & Misra, P. (2016). Ectopic overexpression of WsSGTL1, a sterol glucosyltransferase gene in *Withania somnifera*, promotes growth, enhances glycowithanolide and provides tolerance to abiotic and biotic stresses. *Plant Cell Reports*, *35*, 195–211.
- Santner, A., & Estelle, M. (2007). The JAZ proteins link jasmonate perception with transcriptional changes. *The Plant Cell*, *19*, 3839–3842.
- Shiva, S., Enniful, R., Roth, M. R., Tamura, P., Jagadish, K., & Welti, R. (2018). An efficient modified method for plant leaf lipid extraction results in improved recovery of phosphatidic acid. *Plant Methods*, *14*, 14.
- Shiva, S., Vu, H. S., Roth, M. R., Zhou, Z., Marepally, S. R., Nune, D. S., Lushington, G. H., Visvanathan, M., & Welti, R. (2013). Lipidomic analysis of plant membrane lipids by direct infusion tandem mass spectrometry. *Methods in Molecular Biology (Clifton, N.J.)*, *1009*, 79–91.

- Song, Y., Vu, H. S., Shiva, S., Fruehan, C., Roth, M. R., Tamura, P., & Welti, R. (2020). A Lipidomic Approach to Identify Cold-Induced Changes in Arabidopsis Membrane Lipid Composition. *Methods in Molecular Biology (Clifton, N.J.)*, 2156, 187–202.
- Stucky, D. F., Arpin, J. C., & Schrick, K. (2015). Functional diversification of two UGT80 enzymes required for steryl glucoside synthesis in Arabidopsis. *Journal of Experimental Botany*, 66, 189–201.
- Takahashi, D., Li, B., Nakayama, T., Kawamura, Y., & Uemura, M. (2013). Plant plasma membrane proteomics for improving cold tolerance. *Frontiers in Plant Science*, 4, 90.
- Tan, W.-J., Yang, Y.-C., Zhou, Y., Huang, L.-P., Xu, L., Chen, Q.-F., Yu, L.-J., & Xiao, S. (2018). DIACYLGLYCEROL ACYLTRANSFERASE and DIACYLGLYCEROL KINASE Modulate Triacylglycerol and Phosphatidic Acid Production in the Plant Response to Freezing Stress. *Plant Physiology*, 177, 1303–1318.
- Tarazona, P., Feussner, K., & Feussner, I. (2015). An enhanced plant lipidomics method based on multiplexed liquid chromatography-mass spectrometry reveals additional insights into cold- and drought-induced membrane remodeling. *The Plant Journal: For Cell and Molecular Biology*, 84, 621–633.
- Telfer, A., Bollman, K. M., & Poethig, R. S. (1997). Phase change and the regulation of trichome distribution in Arabidopsis thaliana. *Development (Cambridge, England)*, 124, 645–654.
- Uemura, M., Joseph, R. A., & Steponkus, P. L. (1995). Cold Acclimation of Arabidopsis thaliana (Effect on Plasma Membrane Lipid Composition and Freeze-Induced Lesions). *Plant Physiology*, 109, 15–30.
- Uemura, M., & Steponkus, P. L. (1994). A Contrast of the Plasma Membrane Lipid Composition of Oat and Rye Leaves in Relation to Freezing Tolerance. *Plant Physiology*, 104, 479–496.
- Vu, H. S., Roston, R., Shiva, S., Hur, M., Wurtele, E. S., Wang, X., Shah, J., & Welti, R. (2015). Modifications of membrane lipids in response to wounding of Arabidopsis thaliana leaves. *Plant Signaling & Behavior*, 10, e1056422.
- Vu, H. S., Roth, M. R., Tamura, P., Samarakoon, T., Shiva, S., Honey, S., Lowe, K., Schmelz, E. A., Williams, T. D., & Welti, R. (2014a). Head-group acylation of monogalactosyldiacylglycerol is a common stress response, and the acyl-galactose acyl composition varies with the plant species and applied stress. *Physiologia Plantarum*, 150, 517–528.
- Vu, H. S., Shiva, S., Hall, A. S., & Welti, R. (2014b). A lipidomic approach to identify cold-induced changes in Arabidopsis membrane lipid composition. *Methods in Molecular Biology (Clifton, N.J.)*, 1166, 199–215.
- Vu, H. S., Shiva, S., Roth, M. R., Tamura, P., Zheng, L., Li, M., Sarowar, S., Honey, S., McEllhiney, D., Hinkes, P., Seib, L., Williams, T. D., Gadbury, G., Wang, X., Shah, J., &

- Welti, R. (2014c). Lipid changes after leaf wounding in *Arabidopsis thaliana*: Expanded lipidomic data form the basis for lipid co-occurrence analysis. *The Plant Journal: For Cell and Molecular Biology*, *80*, 728–743.
- Vu, H. S., Shiva, S., Samarakoon, T., Li, M., Sarowar, S., Roth, M. R., Tamura, P., Honey, S., Lowe, K., Porras, H., Prakash, N., Roach, C. A., Stuke, M., Wang, X., Shah, J., Gadbury, G., Wang, H., & Welti, R. (2022). Specific Changes in *Arabidopsis thaliana* Rosette Lipids during Freezing Can Be Associated with Freezing Tolerance. *Metabolites*, *12*, 385.
- Vu, H. S., Tamura, P., Galeva, N. A., Chaturvedi, R., Roth, M. R., Williams, T. D., Wang, X., Shah, J., & Welti, R. (2012). Direct infusion mass spectrometry of oxylipin-containing *Arabidopsis* membrane lipids reveals varied patterns in different stress responses. *Plant Physiology*, *158*, 324–339.
- Welti, R., Li, W., Li, M., Sang, Y., Biesiada, H., Zhou, H.-E., Rajashekar, C. B., Williams, T. D., & Wang, X. (2002). Profiling membrane lipids in plant stress responses. Role of phospholipase D alpha in freezing-induced lipid changes in *Arabidopsis*. *The Journal of Biological Chemistry*, *277*, 31994–32002.
- Yadav, S. K. (2010). Cold stress tolerance mechanisms in plants. A review. *Agronomy for Sustainable Development*, *30*, 515–527.
- Yang, W.-Y., Zheng, Y., Bahn, S. C., Pan, X.-Q., Li, M.-Y., Vu, H. S., Roth, M. R., Scheu, B., Welti, R., Hong, Y.-Y., & Wang, X.-M. (2012). The patatin-containing phospholipase A pPLAII α modulates oxylipin formation and water loss in *Arabidopsis thaliana*. *Molecular Plant*, *5*, 452–460.
- Zheng, G., Li, L., & Li, W. (2016). Glycerolipidome responses to freezing- and chilling-induced injuries: Examples in *Arabidopsis* and rice. *BMC Plant Biology*, *16*, 70.
- Zhou, Z., Marepally, S. R., Nune, D. S., Pallakollu, P., Ragan, G., Roth, M. R., Wang, L., Lushington, G. H., Visvanathan, M., & Welti, R. (2011). LipidomeDB data calculation environment: Online processing of direct-infusion mass spectral data for lipid profiles. *Lipids*, *46*, 879–884.
- Zien, C. A., Wang, C., Wang, X., & Welti, R. (2001). In vivo substrates and the contribution of the common phospholipase D, PLDalpha, to wound-induced metabolism of lipids in *Arabidopsis*. *Biochimica Et Biophysica Acta*, *1530*, 236–248.
- Zuther, E., Schaarschmidt, S., Fischer, A., Erban, A., Pagter, M., Mubeen, U., Giavalisco, P., Kopka, J., Sprenger, H., & Hinch, D. K. (2018). Molecular signatures of increased freezing tolerance due to low temperature memory in *Arabidopsis*. *Plant, Cell & Environment*, pce.13502.

Chapter 3 - GWAS on lipidomes of *Arabidopsis thaliana* reveals the potential regulators for lipid remodeling under cold stress

Introduction

Low temperature is one of the major abiotic stresses limiting plant distribution and crop yield. To develop more cold- and freezing-resistant crop species, one big challenge is understanding the biochemistry and genetics behind plant response to cold and freezing. Freezing temperature causes great damage to plants at the cellular level and plants have evolved an effective strategy, called cold acclimation, to increase their freezing tolerance. *Arabidopsis* (Columbia-0 accession), during its exposure to low but non-freezing temperatures for a period of one day or more, exhibits greatly enhanced freezing tolerance with the lethal freezing temperature dropping from -2 to -8 °C (Gilmour et al., 1988; Uemura et al., 1995). During cold acclimation, plants utilize various adaptive responses to cope with low temperature, including changes in lipid composition, which functions in maintaining membrane structure, in signaling, or both. Previous studies demonstrated that various lipid modifications, such as fatty acid desaturation, fatty acid oxidation, phospholipid hydrolysis, lipid acylation, and head group glycosylation occurred during cold or freezing stress to modulate plant damage (Hugly & Somerville, 1992; Li & Yu, 2018; Li et al., 2008; Menard et al., 2017; Miquel et al., 1993; Moellering et al., 2010; Nilsson et al., 2012, 2015; Vu et al., 2014a; Welti et al., 2002).

Arabidopsis is widely distributed in nature throughout the Eurasian continent, and the great differences in local environment have shaped natural variation among different accessions. Natural variation of many plant phenotypes is often pronounced along latitudinal gradients. For example, freezing tolerance has been demonstrated for *Arabidopsis* accessions originally collected from geographically diverse habitats, and the results suggest there was significant

correlation between the measured freezing tolerance and the latitude of origin (Hannah et al., 2006; Zhen & Ungerer, 2008; Zuther et al., 2012). Evidence also indicates that lipid composition in seeds and leaves of *Arabidopsis* accessions is under selection by temperature. Therefore, natural *Arabidopsis* accessions are a convenient experimental system in which to investigate the genetic variation in plants to regulate lipid metabolism under low temperature stress. Many studies have focused on the fatty acid composition of seed oil in natural *Arabidopsis* accessions to elucidate the regulation of lipid biosynthesis under unstressed and cold conditions (Branham et al., 2016; Menard et al., 2017; Sanyal & Linder, 2013). To date, only a few works have concentrated on the natural variation in the lipid profile in leaf tissues of *Arabidopsis*. Degenkolbe performed a comparative analysis of the lipidomes of 15 *Arabidopsis* accessions during cold acclimation using LC-MS, allowing the detection of 180 lipid species and found natural variations in some lipid species were highly correlated with freezing tolerance (Degenkolbe et al., 2012).

Genome wide association study (GWAS), utilizing individuals from a large number of natural accessions, is the one of the most popular approaches to uncover genetic associations. Compared to QTL mapping, which is limited to the availability of genetic variations in a segregating population, GWAS can map quantitative traits with higher resolution (Abdurakhmonov & Abdugarimov, 2008). GWAS has been successfully applied in *Arabidopsis* due to the establishment of 1001 Genomes Project, in which genomes of 1135 natural accessions were sequenced with over 10 million biallelic SNPs identified along the whole genome (Weigel & Mott, 2009).

In recent years, the use of GWAS in *Arabidopsis* has identified genes associated with lipid synthesis and composition under various stresses. Branham performed GWAS analysis on

the fatty acid composition in seed oil of 391 wild *Arabidopsis* accessions and identified 19 regions of interest associated with the seed oil composition (Branham et al., 2016). Recently, Menard utilized GWAS to dissect the genetic control of fatty acid desaturation in developing seeds and found that ω -6 desaturation is largely controlled by *cis*-acting sequence variants in *FAD2* (Menard et al., 2017).

Mass spectrometry-based lipidomics offers many advantages in monitoring cold- and freezing-induced lipid changes (Burgos et al., 2011; Degenkolbe et al., 2012; Tarazona et al., 2015; Vu et al., 2022; Zheng et al., 2016). Large numbers of lipid molecular species can be analyzed in a relatively short time, with higher sensitivity and resolution. Vu, Shiva, and coworkers (Shiva et al., 2013; Vu et al., 2014b) established a comprehensive lipidomic approach including lipid extraction, mass spectral analysis, and data processing. They developed a direct infusion ESI-MS method to measure *Arabidopsis* leaf lipid profile by a series of precursor and neutral loss scans. Recently, Song et al. updated and extended this lipidomics method by employing multiple reaction monitoring (MRM) to measure a greater number of analytes in a shorter time (Song et al., 2020). The updated direct infusion MRM method measures selected phospholipids, galactolipids, storage lipids, sphingolipids, and sterol derivatives, with most lipids designated by lipid class, total acyl carbons, and total double bonds, providing a comprehensive view of lipid changes under cold or freezing stress.

In this study, we performed a comparative analysis of the lipid profiles of 360 *Arabidopsis* accessions selected from 1001 Genomes Project. After a “super-cold” treatment (3-day cold acclimation at 4 °C followed by -2 °C for 16 h), most of the investigated lipid species were significantly changed, with most obvious inductions being in eukaryotic TAGs and VLCFA-containing membrane lipids. We performed a joint analysis of two GWAS, based on the

cold-induced lipid profiles from groups of 360 accessions and 320 accessions. The identification of lipid-level-associated SNPs and candidate genes in the jointly analyzed GWAS indicates that the associated genes are under evolutionary selection and allows us to hypothesize that specific lipid remodeling reactions and pathways in Arabidopsis leaves are important in cold stress response. The relative abundances of specific lipid species for the investigated accessions were highly correlated with measured freezing tolerance, latitude of origin, and local temperatures, providing evidence for the role of lipids and related genes in plant freezing tolerance.

Materials and Methods

Plant materials and growth conditions

679 accessions in the two independent groups were selected from the 1001 Genomes Project with a wide geographic distribution to ensure they have large phenotypic variation for GWAS. Information on the 320 accessions in group-1 and the 360 accessions in group-2 is listed in Table S3-1. A complete set of 1001 Genomes accessions (1135 accessions, Stock Number: CS78942) were obtained from Arabidopsis Biological Resource Center (ABRC).

All 679 investigated accessions were grown under the same standard conditions in growth chambers as described in Materials and Methods of Chapter 2. On day 26, soil-grown Arabidopsis plants were moved to a cold room at 4 °C for cold acclimation and plants were cold-acclimated for 3 days. On day 29, cold-acclimated plants were transferred to a programmable freezing chamber at -2 °C for 16 h. After the -2 °C treatment, stressed plants were thawed at 22 °C for 1 h. Leaf #4 was harvested for lipid extraction, while the leaf #5 was harvested for RNA extraction. For control plants in group-2, which didn't go through cold acclimation and -2 °C treatment, leaf #4 was harvested for lipid extraction on day 29. For each accession, there were three biological replicates for lipid analysis.

Lipidomic analysis of Arabidopsis accessions

Lipids in leaf samples were extracted using an optimized extraction method based on Shiva et al. (2018). The lipid extraction procedure, preparation of internal standards, and preparation and use of QC samples are described in Materials and Methods section in Chapter 2. Data were acquired on a triple quadrupole mass spectrometer (Sciex 6500+ mass spectrometer) equipped with an ESI probe, using MRM scanning operated in positive and/or negatives modes. Details of the MS parameters are described in Chapter 2. In the positive mode, 104 transitions and, in the negative mode, 234 transitions were monitored in each MRM cycle. Twenty-seven cycles of MRM scanning were acquired within 5 min. Parameters for each MRM transition are listed in Supplemental Table S3-2 for the plant lipid analytes and internal standards.

Data processing and normalization

As described in Chapter 2, the MRM data were collected using the Sciex 6500+ mass spectrometer, processed using the software MultiQuant, deconvoluted and calculated using the online software LipidomeDB Data Calculation Environment (DCE). An adaptation of the method of Dunn (2011), as described by Vu et al. (2014c), was employed to eliminate variability in instrument response through the entire acquisition period, producing a consistent data set. Coefficient of variation (CoV) values of less than 30% represent analytes with reasonable analytical precision. All lipid analytes with CoVs of less than 30% are summarized in Table S3-3. Finally, the data were corrected for the fraction of the sample analyzed and normalized to the sample “dry masses” to produce data in normalized mass spectral intensity per dry mass mg^{-1} , where a normalized intensity of 1 = the intensity of 1 nmol of internal standard. The average of three biological replicates for each accession was calculated and the mean value of absolute content (normalized intensity mg^{-1}) of all 360 accessions before and after super-cold stress is

shown in Table S3-4. The relative proportions of individual lipid molecular species were expressed as a percentage of the total measured lipid content (normalized intensity mg^{-1}) per sample. The relative level (percentage) of each lipid species of 360 accessions is shown in Table S3-5. Lipid species can be categorized into 32 lipid sub-classes, and the absolute and relative content for 32 lipid classes is shown in Tables S3-6 and S3-7.

Freezing tolerance assays

679 *Arabidopsis* accessions in the two independent populations were used as subjects for freezing tolerance measurements. Planting designs were randomized so that 3 plants of the same accession were included on the same 72-well tray. Before freezing treatments, plants of all accessions went through a growth period (as described in Materials and Methods of Chapter 2) for 26 days and cold acclimation at 4 °C for 3 days which are described before. Then acclimated plants were subjected to freezing stress in a freezing chamber using a programmed temperature gradient: a cooling period from 0 °C to -13 °C at a rate of temperature decrease of 2 °C h^{-1} , hold at minimum temperature (-13 °C) for 2.5 h, then a warming period from -13 °C to 4 °C at a rate of temperature increase of 2 °C h^{-1} , and finally a recovery period at 4 °C for 5.5 h. After the freezing treatment, plants were grown at room temperature of 22 °C. After 2 weeks of recovery, plants were scored as a number ranging from 0 to 100 representing proportion of the plant leaf area that appeared to be alive. The freezing tolerance scores of 679 accessions are shown in Table S3-8. The data represent a semi-quantitative measurement of freezing tolerance of *Arabidopsis*, modified from Zhen & Ungerer (2008).

Genome-wide association study

GWA analysis was performed with the online tool GWA-Portal (URL <https://gwas.gmi.oeaw.ac.at>) using ~10 million single-nucleotide polymorphisms (SNPs)

available from the imputed full sequence dataset. A Box-Cox transformation was applied to assure most lipid phenotypes had approximately normal distributions. Accelerated mixed model (AMM) was chosen to take population structure into accounts. Pseudo-heritability for each BoxCox-transformed lipid phenotype was determined by GWA-Portal and summarized in Table S3-9.

GWAS results were downloaded from GWA-Portal as csv files and then filtered by minor allele frequency (MAF) ≥ 0.05 and score ≥ 2 , using a Python program (<https://github.com/songyu6054677/GWAS-results-analysis-01122021.git>). Using the Python data processing pipeline, additional information was added to each SNP entry, including the associated lipid name, lipid number, transformation method, and stress condition. A summary GWAS result file, consisting of all significant SNPs identified for all lipid species, was generated. The GWAS results were further filtered by matching the SNPs identified from the two GWAS studies based on different groups of Arabidopsis accessions. The “merge” function in the Python program facilitated discovery of SNPs with the same “position”, “lipid name”, and “transformation” between the two GWAS summary files. The common SNPs the from two GWAS studies for the same lipid-level phenotypes under cold stress were summarized and a combined *p*-value was calculated using Fisher's method for each SNP. Finally, all SNPs with criteria of combined *p*-score ≥ 6.5 and *maf* ≥ 0.05 are summarized in Table S3-10. All genes located between 10 kb upstream and downstream of each significant SNP were identified by Python program. By checking the genomic region around significant SNP peaks, all significant SNPs and associated candidate genes were categorized into genomic regions, each containing the SNPs within 20 kb of each other and having alleles associated with the level of a particular lipid or with multiple lipids if the lipids are associated with one or more of the same SNPs in the

region. Gene annotation from candidate genes was obtained from TAIR 10 database (<http://www.arabidopsis.org>). Lipid-related genes and associated lipid phenotypes are summarized in S3-11.

Gene expression analysis (RT-qPCR)

Before RNA extraction, the harvested leaf samples were frozen immediately in liquid nitrogen and stored at -80 °C. Three leaves were harvested from each accession as technical replicates and a total of 50 accessions were selected for gene expression analysis. Information about selected accessions is listed in Table S3-12. Two different sub-groups of accessions were selected for gene expression analysis of 6 candidate genes. Thirty accessions were chosen for AT1G74960, AT3G11170, AT3G19260, AT4G36810 to ensure a high representation of accessions with minor alleles in the measured group, and 20 accessions were measured for AT3G12120 and AT5G16230. Three leaves from each accession were frozen in a 1.5 mL microcentrifuge tube along with a metal bead and ground thoroughly in a tissue lyser. RNA was extracted from the tissue powder using RNeasy Plant Mini Kit from Qiagen following the manufacturer's protocol. Ten µg of total RNA was digested with DNase Max Kit from Qiagen to remove any genomic DNA contamination. RNA concentrations were quantified with a NanoDrop 2000 spectrophotometer (Thermo Scientific). 1 µg of RNA was used for cDNA synthesis using qScript™ cDNA Synthesis Kit from Bio-Rad according to the manufacturer's protocol.

Quantitative PCR was performed on a CFX96 real-time PCR system (Bio-Rad) using the iTaq Universal SYBR Green Supermix chemistry on iCycler iQ from BioRAD. Gene expression levels of all tested genes were normalized to the *TRO* (AT1G51450) and *YLS8* (AT5G08290) genes using the Delta-Delta-CT (DDCT) method (Livak & Schmittgen, 2001). The expression

levels of reference genes *TRO* and *YLS8* are very stable in Arabidopsis leaf tissues across unstressed, cold, and wounding conditions according to microarray data from Genevestigator software (Hruz et al., 2011). Primers used to quantify expression of these genes are listed in Table S3-13.

Statistical analysis

Auto-scaling, the two-sample t-test, and calculation of False Discovery Rate (FDR) were performed (Table S3-14), based on relative content (% of total lipids) of individual lipid species, before and after super-cold stress, and the heat map was produced using utilities at the MetaboAnalyst website. Linear regression analysis was performed using the function in Origin 2021 and the significance of correlations was estimated by calculating Pearson correlation coefficients of lipid level and gene expression level. Pearson correlation analysis was performed using the CORREL function in Excel (Office 365) and the significance (*P*) of correlations was estimated by calculating Pearson correlation coefficients of corresponding variables (freezing tolerance scores, latitudes of accession origin, geoclimatic variables). Correlation results were summarized in Table S3-15, S3-16.

Results

Super-cold treatment induced significant changes of lipid profiles among 360

Arabidopsis natural accessions

All analyzed 270 lipid molecular species are categorized into 32 lipid sub-classes. The changes in the relative contents (%) of the 32 lipid classes or sub-classes after low temperature treatment are depicted in Figure 3-1. One of the most prominent changes in lipid profiles of leaves of plants under super-cold treatment, as compared to those of control plants, is the accumulation of TAGs in most investigated accessions. Another obvious change is the

production of oxidized lipids, especially the ox-acMGDG, ox-ASG, and ox-DGMG sub-classes. Among the lipids reduced in level under super-cold stress, the most significant changes include decreases of GlcCer, ASG, MGDG, and PS classes.

A more detailed view of individual lipid molecular species is shown in Table S3-5 and S3-14. Of the 270 lipid analytes, 225 were significantly different, by unpaired t-test ($P < 0.01$), in level between control plants and those undergoing super-cold treatment. 152 lipid species were significantly increased in level under cold stress while 73 lipid species were decreased. The autoscaled levels of lipid species among 360 accessions are plotted in a heatmap (Figure 3-2). The heatmap not only shows changes in lipid levels before and after cold treatment, also displays the natural variation in the levels of individual lipid species among accessions under control and low-temperature conditions.

Accumulation of TAG in leaves is a major change in lipid profile under low temperature

In most investigated accessions, the total relative content of TAG increased with an average of 2-fold change after super-cold treatment. However, the change in TAG content under cold stress was not uniformly distributed across all molecular species. As shown in Figure 3-3, levels of all tested TAG species with polyunsaturated fatty acyl chains were significantly increased except for TAG(16:0/34:6) and TAG(18:3/34:6), which contain the DAG combination, 18:3 and 16:3, which can be formed through the prokaryotic pathway. Additionally, the long-chain TAGs with a high degree of unsaturation such as TAG(18:3/36:5) and TAG(18:2/36:5) showed more induction compared with other TAG species.

Polar glycerolipid remodeling is a distinct signature under low temperature

In lipid profiles of control and super-cold-treated accessions, 236 polar glycerolipid species were detected. Under super-cold stress, remarkable lipid remodeling occurred in plasma membrane especially for phospholipids. We found that the relative contents of the PC, PE, and PI classes were significantly increased after the super-cold treatment, while the content of PS was decreased. PC is the major phospholipid in Arabidopsis leaves, and, in a more detailed view of PC molecular species (Figure 3-4), it is found that there was a drastic alteration in fatty acid composition. Under cold stress, the 32C-PC species including PC(16:0/16:3), PC(16:0/16:1), PC(16:0/16:0) declined, and most 36C-PC, 38C-PC, and all 40C-PC species tended to increase, particularly the 40C-PC species, PC(22:1/18:3), PC(22:0/18:3), and PC(22:0/18:2), which increased 4 to 6-fold. Changes in FA unsaturation level were also observed in cold-induced lipid profiles. Most 18:2-containing PC species, particularly the major species PC(18:2/18:2) and PC(18:2/18:3), were increased, while levels of some PC species containing saturated FA, including PC(16:0/18:3), PC(18:0/18:3), and PC(20:0/18:3), were reduced under low temperature. Similar to PC, PE showed increased proportions of VLCFA chains (20C, 22C, and 24C) and decreased proportions of 16C-fatty acyl chains (Figure B-1). Additionally, some PE species containing saturated FA, such as PE(16:0/18:3) and PE(18:0/18:3), declined after cold treatment, which is consistent with the changes in PC profile.

The relative abundance of some lipid species is highly correlated with freezing tolerance

Using lipidomics, we evaluated the phenotypic variation for relative proportions (% of total) of individual lipid species and lipid classes under super-cold stress. The means, maximum value, minimum value, ranges, and variability (CoV) of 270 lipid species and 32 lipid classes

were calculated. Different lipid classes exhibited different variability with CoV ranging from 3% to 84% under super-cold stress (Table 3-1).

Latitude and geoclimatic data in the location where the investigated accessions were originally collected are good indicators of freezing tolerance of Arabidopsis. To better explore the relationship between latitude, local climate variables, and freezing tolerance, we performed correlation analysis between freezing tolerance scores and 21 climate variables including latitude and local temperature variables interpolated from weather stations. The climate variables were obtained from AraCLIM—a web-based resource that has compiled existing environmental conditions at the sites of collection of the Arabidopsis. The results in Table S3-15 show that in the investigated group of 360 accessions, latitude was highly correlated with freezing tolerance scores ($r = 0.399$; $P = 3.63E-15$), indicating that the freezing tolerance of these accessions increase with its latitude of origin. Of the 21 climate variables used in correlation analysis, 7 were more correlated with freezing tolerance scores than latitude. These included average land surface day temperature in spring, average land surface day temperature in summer, average land surface night temperature in spring, maximum temperature in spring, annual mean temperature, mean temperature of the driest quarter, and mean temperature of the coldest quarter.

To further explore the role of specific lipids in plant freezing tolerance, we performed Pearson correlation analysis between relative abundances of individual lipid species under super-cold stress and their freezing tolerance scores, between lipid levels and latitude, and between lipid levels and each of the 21 climate variables. The results of all correlation analyses are presented in Tables S3-S16. Many lipid species with levels under super-cold treatment significantly correlated with freezing tolerance scores, latitude, and climate variables were identified. Acclimated freezing tolerance, which is indicated by freezing tolerance scores, was

positively correlated with the relative abundance of several molecular species of polar membrane lipids (e.g. MGDG(18:3/16:2), MGDG(20:2/18:3), PC(18:2/18:2), PE(18:2/18:2), PG(18:3/16:0)). These lipid species also showed positive correlations with latitude and negative correlations with local temperature variables like minimum temperature of coldest month, implying that they are indicators for higher freezing tolerance. On the other hand, other lipid species such as Sitosterol-Glc(16:0), DAG(18:3/18:3), GlcCer(34:1)-2, DGMG(16:0), PC(16:0/18:3), PE(16:0/18:3), PE(24:0/18:3), and PG(18:2/16:1) were negatively correlated with freezing tolerance, with most of them also showing negative correlations with latitude and positive correlations with temperature variables of origin, implying they are indicators of freezing sensitivity.

GWAS study on lipidomics data revealed candidate genes related to lipid metabolism

Among the 360 accessions, most of 270 lipid analytes measured in Arabidopsis leaves under super-cold treatment displayed substantial variation in their relative proportions (% of total). CoVs were calculated and summarized in Table S3-5 for each lipid species. The online tool GWA-Portal was used to perform GWA mapping on individual lipid species. After BOXCOX transformation, the distribution of all lipid phenotypes was greatly improved and the narrow-sense heritability of each transformed phenotype is indicated by the pseudo-heritability. Pseudo-heritabilities for each lipid species are summarized in Table S3-9.

The statistical power to map candidate genes in GWAS depends largely on the investigated population size. Here, association analysis by SNPs was performed using joint analysis of GWAS from two independent studies to increase the power to detect trait associations. After comparison between the GWAS results based on a group of 320 accessions

(group-1) and GWAS results on a different group of 360 accessions (group-2), associations were independently detected for the same SNPs across the nonoverlapping groups of accessions, providing stronger associations between lipid-level and SNPs. Lipid level-associated SNPs identified from both GWAS studies for the same lipid phenotypes under cold stress were summarized and a combined p-score was calculated using Fisher's method for each SNP. Finally, a total of 873 SNPs with criteria of combined p-score ≥ 6.5 , maf ≥ 0.05 , and pseudo-heritability > 0 were identified; these were associated with 66 lipid species. Candidate genes were determined within a 20-kb length region (10 kb upstream and downstream of the significant SNPs). The 873 SNPs identified from both GWAS studies under cold stress were associated with 65 genomic regions. A total of 479 candidate genes were identified for cold-induced lipidomic data. All SNPs, nearby regions, and associated genes are listed in Table S3-10. Based on GO annotation results, 29 of 479 candidate genes identified under cold stress are characterized lipid-related genes or uncharacterized genes which may have lipid biosynthetic or metabolic functions (Table S3-11).

Variation in *FAD2* regulates ω -6 desaturation in leaf phospholipids under cold stress

A reported GWAS on fatty acid composition of seeds from RIL and natural populations of *Arabidopsis* identified the gene *FAD2*, which is responsible for ω -6 fatty acid desaturation under both unstressed and cold conditions (Branham et al., 2016; Menard et al., 2017). Here, using the percentages of individual phospholipid species measured in group-2 of 360 accessions for GWAS using ~10 million SNPs present in imputed full sequence database, *FAD2* was also identified as a candidate gene. Phospholipids species including PC(18:1/18:3), PE(18:1/18:3), and PI(16:0/18:1) were associated with AT3G12120 (*FAD2*), which encodes the enzyme mainly

responsible for the production of 18:2 from 18:1 fatty acids in the endoplasmic reticulum (ER). *FAD2* was located within a large genomic region (#20, containing 17 genes from AT3G12060 to AT3G12150). Figure 3-5a is the Manhattan plot of GWAS analysis on the relative level (%) of PC(18:1/18:3). One significant SNP (Chr3_3862612) within region #20 was strongly associated with PC(18:1/18:3) with a 5.98 p-score ($-\log_{10}(P)$) in group-2. This polymorphism is a single-nucleotide substitution (A/G) situated at the intron within the 5' UTR of the *FAD2*. Haplotype analysis using this SNP (Chr3_3862612) revealed two haplotype groups of *FAD2* in the 360 natural accessions, with 334 and 26 accessions in major allele group and minor allele group, respectively. The haplotype analysis for lipid phenotype PC(18:1/18:3) is summarized in Figure 3-5b, the major allele group with allele A at this SNP position had significantly lower level of PC(18:1/18:3) than minor allele group with allele G (mean of major allele group = 0.43%, mean of minor allele group = 0.52%, $P = 3.81E-08$). Besides PC(18:1/18:3), haplotype analysis using SNP (Chr3_3862612) in group-2 of 360 accessions showed there are significant differences in the relative contents of PC(18:2/18:2), PE(18:2/18:2), PE(18:1/18:3), PE(20:1/18:3), and PI(16:0/18:1). The major allele group had lower levels of PE(18:1/18:3), PE(20:1/18:3), PI(16:0/18:1) and higher level of PC(18:2/18:2), PE(18:2/18:2) compared to minor allele group. In Figure 3-5c, from the geographic distribution of the two haplotype groups, most accessions in the minor allele group are located in southern Europe with average latitude of 41.7 °N, which is significantly lower than the latitude of the accessions in major allele group ($P = 9.98E-4$). These results may indicate this SNP is associated with local temperature and can influence *Arabidopsis* cold/freezing tolerance. In addition, correlation analysis indicated that the relative levels of PC(18:2/18:2) and PE(18:2/18:2) were positively correlated with freezing tolerance and latitude, while PC(18:1/18:3) level was negatively correlated with freezing tolerance and latitude (Figure

3-6). Thus, we hypothesize that the natural variation in 5' UTR of *FAD2* or a linked SNP causes phenotypic variation in ω -6 desaturation in leaf phospholipids under cold stress and that 18:2-PLs in leaves contribute to freezing tolerance in Arabidopsis.

Variation in *FAD7* regulates ω -3 desaturation in leaf galactolipids under cold stress

Lipidomic analysis of MGDG and DGDG molecular species among 360 accessions revealed that changes in the lipid content were not uniformly distributed across different molecular species. Based on variation in the relative abundance of individual MGDG and DGDG species under super-cold stress, we performed GWAS analysis to explore the genetic architecture of MGDG and DGDG composition. Lipid-level phenotypes for MGDG(18:3/16:2), MGDG(18:2/18:3), and DGDG(18:3/16:2) were associated with a genomic region (#19) extending from AT3G11150 to AT3G11210. The gene *FAD7* (AT3G11170) is located within region #19; *FAD7* encodes the major plastid-localized ω -3 desaturase in leaves; *FAD7*'s gene product is responsible for the synthesis of 16:3 and 18:3 fatty acids in galactolipids. For MGDG(18:2/18:3), the SNPs with highest p-score within region #19 are the SNP at Chr3_3501980, the SNP at Chr3_3502171, and the SNP at Chr3_3502209. Among them, the SNP at Chr3_3501980 is the only missense SNP in *FAD7* identified by GWAS, and it showed association with MGDG(18:2/18:3) (p-score = 5.79, group-2; p-score = 2.46, group-1). Figure 3-7a is the Manhattan plot for lipid phenotype MGDG(18:2/18:3) in group-2. Haplotype analysis using the SNP at Chr3_3501980 revealed two haplotype groups of *FAD7* in the 360 natural accessions, with 210 and 150 accessions in the major allele group and minor allele group, respectively. The haplotype analysis for lipid phenotype MGDG(18:2/18:3) is summarized in Figure 3-7b, the major allele group with nucleotide A at this SNP position had significantly higher level of MGDG(18:2/18:3) than did the minor allele group with nucleotide G (mean of

major allele group = 0.23%, mean of minor allele group = 0.20%, $P = 1.83E-8$). Besides MGDG(18:2/18:3), this SNP was also strongly associated with other galactolipid species including MGDG(18:3/16:2), and MGDG(18:3/18:3). From the geographic distribution of the two haplotype groups (Figure 3-7c), there is no significant difference in latitude between the two groups. But correlation analysis showed positive correlations between the relative content of MGDG(18:3/16:2) and MGDG(18:2/18:3) and freezing tolerance (Figure 3-8). Therefore, we hypothesize that the non-synonymous SNP in coding sequence of *FAD7* is linked to the phenotypic variation in ω -3 desaturation in leaf MGDG, and accessions with higher proportions of 18:3-containing MGDGs exhibit more freezing tolerance.

Variation in *LOH2* and *KCS9* regulate GlcCer biosynthesis and fatty acyl elongation under cold stress

Lipidomics analysis on GlcCer molecular species demonstrated that there was an overall reduction in the relative abundance of GlcCer species in most accessions under cold stress. Although GlcCer has been implicated in membrane stability and in various signaling processes, the exact functions of GlcCer species in response to cold remain unclear. Based on variation in the relative abundance of individual GlcCer species before and after cold stress, we performed GWAS to map candidate genes controlling GlcCer metabolism. For two GlcCer species, GlcCer(34:1)-2O, which is GlcCer(d18:1/h16:0) and GlcCer(34:1)-3O, which is GlcCer(t18:1/h16:0) (Markham & Jaworski, 2007), the strongest association was detected in a genomic region (#22) from AT3G19190 to AT3G19380. Within region #22, there were 5 significant SNPs located in the third and fifth intron or the 3' UTR region of *LOH2* (AT3G19260). In the Manhattan plot for lipid-level phenotype GlcCer(d18:1/h16:0) (Figure 3-9a), the SNP at Chr3_6669405 (p-score=11.93, group-2; p-score=11.99, group-1) was situated in

the 3' UTR of *LOH2* (AT3G19260), which encodes a ceramide synthase essential for production of C16-ceramide (the precursor of C16-GlcCer). Haplotype analysis using the SNP at Chr3_6669405 revealed two haplotype groups of *LOH2* in the 360 natural accessions, with 330 and 30 accessions in major allele group and minor allele group, respectively. The haplotype analysis for lipid phenotype GlcCer(d18:1/h16:0) is summarized in Figure 3-9b, and the major allele group with nucleotide G at this SNP position had a significantly higher level of GlcCer(d18:1/h16:0) than the minor allele group with nucleotide A (mean of major allele group = 0.35%, mean of minor allele group = 0.28%, $P = 1.43E-10$). In addition to GlcCer(d18:1/h16:0), this SNP were also strongly associated with another C16-GlcCer species GlcCer(t18:1/h16:0). Haplotype analysis on the SNP at Chr3_6669405 for GlcCer(t18:1/h16:0) showed a similar pattern with a higher level in major allele group.

For GlcCer species GlcCer(40:1)-3O, which is GlcCer(t18:1/h22:0) (Markham & Jaworski, 2007) with VLCFA, GWAS showed the associated genomic region on chromosome 2. Figure 3-10a shows the Manhattan plot for the lipid-level phenotype GlcCer(t18:1/h22:0) and the highest SNP (Chr2_7051376) in region #14, which is situated in the coding sequence of *KCS9* (AT2G16280). *KCS9* is a member of the 3-ketoacyl-CoA synthase family involved in the biosynthesis of VLCFA, converting 22C-FA to 24C-FA (Kim et al., 2013). As shown in Figure 3-10b, haplotype analysis among group-2 of 360 accessions showed that the major allele group with nucleotide T at this SNP position had a significantly lower level of GlcCer(t18:1/h22:0) than the minor allele group with nucleotide C (mean of major allele group = 0.23%, mean of minor allele group = 0.25%, $P = 8.15E-05$). The haplotype analysis of GlcCer(42:2)-3O, which is GlcCer(t18:1/h24:1) (Markham & Jaworski, 2007), demonstrated a reverse pattern with a higher level of GlcCer(t18:1/h24:1) in the major allele group. From the geographic distribution

of the two haplotype groups in 360 accessions (Figure 3-10c), more accessions in the minor allele group are located in northern Europe with an average latitude of 49.5 °N, which is significantly higher than the average latitude (44.8 °N) in the major allele group ($P = 3.53E-9$). In group-1 of 320 accessions, accessions in minor allele group also have significantly higher latitude than accessions in major allele group (minor allele group: 54.5 °N, major allele group: 51.3 °N, $P = 3.28E-6$).

To investigate the roles of *LOH2* and *KCS9* in plant freezing tolerance, we performed correlation analysis between the relative content of 4 GlcCer species and freezing tolerance. As shown in Figure 3-11, the level of GlcCer(d18:1/h16:0) and GlcCer(t18:1/h22:0) under cold conditions had strong negative correlations with freezing tolerance and latitude. On the other hand, these two species were negatively correlated with local temperatures. Correlation results demonstrate that specific GlcCer species might be indicators for freezing susceptibility.

Variation in other lipid related genes regulate lipid metabolism under cold stress

Fatty Acid Biosynthesis 1 (FAB1), which catalyzes the elongation of 16:0 to 18:0 in plastid, was significantly associated with variation in the proportions of PG(16:0/16:1) after cold treatment. From our GWAS, a SNP at Chr1_28156734 had significant associations with PG(16:0/16:1) with a p-score of 4.64 (Figure B-2). This SNP was located at 384 bp upstream of *FAB1* (AT1G74960) and might affect gene expression and fatty acid composition in PG. Haplotype analysis for the SNP (Chr1_28156734) showed that the major allele group with nucleotide T at this SNP position had significantly higher average levels of PG(16:0/16:1) than the minor allele group with nucleotide A. Although accessions in the major allele group have significantly lower average latitude than accessions in the minor allele group, the correlation

analysis didn't reveal a significant correlation between relative content of PG(16:0/16:1), PG(16:0/16:0) and freezing tolerance.

GERANYLGERANYL PYROPHOSPHATE SYNTHASE 11 (GGPPS11) encodes a geranylgeranyl diphosphate synthase with two differentially targeted enzyme isoforms. Although GGPPS11 is a hub isozyme required for the production of most photosynthesis-related isoprenoids through the MEP pathway in plastid, it might affect the isopentenyl diphosphate flux and cytosolic MVA pathway for the production of sterols (Ruiz-Sola et al., 2016b). As shown in Figure B-3, a SNP at Chr4_17343444 was detected in the 5' UTR region of *GGPPS11* (AT4G36810) for two lipid phenotypes sitosterol(18:2) and sitosterol(18:3). Both sitosterol(18:2) and sitosterol(18:3) had associations with the SNP with combined p-score of 7.15 and 7.25, respectively. Haplotype analysis for the SNP in group-2 of 360 accessions showed that the major allele group with nucleotide A at this SNP position had a significantly higher average level of sitosterol esters than minor allele group with nucleotide C. From the geographic distribution of the two haplotype groups, most accessions in the major allele group are located in southern Europe with average latitude of 44.1 °N, which is significantly lower than the accessions in minor allele group ($P = 7.44E-9$). Correlation analysis showed that the relative content of sitosterol(18:3) was negatively correlated with freezing tolerance, latitude, and positively correlated with local temperatures, indicating sitosterol(18:3) is a lipid marker for less freezing resistance in *Arabidopsis*.

SNPs in *FAD2* determine the expression level of the gene

To determine whether the SNPs located in 5' UTR, 3' UTR or upstream regions influence the expression level of candidate genes, 50 accessions from group 2 were selected and RT-qPCR was used to measure transcript the abundance of *FAD2*, *FAD7*, *LOH2*, *FAB1*, and

GGPPS11. Among these genes, only *FAD2* showed a significant difference in expression level between its two haplotype groups. In Figure 3-12a, among the 20 accessions tested for gene *FAD2*, the gene expression level of the major allele group (10 accessions) with A at Chr3_3862612 was higher than gene expression level of the minor allele group (10 accessions) with G. The gene expression results for *FAD2* were consistent with our lipidomics results on PC(18:1/18:3) and PC(18:2/18:2), suggesting that higher *FAD2* expression leads to higher proportion of 18:2 FA and lower proportion of 18:1 FA in PC, PE, and PI. As shown in Figure 3-12(b, c), in the investigated 20 accessions, *FAD2* expression was negatively correlated with the relative content of PC(18:1/18:3) and positively correlated with the relative content of PC(18:2/18:2), revealing the effect of the SNP at Chr3_3862612 or a linked SNP on gene expression and ω -6 desaturation in leaf phospholipids under cold stress.

Discussion

During the past twenty years, scientists investigated lipid changes in Arabidopsis under low temperature (cold and freezing stress) with the help of lipidomics, especially for the major membrane lipids like phospholipids, galactolipids, and storage lipids (Barrero-Sicilia et al., 2017; Burgos et al., 2011; Degenkolbe et al., 2012; Li et al., 2008; Sanyal & Linder, 2013; Tarazona et al., 2015; Vu et al., 2022; Wang et al., 2006; Welti et al., 2002; Zheng et al., 2016). It has been found that the lipid metabolism under cold and freezing result in distinctly different lipid changes. Freezing stress is a more severe stress compared with cold stress, leading directly to membrane damage and cell death. Therefore, the lipid remodeling of cell membrane during freezing is different from cold stress; for example, in Arabidopsis, freezing induced a dramatic degradation of PC, along with large accumulation of PA, catalyzed by PLD α 1 (Li et al., 2008; Welti et al., 2002; Zheng et al., 2016). On the other hand, while under cold stress, there was a

slight increase in the content of PC in most accessions (Degenkolbe et al., 2012; Tarazona et al., 2015).

To ensure freezing wouldn't cause obvious damage to Arabidopsis, a super-cold treatment (3-day cold acclimation followed by -2°C freezing for 16 h) was applied in Chapter 2 to detect changes in lipid profile of Col-0 under low temperature. The results showed that cold acclimation and super-cold treatment induced similar changes for most lipids in leaves of Col-0 compared to the unstressed plants, with the most significant changes in lipid levels being increases in TAG, SE, and LPLs and decreases in MGDG, GlcCer, PS, and ASG.

In this study, we quantified cold-induced lipidomes on 679 accessions from the 1001 Genomes Project. These accessions are locally adapted lines and have tremendous phenotypic variation in lipid composition and freezing tolerance (Weigel & Mott, 2009). The discovery of genome-wide variants among accessions in 1001 Genomes Project provides a powerful tool for GWAS. Recently, an interactive web-based database of the environment variables was developed containing 204 geoclimatic variables to describe the local environments of Arabidopsis accessions from 1001 Genomes Project (Ferrero-Serrano & Assmann, 2019). It provides more evidence about the relationship between the geoclimatic variables, freezing tolerance, and cold-induced lipidomes in natural Arabidopsis accessions.

The overall changes in lipid profile in most accessions under the super-cold treatment at -2°C are similar to the lipid changes during cold acclimation. From our lipidomics results, there was a large accumulation of TAGs after super-cold treatment, which is consistent with the previous lipidomic results in Arabidopsis during cold acclimation (Degenkolbe et al., 2012; Tarazona et al., 2015). Additionally, the significant increase of PC and PE and decrease of MGDG, and GlcCer observed in this study were also reported before by Degenkolbe in cold-

acclimated accessions (Degenkolbe et al., 2012). PC hydrolysis along with the production of PA was not observed in this study under the super-cold stress. There was an increase of acMGDG and TrGDG during super-cold stress, but to a much lesser extent than at -8 °C (Moellering et al., 2010; Vu et al., 2014a; Vu et al., 2022).

In addition to the increase in total TAG content, there was a preferential accumulation of TAG species with four to nine double bonds in their three fatty acyl chains except for 34:6-TAG. In Arabidopsis, TAG is produced from *de novo* synthesized DAG through the acyl-CoA-dependent pathway (catalyzed by DGAT1) or from PC-derived DAG through the acyl-CoA independent pathway (catalyzed by PDAT) (Fan et al., 2013b). Previous findings suggested that plants can maintain cell membrane stability and fluidity by converting DAG to TAG in response to freezing (Chen et al., 2015). Environmental stress causes degradation of membrane lipids, leading to accumulation of toxic lipid intermediates (free FA, DAG), TAG functions as a pool to sequester these toxic compounds and prevent cellular damages under unfavorable conditions (Fan et al., 2013a; Lippold et al., 2012). It is possible the accumulation of polyunsaturated TAGs during cold acclimation or -2 °C treatment helps Arabidopsis reduce damage caused by toxic free FA. Our correlation analysis didn't show significant correlation between the relative level of TAG species and freezing tolerance. The precise mechanism in which TAG biosynthesis contributes to plant freezing tolerance needs to be elucidated in the future.

Many studies have revealed the ability of plants to modulate membrane fluidity in response to low temperature by changing fatty acid desaturation of membrane glycerolipids. The fluid state of plasma membrane or chloroplast membrane is a structural asset for their normal functions and low temperature results in the transition from a fluid state to a rigid gel phase. Plants can increase the fatty acyl unsaturation level in membrane lipids to enhance membrane

fluidity and stabilization under cold (Chen & Thelen, 2013; Harayama & Riezman, 2018; Hugly & Somerville, 1992; Matos et al., 2007; Miquel et al., 1993). In our study, the two major phospholipids PC and PE displayed drastic changes in their fatty acid composition under cold stress. Most PC and PE species containing saturated fatty acids, e.g., 18:0, were significantly reduced, while 18:2-containing species were increased. Interestingly, the relative contents of PC(18:2/18:2) and PE(18:2/18:2) among investigated accessions were positively correlated with freezing tolerance, latitude and negatively correlated with local temperature variables such as minimum temperature of coldest month. Previous work also showed PC(38:4) was correlated with acclimated freezing tolerance (Degenkolbe et al., 2012). PC and PE containing 18:2 fatty acid chains might be very important lipid compounds for freezing tolerance. VLCFAs are specifically present in several membrane lipids and essential for membrane homeostasis under various stresses, VLCFAs are enriched in PC, PE, and PS, where they play a role in membrane domain organization and interleaflet coupling (Batsale et al., 2021). In recent years, VLCFAs have been reported to contribute to plant chilling tolerance. Overexpression of *KCSI* in *Arabidopsis* enhanced VLCFA content and chilling tolerance (Chen et al., 2020). The increase of fatty acid chain length in PC and PE under cold was the prominent change in the lipid profile in plants exposed to super cold. All 32C-PC and PE species with two 16C fatty acid chains declined while 38C-, 40C-, 42C-species containing one 18C fatty acid chain and one VLCFA (20C, 22C, 24C) were largely increased in response to cold. PE(24:1/18:2) was positively correlated with freezing tolerance, latitude and negatively correlated with several local temperature variables like minimum temperature in spring. Therefore, some VLCFA-containing membrane lipids like VLCFA-PCs and VLCFA-PEs might contribute to freezing tolerance in *Arabidopsis*. Different from PC and PE, PG is mainly synthesized in chloroplast by the prokaryotic pathway and has

been shown to influence plant chilling tolerance. Studies on *fabI* mutants indicated that high levels of high-melting-point (HMP)-PG cause deficient photosynthesis and eventual death of plants under chilling stress (Gao et al., 2020; Gao et al., 2015; Kim et al., 2010). In the PG profile under cold stress, there was a remarkable reduction of two 32C-PG species, PG(16:0/16:0) and PG(16:0/16:1), which are HMP-PG species. At the same time, there was a significant increase of 18C FA-containing unsaturated PG species. The relative levels of several 18:3-containing PG species, e.g., PG(18:3/16:0), were positively correlated with freezing tolerance and latitude and negatively correlated with some local temperature variables including mean temperature of the coldest quarter, providing more evidence as to the role of 18:3-PGs in plant freezing tolerance.

Under super-cold stress, lipid changes were also observed in low abundant lipid classes such as GlcCer and ASG. There was an overall reduction in the contents of four GlcCer species. Among the four GlcCer species, the relative content of GlcCer(d18:1-h16:0) and GlcCer(t18:1-h22:0) after super-cold treatment were highly correlated with freezing tolerance. These results are consistent with previous observations on GlcCer during cold acclimation, in which GlcCer significantly declined and GlcCer (d18:1/h16:0) was negatively correlated with leaf freezing tolerance after acclimation (Degenkolbe et al., 2012). Arabidopsis mutants deficient in sphingoid long-chain base $\Delta 8$ desaturase activity were cold-sensitive, displaying impaired growth and survival at low temperature, indicating the role of specific GlcCer species for cold tolerance (Chen et al., 2012). As essential component of plasma membrane and tonoplasts, GlcCer probably contributes to physiological properties and functions of membranes under cold and freezing stress (Minami et al., 2009; Uemura et al., 1995). Sphingolipids are present in rafts and can function as signaling messenger in response to cold, and phytosphingosine phosphate was

reported to play important roles upstream of cold-induced CBF signaling pathway during cold acclimation (Dutilleul et al., 2012). Here, the decrease of GlcCer is hypothesized contribute to a greater hydration of the plasma membrane that could, in turn, increase membrane stability during cold stress.

Our lipidomics study also revealed a significant reduction in the total content of ASG, especially the glycosylated forms of sitosterol and stigmasterol. Sitosterol-Glc(16:0), Sitosterol-Glc(18:3), and Campesterol-Glc(16:0) were negatively correlated with freezing tolerance, latitude, and positively correlated with some local temperature variables such as annual mean temperature, indicating some ASG species might be negative indicators for freezing tolerance. Our observations of the changes in sterol profiles are inconsistent with previous publications showing that in *Arabidopsis* ASGs largely increased after a 10-day cold acclimation (Tarazona et al., 2015). Transgenic experiments using knockout and overexpression mutants for a sterol glycosyltransferases TTG15 demonstrated roles of SG and ASG in freezing tolerance (Mishra et al., 2015).

Among the 30 candidate genes (Table S4-11) related to lipid metabolism under super-cold stress, 6 of these genes encode enzymes with functions directly related to the lipid-level phenotypes associated with them. The associations identified in our study are in accordance with known effects on lipid metabolism characterized by previous work for 6 characterized genes (*FAD2*, *FAD7*, *LOH2*, *KCS9*, *FAB1*, *GGPPS11*).

FAD2 encodes an ω -6 desaturase which is mainly responsible for the biosynthesis of 18:2-PLs in ER (Browse et al., 1993; Miquel & Browse, 1992). The highest SNP in genomic region #20 identified from our GWAS linked to *FAD2* was located at the intron within the 5' UTR and was associated with 3 lipid-level phenotypes (PC(18:1/18:3), PE(18:1/18:3),

PI(16:0/18:1)). Interestingly, previous QTL mapping found a QTL containing *FAD2* for fatty acid composition in seed oil of *Arabidopsis* (Hobbs et al., 2004; O'Neill et al., 2012; Sanyal & Linder, 2012). More recently, a GWAS based on the MAGIC population and another natural population of 391 accessions also revealed the same sequence variant strongly associated with 18:1, 18:2, and 20:2 proportions in seed oil (Branham et al., 2016; Menard et al., 2017). The most significant SNP (Chr3_3862256) identified in their GWAS was situated in the intron of the 5' UTR of *FAD2*, and variation in this SNP was highly associated with the gene expression level (Menard et al., 2017). Our GWAS analysis focused on molecular species composition of leaf phospholipids and also detected a significant SNP located in 5' UTR of the *FAD2* but at different locus (Chr3_3862612). Haplotype analysis using this SNP (Chr3_3862612) showed that the major allele group with nucleotide A had significantly lower average level of 18:1-PL species and higher average level of 18:2-PL species than the minor allele group with nucleotide G. Under super-cold stress, the transcript abundance of *FAD2* in the major allele group with allele A was significantly higher than *FAD2* level in the minor group with allele G among 20 investigated accessions. Additionally, there was significant difference in latitude between the two haplotypes in 360 accessions, and accessions in the minor allele group had a world distribution with a lower average latitude. In addition, the relative contents of several PC and PE species, including PC(18:1/18:3) and PC(18:2/18:2), were significantly correlated with freezing tolerance, which is consistent with predictions based on the haplotype analysis of lipid level and latitude. Finally, we propose a model illustrating the role of ω -6 phospholipids in plant freezing tolerance: the natural non-coding variant SNP at Chr3_3862612 in the 5' UTR of *FAD2* affects gene expression, causing phenotypic variation in ω -6 desaturation in leaf phospholipids after super-cold treatment, and variation in freezing tolerance, and geographic distribution. Accessions in the major allele

group tends to better maintain their membrane fluidity and have higher freezing tolerance than accessions in minor allele group during cold due to higher proportion of 18:2 in major PLs.

FAD7, which is a chloroplast localized ω -3 desaturase and responsible for the synthesis of 16:3 and 18:3 fatty acids from galactolipids (Iba et al., 1993), was significantly associated with variation in MGDG(18:3/16:2), MGDG(18:2/18:3), and DGDG(18:3/16:2) under super-cold condition. Although *FAD7* is the major ω -3 desaturase in leaves, another highly homologous ω -3 desaturase, *FAD8*, has been reported to be a cold-specific desaturase and to have different substrate specificity from *FAD7* (Román et al., 2015; Soria-Garci A et al., 2019), leaving open the possibility that *FAD7* and *FAD8* may play complementary roles related to cold and freezing tolerance. Transgenic tobacco and tomato lines with increased expression of *FAD7* had enhanced resistance to cold stress (Domínguez et al., 2010; Kodama et al., 1994), indicating the potential role of *FAD7* in cold tolerance. In our GWAS results, 3 significant SNPs linked to *FAD7* were associated with lipid-level phenotypes of MGDG(18:3/16:2), MGDG(18:2/18:3), and DGDG(18:3/16:2). Haplotype analysis using the missense SNP (Chr3_3501980) showed that the major allele group had higher levels of MGDG(18:3/16:2) and MGDG(18:2/18:3) than the minor allele group. Correlation analysis showed that MGDG(18:3/16:2) and MGDG(18:2/18:3) levels were positively correlated with freezing tolerance, indicating the potential role of 18:3-MGDGs for freezing tolerance. The membrane physiochemical properties in plastid are modulated by fatty acyl desaturation level in MGDG, DGDG, and PG. Lower temperatures are often associated with an increase in the production of PUFAs, such as 18:3, which is thought to maintain membrane fluidity because of their lower melting temperatures (Iba, 2002; Nishida & Murata, 1996). Our lipidomics and GWAS results revealed that *FAD7*

regulates ω -3 desaturation in galactolipids, and an increased proportion of 18:3 in chloroplast membranes results in better performance of *Arabidopsis* under low temperature.

LOH2 and *KCS9* were identified from GWAS using the relative content of GlcCer species under cold stress as the phenotype. *LOH2* is a ceramide synthase essential for production of C16-ceramides using palmitoyl-CoA and dihydroxy LCB substrates (Markham et al., 2011). Ceramides are precursors for more complex sphingolipids like GlcCer, so the level in GlcCer can be regulated by *LOH2*. Haplotype analysis showed that sequence variant (G/A, Chr3_6669405) in the 3' UTR of *LOH2* was responsible for variation in GlcCer(d18:1/h16:0) and GlcCer(t18:1-h16:0) levels. The gene *KCS9*, which was identified for GlcCer (t18:1-h22:0), encodes a 3-ketoacyl-CoA synthase involved in biosynthesis of VLCFA (from 22C-FA to 24C-FA) in *Arabidopsis* (Kim et al., 2013). Only one significant SNP was linked to *KCS9* and it is a nonsynonymous mutation in the coding sequence (T/C, Chr2_7051376). Haplotype analysis using the SNP (Chr2_7051376) showed that this nonsynonymous mutation in *KCS9* was associated with natural variation in the relative level of VLCFA-GlcCer. The relative levels of GlcCer (d18:1-h16:0) and GlcCer (t18:1-h22:0) were negatively correlated with freezing tolerance and latitude, indicating lower levels of specific GlcCer species lead to better performance of *Arabidopsis* in response to low temperature. Sphingolipids and sterols are essential components of plasma membrane, and the decrease of GlcCer is hypothesized contribute to a greater hydration of the plasma membrane that could, in turn, increase membrane stability during cold stress. Accessions with lower GlcCers during cold may have higher membrane stability and freezing tolerance.

FABI, encodes a plastidic beta-ketoacyl-ACP synthase II (KASII), involved in fatty acid elongation from 16:0-ACP to 18:0-ACP (Wu et al., 1994). PG is the only chloroplast

glycerolipid that is produced solely by the prokaryotic pathway so fatty acid composition in PG is largely regulated by FAB1. *fab1* mutants of Arabidopsis had high levels of HMP-PG similar to many chilling-sensitive plant species and showed a collapse of photosynthesis after >10 d of exposure to 2°C (Wu et al., 1997). Recently, a study provided more evidence demonstrating the role of FAB1 for chloroplast photosynthetic function and chilling tolerance (Gao et al., 2020). In our study, a SNP (Chr1_28156734) situated upstream of *FAB1* (AT1G74960) had significant associations with the relative level of PG(16:0/16:1). Haplotype analysis showed SNP (Chr1_28156734) caused the difference in relative abundance of 32C-PG between major allele group and minor allele group. HMP-PG species can induce a phase change from liquid crystalline to gel phase under cold and thereby disrupt membrane and chloroplast functions (Murata & Yamaya, 1984). Our GWAS results are consistent with previous studies on FAB1 suggesting an important role of 32C-PG in chilling tolerance.

GGPPS11, encodes a protein with geranylgeranyl pyrophosphate synthase activity involved in isoprenoid biosynthesis. GGPPS11 is a hub isozyme for the production of most photosynthesis-related isoprenoids, which are essential for photosynthesis (Ruiz-Sola et al., 2016b). Another study revealed that *GGPPS11* encodes two differentially targeted isoforms. The short enzyme localizes in the cytosol and is involved in the mevalonic acid (MVA) pathway for geranylgeranyl diphosphate (GGPP) biosynthesis (Ruiz-Sola et al., 2016a). Although sterols are synthesized from farnesyl diphosphate (FPP), its level might be regulated by GGPPS11 because FPP and GGPP are synthesized from same precursor dimethylallyl diphosphate (DMAPP) (Ruiz-Sola et al., 2016b). Our GWAS results on two sterol ester species sitosterol(18:2) and sitosterol(18:3) showed a significant SNP (Chr4_17343444) located in 5' UTR of *GGPPS11*.

However, the exact role of GGPPS11 in sterol lipids biosynthesis and freezing tolerance is still elusive.

Figures

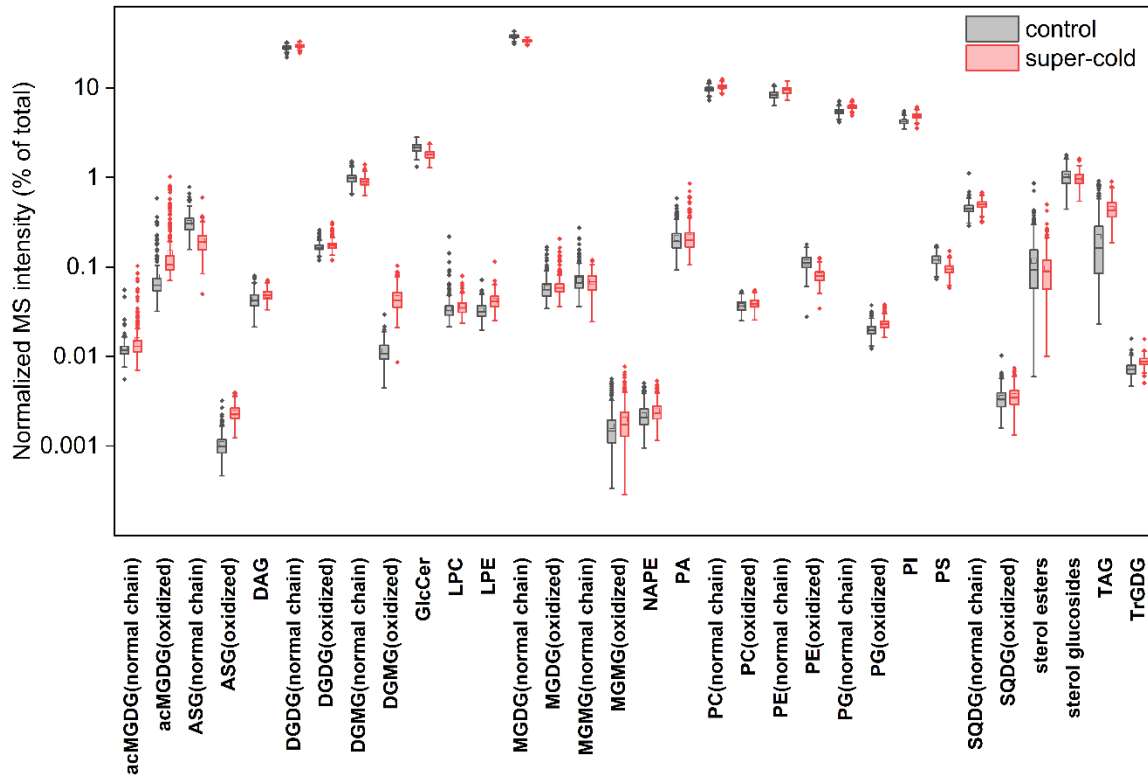


Figure 3-1. Changes in the relative contents of 32 lipid classes in leaf tissues among the 360 investigated Arabidopsis accessions in unstressed and super-cold treated group

Changes in the leaf relative contents (% of total) of 32 lipid classes in the 360 investigated Arabidopsis accessions in unstressed (grey boxes) and super-cold (red boxes) group. Standard box plots are shown with horizontal bars in the boxes representing the median, bottom and top of the box indicate the 25th and 75th percentiles (lower and upper quartiles). Whiskers indicate 1.5-fold interquartile range, diamonds represent potential outliers. Note that the y-axis is log₁₀ scaled, due to the large differences in the relative contents of various lipids.

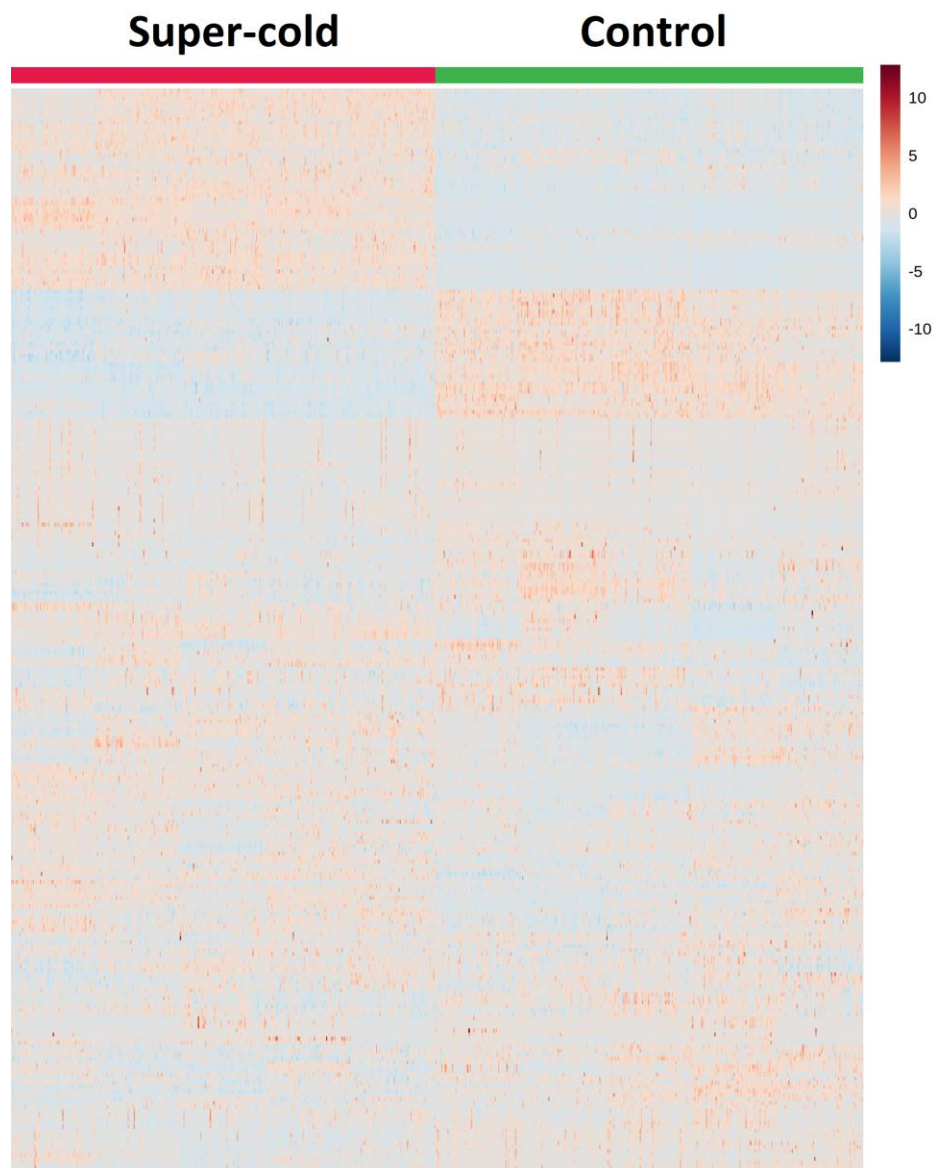


Figure 3-2. Heatmap of autoscaled lipid levels in unstressed (control) and super-cold treated leaves in 360 accessions

Note: 270 analytes are shown in 720 columns. Each column represents the mean value of 3 replicates for every investigated accession (a total of 360 accessions) under unstressed (control) or super-cold stress.

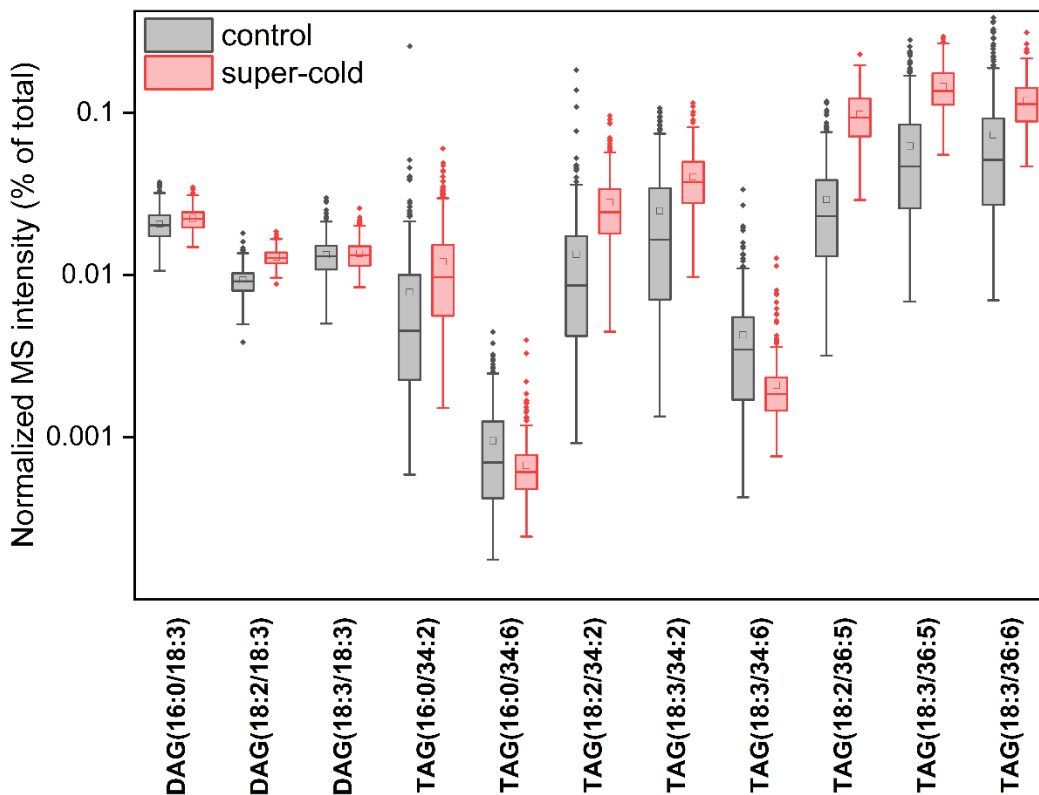


Figure 3-3. Changes in the relative contents of 11 DAG, TAG species in leaf tissues in the 360 investigated Arabidopsis accessions in standard condition (control) and after super-cold treatment

Changes in the leaf relative contents (% of total) of 11 DAG, TAG species in the 360 investigated Arabidopsis accessions of unstressed (grey boxes) and super-cold (red boxes) group. Standard box plots are shown with horizontal bars in the boxes representing the median, bottom and top of the box indicate the 25th and 75th percentiles (lower and upper quartiles). Whiskers indicate 1.5-fold interquartile range, diamonds represent potential outliers. Note that the y-axis was log₁₀ scaled, due to the large differences in the contents of the lipid classes.

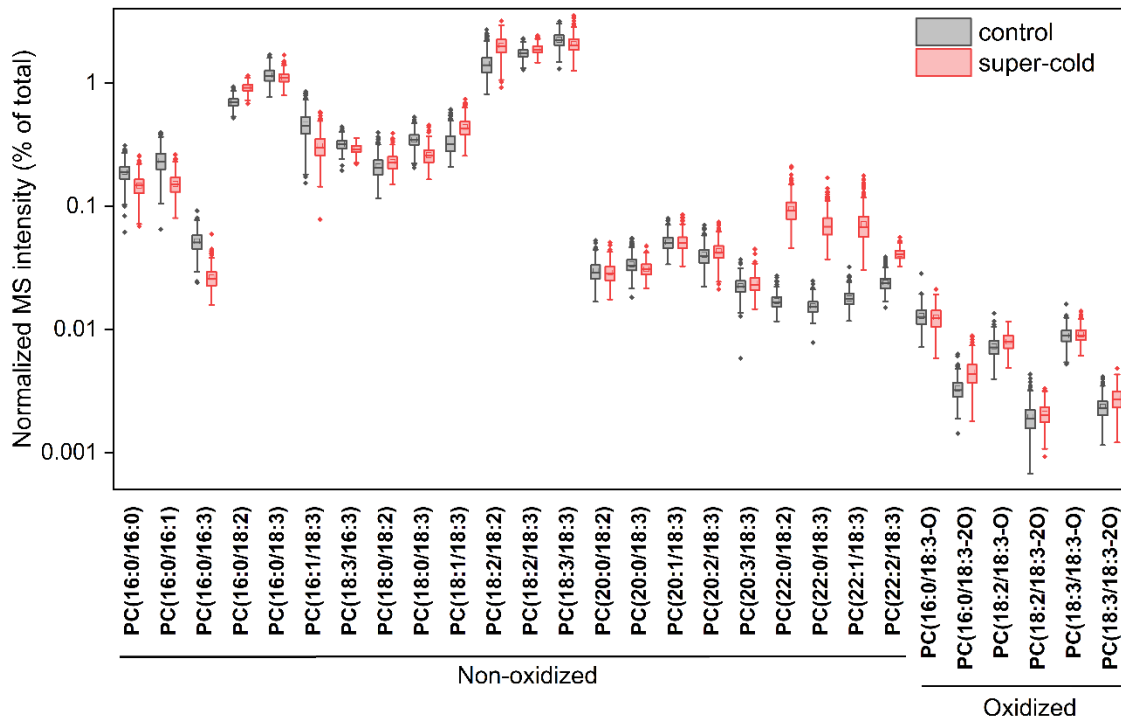


Figure 3-4. Changes in the relative contents of 28 PC species in leaf tissues among the 360 investigated Arabidopsis accessions in unstressed and super-cold treated group

Changes in the leaf relative contents (% of total) of 28 PC species in the 360 investigated Arabidopsis accessions in unstressed (grey boxes) and super-cold (red boxes) group. Standard box plots are shown with horizontal bars in the boxes representing the median, bottom and top of the box indicate the 25th and 75th percentiles (lower and upper quartiles). Whiskers indicate 1.5-fold interquartile range, diamonds represent potential outliers. Note that the y-axis was log₁₀ scaled, due to the large differences in the relative contents of various lipids.

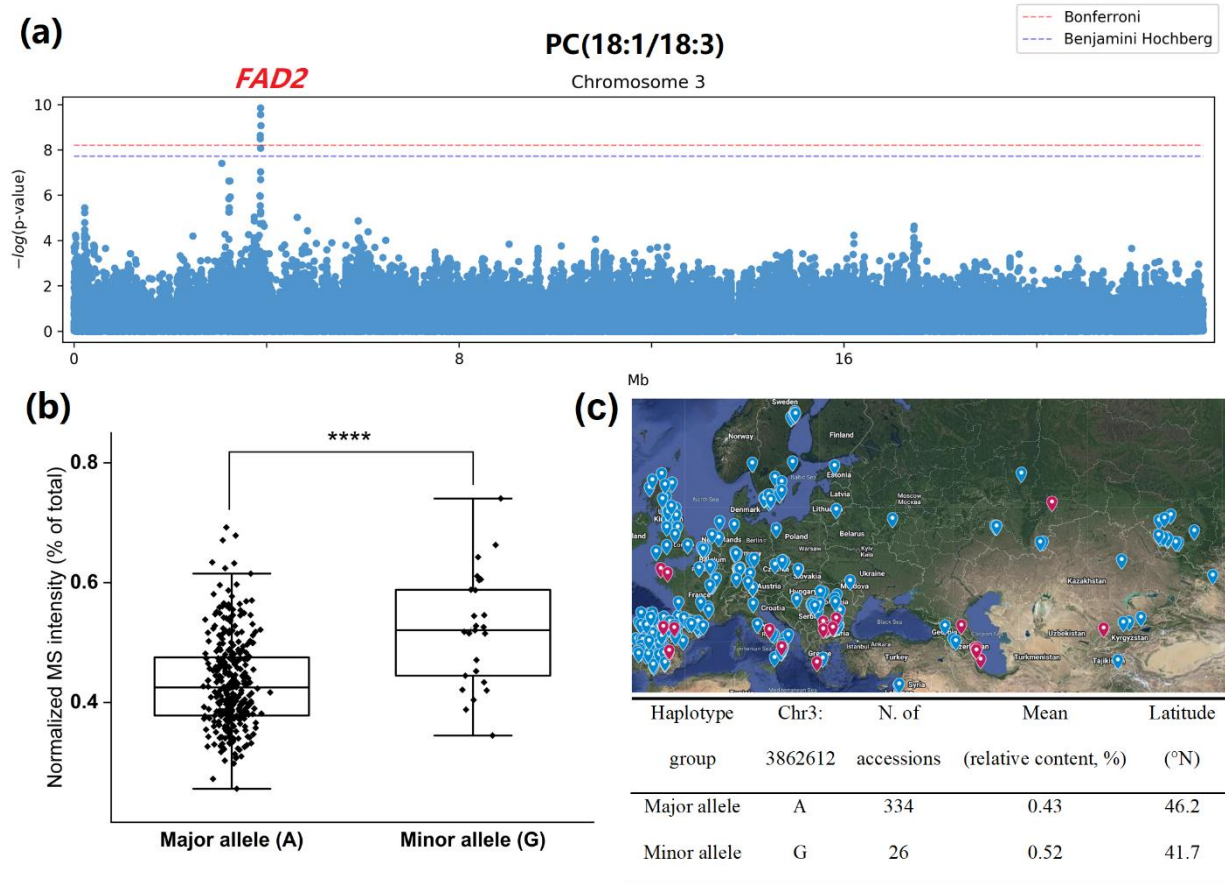


Figure 3-5. The relative level of PC (18:1/18:3) is associated with the SNP in the 5' UTR intron of *FAD2*

(a) Manhattan plot of GWAS of relative level (%) of PC(18:1/18:3). (b) Haplotype analysis of relative level of PC(18:1/18:3) in 360 natural accessions based on the SNP at Chr3_3862612.

Symbols show the distribution of relative level of PC(18:1/18:3) in two haplotype groups. Error bars represent SD. Asterisks above the bars indicate significant difference between groups (Student's t-test, $P < 0.0001$).

(c) Geographic distribution of the two haplotype groups in the world. Blue pins represent accessions in major allele group, and red pins represent accessions in minor allele group.

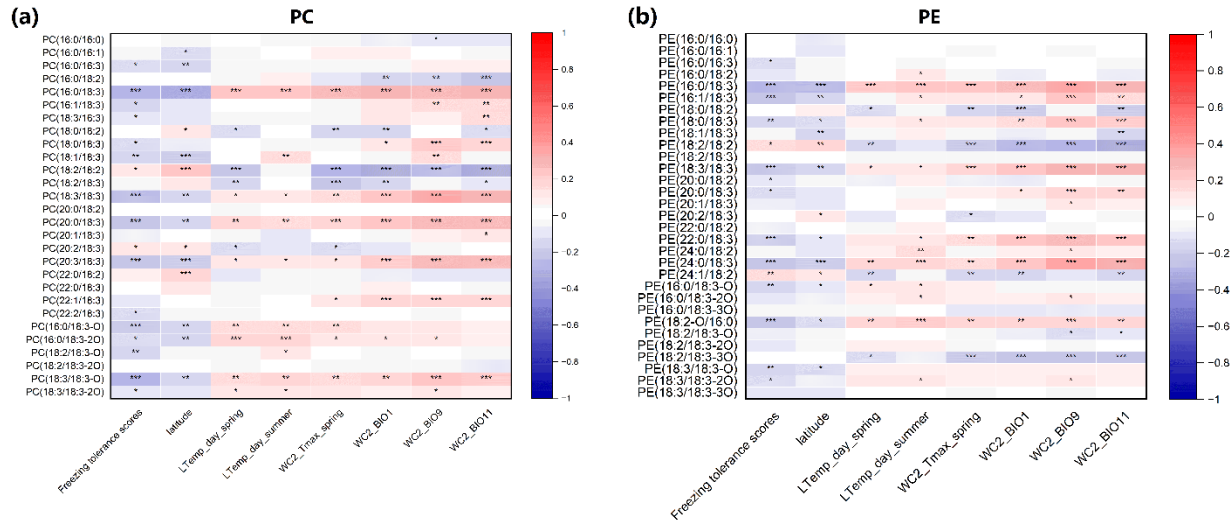


Figure 3-6. Correlation heatmaps of correlations of relative contents of individual PC and PE species with freezing tolerance, latitude, and some local temperature variables

Correlation heatmaps were constructed based on correlations of relative content of PC and PE species with freezing tolerance, latitude, and some local temperature variables. Color in each cell indicates the Pearson’s correlation coefficients. Red indicates positive correlations and blue indicates negative correlations. The number of asterisks indicates the significance of correlation,

* $P \leq 0.05$, ** $P \leq 0.01$, *** $P \leq 0.001$.

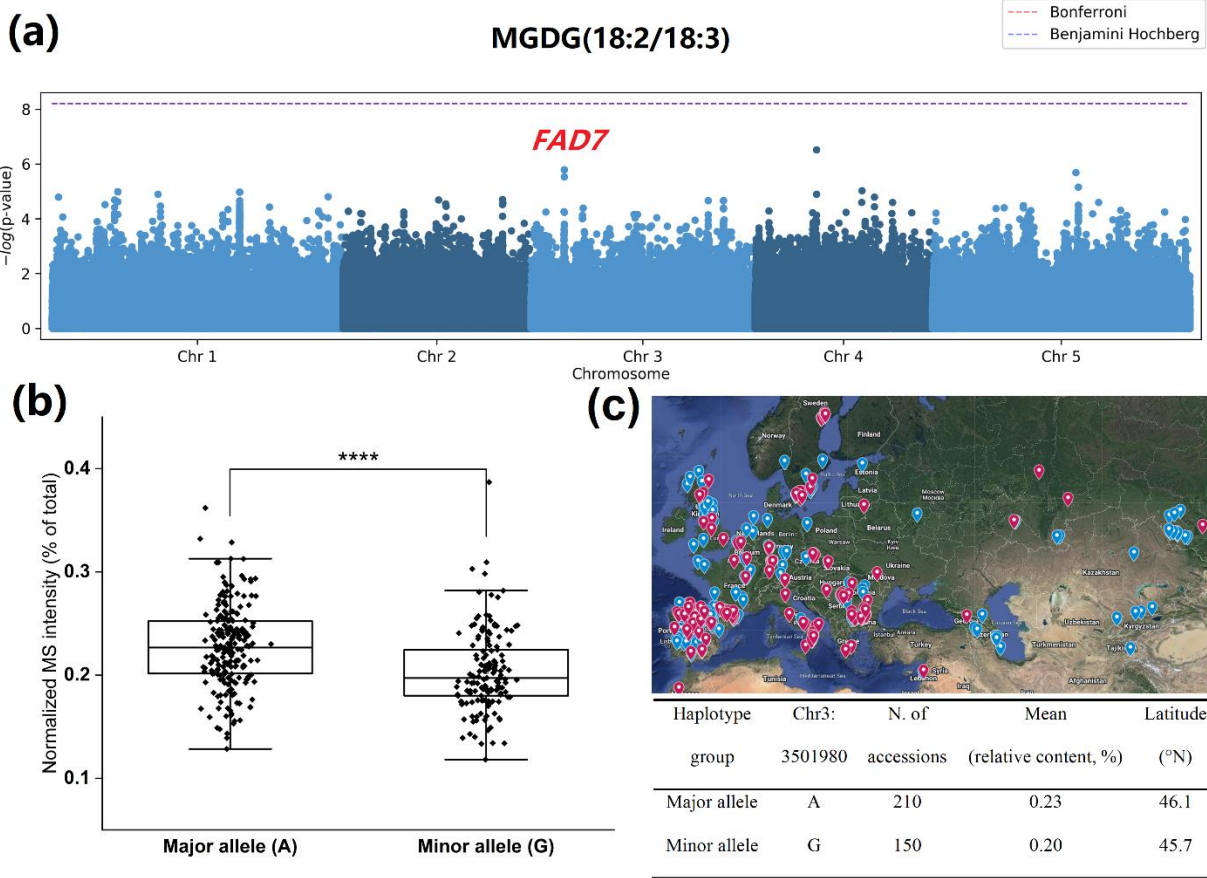


Figure 3-7. The relative level of MGDG (18:2/18:3) is associated with missense SNP in *FAD7*

(a) Manhattan plot of GWAS of relative level (%) of MGDG(18:2/18:3). (b) Haplotype analysis of relative level of MGDG(18:2/18:3) in 360 natural accessions based on the SNP at Chr3_3501980. Symbols show the distribution of relative level of MGDG(18:2/18:3) in two haplotype groups. Error bars represent SD. Asterisks above the bars indicate significant difference between groups (Student's t-test, $P < 0.0001$). (c) Geographic distribution of the two haplotype groups in the world. Blue pins represent accessions in major allele group, red pins represent accessions in minor allele group.

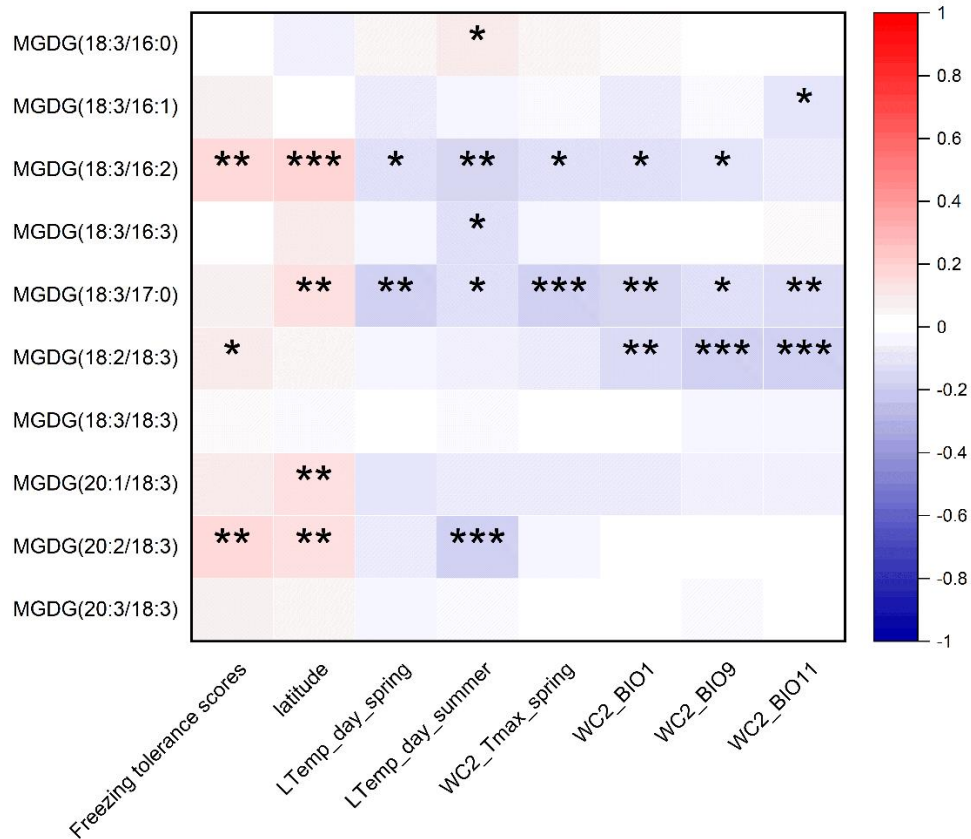


Figure 3-8. Correlation heatmaps of correlations of relative contents of individual MGDG species with freezing tolerance, latitude, and some local temperature variables

Correlation heatmaps were constructed based on correlations of relative content of MGDG species with freezing tolerance, latitude, and some local temperature variables. Color in each cell indicates the Pearson's correlation coefficients. Red indicates positive correlations and blue indicates negative correlations. The number of asterisks indicates the significance of correlation,

* $P \leq 0.05$, ** $P \leq 0.01$, *** $P \leq 0.001$.

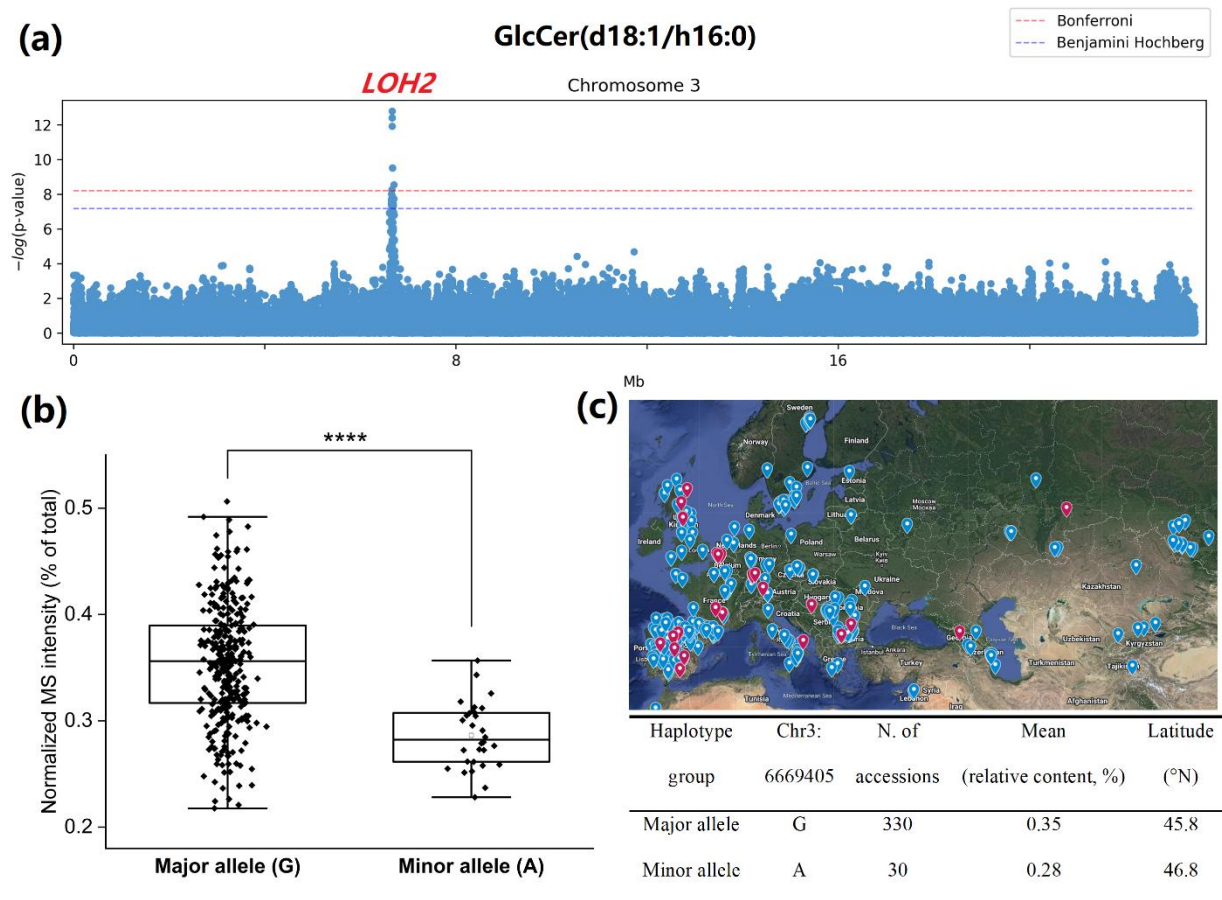


Figure 3-9. The relative level of GlcCer (d18:1-h16:0) is associated with the SNP in 3' UTR of *LOH2*

(a) Manhattan plot of genome-wide association study (GWAS) of relative level (%) of GlcCer(d18:1-h16:0). (b) Haplotype analysis of relative level of GlcCer(d18:1-h16:0) in 360 natural accessions based on the SNP (Chr3_6669405) and geographic distribution of the two haplotype groups in the world. Diamond plots showing the distribution of relative level of GlcCer(d18:1-h16:0) in two haplotype groups. Error bars represent SD. Asterisks above the bars indicate significant difference between groups (Student's t-test, $P < 0.0001$). Blue pins represent accessions in major allele group, red pins represent accessions in minor allele group.

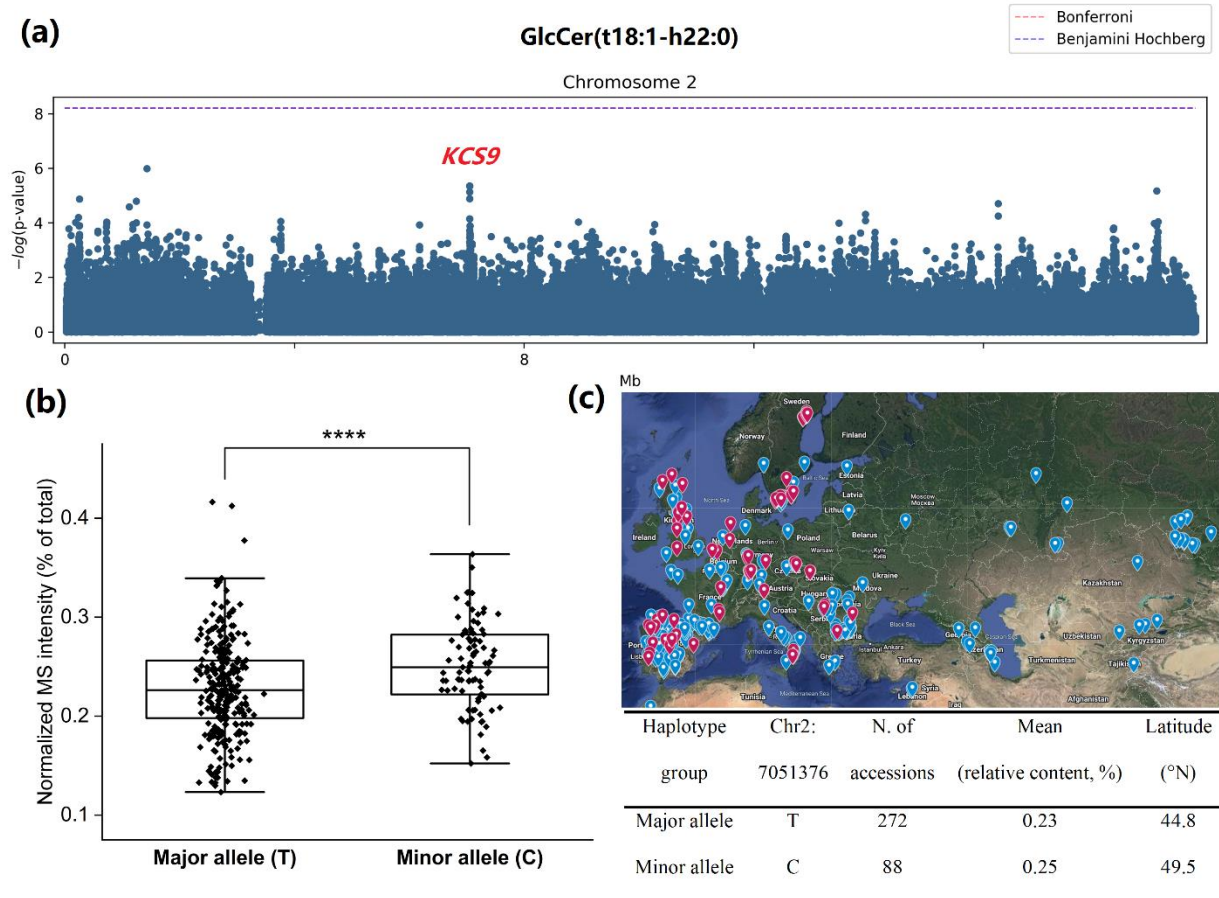


Figure 3-10. The relative level of GlcCer (t18:1-h22:0) is associated with missense SNP of *KCS9*

(a) Manhattan plot of genome-wide association study (GWAS) of relative level (%) of GlcCer (t18:1-h22:0). (b) Haplotype analysis of relative level of GlcCer (t18:1-h22:0) in 360 natural accessions based on the SNP (Chr3_6669405) and geographic distribution of the two haplotype groups in the world. Diamond plots showing the distribution of relative level of GlcCer (t18:1-h22:0) in two haplotype groups. Error bars represent SD. Asterisks above the bars indicate significant difference between groups (Student's t-test, $P < 0.0001$). Blue pins represent accessions in major allele group, red pins represent accessions in minor allele group.

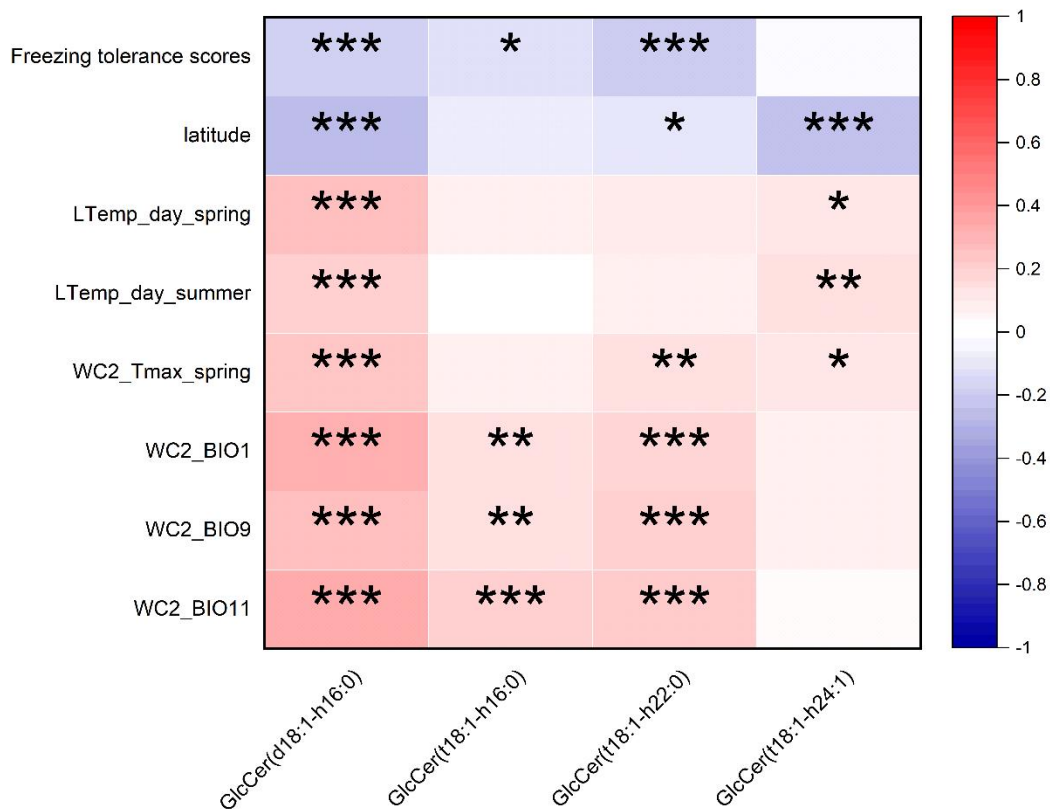


Figure 3-11. Correlation heatmaps of correlations of relative contents of individual GlcCer species with freezing tolerance, latitude, and some local temperature variables

Correlation heatmaps were constructed based on correlations of relative content of GlcCer species with freezing tolerance, latitude, and some local temperature variables. Color in each cell indicates the Pearson's correlation coefficients. Red indicates positive correlations and blue indicates negative correlations. The number of asterisks indicates the significance of correlation, * $P \leq 0.05$, ** $P \leq 0.01$, *** $P \leq 0.001$.

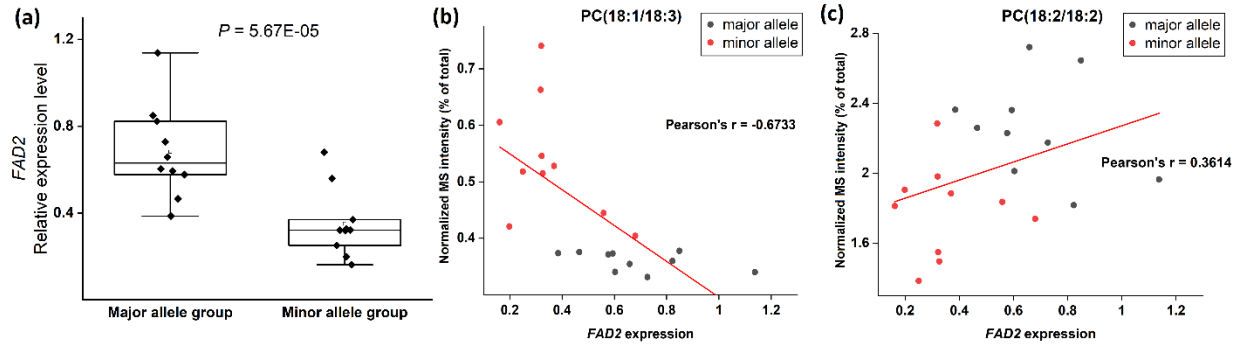


Figure 3-12. Relationship between *FAD2* expression level and the relative content of two PC species

(a) Haplotype analysis of *FAD2* expression level under super-cold stress in 20 natural accessions. Diamond plots showing the distribution of gene expression in two haplotype groups categorized by the SNP at Chr3_3862612. Error bars represent SD. The exact *P*-values from Student's t-test are shown above. Linear regression between *FAD2* expression and the relative content of PC(18:1/18:3) (b) and PC(18:2/18:2) (c). Black circles represent 10 accessions that have nucleotide variant A and red circles represent 10 accessions that have nucleotide variant G at the SNP (Chr3_3862612).

Tables

Table 3-1. Summary statistics of variation and heritability for 32 lipid classes in 360 accessions of Arabidopsis after super-cold treatment

Lipid class/ sub-class	Mean	SD ^a	Minimum	Maximum	Range	CoV ^b	H ^{2c} (%)
acMGDG (normal chain)	0.015	0.0097	0.0070	0.10	0.095	64.10	10
acMGDG (oxidized)	0.14	0.12	0.070	1.02	0.95	84.36	12
ASG (normal chain)	0.19	0.053	0.050	0.60	0.55	27.13	44
ASG (oxidized)	0.0023	0.00049	0.0012	0.0039	0.0027	20.95	29
sterol glucosides	0.97	0.17	0.54	1.61	1.07	17.20	65
sterol esters	0.097	0.058	0.010	0.50	0.49	59.48	81
DAG	0.049	0.0069	0.033	0.071	0.038	14.12	73
TAG	0.44	0.13	0.18	0.90	0.71	28.39	64
GlcCer	1.80	0.21	1.28	2.40	1.11	11.68	42
NAPE	0.0024	0.00064	0.0011	0.0053	0.042	25.94	69
DGDG (normal chain)	29.53	1.31	24.59	32.99	8.40	4.44	60
DGDG (oxidized)	0.17	0.022	0.12	0.31	0.20	12.67	18
DGMG (normal chain)	0.91	0.11	0.62	1.39	0.77	11.77	65
DGMG (oxidized)	0.045	0.013	0.0086	0.10	0.095	30.23	22
LPC	0.036	0.069	0.023	0.079	0.056	19.24	14
LPE	0.042	0.085	0.025	0.11	0.089	20.18	16
MGDG (normal chain)	33.60	1.13	29.89	36.70	6.81	3.35	44
MGDG (oxidized)	0.061	0.017	0.036	0.21	0.17	27.64	23
MGMG (normal chain)	0.068	0.017	0.024	0.12	0.095	24.54	10
MGMG (oxidized)	0.0020	0.0010	0.00029	0.0077	0.0074	53.09	14
PA	0.22	0.083	0.10	0.86	0.75	38.27	18
PC (normal chain)	10.30	0.66	8.56	12.57	4.01	6.46	58
PC (oxidized)	0.039	0.0054	0.025	0.055	0.029	13.85	43
PE (normal chain)	9.39	0.89	7.28	11.97	4.69	9.47	45
PE (oxidized)	0.080	0.013	0.034	0.12	0.091	16.25	60
PG (normal chain)	6.17	0.34	4.92	7.33	2.41	5.48	76
PG (oxidized)	0.023	0.0034	0.016	0.038	0.022	14.47	34
PI	4.88	0.34	3.55	6.10	2.55	6.90	58
PS	0.095	0.013	0.058	0.15	0.092	14.18	50
SQDG (normal chain)	0.50	0.052	0.32	0.68	0.36	10.51	60
SQDG (oxidized)	0.0036	0.00096	0.0013	0.0075	0.0061	26.73	11
TrGDG	0.0088	0.0011	0.0050	0.016	0.011	12.05	50

^astandard deviation, ^bcoefficient of variation, ^cnarrow-sense heritability.

References

- Abdurakhmonov, I. Y., & Abdukarimov, A. (2008). Application of association mapping to understanding the genetic diversity of plant germplasm resources. *International Journal of Plant Genomics*, 2008, 574927.
- Barrero-Sicilia, C., Silvestre, S., Haslam, R. P., & Michaelson, L. V. (2017). Lipid remodelling: Unravelling the response to cold stress in *Arabidopsis* and its extremophile relative *Eutrema salsugineum*. *Plant Science: An International Journal of Experimental Plant Biology*, 263, 194–200.
- Batsale, M., Bahammou, D., Fouillen, L., Mongrand, S., Joubès, J., & Domergue, F. (2021). Biosynthesis and Functions of Very-Long-Chain Fatty Acids in the Responses of Plants to Abiotic and Biotic Stresses. *Cells*, 10, 1284.
- Branham, S. E., Wright, S. J., Reba, A., & Linder, C. R. (2016). Genome-Wide Association Study of *Arabidopsis thaliana* Identifies Determinants of Natural Variation in Seed Oil Composition. *The Journal of Heredity*, 107, 248–256.
- Browse, J., McConn, M., James, D., & Miquel, M. (1993). Mutants of *Arabidopsis* deficient in the synthesis of alpha-linolenate. Biochemical and genetic characterization of the endoplasmic reticulum linoleoyl desaturase. *The Journal of Biological Chemistry*, 268, 16345–16351.
- Burgos, A., Szymanski, J., Seiwert, B., Degenkolbe, T., Hannah, M. A., Giavalisco, P., & Willmitzer, L. (2011). Analysis of short-term changes in the *Arabidopsis thaliana* glycerolipidome in response to temperature and light. *The Plant Journal: For Cell and Molecular Biology*, 66, 656–668.
- Chen, L., Hu, W., Mishra, N., Wei, J., Lu, H., Hou, Y., Qiu, X., Yu, S., Wang, C., Zhang, H., Cai, Y., Sun, C., & Shen, G. (2020). AKR2A interacts with KCS1 to improve VLCFAs contents and chilling tolerance of *Arabidopsis thaliana*. *The Plant Journal: For Cell and Molecular Biology*, 103, 1575–1589.
- Chen, Ming, Markham, J. E., & Cahoon, E. B. (2012). Sphingolipid $\Delta 8$ unsaturation is important for glucosylceramide biosynthesis and low-temperature performance in *Arabidopsis*. *The Plant Journal: For Cell and Molecular Biology*, 69, 769–781.
- Chen, Mingjie, & Thelen, J. J. (2013). ACYL-LIPID DESATURASE2 is required for chilling and freezing tolerance in *Arabidopsis*. *The Plant Cell*, 25, 1430–1444.
- Chen, Q.-F., Xu, L., Tan, W.-J., Chen, L., Qi, H., Xie, L.-J., Chen, M.-X., Liu, B.-Y., Yu, L.-J., Yao, N., Zhang, J.-H., Shu, W., & Xiao, S. (2015). Disruption of the *Arabidopsis* Defense Regulator Genes SAG101, EDS1, and PAD4 Confers Enhanced Freezing Tolerance. *Molecular Plant*, 8, 1536–1549.

- Degenkolbe, T., Giavalisco, P., Zuther, E., Seiwert, B., Hinch, D. K., & Willmitzer, L. (2012). Differential remodeling of the lipidome during cold acclimation in natural accessions of *Arabidopsis thaliana*. *The Plant Journal: For Cell and Molecular Biology*, *72*, 972–982.
- Domínguez, T., Hernández, M. L., Pennycooke, J. C., Jiménez, P., Martínez-Rivas, J. M., Sanz, C., Stockinger, E. J., Sánchez-Serrano, J. J., & Sanmartín, M. (2010). Increasing omega-3 desaturase expression in tomato results in altered aroma profile and enhanced resistance to cold stress. *Plant Physiology*, *153*, 655–665.
- Dunn, W. B., Broadhurst, D., Begley, P., Zelena, E., Francis-McIntyre, S., Anderson, N., Brown, M., Knowles, J. D., Halsall, A., Haselden, J. N., Nicholls, A. W., Wilson, I. D., Kell, D. B., Goodacre, R., & Human Serum Metabolome (HUSERMET) Consortium. (2011). Procedures for large-scale metabolic profiling of serum and plasma using gas chromatography and liquid chromatography coupled to mass spectrometry. *Nature Protocols*, *6*, 1060–1083.
- Dutilleul, C., Benhassaine-Kesri, G., Demandre, C., Rézé, N., Launay, A., Pelletier, S., Renou, J.-P., Zachowski, A., Baudouin, E., & Guillas, I. (2012). Phytosphingosine-phosphate is a signal for AtMPK6 activation and *Arabidopsis* response to chilling. *The New Phytologist*, *194*, 181–191.
- Fan, J., Yan, C., & Xu, C. (2013a). Phospholipid:diacylglycerol acyltransferase-mediated triacylglycerol biosynthesis is crucial for protection against fatty acid-induced cell death in growing tissues of *Arabidopsis*. *The Plant Journal*, *76*, 930–942.
- Fan, J., Yan, C., Zhang, X., & Xu, C. (2013b). Dual role for phospholipid:diacylglycerol acyltransferase: Enhancing fatty acid synthesis and diverting fatty acids from membrane lipids to triacylglycerol in *Arabidopsis* leaves. *The Plant Cell*, *25*, 3506–3518.
- Ferrero-Serrano, Á., & Assmann, S. M. (2019). Phenotypic and genome-wide association with the local environment of *Arabidopsis*. *Nature Ecology & Evolution*, *3*, 274–285.
- Gao, J., Lunn, D., Wallis, J. G., & Browse, J. (2020). Phosphatidylglycerol Composition Is Central to Chilling Damage in the *Arabidopsis fab1* Mutant. *Plant Physiology*, *184*, 1717–1730.
- Gao, J., Wallis, J. G., & Browse, J. (2015). Mutations in the Prokaryotic Pathway Rescue the fatty acid biosynthesis1 Mutant in the Cold. *Plant Physiology*, *169*, 442–452.
- Gilmour, S. J., Hajela, R. K., & Thomashow, M. F. (1988). Cold Acclimation in *Arabidopsis thaliana*. *Plant Physiology*, *87*, 745–750.
- Hannah, M. A., Wiese, D., Freund, S., Fiehn, O., Heyer, A. G., & Hinch, D. K. (2006). Natural genetic variation of freezing tolerance in *Arabidopsis*. *Plant Physiology*, *142*, 98–112.
- Harayama, T., & Riezman, H. (2018). Understanding the diversity of membrane lipid composition. *Nature Reviews. Molecular Cell Biology*, *19*, 281–296.

- Hobbs, D. H., Flintham, J. E., & Hills, M. J. (2004). Genetic control of storage oil synthesis in seeds of *Arabidopsis*. *Plant Physiology*, *136*, 3341–3349.
- Hruz, T., Wyss, M., Docquier, M., Pfaffl, M. W., Masanetz, S., Borghi, L., ... Zimmermann, P. (2011). RefGenes: Identification of reliable and condition specific reference genes for RT-qPCR data normalization. *BMC Genomics*, *12*, 156.
- Hugly, S., & Somerville, C. (1992). A role for membrane lipid polyunsaturation in chloroplast biogenesis at low temperature. *Plant Physiology*, *99*, 197–202.
- Iba, K. (2002). Acclimative response to temperature stress in higher plants: Approaches of gene engineering for temperature tolerance. *Annual Review of Plant Biology*, *53*, 225–245.
- Iba, K., Gibson, S., Nishiuchi, T., Fuse, T., Nishimura, M., Arondel, V., Hugly, S., & Somerville, C. (1993). A gene encoding a chloroplast omega-3 fatty acid desaturase complements alterations in fatty acid desaturation and chloroplast copy number of the *fad7* mutant of *Arabidopsis thaliana*. *The Journal of Biological Chemistry*, *268*, 24099–24105.
- Kim, H. U., Vijayan, P., Carlsson, A. S., Barkan, L., & Browse, J. (2010). A mutation in the LPAT1 gene suppresses the sensitivity of *fab1* plants to low temperature. *Plant Physiology*, *153*, 1135–1143.
- Kim, J., Jung, J. H., Lee, S. B., Go, Y. S., Kim, H. J., Cahoon, R., Markham, J. E., Cahoon, E. B., & Suh, M. C. (2013). *Arabidopsis* 3-ketoacyl-coenzyme a synthase9 is involved in the synthesis of tetracosanoic acids as precursors of cuticular waxes, suberins, sphingolipids, and phospholipids. *Plant Physiology*, *162*, 567–580.
- Kodama, H., Hamada, T., Horiguchi, G., Nishimura, M., & Iba, K. (1994). Genetic Enhancement of Cold Tolerance by Expression of a Gene for Chloroplast [omega]-3 Fatty Acid Desaturase in Transgenic Tobacco. *Plant Physiology*, *105*, 601–605.
- Li, H.-M., & Yu, C.-W. (2018). Chloroplast Galactolipids: The Link Between Photosynthesis, Chloroplast Shape, Jasmonates, Phosphate Starvation and Freezing Tolerance. *Plant & Cell Physiology*, *59*, 1128–1134.
- Li, W., Wang, R., Li, M., Li, L., Wang, C., Welti, R., & Wang, X. (2008). Differential degradation of extraplastidic and plastidic lipids during freezing and post-freezing recovery in *Arabidopsis thaliana*. *The Journal of Biological Chemistry*, *283*, 461–468.
- Lippold, F., vom Dorp, K., Abraham, M., Hölzl, G., Wewer, V., Yilmaz, J. L., Lager, I., Montandon, C., Besagni, C., Kessler, F., Stymne, S., & Dörmann, P. (2012). Fatty acid phytyl ester synthesis in chloroplasts of *Arabidopsis*. *The Plant Cell*, *24*, 2001–2014.
- Livak, K. J., & Schmittgen, T. D. (2001). Analysis of relative gene expression data using real-time quantitative PCR and the 2^{(-Delta Delta C(T))} Method. *Methods (San Diego, Calif.)*, *25*, 402–408.

- Markham, J. E., & Jaworski, J. G. (2007). Rapid measurement of sphingolipids from *Arabidopsis thaliana* by reversed-phase high-performance liquid chromatography coupled to electrospray ionization tandem mass spectrometry. *Rapid Communications in Mass Spectrometry*, *21*, 1304–1314.
- Markham, J. E., Molino, D., Gissot, L., Bellec, Y., Hématy, K., Marion, J., Belcram, K., Palauqui, J.-C., Satiat-Jeunemaître, B., & Faure, J.-D. (2011). Sphingolipids containing very-long-chain fatty acids define a secretory pathway for specific polar plasma membrane protein targeting in *Arabidopsis*. *The Plant Cell*, *23*, 2362–2378.
- Matos, A. R., Hourton-Cabassa, C., Çiçek, D., Rezé, N., Arrabaça, J. D., Zachowski, A., & Moreau, F. (2007). Alternative oxidase involvement in cold stress response of *Arabidopsis thaliana* fad2 and FAD3+ cell suspensions altered in membrane lipid composition. *Plant & Cell Physiology*, *48*, 856–865.
- Menard, G. N., Moreno, J. M., Bryant, F. M., Munoz-Azcarate, O., Kelly, A. A., Hassani-Pak, K., Kurup, S., & Eastmond, P. J. (2017). Genome Wide Analysis of Fatty Acid Desaturation and Its Response to Temperature. *Plant Physiology*, *173*, 1594–1605.
- Minami, A., Fujiwara, M., Furuto, A., Fukao, Y., Yamashita, T., Kamo, M., Kawamura, Y., & Uemura, M. (2009). Alterations in detergent-resistant plasma membrane microdomains in *Arabidopsis thaliana* during cold acclimation. *Plant & Cell Physiology*, *50*, 341–359.
- Miquel, M., & Browse, J. (1992). *Arabidopsis* mutants deficient in polyunsaturated fatty acid synthesis. Biochemical and genetic characterization of a plant oleoyl-phosphatidylcholine desaturase. *The Journal of Biological Chemistry*, *267*, 1502–1509.
- Miquel, M., James, D., Dooner, H., & Browse, J. (1993). *Arabidopsis* requires polyunsaturated lipids for low-temperature survival. *Proceedings of the National Academy of Sciences of the United States of America*, *90*, 6208–6212.
- Mishra, M. K., Singh, G., Tiwari, S., Singh, R., Kumari, N., & Misra, P. (2015). Characterization of *Arabidopsis* sterol glycosyltransferase TTG15/UGT80B1 role during freeze and heat stress. *Plant Signaling & Behavior*, *10*, e1075682.
- Moellering, E. R., Muthan, B., & Benning, C. (2010). Freezing tolerance in plants requires lipid remodeling at the outer chloroplast membrane. *Science (New York, N.Y.)*, *330*, 226–228.
- Murata, N., & Yamaya, J. (1984). Temperature-dependent phase behavior of phosphatidylglycerols from chilling-sensitive and chilling-resistant plants. *Plant Physiology*, *74*, 1016–1024.
- Nilsson, A. K., Fahlberg, P., Ellerström, M., & Andersson, M. X. (2012). Oxo-phytodienoic acid (OPDA) is formed on fatty acids esterified to galactolipids after tissue disruption in *Arabidopsis thaliana*. *FEBS Letters*, *586*, 2483–2487.
- Nilsson, A. K., Johansson, O. N., Fahlberg, P., Kommuri, M., Töpel, M., Bodin, L. J., Sikora, P., Modarres, M., Ekengren, S., Nguyen, C. T., Farmer, E. E., Olsson, O., Ellerström, M., &

- Andersson, M. X. (2015). Acylated monogalactosyl diacylglycerol: Prevalence in the plant kingdom and identification of an enzyme catalyzing galactolipid head group acylation in *Arabidopsis thaliana*. *The Plant Journal: For Cell and Molecular Biology*, *84*, 1152–1166.
- Nishida, I., & Murata, N. (1996). CHILLING SENSITIVITY IN PLANTS AND CYANOBACTERIA: The Crucial Contribution of Membrane Lipids. *Annual Review of Plant Physiology and Plant Molecular Biology*, *47*, 541–568.
- O'Neill, C. M., Morgan, C., Hattori, C., Brennan, M., Rosas, U., Tschoep, H., Deng, P. X., Baker, D., Wells, R., & Bancroft, I. (2012). Towards the genetic architecture of seed lipid biosynthesis and accumulation in *Arabidopsis thaliana*. *Heredity*, *108*, 115–123.
- Román, Á., Hernández, M. L., Soria-García, Á., López-Gomollón, S., Lagunas, B., Picorel, R., Martínez-Rivas, J. M., & Alfonso, M. (2015). Non-redundant Contribution of the Plastidial FAD8 ω -3 Desaturase to Glycerolipid Unsaturation at Different Temperatures in *Arabidopsis*. *Molecular Plant*, *8*, 1599–1611.
- Ruiz-Sola, M. Á., Barja, M. V., Manzano, D., Llorente, B., Schipper, B., Beekwilder, J., & Rodríguez-Concepcion, M. (2016a). A Single *Arabidopsis* Gene Encodes Two Differentially Targeted Geranylgeranyl Diphosphate Synthase Isoforms. *Plant Physiology*, *172*, 1393–1402.
- Ruiz-Sola, M. Á., Coman, D., Beck, G., Barja, M. V., Colinas, M., Graf, A., Welsch, R., Rütimann, P., Bühlmann, P., Bigler, L., Gruissem, W., Rodríguez-Concepción, M., & Vranová, E. (2016b). *Arabidopsis* GERANYLGERANYL DIPHOSPHATE SYNTHASE 11 is a hub isozyme required for the production of most photosynthesis-related isoprenoids. *The New Phytologist*, *209*, 252–264.
- Sanyal, A., & Linder, C. R. (2013). Plasticity and constraints on fatty acid composition in the phospholipids and triacylglycerols of *Arabidopsis* accessions grown at different temperatures. *BMC Plant Biology*, *13*, 63.
- Sanyal, A., & Randal Linder, C. (2012). Quantitative trait loci involved in regulating seed oil composition in *Arabidopsis thaliana* and their evolutionary implications. *TAG. Theoretical and Applied Genetics. Theoretische Und Angewandte Genetik*, *124*, 723–738.
- Shiva, S., Enniful, R., Roth, M. R., Tamura, P., Jagadish, K., & Welti, R. (2018). An efficient modified method for plant leaf lipid extraction results in improved recovery of phosphatidic acid. *Plant Methods*, *14*, 14.
- Shiva, S., Vu, H. S., Roth, M. R., Zhou, Z., Marepally, S. R., Nune, D. S., Lushington, G. H., Visvanathan, M., & Welti, R. (2013). Lipidomic analysis of plant membrane lipids by direct infusion tandem mass spectrometry. *Methods in Molecular Biology (Clifton, N.J.)*, *1009*, 79–91.

- Song, Y., Vu, H. S., Shiva, S., Fruehan, C., Roth, M. R., Tamura, P., & Welti, R. (2020). A Lipidomic Approach to Identify Cold-Induced Changes in Arabidopsis Membrane Lipid Composition. *Methods in Molecular Biology (Clifton, N.J.)*, 2156, 187–202.
- Soria-García A, Ī. N., Rubio, M. A. C., Lagunas, B., Li Pez-Gomollı N, S., Lujı N, M. A. de L. Ī. N., Dı Az-Guerra, R. L., Picorel, R., & Alfonso, M. (2019). Tissue Distribution and Specific Contribution of Arabidopsis FAD7 and FAD8 Plastid Desaturases to the JA- and ABA-Mediated Cold Stress or Defense Responses. *Plant & Cell Physiology*, 60, 1025–1040.
- Tarazona, P., Feussner, K., & Feussner, I. (2015). An enhanced plant lipidomics method based on multiplexed liquid chromatography-mass spectrometry reveals additional insights into cold- and drought-induced membrane remodeling. *The Plant Journal: For Cell and Molecular Biology*, 84, 621–633.
- Uemura, M., Joseph, R. A., & Steponkus, P. L. (1995). Cold Acclimation of Arabidopsis thaliana (Effect on Plasma Membrane Lipid Composition and Freeze-Induced Lesions). *Plant Physiology*, 109, 15–30.
- Vu, H. S., Roth, M. R., Tamura, P., Samarakoon, T., Shiva, S., Honey, S., Lowe, K., Schmelz, E. A., Williams, T. D., & Welti, R. (2014a). Head-group acylation of monogalactosyldiacylglycerol is a common stress response, and the acyl-galactose acyl composition varies with the plant species and applied stress. *Physiologia Plantarum*, 150, 517–528.
- Vu, H. S., Shiva, S., Hall, A. S., & Welti, R. (2014b). A lipidomic approach to identify cold-induced changes in Arabidopsis membrane lipid composition. *Methods in Molecular Biology (Clifton, N.J.)*, 1166, 199–215.
- Vu, H. S., Shiva, S., Roth, M. R., Tamura, P., Zheng, L., Li, M., Sarowar, S., Honey, S., McElhiney, D., Hinkes, P., Seib, L., Williams, T. D., Gadbury, G., Wang, X., Shah, J., & Welti, R. (2014c). Lipid changes after leaf wounding in Arabidopsis thaliana: Expanded lipidomic data form the basis for lipid co-occurrence analysis. *The Plant Journal: For Cell and Molecular Biology*, 80, 728–743.
- Vu, H. S., Shiva, S., Samarakoon, T., Li, M., Sarowar, S., Roth, M. R., Tamura, P., Honey, S., Lowe, K., Porras, H., Prakash, N., Roach, C. A., Stuke, M., Wang, X., Shah, J., Gadbury, G., Wang, H., & Welti, R. (2022). Specific Changes in Arabidopsis thaliana Rosette Lipids during Freezing Can Be Associated with Freezing Tolerance. *Metabolites*, 12, 385.
- Wang, X., Li, W., Li, M., & Welti, R. (2006). Profiling lipid changes in plant response to low temperatures. *Physiologia Plantarum*, 126, 90–96.
- Weigel, D., & Mott, R. (2009). The 1001 genomes project for Arabidopsis thaliana. *Genome Biology*, 10, 107.

- Welti, R., Li, W., Li, M., Sang, Y., Biesiada, H., Zhou, H.-E., Rajashekar, C. B., Williams, T. D., & Wang, X. (2002). Profiling membrane lipids in plant stress responses. Role of phospholipase D alpha in freezing-induced lipid changes in Arabidopsis. *The Journal of Biological Chemistry*, 277, 31994–32002.
- Wu, J., James, D. W., Dooner, H. K., & Browse, J. (1994). A Mutant of Arabidopsis Deficient in the Elongation of Palmitic Acid. *Plant Physiology*, 106, 143–150.
- Wu, J., Lightner, J., Warwick, N., & Browse, J. (1997). Low-temperature damage and subsequent recovery of fab1 mutant Arabidopsis exposed to 2 degrees C. *Plant Physiology*, 113, 347–356.
- Zhen, Y., & Ungerer, M. C. (2008). Clinal variation in freezing tolerance among natural accessions of Arabidopsis thaliana. *The New Phytologist*, 177, 419–427.
- Zheng, G., Li, L., & Li, W. (2016). Glycerolipidome responses to freezing- and chilling-induced injuries: Examples in Arabidopsis and rice. *BMC Plant Biology*, 16, 70.
- Zuther, E., Schulz, E., Childs, L. H., & Hinch, D. K. (2012). Clinal variation in the non-acclimated and cold-acclimated freezing tolerance of Arabidopsis thaliana accessions. *Plant, Cell & Environment*, 35, 1860–1878.

Chapter 4 - Genome wide association in *Arabidopsis thaliana* accessions, under control conditions and after wounding, identifies genetic variation related to lipid levels and reveals two genes affecting the production of oxophytodienoic acid and related lipids

Introduction

Arabidopsis thaliana is widely distributed in Eurasia, where differences in local environment have shaped natural variations among accessions collected in different geographic locations (Koornneef et al., 2004; Weigel, 2012). A genome wide association study (GWAS) correlates phenotypic differences among accessions with genotypic information about the accessions to identify genes associated with the observed phenotypic variation. The establishment of 1001 Genomes Project, in which genomes of 1135 natural accessions were sequenced, with over 10 million biallelic single nucleotide polymorphism (SNPs) identified (Weigel & Mott, 2009), greatly facilitates the ability of *Arabidopsis* researchers to conduct GWAS. Additionally, the user-friendly and interactive online GWAS analysis tool, GWA-Portal, facilitates analysis (Seren, 2018; Seren et al., 2012). One type of phenotypic variation that can be analyzed by GWAS is differences in lipid composition of various plant tissues among accessions. For example, variations in the seed oil fatty acid composition of natural accessions and recombinant inbred lines have been associated with genes with variant sequences in the structural gene or promoter region including fatty acid desaturase 2 (*FAD2*), fatty acid desaturase 3 (*FAD3*), and ketoacyl-CoA synthase 18 (*KCS18*) (Branham et al., 2016; Jasinski et al., 2012; Menard et al., 2017).

In plants, lipids function in a variety of ways. Some lipids are essential components of cells and organelles as the hydrophobic components of membranes. Other lipids function as a compact energy source for seed germination and plant development. Furthermore, they act as signaling molecules to regulate plant growth and development (Kim, 2020; Li-Beisson et al., 2013). Emerging evidence has revealed potential roles of glycerolipid remodeling in plant stress responses. One of the key biological roles is to adjust membrane physiochemical properties to optimize membrane functions under unfavorable conditions (Moellering & Benning, 2011; Nakamura, 2013). Another important role is to remove oxidized or damaged acyl chains, sequester cytotoxic fatty acids, and release signaling lipids and in stress responses (Hermansson et al., 2011; Nakamura, 2013; Vu et al., 2014a).

Mechanical wounding causes severe damage to plant tissues and great losses in agriculture around the world. Mechanical wounding occurs in nature when plants are subjected to abiotic stresses, such as wind, hail, snow, or biotic stresses, such as insect bites and herbivore grazing. Wounding causes global changes in the metabolome including changes in many lipids (Buseman et al., 2006; Ibrahim et al., 2011; Nakashima et al., 2013; Nilsson et al., 2012; Vu et al., 2015, 2012; Vu et al., 2014a; Vu et al., 2014b; Zien et al., 2001). Among the changes in the lipid profile upon wounding, a prominent change is rapid accumulation of oxidized glycerolipids, especially Arabidopsides, which are a group of 12-oxophytodienoic acid (OPDA) and/or dinor-oxophytodienoic acid (dn-OPDA) containing galactolipids (Buseman et al., 2006; Hisamatsu et al., 2003, 2005; Ibrahim et al., 2011; Kourtchenko et al., 2007; Vu et al., 2015, 2012; Vu et al., 2014a; Vu et al., 2014b). Free OPDAs and dnOPDAs are oxylipins derived from 18:3 and 16:3 fatty acids, respectively, through the lipoxygenase (LOX) and allene oxide synthase (AOS) pathways, which generate many important oxidized metabolites, such as jasmonic acid (JA) and

its derivatives (Vick & Zimmerman, 1983; Wasternack & Feussner, 2018; Wasternack & Strnad, 2018; Weber et al., 1997). Many studies described the role of JA and OPDA as major regulators of gene expression changes under wounding stress (Ahmad et al., 2016; Seo et al., 1997; Taki et al., 2005). However, less is known about the biosynthesis and biological functions of esterified OPDA. Actually, (dn)OPDA is more abundant in its esterified forms in plants compared to its free forms (Andersson et al., 2006; Kourtchenko et al., 2007; Nilsson et al., 2012).

Advances in analytical techniques in mass spectrometry now allow large-scale determination of plant lipid profiles. The levels of a specific lipid in each of a wide range of accessions is a phenotype that can be analyzed in a GWAS to identify genes associated with the variation in lipid level. Here we used a direct-infusion electrospray ionization (ESI) triple quadrupole MS method and a liquid chromatography MS method targeted to phytohormones to quantitatively measure the lipidomes of 360 natural accessions from 1001 Genomes Project. We compared lipidomes of unwounded plants and mechanically wounded plants, and a series of GWASs was carried on using the relative levels of 274 lipid species in the control group and 277 in the wounding group. Our goal was to investigate natural variation in the wound-induced lipidome among natural accessions and identify candidate genes underlying lipid metabolism in response to wounding. As observed previously, after wounding treatment, the large accumulation of oxylipin-containing plastidic lipids was one of the most prominent changes. However, great variability exists among accessions in the wounding-induced lipidome, especially in the oxylipin and esterified oxylipin profiles. The variability facilitated the identification of genes responsible for oxidized lipid metabolism under mechanical wounding stress. Among the candidate genes identified, the most significant were allene oxide cyclase (*AOC2*) and hydroperoxide lyase 1 (*HPL1*), encoding enzymes involved in the production of oxidized fatty acids.

Materials and Methods

Plant materials and growth conditions

360 accessions were selected from the 1001 Genomes Project with a wide geographic distribution to ensure phenotypic variation for GWAS analysis. Information on the 360 accessions is listed in Table S4-1. Seeds from each of the sequenced accessions (1135 accessions, Stock Number: CS78942) used in the 1001 Genomes Project were obtained from Arabidopsis Biological Resource Center (ABRC).

All investigated accessions went through standard growth conditions in growth chamber as described in Materials and Methods in Chapter 2. On day 30, before wounding treatment, we harvested unwounded leaf #4 for lipid extraction as a sample for the control group. For the wounding treatment, a hemostat was used to wound leaves #5 and 6 of 30-day-old plants across the mid-vein, twice and about 6 mm apart. After 45 min, wounded leaf #5 was harvested for lipid extraction while wounded leaf #6 was harvested for RNA extraction. Leaf numbers were determined as described by Telfer et al. (1997). For each accession, there were three biological replicates for lipid analysis in each of the control and wounding groups.

Lipidomic analysis of 360 Arabidopsis accessions

Lipids in leaf samples were extracted using an optimized extraction method based on Shiva et al. (2018). Lipid extraction procedure, preparation of internal standards (IS) and quality control (QC) samples are described in Materials and Methods section in Chapter 2.

Data were acquired on a triple quadrupole mass spectrometer (Sciex 6500+ mass spectrometer) equipped with an ESI probe, using MRM with transitions for some analytes measured in positive and others measured in negative modes. Detailed MS parameters are described in Chapter 2. In the positive mode, 104 transitions and, in the negative mode, 234

transitions were monitored in each MRM cycle. 27 cycles of MRM transitions were acquired in 5 min. Parameters for each MRM transition are listed in Table S4-2 for the plant lipid analytes and internal standards.

Data processing and normalization

As described in Chapter 2, the MRM data were exported from the Sciex 6500+ mass spectrometer, processed using the software MultiQuant, isotopically deconvoluted, and quantified in comparison to internal standards by the online software LipidomeDB Data Calculation Environment (DCE). An adaptation of the method of Dunn (2011) was employed to correct for differences in the response of the instrument over time, to improve the consistency of the data throughout the acquisition period (Vu et al., 2014b). A detailed protocol for the data processing and correction process can be found in Song et al. (2020). Coefficient of variation (CoV) values of less than 30% represent analytes with reasonable analytical precision. Lipid analytes with CoV less than 30% are summarized in Table S4-3. Finally, the data were corrected for the fraction of the sample analyzed and calculated as normalized mass spectral intensity, where a value of 1 represents an intensity equal to that of 1 nmol of internal standard \times mg⁻¹. The average of three biological replicates for each accession was calculated and the mean value of absolute content (normalized mass spectral intensity \times mg⁻¹) of all 360 accessions before and after wounding stress was shown in Table S4-4. Lipid species can be categorized into 32 lipid sub-classes, the absolute content for 32 lipid classes is shown in Table S4-6.

Analysis and quantification of JA, JA-Ile, and OPDA

Jasmonic acid, jasmonoyl-L-isoleucine (JA-Ile), and 12-oxo-phytodienonic acid (OPDA), were quantified as previously described (Koo et al., 2014). Briefly, an aliquot of lipid extracts mixed with dihydro jasmonic acid (dhJA), [¹³C₆]-JA-Ile, and [²H₅]-OPDA as internal standards

was analyzed using an ultraperformance liquid chromatography (ACUITY H-class, Waters), coupled to an electrospray ionization (ESI) triple quadrupole tandem mass spectrometer (Xevo T-QS, Waters, Milford, MA). Seven ml of each sample was injected and the analytes were separated on an Ascentis Express C18 column (2.7 mm, 2.1 x 50 mm; Supelco, Bellefonte, PA) maintained at 40 °C using a 3-min LC gradient program that delivers mobile phase consisting of 0.1% aqueous formic acid and methanol at 0.4 mL/min flow rate. The MS method was operated in a negative ion mode and the characteristic m/z transitions from precursor to product ions for jasmonic acid (209 > 59), dhJA (211>59), JA-Ile (322>130), [¹³C₆]-JA-Ile (328>136), OPDA (291>165), and [²H₅]-OPDA (296>170) were monitored by multiple reaction monitoring (MRM). Data acquisition and quantification were performed using MassLynx 4.1 and TargetLynx software (Waters). Standard curves comparing relative contents of the hormones to their respective internal standards were used to calculate endogenous hormone contents that were normalized by their sample dry weights, resulting in data in nmol mg⁻¹.

Data as percentages

Data were divided by the total of the normalized mass spectral intensity for the complex lipid data. Thus, the total lipid (%) was 100% for the control data and slightly over 100% for the wounded data, since JA, OPDA, and JA-Ile were measured separately by LC/MS only in wounded samples. The average of three biological replicates for each accession was calculated and the relative proportions of individual lipid molecular species were expressed as a percentage of the total lipid content per sample (Table S4-5). Total lipid levels for 32 lipid sub-classes also were determined (Table S4-7).

Lipid data analysis

The two-sample t-test and calculation of False Discovery Rate (FDR) were performed (Table S4-8) based on percentage data indicating levels of individual lipid species before and after wounding stress, and the heat map were produced using utilities in MetaboAnalyst (Xia et al., 2015). Linear regression analysis was performed in Origin 2020, and the significance of correlations was estimated by calculating Pearson correlation coefficients of lipid level and gene expression level.

Genome-wide association study (GWAS)

GWAS analysis was performed using the online tool GWA-Portal (URL <https://gwas.gmi.oeaw.ac.at>) with ~10 million single-nucleotide polymorphisms (SNPs) available from the imputed full sequence dataset. Box-Cox transformation was applied to assure most lipid phenotypes to approximately normal distributions. The narrow-sense heritability (pseudo-heritability) of each Box-Cox-transformed lipid phenotype after wounding treatment is summarized in Table S4-9. Accelerated mixed model (AMM) was chosen to take population structure into account.

GWAS results were downloaded from GWA-Portal as csv files and then filtered by minor allele frequency (MAF) ≥ 0.05 and p-score ≥ 6 , which is processed in a Python program (<https://github.com/songyu6054677/GWAS-results-analysis-01122021.git>). With the help of the Python data processing pipeline, more information was annotated for each SNP entry including associated lipid name, lipid number, transformation methods, and stress conditions. Annotation information including lipid name, lipid number, GWAS file name, and transformation method used in this study is documented in Table S4-10. A summary GWAS result file was generated consisting of all significant SNPs identified for individual lipid phenotypes. Because linkage

disequilibrium (LD) in *Arabidopsis* decays within 10 kb on average, all genes located between 10 kb upstream and downstream of each significant SNP ($p\text{-score} \geq 6$) were identified by Python program. By checking the genomic region around significant SNPs, all SNPs and associated candidate genes were categorized into different genomic regions. Gene annotation information for candidate genes was obtained from TAIR 10 database (<http://www.arabidopsis.org>). Genes known to be lipid-related and associated lipid-level phenotypes are summarized in S4-11.

The GWAS results can be further analyzed by comparing SNPs between control and wounding conditions. The “merge” function in our Python program facilitated discovery of common SNPs with exactly same information of “position”, “lipid name”, and “transformation” between two GWAS summary files.

Gene expression analysis (RT-qPCR)

Before RNA extraction, the harvested leaf samples were frozen immediately in liquid nitrogen and stored at $-80\text{ }^{\circ}\text{C}$. Three leaves harvested from each accession were combined; a total of 40 accessions were selected for gene expression analysis (Table S4-13). Three leaves from each accession and frozen in a 1.5 mL microcentrifuge tube along with a metal bead were ground thoroughly in a tissue lyser. RNA was extracted from the tissue powder using RNeasy Plant Mini Kit from Qiagen following the manufacturer’s protocol. 10 μg of total RNA was digested with DNase Max Kit from Qiagen to remove any genomic DNA contamination. RNA concentrations were quantified with a NanoDrop 2000 spectrophotometer (Thermo Scientific). 1 μg of RNA was used for cDNA synthesis using qScriptTM cDNA Synthesis Kit from Bio-Rad according to the manufacturer’s protocol.

Quantitative PCR was performed on a CFX96 real-time PCR system (Bio-Rad) using the iTaq Universal SYBR Green Supermix chemistry on iCycler iQ from BioRAD. *AOC1*, *AOC2*,

AOC3, and *HPL1* gene expression levels were normalized to the *TRO* (AT1G51450) and *YLS8* (AT5G08290) genes using the Delta-Delta-CT (DDCT) method. Primers used to quantify expression of these genes are listed in Table S4-14.

Results

Natural variation of the leaf lipid composition occurs in *Arabidopsis thaliana* under control and wounding conditions

Using direct-infusion triple quadrupole mass spectrometry, lipidomic analysis was performed on 360 *Arabidopsis thaliana* accessions, selected from the 1001 Genomes Project to include a wide geographic distribution (e.g. latitude ranging from 31.48° N to 63.08° N). The phenotypic variation in individual lipid species and different lipid classes in their relative proportions under control conditions and 45 min after mechanical wounding across the leaf mid-vein with a hemostat was investigated. The lipidomic data, as normalized mass spectral intensity per dry mass and as percent of total mass spectral intensity of the analyzed lipids, are presented in Tables S4-4 and S4-5. Although the datasets are very similar, we chose to work further with the percent data because the agreement among the biological replicates tended to be better for the control group and was significantly better for the wounding group [average among lipid species for the coefficient of variation (CoV; standard deviation x 100% /average) among biological replicates: 41.5% (for % of total intensity) vs. 44.5% (for normalized intensity per dry mass) for control plants and 33.5% (for % of total intensity) vs 36.7% (for normalized intensity per dry mass) for wounded plants].

The analyzed lipids include 270 lipid molecular species that can be classified into 32 lipid classes or sub-classes. The means, ranges, and variabilities of the lipid species in the group of 360 accessions are shown in Table S4-5. The amount of variability of relative content among

accessions in lipid classes measured as CoV ranges from 5% to 81% under control conditions and from 5% to 105% after wounding (Table 4-1).

Wounding induced overall changes of lipid composition in 360 Arabidopsis accessions

The levels and variation among the analyzed 360 Arabidopsis accessions of 32 lipid classes and sub-classes under control conditions and after wounding stress are depicted in Figure 4-1a. Differences in the lipid composition of control and wounded plants indicate wounding induces lipid oxidation, hydrolysis, head-group acylation, and changes in levels of sterol derivatives. Lipid classes that increased, on average among the accessions, during wounding include acMGDG, ASG, LPC, LPE, PA, oxidized galactolipids, oxidized PC, and oxidized PG. These results are consistent with previous data from the Columbia-0 accession (Vu et al., 2014a; Vu et al., 2014b; Vu et al., 2012). In particular, a large accumulation of galactolipids containing the oxidized fatty acids, OPDA (detected by mass spectrometry as 18:4-O, indicating 18 carbons, 4 double bond equivalents, and one oxygen beyond the carbonyl oxygen) and/or dnOPDA (16:4-O), occurred (Figure 4-1b). Non-oxidized precursor lipids decreased as oxidized lipid species increased (Figure 4-1a). While the percentages of oxidized MGDG and oxidized DGDG were increased 7-fold and 4-fold, on average among the accessions, respectively, 45 min after wounding, the percentages of the non-oxidized forms were reduced (5% for MGDG and 11% reduction for DGDG) (Figure 4-1a).

Significant increases in mono-acyl phospholipids and PA, and significant decreases in PC, PI, and PS, were observed, and were most likely due to phospholipid hydrolysis (Table S4-7). The abundant phospholipid PC decreased in most accessions, with an average reduction of 3%, while levels of its hydrolysis products PA and LPC increased by an average of 4- and 2-fold.

Head-group acylation mainly occurred in MGDG, generating acMGDG, as well as DGMG or MGMG, as an acyl chain is transferred from DGDG or MGDG to the MGDG head group, upon wounding of Arabidopsis leaves (Andersson et al., 2006; Heinz, 1967; Nilsson et al., 2015). The most induced lipids were oxidized acMGDGs, which were increased, on average across the accessions, by 36-fold at 45 min after wounding. However, the oxidized lipid classes showed great variability among natural accessions. TRa 01 produced low levels of oxidized DGDG, MGDG, DGMG, MGMG, PG, and SQDG in response to wounding, while Map-35 produced particularly large amounts of oxidized lipids. Lipid oxidation also occurred in extraplastidic lipids, as indicated by an increase in oxidized PCs (1.2-fold) in response to wounding. Acyl sterol glucosides (ASGs) with an OPDA as the acyl chain increased 2.5-fold. Additionally, there were significant increases in sterol glucosides (SG) and other ASGs in response to wounding stress (both ~1.5-fold increase).

The detailed molecular species profiles for all lipids analyzed are displayed in Figures S4-1-S4-15. Of the 270 lipid analytes, analyzed as percent of total normalized MS intensity, 247 were significantly different after wounding, compared to the control, by unpaired t-tests ($P < 0.01$) (Table S4-8). 193 lipid species were significantly higher after wounding while 56 lipid species were lower. Some changes due to wounding were observed in particular molecular species, rather than in entire lipid classes. For example, there was an overall reduction of TAGs after wounding, except for TAG (18:3/34:6), which increased 4-fold ($P = 3.7E-111$). It was previously suggested that TAG (18:3/34:6) was produced as a side product through upregulation of SFR2 activity utilizing MGDG (34:6), i.e., MGDG(18:3/16:3), under wounding stress (Vu et al., 2015). There was great difference among MGDG and DGDG molecular species in response to wounding. Highly unsaturated species, including 34:6, 36:5, and 36:6, showed significant

reduction after wounding, consistent with the notion that they are substrates for lipid oxidation, while incompletely unsaturated species, including 34:1 and 34:5, showed no significant change or a slight increase. 32-carbon and 34-carbon normal-chain PG species containing 16:1 were also lower in leaves of wounded plants compared to their level in the leaves of control plants. 34-carbon PG species containing 16:0 and an 18C fatty acyl chain and 36C PG species, containing two 18C acyl chains, displayed significant increases after wounding. Similarly, various oxidized lipid molecular species exhibited varied changes after wounding. Fully oxidized acMGDG with 3 OPDA or dnOPDA chains was induced most, with an average of 89-fold increase at 45 min after wounding (Figure 4-1b). Ox-acMGDG with 2 OPDA or dnOPDA also were present at high levels after wounding with a 25-fold increase over control, on average across all accessions, at 45 min. Other ox-MGDG with 1 or 0 OPDA or dnOPDA acyl chains were induced less (4-fold increase) 45 min after wounding (Figure C-1).

GWAS study on lipidomics data revealed candidate genes related to lipid metabolism

A GWAS, using the Box-Cox-transformed percentages of individual lipid species as phenotypes, was performed, using the online tool GWA-Portal and its accelerated mixed model (AMM) (Seren, 2018; Seren et al., 2012). In addition to the data from the direct-infusion lipidomic analysis, data from LC-MS analysis of levels OPDA, JA, and JA-Ile in the accessions under wounding stress (included in Table S4-5) were also included in the GWAS. The fraction of the genetic variance of each phenotype that can be explained by genetic relatedness is indicated by pseudo-heritability, which is an estimate of the narrow sense heritability (Table S4-9) (Korte & Farlow, 2013). Pseudo-heritability varies from 0 to 0.84 for levels of various lipids under control conditions and 0 to 0.96 after wounding.

Under the control condition, 1247 SNPs were identified with a $p\text{-score} \geq 6$, $\text{maf} \geq 0.05$, and pseudo-heritability > 0 for 172 lipid level phenotypes. This includes 1576 unique SNPs, since some SNPs were identified for multiple lipid level phenotypes. Under wounding stress, 1433 SNPs were identified that meet the stated criteria for 199 lipid level phenotypes, including 1083 unique SNPs. Comparison of the total number of SNPs identified under control condition and wounding stress is summarized in Figure 4-2a. Among all unique SNPs, 897 were identified only in control group while 1083 were identified only in the wounding group. There are 350 SNPs identified with phenotypes same lipid's levels under control and wounding conditions.

Candidate genes were selected within a 20-kb length chromosomal region upstream and downstream (10 kb in each direction) of the significant SNPs. Each genomic region of interest contains all the SNPs within 20-kb of each other with alleles associated with the level of a particular lipid or with multiple lipids that are associated with the same SNPs in the region. Figure 4-2b is a Venn diagram depicting the comparison of the identified genomic regions between control and wounding groups, with 320 regions specific to control group and 275 specific to the wounding group, and 19 overlapping regions which share at least one SNPs and are associated with at least one of the same lipids. All SNPs, corresponding chromosomal regions, and associated candidate genes are listed in Table S4-10 and S4-11 and overlapping regions are indicated in Table S4-12. Based on GO annotation, 86 of 1758 candidate genes identified under wounding stress and 90 of 1889 under the control condition are characterized lipid-related genes or uncharacterized genes (shown in Table S4-13) that may have lipid biosynthesis or metabolic functions.

Chromosomal regions identified in both control and wounding conditions suggest natural variation in several genes related to lipid metabolism

Of the genomic regions identified under both control and wounding conditions (Table S4-10, S4-11, S4-12), four contain candidate genes previously described as carrying out reactions likely to affect the associated lipid-level phenotypes. As shown in Figure 4-3a, region C-19/W-22 was identified as associated with the levels of campesterol-Glc(18:3), campesterol-Glc(18:2), and campesterol-Glc(16:0) under both control and wounding conditions. This area contains the gene AT1G20330, which encodes sterol methyltransferase 2 (SMT2). SMT2 catalyzes the first reaction in the pathway leading to sitosterol and stigmasterol, and SMT2 activity can regulate the ratio of campesterol to sitosterol (Schaeffer et al., 2001), so it's reasonable that variation in *SMT2* is associated with differences in levels of campesterol derivatives. Region C-137/W-122 was identified as associated with the levels of PI(16:0/18:1) and PC(18:1/18:3) (Figure 4-3a). This region contains fatty acid desaturase 2 (*FAD2*; AT3G12120), which encodes an enzyme catalyzing the desaturation of 18:1 to 18:2 in the endoplasmic reticulum (ER) (Okuley et al., 1994). Although the enzyme works directly on 18:1 in PC, it is likely that PI(16:0/18:1) is formed from PC(16:0/18:1) via phosphatidic acid (PA) and CDP-DAG, and reasonable to hypothesize that levels of PI(16:0/18:1) are regulated by variation in *FAD2*. *FAD4*, AT4G27030, encoding the desaturase that catalyzes the formation of a 3-*trans* bond in 16:0 of PG, is associated with region C-249/W-219 for the lipid phenotypes PG(18:2/16:0-O), PG(18:2/16:1), PG(18:3/16:1), PG(18:2/16:0), and PG(18:3/16:0) under both control and wounding condition. Lipid level phenotypes associated with this region include the *FAD4* substrate, PG(18:2/16:0), PG(18:3/16:0) and product, PG(18:2/16:1), PG(18:3/16:1). The levels of these lipids are associated in reciprocal fashion with the SNP variation (Figure 4-3(b, c)). Interestingly, the level

of PG(18:2/16:0-O) is also associated with this region and its levels parallel those of product lipid, PG(18:2/16:1) (Figure 4-5c), suggesting that there are measurable levels of hydroxylation of 16:0 by FAD4. Indeed, desaturases are known to have the potential to carry out hydroxylation, as well as desaturation reactions (Broun et al., 1998), although this has not been demonstrated directly for FAD4 to our knowledge. Finally, levels of DGDG(18:1/18:3) were associated with region C-270/W-247, which contains gene AT5G16230, encoding the plastidic acyl-acyl carrier protein desaturase 3 (AAD3). AAD3 catalyzes the ω -7 desaturation of 16:0 to 9-*cis* 16:1, which can be elongated to 11-*cis* 18:1 (Kachroo et al., 2007). AAD3 is expressed at low levels in leaves, compared to its expression in the aleurone of seeds (Bryant et al., 2016). In leaves, other acyl-acyl carrier protein desaturases, including FATTY ACID BIOSYNTHESIS 2 (FAB2), act to form 9-*cis* 18:1, the prominent 18:1 isomer in galactolipids; 9-*cis* 18:1 can be further desaturated by FAD6 to 18:2 and FAD7 to 18:3. 11-*cis* 18:1 is not a substrate for further desaturation and might reasonably be expected to accumulate in plastidic membrane lipids, such as DGDG(18:1/18:3). Figure 4-3b shows how the variation in the SNP with the highest p-score relates to DGDG(18:1/18:3) levels. The available information suggests that higher levels of DGDG(18:1/18:3) are reasonably associated with natural variation in AAD3 affecting its function. Taken together, the identification under both control and wounding conditions by GWAS of candidate genes encoding enzymes with the ability to affect the levels of the associated lipid-level phenotypes provides confidence in the GWAS results and implies that natural variation among Arabidopsis accessions affects the levels of specific lipids.

Natural variation in allene oxide cyclase-encoding genes and HYDROPEROXIDE LYASE 1 regulates lipid oxidation in leaves during wounding

There are two genomic regions, identified only under wounding stress, associated with large numbers of lipids. Region W-144 is associated with 30 lipid-level phenotypes and region W-201 is associated with 62 lipid-level phenotypes. The lipids associated with each of these regions are shown in Table 4-2 and Table S4-15. Both regions are strongly associated with levels of 25 molecular species including esterified OPDA and esterified dnOPDA (Table 4-2). Region W-144, on chromosome 3, contains three characterized genes involved in oxylipin biosynthesis, AT3G25760, AT3G25770, and AT3G25780, while region W-201, on chromosome 4, contained one characterized gene associated with oxylipin metabolism, AT4G15440. Figure 4-4a is the Manhattan plot of GWAS analysis on one lipid-level phenotype associated with both regions, i.e., acMGDG (18:4-O/34:8-2O). This acylated MGDG, also known as Arabidopside E, has oxidized fatty acids, OPDA and dnOPDA esterified to the glycerol, and OPDA esterified to the galactose ring (Andersson et al., 2006).

Multiple SNPs in region W-144 displayed strong associations with oxidized lipid-level phenotypes (Table 4-3). The SNP with the highest p-score (lowest *p* value) for most of associated lipid species was at position 9406789 on chromosome 3, in the 5'UTR of AT3G25770 (*ALLENE OXIDE CYCLASE 2*; *AOC2*). Allene oxide cyclase (AOC) catalyzes cyclization (formation of a cyclopentenone ring) to generate dnOPDA and OPDA, whose structures are indicated as 16:4-O and 18:4-O in many of the lipids listed in Table 4-2. dnOPDA and OPDA can serve as a phytohormone and as precursors to JA (Gfeller et al., 2010). Four genes encode AOCs in Arabidopsis and three, *AOC1*, *AOC2*, and *AOC3*, lie in tandem on chromosome 3. Correlations of the SNPs in genomic region W-144 for the lipid-level phenotype of acMGDG

(18:4-O/34:8-2O) (Arabidopside E) are shown in Table 4-3, with positive values indicating linkage. Linked SNP (Chr3_9403749) is situated upstream of AT3G25760 (AOC1), and linked SNPs at Chr3_9408202 and Chr3_9408340) are located upstream of AT3G25780 (AOC3). Haplotype analysis using the SNP at Chr3_9406789 revealed two haplotype groups in the 360 natural accessions, with 198 and 162 accessions in major allele group and minor allele group, respectively. The haplotype analysis for the lipid-level phenotype of Arabidopside E is summarized in Figure 4-4b. The major allele group with nucleotide T at the SNP position Chr3_9406789 had a significantly higher level of Arabidopside E than the minor allele group with nucleotide C (mean of major allele group, 1.49% Arabidopside E; mean of minor allele group, 0.99%; $P = 6.81E-10$). The levels of other oxidized lipids were also higher in the major allele group.

Genomic region W-201 contained multiple SNPs in the upstream regions of AT4G15440 (*HYDROPEROXIDE LYASE 1; HPL1*) (Table 4-3). Among these SNPs, the most significant (p-score = 10.41) for levels of most of the related lipid species is at position 8834169 on chromosome 4, 1198 nucleotides upstream of *HPL1*. Haplotype analysis of the SNP at Chr4_8834169 revealed two haplotype groups in 360 natural accessions with 211 and 149 accessions in major allele group (nucleotide C) and minor allele group (nucleotide T). As shown in Figure 4-4c, the average level of Arabidopside E in the major allele group is higher than the level in minor allele group (mean level in major allele group = 1.46%, mean level in minor allele group = 0.99%, $P = 1.27E-08$). The enzyme encoded by *HPL1* can cleave the C12-C13 bond of fatty acid hydroperoxides to generate hexanol and traumatin or dn-traumatin. It has been proposed that the HPL pathway and the jasmonic acid synthetic pathway compete for substrate hydroperoxy fatty acids, and previous work identified *HPL1* as a negative regulator of OPDA

and Arabidopside production (Nilsson et al., 2016; Rustgi et al., 2019). For associated lipid level phenotypes, except for levels of nonoxidized lipid species and acMGDG with 34:7-O of fatty acyl chain combination in glycerol backbone, the lipid level in major allele group with nucleotide C for SNP (Chr4_8834169) was significantly higher than lipid level in minor allele group with nucleotide T. In contrast, seven lipid level-phenotypes, i.e., levels of acMGDG(16:0/34:6), acMGDG(18:2/34:6), DGDG(18:1/18:3), acMGDG(16:0/34:7-O), acMGDG(18:2/34:7-O), acMGDG(18:3/34:7-O), and acMGDG(18:4-20/34:7-O) were higher in minor allele group. It is likely that nonoxidized acylated galactolipids acMGDG(16:0/34:6) and acMGDG(18:2/34:6) are formed by MGDG head-group acylation in accessions with low levels of dnOPDA and OPDA synthesis. The 34:7-O acyl chains represent the fatty acids 18:3 and 16:4-O (dnOPDA) or 16:3 and 18:4-O (OPDA). MGDGs with these combinations are found at higher basal levels in accession Columbia-0 than diOPDA or OPDA/dnOPDA MGDGs and the accumulation of 34:7-O species occurs more slowly after wounding (Buseman et al., 2006; Vu et al., 2014b). How and whether those factors relate to the reversed pattern of accumulation of 34:7-O-containing acMGDGs is not clear. Besides the SNP at Chr4_8834169, there are another several lipid-level associated SNPs situated in upstream region of *HPL1*, i.e., Chr4_8834257, Chr4_8834258, Chr4_8834584 (Table 4-3).

From the GWAS results above, it was observed that many oxidized lipid species were associated with both genomic regions. In order to determine the combined effect of polymorphisms in each region, the most significant SNPs in the two regions, the SNPs at Chr3_9406789 and Chr4_8834169 were considered together. Haplotype analysis for the Arabidopside E-level phenotype, using these most significant SNPs from each region, is shown in Figure 4-4d. Group A represents accessions with nucleotide C at Chr3_9406789 and C at

Chr4_8834169, group B represents accessions with nucleotide C at Chr3_9406789 and T at Chr4_8834169, group C represents accessions with nucleotide T at Chr3_9406789 and C at Chr4_8834169, and group D represents accessions with nucleotide T at Chr3_9406789 and T at Chr4_8834169. The largest difference was observed between group B and group C with group C having the highest level of Arabidopside E (mean = 1.61%) and group B the lowest (mean = 0.82%). A Student's T-test between group B and C showed $P = 4.54E-14$, i.e., the groups are more significantly different than when only one SNP was considered (Figure 4-4(b, c)), indicating an additive effect of the two SNPs on Arabidopside E production under wounding stress.

To investigate the how natural variation of *AOCs* and *HPLI* regulate free oxylipin production, we measured the content of free OPDA, JA, and jasmonic acid-isoleucine (JA-Ile) in wounded leaves of the investigated 360 accessions. There is large phenotypic variation for OPDA, JA, and JA-Ile in their relative content (% of total) under mechanical wounding stress (Table S4-5) with relatively high CoV ranging from 41% to 55%. As shown in Table S4-16, the relative contents of free OPDA and JA in the 360 accessions analyzed were highly correlated with the relative levels of esterified (dn)OPDA species. For example, accession Tra 01 generated the lowest level of OPDA (0.00098%) and JA (0.0095%) among 360 accessions under wounding stress, which is consistent with the lipidomics results showing that Tra 01 showed the lowest ability to produce esterified OPDA and dnOPDA. GWAS of the free OPDA-level phenotype revealed strong association between OPDA level and genomic region W-144 and W-201, which contains same SNPs (Chr3_9403749, Chr3_9405475, Chr3_9406130, Chr3_9406789, Chr3_9408202, Chr3_9408340, Chr3_9411074, Chr4_8834169, Chr4_8834584) in GWAS results for esterified (dn)OPDA (Table S4-11). Figure 4-5a is the Manhattan plot of GWAS

analysis on free OPDA associated with region W-144 and region W-201. As shown in Figure 4-5b, haplotype analysis using the SNP at Chr3_9406789 revealed the major allele group with nucleotide T had a significantly higher level of free OPDA than the minor allele group with nucleotide C (mean of major allele group, 0.033% OPDA; mean of minor allele group, 0.021%; $P = 1.12E-13$). In Figure 4-5c, haplotype analysis using the SNP at Chr4_8834169 revealed the major allele group with nucleotide C had a significantly higher level of free OPDA than the minor allele group with nucleotide T (mean of major allele group, 0.031% OPDA; mean of minor allele group, 0.023%; $P = 2.01E-6$). Haplotype analysis using both SNPs (Figure 4-5d) showed that the largest difference was observed between group B and group C with group C having the highest level of Arabidopside E (mean = 0.035%) and group B the lowest (mean = 0.020%), indicating an additive effect of the two SNPs on free OPDA production under wounding stress. The haplotype analysis of free OPDA levels is consistent with the haplotype analysis of compounds with esterified OPDA and dnOPDA, suggesting that the candidate SNPs are related in the same way to levels of esterified OPDA and dnOPDA-containing lipids and to levels of free OPDA in natural accessions upon wounding. Thus, the data are consistent with the levels of these free and esterified oxylipins having similar evolutionary drivers.

SNPs in or near *AOC2* and *HPL1* are associated with the expression levels of the genes

To test if SNPs located in 5'UTR or upstream of genes may influence gene expression level, we selected a subset of 20 accessions from the investigated 360 accessions and used RT-qPCR to measure transcript abundance of *AOC1*, *AOC2*, *AOC3*, and *HPL1*. For the SNP at Chr3_9406789, 9 accessions belong to major allele group with allele T and 11 accessions belong to minor allele group with allele C. Among the three AOC genes tested, only *AOC2* showed a

significant difference in the gene expression level between the two haplotype groups ($P = 0.011$, Figure 4-6a). However, there was no significant correlation between *AOC2* expression level and relative level of Arabidopside E in the chosen accessions (Pearson's $r = -0.101$, $P = 0.672$; Figure 4-6b). To investigate the influence of the SNP at Chr4_8834169 on gene expression of *HPL1*, RT-qPCR of *HPL1* was performed in wounded leaf samples of same subset of accessions. The gene expression level of *HPL1* in major allele group (14 accessions) with allele C is significantly lower than minor allele group (6 accessions) with allele T ($P = 6.8E-04$, Figure 4-6c). Additionally, we found that there was a negative correlation between *HPL1* expression level and relative level of Arabidopside E (Pearson's $r = -0.418$, $P = 0.066$; Figure 4-6d). The gene expression results are consistent with lipidomics results, supporting our hypothesis that the SNP at Chr4_8834169 has an effect on gene expression of *HPL1* under wounding stress and contributes to the uneven ability of natural Arabidopsis accessions to produce esterified OPDA and dnOPDA.

To further verify the effects of the SNP at Chr3_9406789 and the SNP at Chr4_8834169 on gene expression of *AOC2* and *HPL1*, we performed a gene expression assay on another subset of 20 accessions. Among the three AOC genes tested including *AOC2*, no significant difference in the gene expression level was observed between the two haplotype groups (major allele: 11 accessions, minor allele: 9 accessions; Figure C-2a). Also, there is no significant correlation between *AOC2* level and relative content of Arabidopside E in both subsets. For *HPL1*, the gene expression level in the major allele group (12 accessions) was significantly lower than the expression in the minor allele group (8 accessions) ($P = 0.019$, Figure C-2c). There was also a negative correlation between the *HPL1* level and the relative content of Arabidopside E in this subset of 20 accessions (Pearson's $r = -0.672$; Figure C-2d). In summary, based on the gene

expression and lipid results among the two subsets of accessions, the expression of *HPLI* is likely to be affected by the sequence variant (Chr4_8834169) identified by GWAS and *HPLI* showed inhibitory effects on the production of Arabidopside E under wounding stress. For SNPs identified in non-coding sequences of AOCs, our evidence doesn't reveal a clear relationship between *AOC2* level and Arabidopside E content.

Discussion

Leaf lipid composition in response to mechanical wounding was examined in 360 Arabidopsis natural accessions from the 1001 Genomes Project. Although one study quantified wound-induced esterified oxidized lipids in 14 different accessions after wounding (Nilsson et al., 2016), most studies on leaf lipid profile after wounding have focused on Arabidopsis accession Col-0 (Buseman et al., 2006; Ibrahim et al., 2011; Nakashima et al., 2013; Nilsson et al., 2012; Vu et al., 2015, 2012; Vu et al., 2014b; Zien et al., 2001). Analysis of the 360 accessions revealed that natural variation exists in lipid profile of both unwounded (control) and wounded plants. The variation in the level of oxidized lipid classes among investigated accessions was much larger than the variation in non-oxidized lipids. For example, oxidized MGDG showed higher variation (CoV = 48%) than the variation in non-oxidized MGDG (CoV = 5%) after wounding. Additionally, oxidized lipid classes after wounding had high heritability with pseudo-heritabilities ranging from 36% to 85%, suggesting, that the level of oxidized lipids in response to wounding, may be strongly controlled by genetic variation among natural accessions and that oxidized lipid traits are likely to be amenable to genetic dissection and prediction using quantitative genetic approaches.

Among the changes in lipid profile after wounding, oxidized lipids, especially plastidic oxidized lipids, showed the largest fold changes. Studies on leaf lipid changes of Col-0 under

wounding stress have found that the rapid accumulation of esterified oxylipins is a major signature of wounding responses (Buseman et al., 2006; Ibrahim et al., 2011; Kourtchenko et al., 2007; Vu et al., 2015, 2012; Vu et al., 2014a; Vu et al., 2014b). Mechanical wounding and bacterial infection induce the oxylipin biosynthetic pathway, generating esterified, as well as free, oxylipin compounds, which have potential functions as antifungal and antibacterial activities or in modulation of gene expression (Andersson et al., 2006; Kourtchenko et al., 2007; Pedras & To, 2017; Schäfer et al., 2011; Stintzi et al., 2001; Taki et al., 2005; Wasternack & Strnad, 2016). In addition to the increase in total content of oxidized lipid classes, there was a preferential accumulation of highly or fully oxidized galactolipids at 45 min after wounding treatment, consistent with previous time-course data showing that fully oxidized species were formed most quickly and other galactolipid species with a mixture of oxidized and normal chains were formed more slowly (levels were higher at 6 h after wounding) (Buseman et al., 2006; Nilsson et al., 2012; Vu et al., 2014b; Vu et al., 2012).

The percentage of oxidized acMGDG and oxidized MGDG increased with an average change of 36- and 7-fold, respectively, in the 45 min after wounding, on average among the tested accessions. The accessions ranged from accession Tra 01, generating just a 5-fold change in oxidized acMGDG, to accession Omn-1 with a 127-fold increase at 45 min after wounding. The identified lipid-level phenotype variations may provide valuable information for further analysis of the genetic architecture underlying the most extreme differences. Analysis of recombinant inbred lines produced from accessions with extreme lipid-level phenotypes has potential to identify novel quantitative trait loci that were not detected using GWAS.

Another notable lipid-level phenotype change after wounding was the head-group acylation of MGDG and ASG. Head-group acylation of MGDG was originally described by

Heinz (Heinz, 1967) and many studies showed that drastic accumulation of acMGDG occurred in different plant species under wounding stress (Nilsson et al., 2015; Vu et al., 2014a; Vu et al., 2014b). In *Arabidopsis*, head-group acylation of MGDG was strongly enhanced by wounding, generating acMGDGs, in which oxidized acMGDGs were prominent. In this study, most of the investigated accessions rapidly produced acMGDG with an average of 32-fold change in total oxidized and non-oxidized acMGDGs at 45 min after wounding treatment. Besides acMGDG, there was a significant increase of ASG among the 360 accessions after wounding, consistent with the previous lipidomics study on Col-0 by Vu (Vu et al., 2015; Vu et al., 2014b).

The phenotypic variation in leaf lipid profile implies that the investigated group of 360 accessions from 1001 Genomes Project is a great resource for genetic trait dissection via GWAS. By analyzing the relative content of oxidized lipid species in leaf tissues from 360 accessions after wounding, we found most oxidized lipid species are highly controlled by genetic differences with high heritabilities. For most oxidized lipid species induced by wounding, two major genomic regions were detected on chromosome 3 and 4. Of the ~10 million SNPs present in imputed full sequence database, the one that is most strongly associated with most oxidized lipid species in region W-144 is SNP (Chr3_9406789) which is located in 5' UTR of *AOC2*, the other one (Chr4_8834169) that is most significant in region W-201 is situated in upstream regions of *HPL1*. Among all significant SNPs detected in region W-144 and region W-201, there is no nonsynonymous sequence variants in *AOC2* or *HPL1*, and other nearby genes. Therefore, we hypothesize that these SNPs in 5' UTR or upstream regions are most likely to control the gene expression under wounding stress.

The most significant SNP in region W-144 which contains *AOC1*, *AOC2*, and *AOC3* encompassed 30 lipid species including species of ox-acMGDG, ox-MGDG, ox-acDGDG, ox-

DGDG, ox-DGMG, ox-PG, and free OPDA. Previous studies on *AOC2* found it encodes an allele oxide cyclase, which catalyzes the cyclization of unstable allene oxides to OPDA and dnOPDA (Creelman & Mulpuri, 2002; Hofmann et al., 2006; Neumann et al., 2012). The *Arabidopsis* genome includes four *AOC* genes (*AOC1*, *AOC2*, *AOC3*, and *AOC4*) with functional redundancies among individual AOCs for free OPDA and JA production (Schaller et al., 2008; Stenzel et al., 2012). *AOC2* is the most characterized isoform and can form a trimer *in vitro* (Hofmann et al., 2006). Recently, *in vivo* and *in vitro* analysis shows that all four AOCs can interact with each other, and different heteromeric combinations result in different AOC activities for JA production (Otto et al., 2016; Stenzel et al., 2012). However, the biological role of each isoform is still elusive. More recently, biochemical experiments identified an enzyme complex LOX2–AOS–(*AOC2*)₃ in chloroplasts that drives OPDA synthesis from α -linolenic acid in consecutive steps (Pollmann et al., 2019). The haplotype analysis for the SNP at Chr3_9406789 for all associated lipid phenotypes suggested that the major allele group (198 accessions) with nucleotide T at this SNP position had a significantly higher level of esterified oxylipins (e.g., Arabidopside E) than the minor allele group with nucleotide C (162 accessions). Although *AOC2* showed a significant difference in the gene expression level between the two haplotype groups, indicating accessions with higher *AOC2* level generated lower level Arabidopside E in this subset of 20 accessions, there is no significant correlation between *AOC2* expression level and relative level of Arabidopside E (Pearson's $r = -0.101$, $P > 0.05$) and haplotype analysis in another subset of 20 accessions didn't show a significant difference in the *AOC2* expression level between the two haplotype groups. Therefore, current evidence demonstrates a strong association between SNPs in non-coding sequences of in the region of *AOC1/2/3* and levels of oxidized lipids, but doesn't support the notion that the effects of these

SNPs are mediated by differences in *AOC* expression level among accessions after wounding. The mechanism by which the *AOC* genes and variation in the region affects levels of various oxylipin-containing lipid species needs to be clarified in the future.

Another genomic region that is strongly associated with most esterified (dn)OPDA species under wounding stress is situated on chromosome 4. There were several significant SNPs within region W-201 located in upstream region of the gene *HPL1*, which encodes hydroperoxide lyase 1 involved in HPL pathway. The HPL pathway competes with the AOS pathway for the same substrate in free oxylipin biosynthesis pathways (Duan et al., 2005; Matsui, 2006; Nakashima et al., 2013; Nilsson et al., 2016). In *Arabidopsis*, lipoxygenase-derived (dn)HPOTs are cleaved by HPL1 into short-chain aldehydes including a C6 aldehyde and a (dinor)traumatin (Croft et al., 1993; Duan et al., 2005; Nakashima et al., 2013). The C6 aldehydes can be further metabolized to green leaf volatiles, which have well established roles in wounding and defense responses in plants (Arimura et al., 2009; Matsui et al., 2012). Evidence is accumulating to support the idea that HPL1 negatively influences Arabidopside formation by consuming galactolipid-bound hydroperoxide fatty acids (Nilsson et al., 2016). Differential expression of *HPL1* in different *Arabidopsis* accessions can contribute to variation in Arabidopsides, esterified traumatin, and green leaf volatile abundance (Duan et al., 2005; Nakashima et al., 2013; Nilsson et al., 2016). Our GWAS identified a SNP (Chr4_8834169) in the upstream region of *HPL1*, showing strong associations with a large number of esterified OPDA and dnOPDA molecular species. Haplotype analysis at the SNP at Chr4_8834169 for all associated esterified OPDA or dnOPDA-containing lipid species suggested that the major allele group (211 accessions) with nucleotide C at this SNP position had a significantly higher level of most esterified oxylipins than minor allele group with nucleotide T (149 accessions).

Additionally, haplotype analysis of *HPLI* expression level in showed that accessions in the major allele group had lower *HPLI* expression than the accessions in the minor allele group, and there were negative correlations between *HPLI* level and the relative content of Arabidopside E in both subsets of accessions under wounding. The evidence is consistent with our hypothesis that the natural genetic variant at Chr4_8834169 in the *HPLI* promoter region affects the gene expression level of *HPLI*, leading to variation in esterified oxylipins under wounding stress. The SNP at Chr4_8834169 is predicted, with the help of *Arabidopsis thaliana* cis-regulatory database (AtCisDB) (Davuluri et al., 2003), to be situated in a G-box promoter motif (CACGTG) or a DPBF1&2 binding site motif (ACACGTG). It is known that the highly conserved G-box motif (CACGTG) and the DPBF1&2 binding site motif (ACACGTG) are bound by TFs in the basic helix-loop-helix (bHLH) and basic Leu zipper (bZIP) families in Arabidopsis (Ezer et al., 2017). Therefore, it is possible that mutation at Chr4_8834169 in these promoter motifs can directly affect the physical binding of bHLH or bZIP TFs to the *HPLI* promoter, enhancing or inhibiting *HPLI* expression under wounding. Nilsson identified a region containing *HPLI* from QTL analysis of an F2 population created from a cross between C24 and Col-0 and suggested that high abundance of *HPLI* transcripts in some accessions could be attributed to accession-specific *trans*-acting elements. However, the identification of natural variation in the SNP at Chr4_8834169, 1198 bp upstream of start codon of *HPLI*, opens the possibility that a *cis*-regulatory element of *HPLI* can influence the gene expression level under wounding. Further work will be required to identify the TFs targeting *HPLI* under wounding stress and determine if the SNP at Chr4_8834169 is causal to transcription and esterified oxylipin production.

Based on previous discoveries about AOS and HPL pathways for OPDA and dnOPDA biosynthesis and our lipidomics and GWAS results, a refined model for free and esterified

OPDA and dnOPDA production in *Arabidopsis* upon mechanical wounding is proposed (Figure 4-7). Upon wounding, free and esterified OPDA and dnOPDA are produced directly from polyunsaturated FAs and polyunsaturated membrane lipids in reactions catalyzed by LOX2, AOS, and AOCs through the AOS pathway. HPL1 is a negative regulator because it competes with AOS for the same substrate (hydroperoxides and esterified hydroperoxides).

As the most induced lipid compounds under wounding, esterified OPDA or dnOPDA have indirect or direct functions in plant wounding response. They might act as a pool of free OPDA or dnOPDA that could be released when necessary, the released OPDA could be used as a substrate for JA production, which is an essential hormone in defense mechanisms (Chini et al., 2007; Santner & Estelle, 2007). On the other hand, esterified OPDA or dnOPDA may play a role in sequestration of excess free OPDA and dnOPDA which are toxic for plant cells (Song et al., 2021). Moreover, they *in vitro* studies showed that some esterified OPDA such as arabidopside A, E, G have antifungal and antibacterial activities (Andersson et al., 2006; Kourtchenko et al., 2007; Pedras & To, 2017). The accumulation of arabidopsides can help *Arabidopsis* prevent microbe infection in wounding site, reducing further damages after wounding. Specific genomic variants in *AOC1/2/3* and *HPL1* in natural accessions improve the ability of *Arabidopsis* to generate esterified OPDA or dnOPDA, resulting in better performance after wounding damage.

Figures

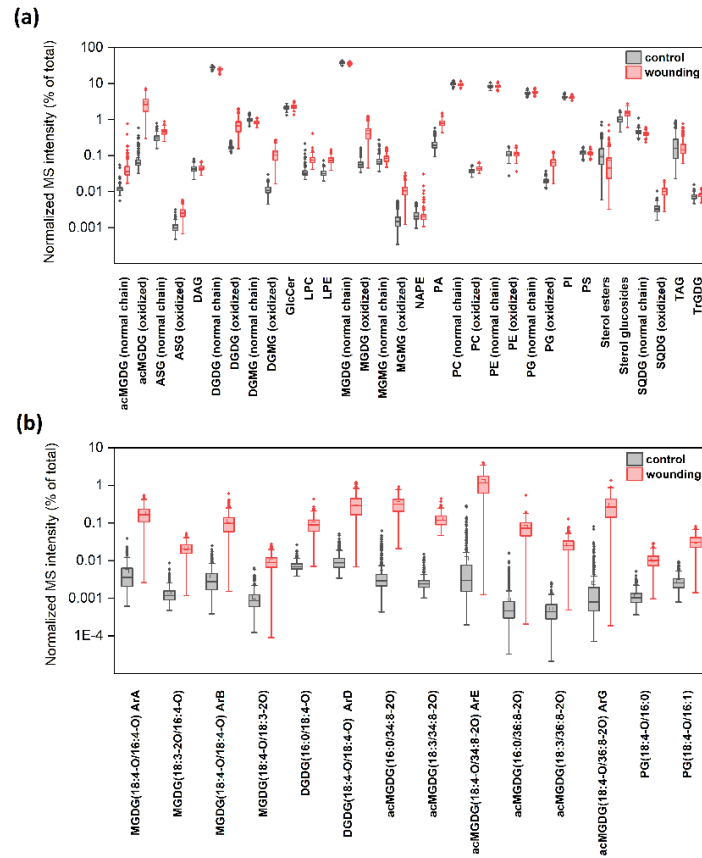


Figure 4-1. Changes in the relative contents of 32 lipid classes and 14 esterified (dn)OPDA species in leaf tissues in the 360 investigated Arabidopsis accessions before and 45 min after wounding treatment

Changes in the leaf relative contents (% of total) of 32 lipid classes (a) and 14 esterified (dn)OPDA species (b) in the 360 investigated Arabidopsis accessions before (grey boxes) and after (red boxes) wounding treatment. Standard box plots are shown with horizontal bars in the boxes representing the median, bottom and top of the box indicate the 25th and 75th percentiles (lower and upper quartiles). Whiskers indicate 1.5-fold interquartile range, diamonds represent potential outliers. Note that the y-axis was log10 scaled, due to the large differences in the relative contents of various lipids.

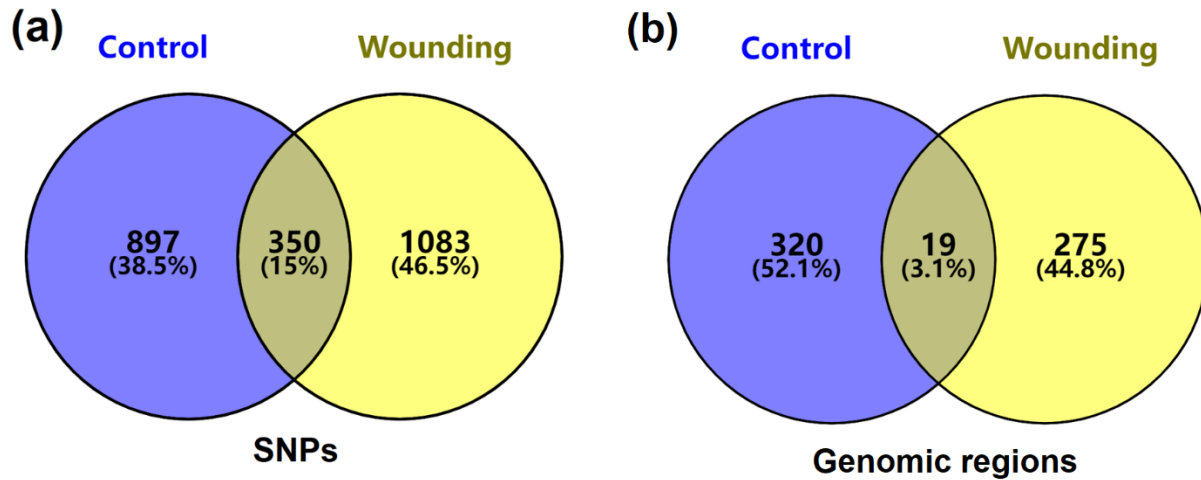


Figure 4-2. Significant SNPs and candidate genes identified from GWAS

(a) Venn diagrams comparing the number of significant SNPs ($p\text{-score} \geq 6$, $\text{maf} \geq 0.05$) identified under unstressed (control) and wounding conditions. (b) Venn diagrams comparing the genomic region of interest in standard and wounding condition. Each genomic region of interest contains all the SNPs within 20 kb of each other with alleles associated with the level of a particular lipid or with multiple lipids that are associated with the same SNPs in the region. overlapping regions which share at least one SNPs and are associated with at least one of the same lipids.

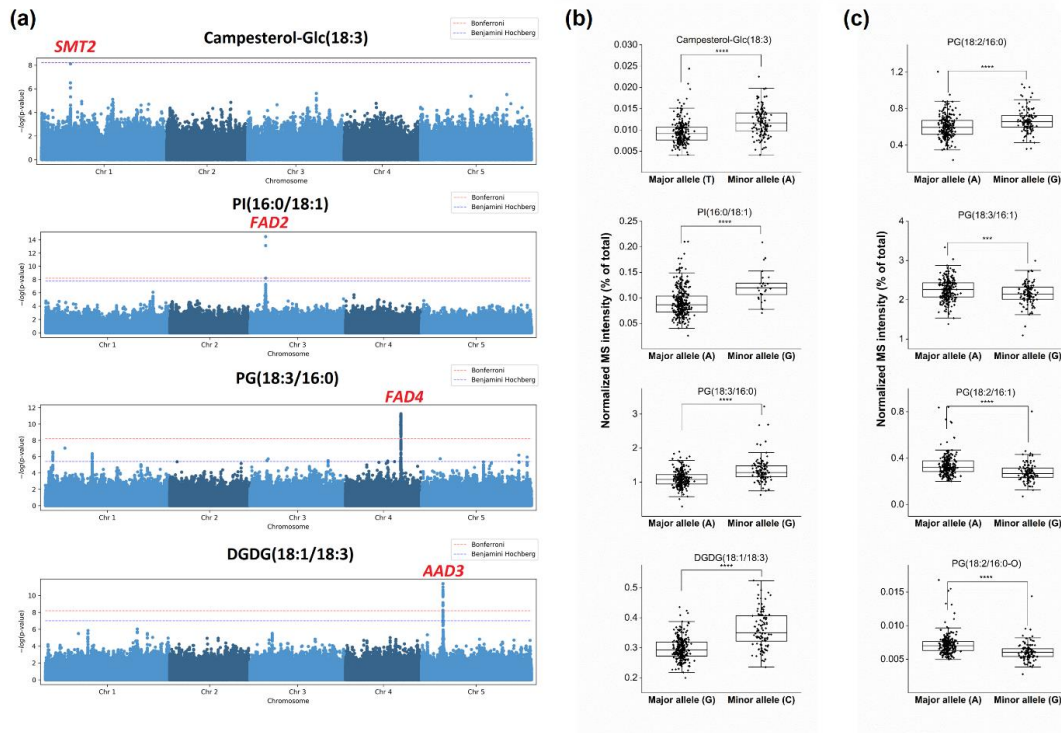


Figure 4-3. GWAS mapping (Manhattan plot) and haplotype analysis for lipid species identified in unstressed population of Arabidopsis

(a) Manhattan plot for relative contents of Campesterol-Glc(18:3), PI(16:0/18:1), PG(18:3/16:0), DGDG(18:1/18:3). Candidate genes SMT2, FAD2, FAD4, AAD3 located in the associated genomic regions correspond to Campesterol-Glc(18:3), PI(16:0/18:1), PG(18:3/16:0), and DGDG(18:1/18:3) respectively. (b) Haplotype analysis in unstressed 360 natural accessions based on the highest SNPs within the most associated genomic regions. (c) Haplotype analysis of various PG species in unstressed 360 natural accessions based on the SNP(Chr4_13572006) within the most associated genomic regions. Diamonds showing the distribution of the relative content of specific lipids in two haplotype groups of accessions. The horizontal lines within the boxes represent the medians, the boxes indicate the 25th and 75th percentiles, and the Error bars represent \pm SD. ****, $P < 0.0001$ (Student's t-test).

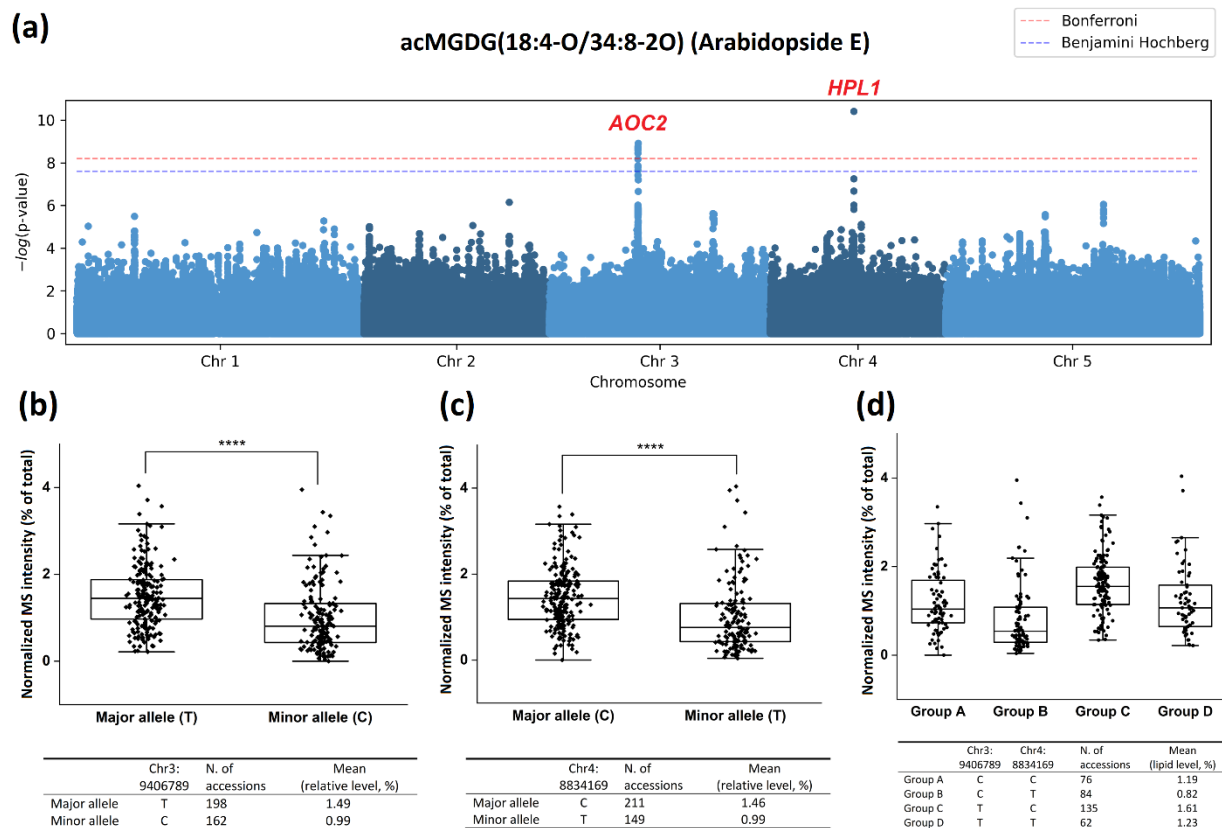


Figure 4-4. The relative level of acMGDG (18:4-O/34:8-2O) (Arabidopsis E) is associated with the SNPs in non-coding sequence of *AOC2* and *HPL1*

(a) Manhattan plot of genome-wide association of SNPs with levels (%) of acMGDG (18:4-O/34:8-2O) (Arabidopsis E). Haplotype analysis of Arabidopsis E level in 360 natural accessions under wounding based on SNP Chr3:9406789 (b), SNP Chr4:8834169 (c), and on both SNPs (d). Plots show the distribution of the relative content of Arabidopsis E in different haplotype groups of accessions. The horizontal lines within the boxes represent the medians, the boxes indicate the 25th and 75th percentiles, and the Error bars represent \pm SD.

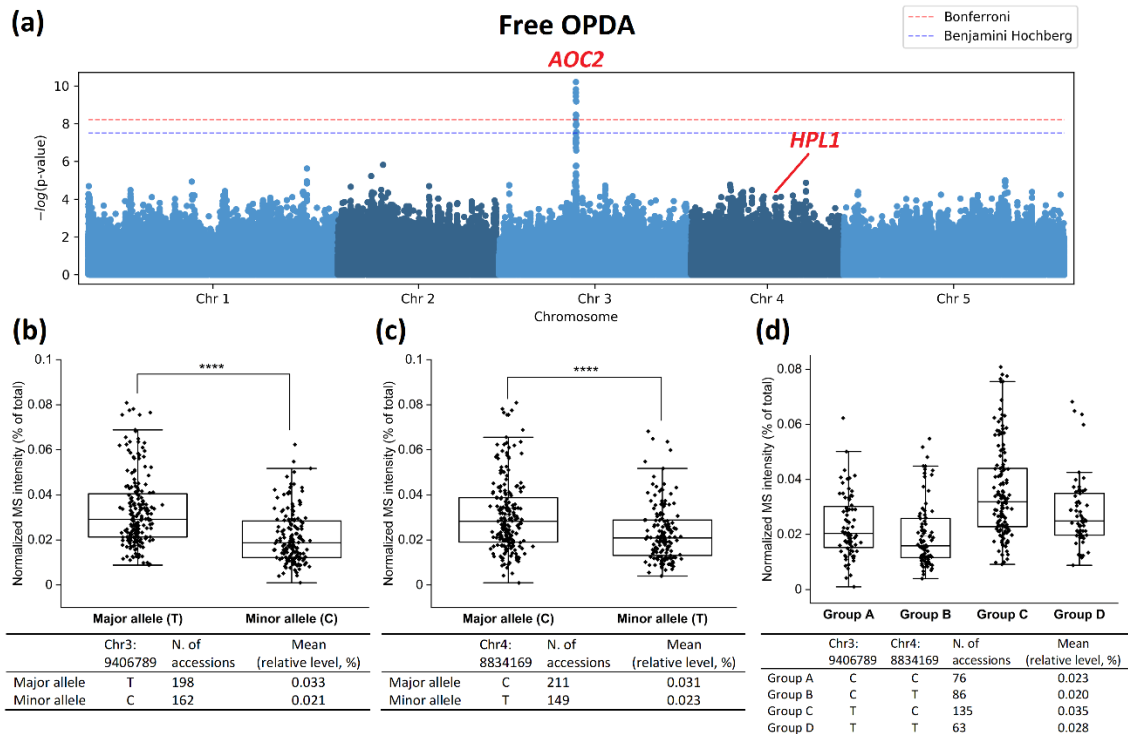


Figure 4-5. The relative level of free OPDA is associated with the SNPs in non-coding sequence of *AOC2* and *HPL1*

(a) Manhattan plot of genome-wide association of SNPs with levels (%) of free OPDA.

Haplotype analysis of OPDA level in 360 natural accessions under wounding based on SNP Chr3:9406789 (b), SNP Chr4:8834169 (c), and on both SNPs (d). Plots show the distribution of the relative content of OPDA in different haplotype groups of accessions. The horizontal lines within the boxes represent the medians, the boxes indicate the 25th and 75th percentiles, and the Error bars represent \pm SD.

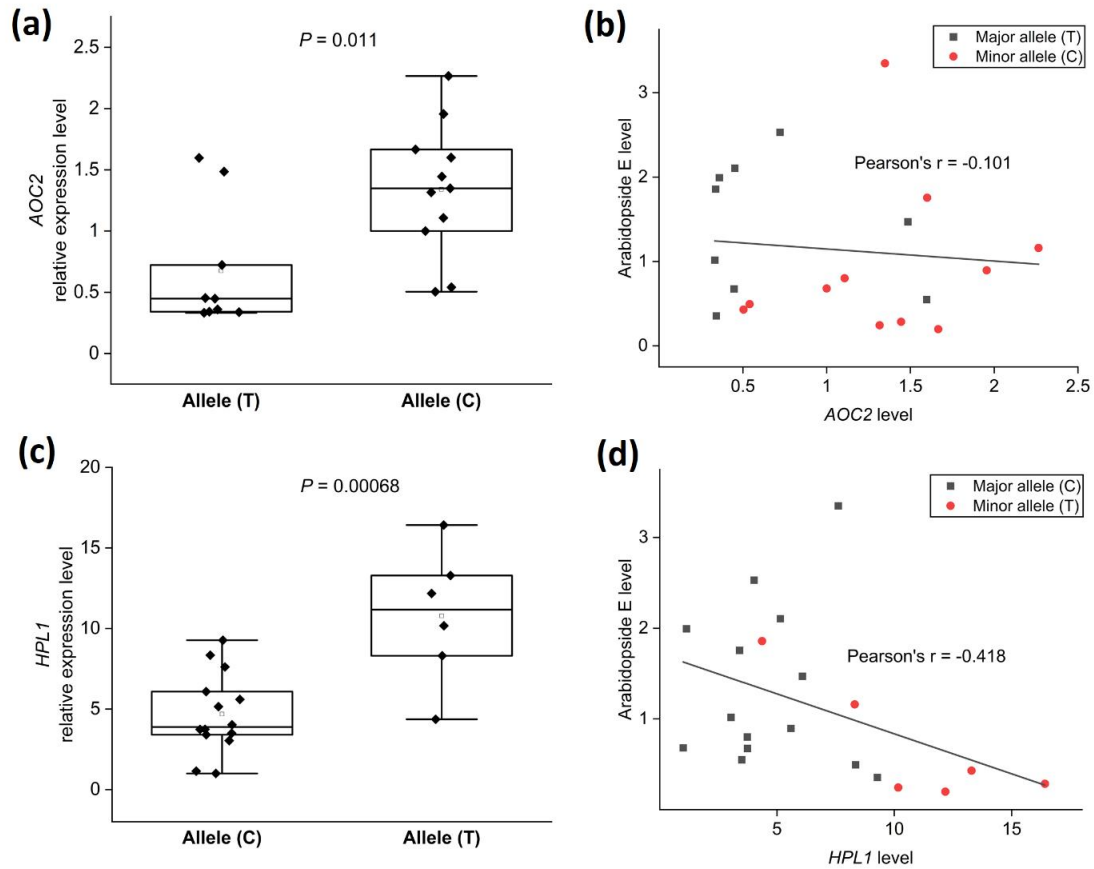


Figure 4-6. Association between SNPs, gene expression level, and Arabidopside E level

The distribution of *AOC2* (a) and *HPL1* (c) expression level among two haplotype groups.

Relationship between the relative level of *AOC2* and relative content of Arabidopside E (b) and

relationship between *HPL1* and Arabidopside E (d). Symbols indicate the distribution of *AOC2*

and *HPL1* levels in two haplotype groups of accessions (black squares represent major allele

group, red dots represent minor allele group). The horizontal lines within the boxes represent the

medians, the boxes indicate the 25th and 75th percentiles, and the Error bars represent \pm SD.

Exact *P*-values (Student's *t*-test) are shown above. Pearson correlation coefficient (Pearson's *r*)

is shown above the trend line indicating the linear correlation between gene expression and lipid

level.

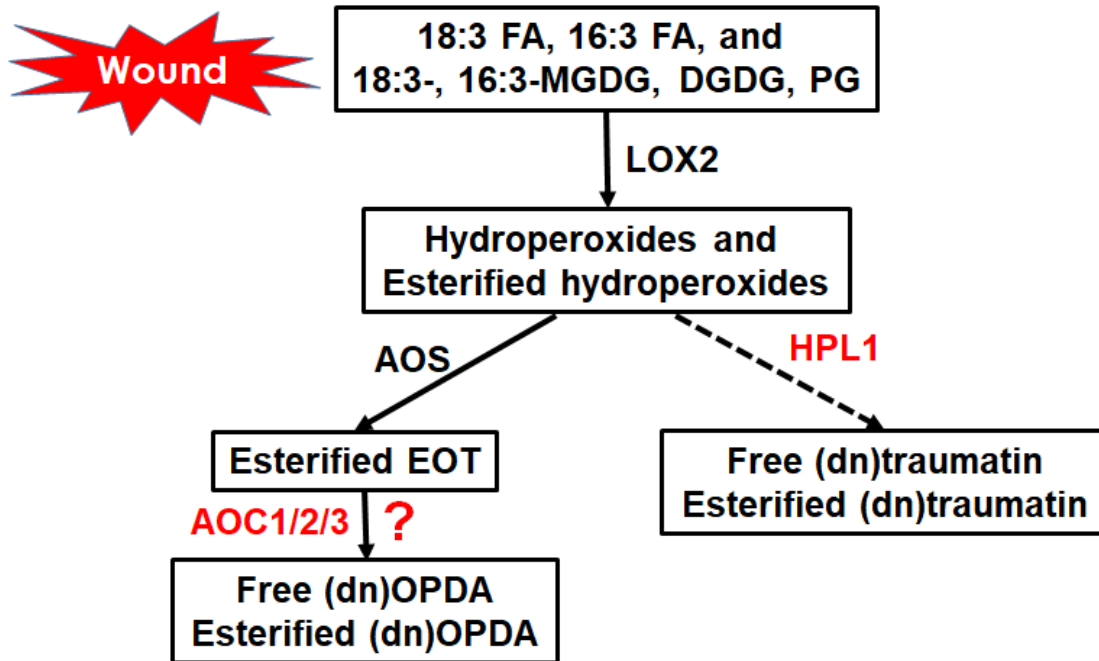


Figure 4-7. Proposed model of free and esterified (dn)OPDA biosynthesis in Arabidopsis leaves under mechanical wounding stress

Solid black lines indicate the AOS pathway for the biosynthesis of free and esterified (dn)OPDA, while the dashed line indicates HPL pathway which reduces the flux through AOS pathway. Enzymes labeled in red (AOC1/2/3, HPL1) are candidate regulator identified from GWAS.

Tables

Table 4-1. Summary statistics of variation and heritability for 32 lipid classes in 360 accessions of Arabidopsis before and after wounding

The total relative content for each lipid class was calculated for each accession and summarized in Table S4-7. The mean, CoV were calculated among the 360 accessions, heritability was calculated from GWA-Portal.

Lipid class	Mean		CoV ^a (%)		<i>h</i> ^{2b} (%)	
	control	wound	control	wound	control	wound
acMGDG (normal)	0.012	0.045	30.63	105.34	22	47
acMGDG (oxidized)	0.078	2.82	76.61	49.06	6	85
ASG (normal chain)	0.31	0.45	23.84	19.94	54	70
ASG (oxidized)	0.0011	0.0027	31.27	31.18	22	64
sterol glucosides	1.02	1.49	24.24	21.12	58	65
sterol esters	0.12	0.066	79.09	103.52	77	53
DAG	0.043	0.046	22.11	15.80	46	47
TAG	0.22	0.18	81.51	53.97	11	8
GlcCer	2.16	2.29	11.70	11.73	51	64
NAPE	0.0022	0.0022	31.17	83.90	36	37
DGDG (normal chain)	28.26	25.16	5.24	6.59	43	31
DGDG (oxidized)	0.17	0.71	10.75	45.59	4	67
DGMG (normal chain)	0.98	0.83	13.94	11.88	62	47
DGMG (oxidized)	0.011	0.11	25.64	41.58	8	61
LPC	0.035	0.078	42.08	32.11	24	37
LPE	0.033	0.076	20.78	22.44	5	29
MGDG (normal chain)	37.76	35.81	5.16	4.73	46	55
MGDG (oxidized)	0.059	0.44	30.71	47.79	12	51
MGMG (normal chain)	0.072	0.086	34.08	25.55	10	7
MGMG (oxidized)	0.0017	0.011	50.74	40.38	12	39
PA	0.21	0.80	32.83	21.63	26	61
PC (normal chain)	9.68	9.50	6.60	7.60	54	54
PC (oxidized)	0.037	0.044	14.30	14.27	36	36
PE (normal chain)	8.36	8.47	9.23	8.89	59	59
PE (oxidized)	0.11	0.11	18.76	18.46	44	66
PG (normal chain)	5.43	5.72	7.42	8.37	75	54
PG (oxidized)	0.020	0.065	15.92	28.85	29	54
PI	4.21	4.04	7.42	6.62	40	55
PS	0.12	0.11	13.51	11.41	57	59
SQDG (normal chain)	0.45	0.40	14.44	11.90	31	55
SQDG (oxidized)	0.0034	0.010	29.35	28.98	0	33
TrGDG	0.0073	0.0081	17.31	14.78	12	11
OPDA	n.d. ^d	0.028	n.d.	55.80	n.d.	53
JA	n.d.	0.051	n.d.	40.60	n.d.	45

^astandard deviation, ^bcoefficient of variation, ^cnarrow-sense heritability, ^dnot determined.

Table 4-2. Lipid species showing strong associations with genomic region W-144 and region W-201

All lipid phenotypes uploaded for GWAS which showed strong associations (pscore \geq 6, maf \geq 5%, and pseudo-heritability > 0) with the genomic region W-144 and W-201.

Region W-144	Region W-201		Both regions
acDGDG(18:4-O/34:8-2O)	acDGDG(18:4-O/34:8-2O)	acMGDG(18:4-O/36:6-O)	acDGDG(18:4-O/34:8-2O)
acMGDG(16:0/34:8-2O)	acMGDG(16:0/34:6)	acMGDG(18:4-O/36:7-O)	acMGDG(16:0/34:8-2O)
acMGDG(16:0/36:8-2O)	acMGDG(16:0/34:7-O)	acMGDG(18:4-O/36:8-2O)	acMGDG(16:0/36:8-2O)
acMGDG(16:1/34:8-2O)	acMGDG(16:0/34:8-2O)	acMGDG(18:5-2O/34:8-2O)	acMGDG(16:1/34:8-2O)
acMGDG(16:3-2O/34:8-2O)	acMGDG(16:0/36:8-2O)	acMGDG(18:5-2O/36:8-2O)	acMGDG(16:3-2O/34:8-2O)
acMGDG(16:3-O/34:8-2O)	acMGDG(16:1/34:8-2O)	DGDG(16:0/18:3-2O)	acMGDG(16:3-O/34:8-2O)
acMGDG(16:3-O/36:8-2O)	acMGDG(16:3-2O/34:8-2O)	DGDG(16:0/18:3-O)	acMGDG(16:3-O/36:8-2O)
acMGDG(16:4-O/34:8-2O)	acMGDG(16:3-2O/36:8-2O)	DGDG(16:0/18:4-O)	acMGDG(16:4-O/34:8-2O)
acMGDG(16:4-O/36:8-2O)	acMGDG(16:3-O/34:8-2O)	DGDG(18:3-2O/16:3)	acMGDG(16:4-O/36:8-2O)
acMGDG(18:0/34:8-2O)	acMGDG(16:3-O/36:8-2O)	DGDG(18:4-O/16:3)	acMGDG(18:0/34:8-2O)
acMGDG(18:3-2O/34:6)	acMGDG(16:4-O/34:8-2O)	DGDG(18:4-O/16:4-O)	acMGDG(18:3-2O/34:6)
acMGDG(18:3-O/34:8-2O)	acMGDG(16:4-O/36:8-2O)	DGDG(18:4-O/18:4-2O)	acMGDG(18:3-O/34:8-2O)
acMGDG(18:4-2O/34:8-2O)	acMGDG(18:0/34:8-2O)	DGDG(18:4-O/18:4-O)	acMGDG(18:4-2O/34:8-2O)
acMGDG(18:4-2O/36:8-2O)	acMGDG(18:2/34:6)	DGMG(16:4-O)	acMGDG(18:4-2O/36:8-2O)
acMGDG(18:4-O/34:6)	acMGDG(18:2/34:7-O)	DGMG(18:4-O)	acMGDG(18:4-O/34:6)
acMGDG(18:4-O/34:8-2O)	acMGDG(18:2-3O/34:8-2O)	MGDG(18:3-O/16:4-O)	acMGDG(18:4-O/34:8-2O)
acMGDG(18:4-O/36:6-O)	acMGDG(18:3/34:6)	MGDG(18:4-O/16:3-O)	acMGDG(18:4-O/36:6-O)
acMGDG(18:4-O/36:7-O)	acMGDG(18:3/34:7-O)	MGDG(18:4-O/16:4-O)	acMGDG(18:4-O/36:7-O)
acMGDG(18:4-O/36:8-2O)	acMGDG(18:3-2O/34:6)	MGDG(18:4-O/18:1)	acMGDG(18:4-O/36:8-2O)
DGDG(16:0/18:4-O)	acMGDG(18:3-2O/34:8-2O)	MGDG(18:4-O/18:3-2O)	DGDG(16:0/18:4-O)
DGDG(18:3-2O/16:3)	acMGDG(18:3-2O/36:8-2O)	MGDG(18:4-O/18:3-3O)	DGDG(18:3-2O/16:3)
DGDG(18:4-O/18:4-2O)	acMGDG(18:3-3O/36:8-2O)	MGDG(18:4-O/18:3-O)	DGDG(18:4-O/18:4-2O)
DGDG(18:4-O/18:4-O)	acMGDG(18:3-O/34:8-2O)	MGDG(18:4-O/18:4-3O)	DGDG(18:4-O/18:4-O)
DGMG(16:4-O)	acMGDG(18:3-O/36:6-O)	MGDG(18:4-O/18:4-O)	DGMG(16:4-O)
MGDG(18:4-O/16:4-O)	acMGDG(18:4-2O/34:7-O)	MGDG(18:5-2O/16:4-O)	MGDG(18:4-O/16:4-O)
OPDA	acMGDG(18:4-2O/34:8-2O)	MGDG(18:5-2O/18:4-O)	
PE(16:0/16:3)	acMGDG(18:4-2O/36:8-2O)	NAPE(18:3/36:6)	
PG(18:4-O/16:0)	acMGDG(18:4-3O/34:8-2O)	PC(18:3/18:3-2O)	
PG(18:4-O/18:2)	acMGDG(18:4-O/34:6)	PG(18:3-O/16:0)	
PG(18:4-O/18:3)	acMGDG(18:4-O/34:8-2O)	PG(18:4-O/16:1)	
	acMGDG(18:4-O/36:6-2O)	Sitosterol-Glc(18:4-O)	

Table 4-3. Single nucleotide polymorphisms (SNPs) in non-coding regions of AOCs and HPL1 are associated with arabidopside E under wounding stress

Polymorphisms situated in W-144 and W-201 of phenotype arabidopside E with p-score ≥ 6 and maf $\geq 5\%$ were analyzed. The significant SNPs are shown with the physical position (Chr., Position), candidate gene ID, genomic region in which SNP is located, allele frequency, number of accessions for each SNP allele, P-value ($-\log_{10}(P)$), and Pearson's correlation coefficient with the most significant SNP.

Chr.	Position	Gene	Genomic region	Location versus gene start	$-\log_{10}(P)$	Allele frequency	Major allele	Minor allele	Effect type	Linkage to the highest SNP
3	9403749	AT3G25760	W-144	-29	7.80	241/119	C	A	Upstream	0.5644
3	9405475	AT3G25770	W-144	-1193	8.59	244/116	A	C	Upstream	0.6237
3	9406130	AT3G25770	W-144	-538	8.17	239/121	C	T	Upstream	0.5845
3	9406789	AT3G25770	W-144	+121	8.61	198/162	T	C	5'UTR	1.0000
3	9408202	AT3G25780	W-144	-957	7.87	197/163	C	T	Upstream	0.9944
3	9408340	AT3G25780	W-144	-819	8.46	243/117	C	T	Upstream	0.6276
3	9411074	AT3G25780	W-144	+1915	7.66	250/110	C	T	3'UTR	0.5879
4	8834169	AT4G15440	W-201	-1198	10.41	211/149	C	T	Upstream	1.0000
4	8834257	AT4G15440	W-201	-1110	7.25	322/38	G	T	Upstream	0.4088
4	8834258	AT4G15440	W-201	-1109	6.02	199/161	G	A	Upstream	0.9002
4	8834584	AT4G15440	W-201	-783	6.67	325/35	A	G	Upstream	0.3715

References

- Ahmad, P., Rasool, S., Gul, A., Sheikh, S. A., Akram, N. A., Ashraf, M., Kazi, A. M., & Gucel, S. (2016). Jasmonates: Multifunctional Roles in Stress Tolerance. *Frontiers in Plant Science*, 7, 813.
- Andersson, M. X., Hamberg, M., Kourtchenko, O., Brunnström, A., McPhail, K. L., Gerwick, W. H., Göbel, C., Feussner, I., & Ellerström, M. (2006). Oxylin profiling of the hypersensitive response in *Arabidopsis thaliana*. Formation of a novel oxo-phytodienoic acid-containing galactolipid, arabidopside E. *The Journal of Biological Chemistry*, 281, 31528–31537.
- Arimura, G.-I., Matsui, K., & Takabayashi, J. (2009). Chemical and molecular ecology of herbivore-induced plant volatiles: Proximate factors and their ultimate functions. *Plant & Cell Physiology*, 50, 911–923.
- Banas, A., Carlsson, A. S., Huang, B., Lenman, M., Banas, W., Lee, M., Noiriél, A., Benveniste, P., Schaller, H., Bouvier-Navé, P., & Stymne, S. (2005). Cellular sterol ester synthesis in plants is performed by an enzyme (phospholipid:sterol acyltransferase) different from the yeast and mammalian acyl-CoA:sterol acyltransferases. *The Journal of Biological Chemistry*, 280, 34626–34634.
- Branham, S. E., Wright, S. J., Reba, A., & Linder, C. R. (2016). Genome-Wide Association Study of *Arabidopsis thaliana* Identifies Determinants of Natural Variation in Seed Oil Composition. *The Journal of Heredity*, 107, 248–256.
- Broun, P., Shanklin, J., Whittle, E., & Somerville, C. (1998). Catalytic plasticity of fatty acid modification enzymes underlying chemical diversity of plant lipids. *Science (New York, N.Y.)*, 282, 1315–1317.
- Bryant, F. M., Munoz-Azcarate, O., Kelly, A. A., Beaudoin, F., Kurup, S., & Eastmond, P. J. (2016). ACYL-ACYL CARRIER PROTEIN DESATURASE2 and 3 Are Responsible for Making Omega-7 Fatty Acids in the *Arabidopsis* Aleurone. *Plant Physiology*, 172, 154–162.
- Buseman, C. M., Tamura, P., Sparks, A. A., Baughman, E. J., Maatta, S., Zhao, J., Roth, M. R., Esch, S. W., Shah, J., Williams, T. D., & Welti, R. (2006). Wounding stimulates the accumulation of glycerolipids containing oxophytodienoic acid and dinor-oxophytodienoic acid in *Arabidopsis* leaves. *Plant Physiology*, 142, 28–39.
- Catz, D. S., Tandecarz, J. S., & Cardini, C. E. (1985). UDP-Glucose: Sterol Glucosyltransferase and a Steryl Glucoside Acyltransferase Activity in Amyloplast Membranes from Potato Tubers. *Journal of Experimental Botany*, 36, 602–609.
- Chen, Q., Steinhauer, L., Hammerlindl, J., Keller, W., & Zou, J. (2007). Biosynthesis of phytosterol esters: Identification of a sterol o-acyltransferase in *Arabidopsis*. *Plant Physiology*, 145, 974–984.

- Creelman, R. A., & Mulpuri, R. (2002). The oxylipin pathway in Arabidopsis. *The Arabidopsis Book*, 1, e0012.
- Croft, K. P. C., Juttner, F., & Slusarenko, A. J. (1993). Volatile Products of the Lipoxygenase Pathway Evolved from *Phaseolus vulgaris* (L.) Leaves Inoculated with *Pseudomonas syringae* pv *phaseolicola*. *Plant Physiology*, 101, 13–24.
- Davuluri, R. V., Sun, H., Palaniswamy, S. K., Matthews, N., Molina, C., Kurtz, M., & Grotewold, E. (2003). AGRIS: Arabidopsis gene regulatory information server, an information resource of Arabidopsis cis-regulatory elements and transcription factors. *BMC Bioinformatics*, 4, 25.
- Duan, H., Huang, M.-Y., Palacio, K., & Schuler, M. A. (2005). Variations in CYP74B2 (hydroperoxide lyase) gene expression differentially affect hexenal signaling in the Columbia and Landsberg erecta ecotypes of Arabidopsis. *Plant Physiology*, 139, 1529–1544.
- Dunn, W. B., Broadhurst, D., Begley, P., Zelena, E., Francis-McIntyre, S., Anderson, N., Brown, M., Knowles, J. D., Halsall, A., Haselden, J. N., Nicholls, A. W., Wilson, I. D., Kell, D. B., Goodacre, R., & Human Serum Metabolome (HUSERMET) Consortium. (2011). Procedures for large-scale metabolic profiling of serum and plasma using gas chromatography and liquid chromatography coupled to mass spectrometry. *Nature Protocols*, 6, 1060–1083.
- Ezer, D., Shepherd, S. J. K., Brestovitsky, A., Dickinson, P., Cortijo, S., Charoensawan, V., Box, M. S., Biswas, S., Jaeger, K. E., & Wigge, P. A. (2017). The G-Box Transcriptional Regulatory Code in Arabidopsis. *Plant Physiology*, 175, 628–640.
- Ferrer, A., Altabella, T., Arró, M., & Boronat, A. (2017). Emerging roles for conjugated sterols in plants. *Progress in Lipid Research*, 67, 27–37.
- Gfeller, A., Dubugnon, L., Liechti, R., & Farmer, E. E. (2010). Jasmonate biochemical pathway. *Science Signaling*, 3, cm3.
- Heinz, E. (1967). [Acylgalactosyldiglyceride from leaf homogenates]. *Biochimica Et Biophysica Acta*, 144, 321–332.
- Hermansson, M., Hokynar, K., & Somerharju, P. (2011). Mechanisms of glycerophospholipid homeostasis in mammalian cells. *Progress in Lipid Research*, 50, 240–257.
- Hofmann, E., Zerbe, P., & Schaller, F. (2006). The crystal structure of Arabidopsis thaliana allene oxide cyclase: Insights into the oxylipin cyclization reaction. *The Plant Cell*, 18, 3201–3217.
- Ibrahim, A., Schütz, A.-L., Galano, J.-M., Herrfurth, C., Feussner, K., Durand, T., Brodhun, F., & Feussner, I. (2011). The Alphabet of Galactolipids in Arabidopsis thaliana. *Frontiers in Plant Science*, 2, 95.

- Jasinski, S., Lécureuil, A., Miquel, M., Loudet, O., Raffaele, S., Froissard, M., & Guerche, P. (2012). Natural variation in seed very long chain fatty acid content is controlled by a new isoform of KCS18 in *Arabidopsis thaliana*. *PLoS One*, *7*, e49261.
- Kachroo, A., Shanklin, J., Whittle, E., Lapchyk, L., Hildebrand, D., & Kachroo, P. (2007). The *Arabidopsis* stearyl-acyl carrier protein-desaturase family and the contribution of leaf isoforms to oleic acid synthesis. *Plant Molecular Biology*, *63*, 257–271.
- Kim, H. U. (2020). Lipid Metabolism in Plants. *Plants (Basel, Switzerland)*, *9*, E871.
- Koo, A. J., Thireault, C., Zemelis, S., Poudel, A. N., Zhang, T., Kitaoka, N., Brandizzi, F., Matsuura, H., & Howe, G. A. (2014). Endoplasmic Reticulum-associated Inactivation of the Hormone Jasmonoyl-l-Isoleucine by Multiple Members of the Cytochrome P450 94 Family in *Arabidopsis*. *Journal of Biological Chemistry*, *289*, 29728–29738.
- Koornneef, M., Alonso-Blanco, C., & Vreugdenhil, D. (2004). Naturally occurring genetic variation in *Arabidopsis thaliana*. *Annual Review of Plant Biology*, *55*, 141–172.
- Korte, A., & Farlow, A. (2013). The advantages and limitations of trait analysis with GWAS: A review. *Plant Methods*, *9*, 29.
- Kourtchenko, O., Andersson, M. X., Hamberg, M., Brunnström, A., Göbel, C., McPhail, K. L., Gerwick, W. H., Feussner, I., & Ellerström, M. (2007). Oxo-phytodienoic acid-containing galactolipids in *Arabidopsis*: Jasmonate signaling dependence. *Plant Physiology*, *145*, 1658–1669.
- Li-Beisson, Y., Shorrosh, B., Beisson, F., Andersson, M. X., Arondel, V., Bates, P. D., Baud, S., Bird, D., Debono, A., Durrett, T. P., Franke, R. B., Graham, I. A., Katayama, K., Kelly, A. A., Larson, T., Markham, J. E., Miquel, M., Molina, I., Nishida, I., ... Ohlrogge, J. (2013). Acyl-lipid metabolism. *The Arabidopsis Book*, *11*, e0161.
- Matsui, K. (2006). Green leaf volatiles: Hydroperoxide lyase pathway of oxylipin metabolism. *Current Opinion in Plant Biology*, *9*, 274–280.
- Matsui, K., Sugimoto, K., Mano, J., Ozawa, R., & Takabayashi, J. (2012). Differential metabolisms of green leaf volatiles in injured and intact parts of a wounded leaf meet distinct ecophysiological requirements. *PLoS One*, *7*, e36433.
- Menard, G. N., Moreno, J. M., Bryant, F. M., Munoz-Azcarate, O., Kelly, A. A., Hassani-Pak, K., Kurup, S., & Eastmond, P. J. (2017). Genome Wide Analysis of Fatty Acid Desaturation and Its Response to Temperature. *Plant Physiology*, *173*, 1594–1605.
- Misiak, M., Kalinowska, M., & Wojciechowski, Z. A. (1991). Characterization of acyl lipid: Sterol glucoside acyltransferase from oat (*Avena sativa* L.) seedlings. *Acta Biochimica Polonica*, *38*, 43–45.
- Moellering, E. R., & Benning, C. (2011). Galactoglycerolipid metabolism under stress: A time for remodeling. *Trends in Plant Science*, *16*, 98–107.

- Nakamura, Y. (2013). Phosphate starvation and membrane lipid remodeling in seed plants. *Progress in Lipid Research*, *52*, 43–50.
- Nakashima, A., von Reuss, S. H., Tasaka, H., Nomura, M., Mochizuki, S., Iijima, Y., Aoki, K., Shibata, D., Boland, W., Takabayashi, J., & Matsui, K. (2013). Traumatins- and dinortraumatins-containing galactolipids in Arabidopsis: Their formation in tissue-disrupted leaves as counterparts of green leaf volatiles. *The Journal of Biological Chemistry*, *288*, 26078–26088.
- Neumann, P., Brodhun, F., Sauer, K., Herrfurth, C., Hamberg, M., Brinkmann, J., Scholz, J., Dickmanns, A., Feussner, I., & Ficner, R. (2012). Crystal structures of Physcomitrella patens AOC1 and AOC2: Insights into the enzyme mechanism and differences in substrate specificity. *Plant Physiology*, *160*, 1251–1266.
- Nilsson, A. K., Fahlberg, P., Ellerström, M., & Andersson, M. X. (2012). Oxo-phytodienoic acid (OPDA) is formed on fatty acids esterified to galactolipids after tissue disruption in Arabidopsis thaliana. *FEBS Letters*, *586*, 2483–2487.
- Nilsson, A. K., Fahlberg, P., Johansson, O. N., Hamberg, M., Andersson, M. X., & Ellerström, M. (2016). The activity of HYDROPEROXIDE LYASE 1 regulates accumulation of galactolipids containing 12-oxo-phytodienoic acid in Arabidopsis. *Journal of Experimental Botany*, *67*, 5133–5144.
- Nilsson, A. K., Johansson, O. N., Fahlberg, P., Kommuri, M., Töpel, M., Bodin, L. J., Sikora, P., Modarres, M., Ekengren, S., Nguyen, C. T., Farmer, E. E., Olsson, O., Ellerström, M., & Andersson, M. X. (2015). Acylated monogalactosyl diacylglycerol: Prevalence in the plant kingdom and identification of an enzyme catalyzing galactolipid head group acylation in Arabidopsis thaliana. *The Plant Journal: For Cell and Molecular Biology*, *84*, 1152–1166.
- Okuley, J., Lightner, J., Feldmann, K., Yadav, N., Lark, E., & Browse, J. (1994). Arabidopsis FAD2 gene encodes the enzyme that is essential for polyunsaturated lipid synthesis. *The Plant Cell*, *6*, 147–158.
- Otto, M., Naumann, C., Brandt, W., Wasternack, C., & Hause, B. (2016). Activity Regulation by Heteromerization of Arabidopsis Allene Oxide Cyclase Family Members. *Plants (Basel, Switzerland)*, *5*, E3.
- Pedras, M. S. C., & To, Q. H. (2017). Defense and signalling metabolites of the crucifer Erucastrum canariense: Synchronized abiotic induction of phytoalexins and galactolipins. *Phytochemistry*, *139*, 18–24.
- Pollmann, S., Springer, A., Rustgi, S., von Wettstein, D., Kang, C., Reinbothe, C., & Reinbothe, S. (2019). Substrate channeling in oxylipin biosynthesis through a protein complex in the plastid envelope of Arabidopsis thaliana. *Journal of Experimental Botany*, *70*, 1483–1495.

- Potocka, A., & Zimowski, J. (2008). Metabolism of conjugated sterols in eggplant. Part 2. Phospholipid: Steryl glucoside acyltransferase. *Acta Biochimica Polonica*, *55*, 135–140.
- Rustgi, S., Springer, A., Kang, C., von Wettstein, D., Reinbothe, C., Reinbothe, S., & Pollmann, S. (2019). ALLENE OXIDE SYNTHASE and HYDROPEROXIDE LYASE, Two Non-Canonical Cytochrome P450s in *Arabidopsis thaliana* and Their Different Roles in Plant Defense. *International Journal of Molecular Sciences*, *20*, E3064.
- Schaeffer, A., Bronner, R., Benveniste, P., & Schaller, H. (2001). The ratio of campesterol to sitosterol that modulates growth in *Arabidopsis* is controlled by STEROL METHYLTRANSFERASE 2;1. *The Plant Journal: For Cell and Molecular Biology*, *25*, 605–615.
- Schäfer, M., Fischer, C., Meldau, S., Seebald, E., Oelmüller, R., & Baldwin, I. T. (2011). Lipase activity in insect oral secretions mediates defense responses in *Arabidopsis*. *Plant Physiology*, *156*, 1520–1534.
- Schaller, F., Zerbe, P., Reinbothe, S., Reinbothe, C., Hofmann, E., & Pollmann, S. (2008). The allene oxide cyclase family of *Arabidopsis thaliana* - localization and cyclization: Oxylin cyclization. *FEBS Journal*, *275*, 2428–2441.
- Seo, S., Sano, H., & Ohashi, Y. (1997). Jasmonic acid in wound signal transduction pathways. *Physiologia Plantarum*, *101*, 740–745.
- Seren, Ü. (2018). GWA-Portal: Genome-Wide Association Studies Made Easy. *Methods in Molecular Biology (Clifton, N.J.)*, *1761*, 303–319.
- Shiva, S., Enniful, R., Roth, M. R., Tamura, P., Jagadish, K., & Welti, R. (2018). An efficient modified method for plant leaf lipid extraction results in improved recovery of phosphatidic acid. *Plant Methods*, *14*, 14.
- Song, Y., Vu, H. S., Shiva, S., Fruehan, C., Roth, M. R., Tamura, P., & Welti, R. (2020). A Lipidomic Approach to Identify Cold-Induced Changes in *Arabidopsis* Membrane Lipid Composition. *Methods in Molecular Biology (Clifton, N.J.)*, *2156*, 187–202.
- Song, Y., Zoong Lwe, Z. S., Wickramasinghe, P. A. D. B. V., & Welti, R. (2021). Head-Group Acylation of Chloroplast Membrane Lipids. *Molecules*, *26*, 1273.
- Stenzel, I., Otto, M., Delker, C., Kirmse, N., Schmidt, D., Miersch, O., Hause, B., & Wasternack, C. (2012). ALLENE OXIDE CYCLASE (AOC) gene family members of *Arabidopsis thaliana*: Tissue- and organ-specific promoter activities and in vivo heteromerization. *Journal of Experimental Botany*, *63*, 6125–6138.
- Stintzi, A., Weber, H., Reymond, P., Browse, J., & Farmer, E. E. (2001). Plant defense in the absence of jasmonic acid: The role of cyclopentenones. *Proceedings of the National Academy of Sciences of the United States of America*, *98*, 12837–12842.

- Stucky, D. F., Arpin, J. C., & Schrick, K. (2015). Functional diversification of two UGT80 enzymes required for steryl glucoside synthesis in Arabidopsis. *Journal of Experimental Botany*, *66*, 189–201.
- Taki, N., Sasaki-Sekimoto, Y., Obayashi, T., Kikuta, A., Kobayashi, K., Ainai, T., Yagi, K., Sakurai, N., Suzuki, H., Masuda, T., Takamiya, K.-I., Shibata, D., Kobayashi, Y., & Ohta, H. (2005). 12-oxo-phytodienoic acid triggers expression of a distinct set of genes and plays a role in wound-induced gene expression in Arabidopsis. *Plant Physiology*, *139*, 1268–1283.
- Telfer, A., Bollman, K. M., & Poethig, R. S. (1997). Phase change and the regulation of trichome distribution in Arabidopsis thaliana. *Development (Cambridge, England)*, *124*, 645–654.
- Vu, H. S., Roston, R., Shiva, S., Hur, M., Wurtele, E. S., Wang, X., Shah, J., & Welti, R. (2015). Modifications of membrane lipids in response to wounding of Arabidopsis thaliana leaves. *Plant Signaling & Behavior*, *10*, e1056422.
- Vu, H. S., Roth, M. R., Tamura, P., Samarakoon, T., Shiva, S., Honey, S., Lowe, K., Schmelz, E. A., Williams, T. D., & Welti, R. (2014a). Head-group acylation of monogalactosyldiacylglycerol is a common stress response, and the acyl-galactose acyl composition varies with the plant species and applied stress. *Physiologia Plantarum*, *150*, 517–528.
- Vu, H. S., Shiva, S., Roth, M. R., Tamura, P., Zheng, L., Li, M., Sarowar, S., Honey, S., McEllhiney, D., Hinkes, P., Seib, L., Williams, T. D., Gadbury, G., Wang, X., Shah, J., & Welti, R. (2014b). Lipid changes after leaf wounding in Arabidopsis thaliana: Expanded lipidomic data form the basis for lipid co-occurrence analysis. *The Plant Journal: For Cell and Molecular Biology*, *80*, 728–743.
- Vu, H. S., Tamura, P., Galeva, N. A., Chaturvedi, R., Roth, M. R., Williams, T. D., Wang, X., Shah, J., & Welti, R. (2012). Direct infusion mass spectrometry of oxylipin-containing Arabidopsis membrane lipids reveals varied patterns in different stress responses. *Plant Physiology*, *158*, 324–339.
- Wasternack, C., & Feussner, I. (2018). The Oxylipin Pathways: Biochemistry and Function. *Annual Review of Plant Biology*, *69*, 363–386.
- Wasternack, C., & Strnad, M. (2016). Jasmonate signaling in plant stress responses and development – active and inactive compounds. *New Biotechnology*, *33*, 604–613.
- Wasternack, C., & Strnad, M. (2018). Jasmonates: News on Occurrence, Biosynthesis, Metabolism and Action of an Ancient Group of Signaling Compounds. *International Journal of Molecular Sciences*, *19*, E2539.
- Weigel, D. (2012). Natural variation in Arabidopsis: From molecular genetics to ecological genomics. *Plant Physiology*, *158*, 2–22.

- Weigel, D., & Mott, R. (2009). The 1001 genomes project for *Arabidopsis thaliana*. *Genome Biology*, *10*, 107.
- Xia, J., Sinelnikov, I. V., Han, B., & Wishart, D. S. (2015). MetaboAnalyst 3.0—Making metabolomics more meaningful. *Nucleic Acids Research*, *43*, W251–W257.
- Zien, C. A., Wang, C., Wang, X., & Welti, R. (2001). In vivo substrates and the contribution of the common phospholipase D, PLD α , to wound-induced metabolism of lipids in *Arabidopsis*. *Biochimica Et Biophysica Acta*, *1530*, 236–248.

Chapter 5 - Functional characterization of *AOCs* on esterified (dn)OPDA production in *Arabidopsis* under wounding stress

Introduction

Plant oxylipins are a group of structurally diverse metabolites derived from oxidation of unsaturated fatty acids and they play essential roles in plant development and stress defenses (Wasternack & Hause, 2013; Wasternack & Feussner, 2018). Among plant oxylipins, octadecanoids are the most known signaling molecules in plant responses to biotic and abiotic stresses. Octadecanoids include jasmonic acid (JA), JA-methyl ester (JA-ME), and its amino acid conjugates, as well as *cis*-(+)-12-oxophytodienoic acid (OPDA) and its metabolites. OPDA is the precursor of JA and synthesized through the allene oxide synthase (AOS) pathway, in which an unstable intermediate, (13*S*)-12,13-epoxy-octadecanoic acid (EOT) is synthesized by AOS (Brash, 2009; Laudert et al., 1996). In the presence of allene oxide cyclase (AOC), the unstable EOT can be enzymatically converted to OPDA (González-Pérez et al., 2017). In *Arabidopsis*, four genes *AOC1*, *AOC2*, *AOC3*, and *AOC4* encode four functional AOC isozymes (Stenzel et al., 2003). Schaller et al. explored the enzymatic activities and cellular localization of the AOC family and demonstrated that the four AOCs are all located in the chloroplast and contribute to the cyclization reaction of EOT to OPDA (Schaller et al., 2008). Stenzel and coworkers investigated the tissue- and organ-specific expression of the four *AOCs* in *Arabidopsis* and found that the *AOC1*, *AOC2* and *AOC3* promoters were active in fully developed leaves (Stenzel et al., 2012). Further studies on single and double *aoc* mutants revealed there are functional redundancies among the 4 AOCs in OPDA and JA production. In recent years, more and more evidence has demonstrated that AOCs may function as homotrimers or heterotrimers (Otto et al., 2016; Stenzel et al., 2012). Bimolecular fluorescence complementation (BiFC) showed that all

AOCs can interact with each other *in vivo*. Enzyme activities of recombinantly-expressed AOC heterotrimers were compared with the activity of homotrimers and the results showed some heteromeric combinations had elevated activities than homotrimers. A more complicated hypothesis about the role of AOCs was proposed, i.e., that the production of OPDA and JA in different organs and in response to various stresses is fine-tuned by expression and activity of all 4 AOCs. Recently, biochemical experiments identified an enzyme complex consisting of lipoxygenase 2 (LOX2), AOS, and AOC, enzymes which catalyze consecutive steps in OPDA biosynthesis (Pollmann et al., 2019).

Although many esterified oxylipins found in plants have been structurally characterized during the past two decades, less is known about their biosynthesis. Arabidopsides were the first structurally characterized and are the most abundant esterified oxylipins in Arabidopsis, particularly after wounding. Arabidopsides are OPDA- or dnOPDA-containing monogalactosyldiacylglycerols (MGDGs) (Hisamatsu et al., 2003; Stelmach et al., 2001), digalactosyldiacylglycerols (DGDGs) (Hisamatsu et al., 2005), or head group-acylated monogalactosyldiacylglycerols (acMGDGs) (Andersson et al., 2006; Kourtchenko et al., 2007). Data suggested that the biosynthesis of esterified OPDA and dnOPDA occurs when esterified 18:3 and 16:3 are directly transformed into esterified OPDA and dnOPDA (i.e., Arabidopsides) without hydrolysis and re-esterification (Buseman et al., 2006; Nilsson et al., 2012; Nilsson et al., 2016). However, it is not known which AOC isoforms catalyze the formation of Arabidopsides from polyunsaturated galactolipids. It is possible that the biosynthesis of esterified OPDA is also regulated in a fine-tuning by AOC heteromerization.

In Chapter 4, our GWAS on levels of oxidized lipid molecular species suggested that production of many oxylipin-containing lipid species under mechanical wounding stress was

controlled by natural sequence variants in a genomic region containing *AOC1*, *AOC2*, and *AOC3*. The most significant SNPs for associated lipid species were located in 5' UTR or upstream regions of these genes, indicating they might influence the gene expression level of *AOCs*. However, unexpectedly, the haplotype analysis of *AOC2* expression and relative content of Arabidopside E in 20 accessions implied that *AOC2* may inhibit the production of esterified oxylipins under wounding, which is contrary to the characterized function of *AOC2* in free oxylipin production. Here, we utilized reverse genetic approaches to explore the functions of *AOCs* on esterified oxylipin production in *Arabidopsis*. Lipidomic analysis and gene expression analysis were performed on T-DNA insertion and overexpression lines under mechanical wounding stress.

Materials and Methods

Plant materials and growth conditions

In this research, *Arabidopsis thaliana*, ecotype Columbia-0 (Col-0) and T-DNA insertion mutant lines *aoc1* (SALK_073059, insertion in exon), *aoc2* (SALK_069524, insertion in 5' UTR), *aoc3* (SALK_054568C, insertion in exon) were obtained from Arabidopsis Biological Resource Center (ABRC). The left border primer LBb 1.3 and gene specific primers used to genotype these SALK lines are shown in Table 5-1.

All *Arabidopsis* seeds were sown in 3.5-inch-square pots filled with loosely packed, Pro-Mix "PGX" soil (Hummert International, Springfield, MO, USA) saturated with 0.01% 20-20-20 fertilizer (Hummert International, Springfield, MO, USA). Trays were put in refrigerator or cold room at 4 °C for 2 days for stratification of seeds and then moved into a growth chamber under a 14/10 h light/dark cycle at 21 °C with 60% humidity. Light intensity was maintained at 90

$\mu\text{mol}/\text{m}^2/\text{s}$ with cool white fluorescent lights. Trays were covered with propagation domes for the first 9 days to maintain high humidity. Trays were watered once every four days. On day 12 after sowing, plants were thinned to one plant per well. On day 20, trays were fertilized again with 0.01% 20-20-20 fertilizer.

Cloning of coding sequence of Arabidopsis *AOC1*, *AOC2*, *AOC3*

The coding sequences (CDS) of Arabidopsis *AOC1* (AT3G25760), *AOC2* (AT3G25770), *AOC3* (AT3G25780) were PCR amplified from the sequence of pUni clone U82314 and U12485 containing the CDS of *AOC1* and *AOC2*, respectively, or from total cDNA obtained from wild type Col-0 leaves by high-fidelity PCR using Phusion polymerase (New England Biolabs) and forward/reverse primers (Table 5-2).

Overexpression vector construction and transformation

The PCR products were blunt-end cloned into vector pMiniT 2.0 using NEB PCR Cloning Kit (New England Biolabs), digested using restriction enzymes *EcoRI*-HF and *Sall* (New England Biolabs, USA), agarose gel purified, and ligated (T4 DNA ligase, Life technologies, USA) into the binary vector pBinRed35S containing a CaMV35S promoter and a DsRed fluorescence gene, which can be used for transgenic plant selection. The cloning sequences in the destination vector were verified by Sanger sequencing (GENEWIZ from Azenta Life Sciences). The reconstructed binary vectors harboring each CDS under the control of the CaMV 35S promoter were introduced into *Agrobacterium tumefaciens* GV3101 by electroporation. Transgenic plants were created by floral dip of Arabidopsis (Col-0) (Clough & Bent, 1998). Seeds were screened with a green, light-emitting diode and a Red2 camera filter to identify transformed seeds, based on red fluorescence. The transgenic seeds with red fluorescence were planted along with knockout mutants and WT Col-0 following the same

planting protocols described above. Twelve plants for wild-type Col-0 and each overexpression construct (T1 generation) were grown under normal growth conditions (14/10 h light/dark cycle at 21 °C with 60% humidity) until day 30 when the wounding treatment was applied.

Wounding treatment and leaf harvesting

On day 30, leaf #5 and 6 were mechanically wounded; after 45 min, leaf #5 was harvested for lipid extraction, leaf #6 was harvested for RNA extraction. The detailed protocol was described in Materials and Methods section of Chapter 2.

Quantitative RT-PCR analysis of AOC expression in mutant lines

The harvested leaf samples were frozen immediately in liquid nitrogen and stored at -80 °C. A single leaf from each line was frozen in a 2 mL microcentrifuge tube and ground thoroughly using pestle at extremely low temperature in liquid nitrogen. RNA was extracted from the tissue powder using the RNeasy Plant Mini Kit from Qiagen following the manufacturer's protocol. Total RNA (<10 µg) was digested with DNase Max Kit from Qiagen to remove any genomic DNA contamination. RNA concentrations were quantified with a NanoDrop 2000 spectrophotometer (Thermo Scientific). 300 ng of RNA was used for cDNA synthesis using qScript™ cDNA Synthesis Kit from Bio-Rad according to the manufacturer's protocol.

Quantitative PCR was performed on an ABI 7500 Real-Time PCR System (Applied Biosystems, CA) using the PowerUp SYBR Green PCR Master Mix (Applied Biosystems, CA). *AOC1*, *AOC2*, *AOC3* gene expression levels were normalized to the reference gene *TRO* (AT1G51450) and *YLS8* (AT5G08290) using the Delta-Delta-CT (DDCT) method. Primers used to quantify the expression of these genes are listed in Table 5-3.

Lipid extraction and MS analysis

Lipids in leaf samples were extracted using an optimized extraction method (Shiva et al., 2018) which was described in Materials and Methods section in Chapter 2. Finally, the lipid extract (equivalent to 0.085 mg dry tissue mass) was dissolved in 300 μ L MS solvent, chloroform–methanol–300 mM ammonium acetate in water (30:66.5:3.5, v/v/v). 20 μ L of internal standard mix was added to the MS solvent for background subtraction and lipid quantification in the following data processing steps. QC samples were prepared as described in Chapter 2.

Data processing and lipid profile analysis

The raw MS data was exported from Analyst into MultiQuant for signal summation. The total intensity for each lipid analyte was imported into LipidomeDB DCE for data deconvolution and calculation. Finally, all lipid analytes with CoV values less than 30% were quantified in normalized MS intensity per mg sample “dry weight”, where a value of 1 is equivalent in intensity to that of 1 nmol of internal standard(s) and in relative content, expressed as a percentage (%) of the normalized intensity. The detailed guidelines for data processing, calculation, and normalization are described in the Materials and Methods section of Chapter 2.

Statistical analysis

Auto-scaling, two-sample Student’s t-test, and analysis of variance (ANOVA) with Tukey’s post hoc tests were performed, based on relative MS intensity (% of total) of individual lipid species between WT and transgenic lines, and the heat maps were produced using utilities at the MetaboAnalyst website (<https://www.metaboanalyst.ca/MetaboAnalyst/home.xhtml>).

Results

Overexpression of *AOC1/2/3* in leaf tissues of wild-type *Arabidopsis* (Col-0)

In order to explore the molecular functions of AOC1, AOC2, and AOC3 on esterified OPDA and dnOPDA production after mechanical wounding, we generated transgenic lines with the protein coding sequence of the three AOCs, each expressed under the control of 35S promoter. We analyzed the expression of each target gene in the wounded leaves of 12 plants from the T1 generation (Figure 5-1). Of the 12 independent lines of T1 generation, the 3 putative *AOC2* overexpression lines (*AOC2_OE*#1, #5, #7) were verified to be over-expressing *AOC2* using RT-qPCR, as each displayed a significantly higher level of *AOC2* transcript in leaves, compared to the level in WT leaves. Of the 12 T1 plants designed for *AOC1* overexpression, only #11 showed significantly higher *AOC1* transcript in leaves compared to WT. Of the 10 T1 plants designed to overexpress *AOC3*, four plants (*AOC3_OE* #5, #7, #10, #12) had significantly higher *AOC3* transcript level than WT. In the future, we will focus on these plants as parents of T2 generation and T3 generation, where we will select homozygous overexpression lines. Gene expression and lipid analysis will be performed on plants in these generations.

The relative amounts of esterified OPDA and dnOPDA are affected by the expression level of *AOC1* and *AOC2*

To investigate the roles of AOC1, AOC2, and AOC3 on the production of esterified OPDA and dnOPDA in wounded leaf tissues of *Arabidopsis*, we compared the lipid profiles, including a large number of oxidized lipid species between wild-type (Col-0) and T1 generation overexpression lines. As the most abundant esterified OPDA- and dnOPDA-containing molecular species after wounding of *Arabidopsis*, Arabidopside E (acMGDG(18:4-O/34:8-2O)) was different in level between WT and overexpression plants. As shown in Figure 5-2a, two

AOC1 overexpression lines (#7, #11) had higher Arabidopside E than WT while some lines (#1, #6, #8, #9, #10, and #12) in T1 transgenic plants produced very low levels of Arabidopside E after wounding. In Figure 5-2b, among the 12 T1 overexpression lines for *AOC2*, 3 T1 transgenic plants (#1, #5, #7) showed significantly higher level of Arabidopside E than WT under wounding, which is consistent with their higher expression level of *AOC2*, while others expressed *AOC2* at levels less than WT plants did. All the T1 overexpression lines of *AOC3* generated very low amounts of Arabidopside E after wounding (Figure 5-2c).

To further investigate the relationship between *AOC2* expression and Arabidopside E production in wounded leaves of Arabidopsis, we examined the correlation between *AOC2* expression and Arabidopside E production in the 12 WT and the 12 T1 *AOC2* overexpression lines. As shown in Figure 5-3, we found that there was a positive correlation between *AOC2* expression level and relative amount of Arabidopside E (Pearson's $r = 0.829$, $P < 0.0001$). Thus, the gene expression results are consistent with lipidomics results in the investigated WT and *AOC2* overexpression lines, suggesting that *AOC2* promotes esterified OPDA and dnOPDA production after wounding. However, the reason for the less-than-WT levels of Arabidopside E after wounding in some of the T1 plants is not clear. For *AOC1* and *AOC3*, from T1 overexpression lines, there is no significant correlation between gene expression level and lipid level, and the reason for the extremely low production of Arabidopside E in many of the *AOC1* and *AOC3* T1 overexpression plants is also not clear.

Knockout of *AOC1* and *AOC3* led to complete or partial loss of ability to generate esterified OPDA and dnOPDA under wounding

The T-DNA insertion line SALK_073059 (*aoc1*) putatively has an insertion in second exon of AT3G25760 (*AOC1*), SALK_069524 (*aoc2*) putatively has an insertion in the 5' UTR of

AT3G25770 (*AOC2*), and SALK_054568C (*aoc3*) has a confirmed mutation in second exon of AT3G25780 (*AOC3*). All 12 replicate plants of *aoc1*, *aoc2*, and *aoc3* have been genotyped by PCR using specific primers listed in Table 5-1. All 12 replicate plants of *aoc1* and *aoc3* have been confirmed to be homozygous mutants while plants of *aoc2* contains both WT and heterozygous mutants. Lipidomics analysis in leaf tissues on a large number (12) of replicate plants of *aoc1*, *aoc2*, and *aoc3* revealed differences across the lipidome compared to WT, especially for *aoc1* and *aoc3* which had significantly lower levels of esterified OPDA and dnOPDA than WT. Of the 278 unique lipid analytes, 133 were significantly different between WT and *aoc1* by the two-sample t-test ($P < 0.01$ after correction for FDR, Figure 5-4b) with 79 lipid analytes lower and 54 analytes higher in *aoc1* lines compared to WT. From the heatmap and volcano plot, among the differences in *aoc1*, compared to WT plants, were much lower level of chloroplast esterified OPDA- and dnOPDA-containing lipids, including ox-acMGDGs, ox-MGDGs, and ox-DGDGs. The relative contents (% of total lipids) of ox-acMGDG, ox-MGDG, ox-DGDG, ox-acDGDG, ox-DGMG, ox-PG, and ox-ASG in *aoc1* plants were lower than in WT plants under wounding (Figure 5-5(a and b)). As the most induced and most abundant esterified OPDA- or dnOPDA-containing molecular species in WT after wounding, Arabidopside E showed very low levels (mean = 0.0017%) in all 12 *aoc1* lines (Figure 5-6a), suggesting that the T-DNA insertion in the exon of *AOC1* caused complete loss of ability to generate Arabidopside E in Arabidopsis under wounding stress.

In addition to *aoc1* mutants, we also explored the lipidomes of *aoc2* and *aoc3* mutant lines under wounding stress (Figure 5-5 and Figure 5-6). *aoc3* plants had a significantly lower level of ox-acMGDG (1.87% of total) compared to WT plants (3.17% of total) with a P -value of 0.0016. For Arabidopside E, *aoc3* lines had a 48% reduction compared to WT ($P = 0.002$).

Lipidomics results on *aoc3* plants suggested that T-DNA insertion in exon of *AOC3* led to partial loss of ability to generate Arabidopsides after wounding. Lipidomics analysis on *aoc2* plants didn't show any significant differences in esterified OPDA- or dnOPDA-containing lipids compared to WT under wounding stress.

Discussion

Previous studies on Arabidopsis AOCs characterized the structure of AOC2 and proposed a model of the interaction between the AOC2 homotrimer and the bound substrate EOT (Hofmann et al., 2006). In early work, *AOC2* was shown to be highly expressed *in planta* and was described as being the most active of the four Arabidopsis AOCs by *in vitro* assays (Schaller et al., 2008; Stenzel et al., 2003). In recent years, functional redundancy or, potentially, diversification of the 4 AOC isozymes in Arabidopsis have been suggested. Gene expression analysis, mutant characterization, and protein interaction studies on AOCs have indicated functional redundancies among individual AOCs. All AOCs can interact to form trimers and the composition of the trimers affects AOC activity (Otto et al., 2016; Stenzel et al., 2012). Recently, Pollmann and coworkers identified an enzyme complex located in plastid envelope containing LOX2, AOS, and AOC2, which is responsible for JA production in response to biotic and abiotic stimuli (Pollmann et al., 2019). These evidence supports a fine-tuning mechanism for free OPDA and JA biosynthesis in Arabidopsis depending on the physical interactions between LOX2, AOS, and AOC as well as the heteromerization of 4 AOCs. However, oxylipins especially OPDAs and dnOPDAs exist predominantly in esterified forms in Arabidopsis under wounding stress, and the biosynthetic pathways and regulation of the pathways for esterified OPDA and dnOPDA production in Arabidopsis under wounding is still elusive. According to our GWAS results

identified in Chapter 4 and current mutant characterization results, we can make a hypothesis that individual AOCs play different roles for esterified OPDA and dnOPDA production. Here, AOC2 might promote esterified OPDA and dnOPDA production due to the observed positive correlation between AOC2 expression and the relative contents of Arabidopsides. In addition, from the lipidomics analysis of T-DNA insertion lines of AOC1 and AOC3, AOC1 is indispensable in the biosynthesis of esterified OPDA and dnOPDA in Arabidopsis and AOC3 also has enhanced effect on esterified OPDA and dnOPDA production. The functions of AOC1/2/3 in esterified OPDA and dnOPDA production under wounding stress are not redundant, and each of them may play unique and essential roles in the biosynthetic pathway. After genetic and phenotypic characterization on T2 and T3 generation of transgenic lines, the exact molecular function of AOC1/2/3 in OPDA and dnOPDA production will be better elucidated in the future.

Figures

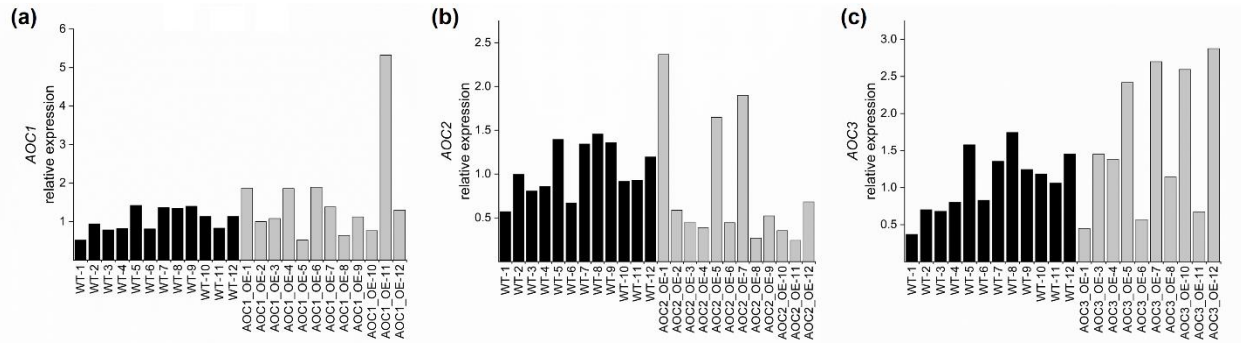


Figure 5-1. Gene expression analysis of wounded leaves of wild-type and T1 generation *AOC1/2/3* overexpression lines

AtAOC transcript levels in the wounded leaves of wild-type (WT) and heterozygous T1 lines overexpressing *AOC1* (a), *AOC2* (b), *AOC3* (c). *AOC1/2/3* transcript levels were quantified using RT-qPCR and normalized to two *Arabidopsis* reference genes (*TRO* and *YLS8*).

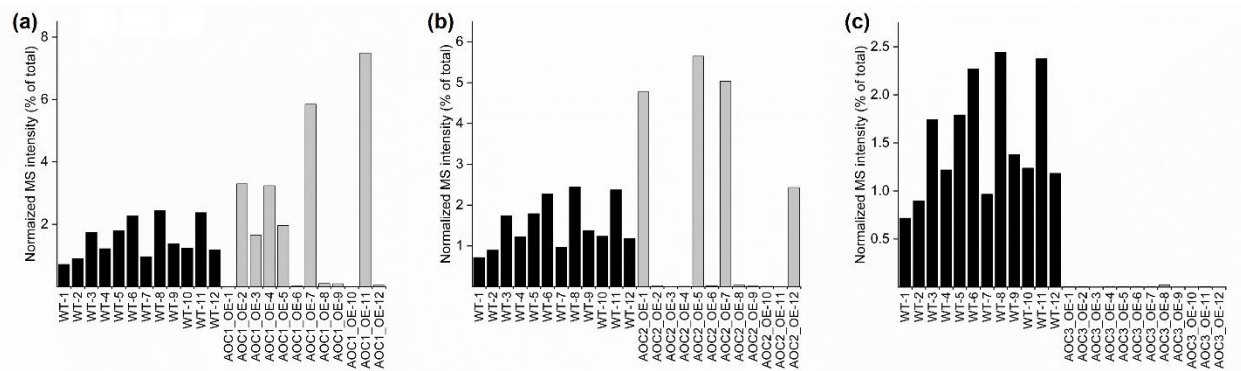


Figure 5-2. Analysis of arabidopside E in wounded leaves of wild-type and T1 generation *AOC1/2/3* overexpression lines

The normalized MS intensity (% of total lipids) of Arabidopside E in the wounded leaves of wild-type (WT) and heterozygous T1 lines overexpressing *AOC1* (a), *AOC2* (b), and *AOC3* (c).

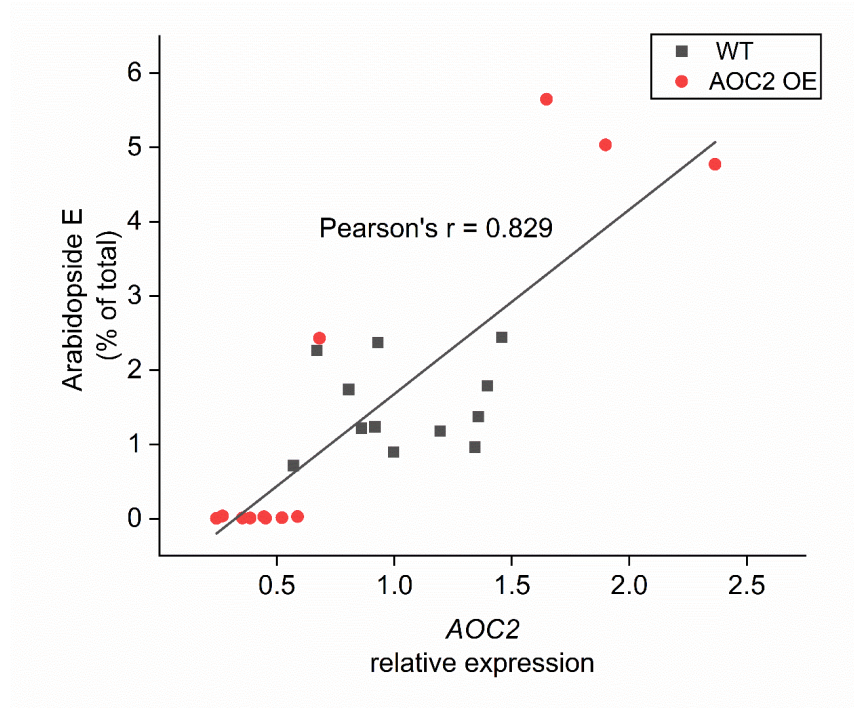


Figure 5-3. Relationship between *AOC2* expression level and Arabidopside E level in WT and T1 generation *AOC2* overexpression plants

The x-axis shows *AOC2* transcript levels quantified using RT-qPCR, and the y-axis shows the relative amounts (% of total) of Arabidopside E among all tested lines. Black squares represent 12 WT lines and red circles represent 12 T1 generation *AOC2* overexpression lines.

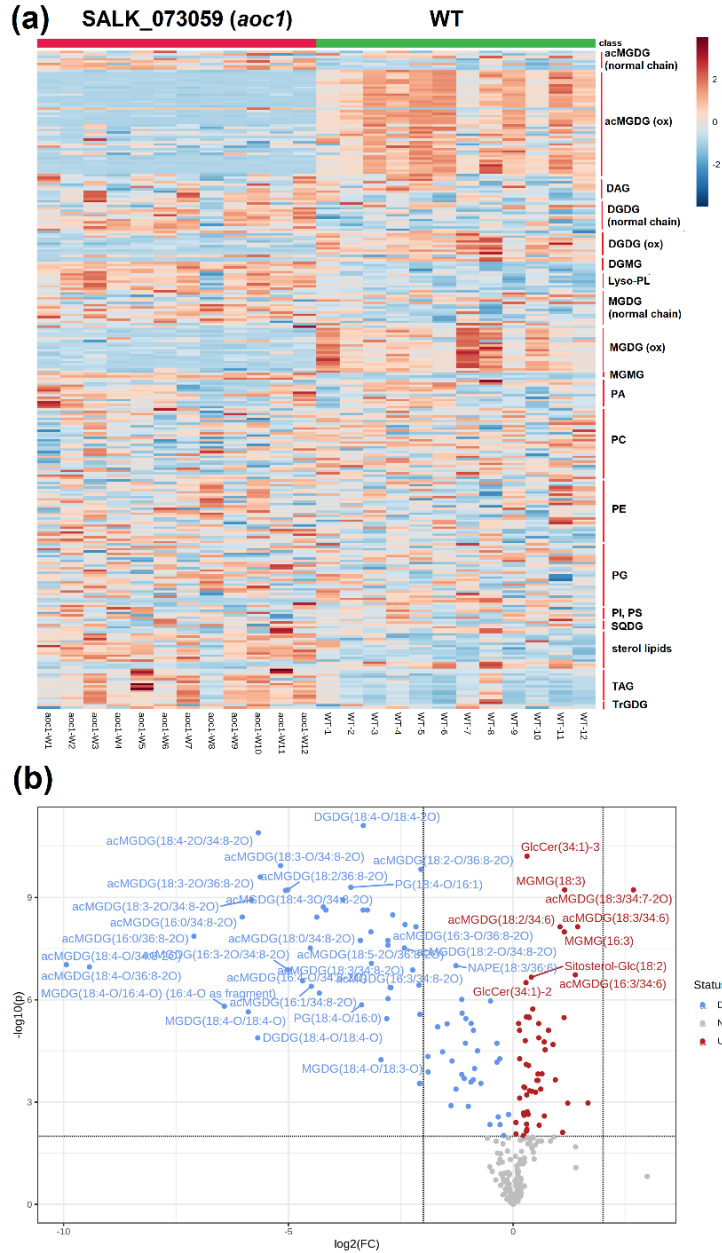


Figure 5-4. Comparison of lipid profiles between WT and SALK_073059 (*aoc1*)

(a) Heatmap of autoscaled lipid levels in wounded leaves of WT and *aoc1*. Note that 278 analytes are shown in 24 samples. Each sample represents one plant in WT and transgenic group ($n = 12$). (b) Volcano plot of 278 lipid analytes of WT and *aoc1*, revealing 79 lipid species lower and 54 higher in *aoc1* group compared to WT with a p -value < 0.01 and a fold change > 1.0 . x-axis corresponds to $\log_2(\text{fold change})$ and y-axis to $-\log_{10}(p\text{-value})$.

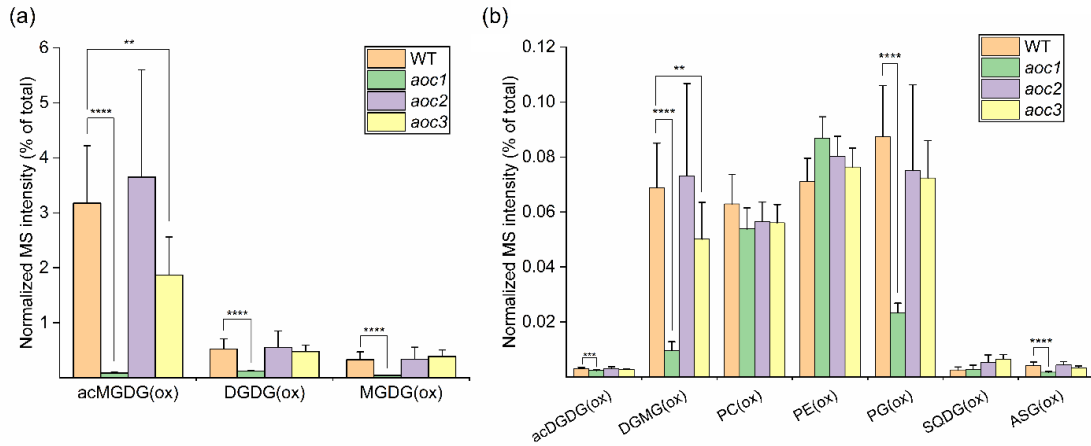


Figure 5-5. Analysis of oxidized lipid classes in wounded leaves of wild-type and T-DNA insertion lines of *AOC1/2/3*

The normalized MS intensity (% of total lipids) of oxidized lipid classes/subclasses in the wounded leaves of wild-type (WT) and T-DNA insertion lines for *AOC1* (SALK_073059), *AOC2* (SALK_069524), and *AOC3* (SALK_054568C). The number of asterisks shows the significance of correlation after Student's t-test, * $P \leq 0.05$, ** $P \leq 0.01$, *** $P \leq 0.001$.

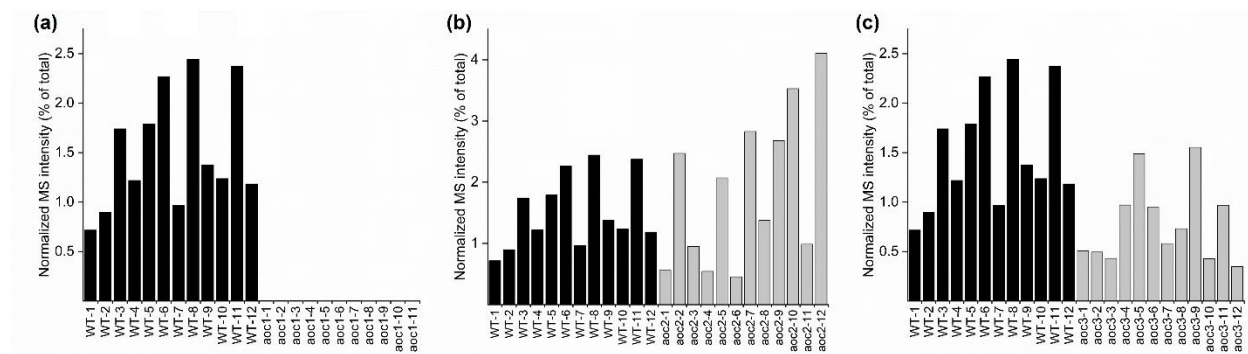


Figure 5-6. Analysis of Arabidopside E in wounded leaves of wild-type and T-DNA insertion lines of *AOC1/2/3*

The normalized MS intensity (% of total lipids) of Arabidopside E in the wounded leaves of wild-type (WT) and T-DNA insertion lines for *AOC1* (SALK_073059), *AOC2* (SALK_069524), and *AOC3* (SALK_054568C).

Tables

Table 5-1. Primers used for genotyping

Mutant lines	Primers
	F: CTCAC TTTACGACCATGGT
SALK_073059	R: TGATTTAGATCGACACAGCC
	F: TCAAGTATGGTCCTTGAACG
SALK_069524	R: TTGCCTTATCCGTTTATGCT
	F: CCTCCAACACATGTTTTGAC
SALK_054568C	R: AACAGAGCTTTGTCTCGG
	LBb 1.3: ATTTTGCCGATTTTCGGAAC

Table 5-2. Primers used for gene cloning

Gene ID	Primers
AT3G25760	F: CCCGAATTCATGGCTTCTTCTACAATCTC
	R: CCCGTCGACCTAATTTGTAAAGTTGCTTACAA
AT3G25770	F: CCCGAATTCATGGCTTCTTCAGCAGTG
	R: CCCGTCGACTTAGTTGGTATAGTTACTTATAACTCC
AT3G25780	F: CCCGAATTCATGGCTTCTTCTTCTGC
	R: CCCGTCGACTTAATTAGTAAAGTTACTTATAACTCCA

Table 5-3. Primers used for RT-qPCR

Gene ID	Primers
<i>TRO</i> (AT1G51450)	F: CTAAAGTTGTACCAGGCAGTG R: TAGTAACGACCGCCAACAAT
<i>YLS8</i> (AT5G08290)	F: GCAGTCATTTATCTGGTGGA R: TGCTTGTCCTTGAGAGCC
<i>AOC1</i> (AT3G25760)	F: AAGAACTCACTCCTACTCG R: TCTTGAACCTTGCTTGGTCTG
<i>AOC2</i> (AT3G25770)	F: CCCTAGACCAAGCAAAGTTC R: GATCGCCTGTGTAGAGTTTG
<i>AOC3</i> (AT3G25780)	F: TCCAGATTTCTCCTCCCGAT R: TCTTGGATCTTACTTGGTCTG

References

- Andersson, M. X., Hamberg, M., Kourtchenko, O., Brunnström, A., McPhail, K. L., Gerwick, W. H., Göbel, C., Feussner, I., & Ellerström, M. (2006). Oxylipin profiling of the hypersensitive response in *Arabidopsis thaliana*. Formation of a novel oxo-phytodienoic acid-containing galactolipid, arabidopside E. *The Journal of Biological Chemistry*, *281*, 31528–31537.
- Brash, A. R. (2009). Mechanistic aspects of CYP74 allene oxide synthases and related cytochrome P450 enzymes. *Phytochemistry*, *70*, 1522–1531.
- Buseman, C. M., Tamura, P., Sparks, A. A., Baughman, E. J., Maatta, S., Zhao, J., Roth, M. R., Esch, S. W., Shah, J., Williams, T. D., & Welti, R. (2006). Wounding stimulates the accumulation of glycerolipids containing oxophytodienoic acid and dinor-oxophytodienoic acid in *Arabidopsis* leaves. *Plant Physiology*, *142*, 28–39.
- Clough, S. J., & Bent, A. F. (1998). Floral dip: A simplified method for *Agrobacterium*-mediated transformation of *Arabidopsis thaliana*. *The Plant Journal: For Cell and Molecular Biology*, *16*, 735–743.
- Genva, M., Obounou Akong, F., Andersson, M. X., Deleu, M., Lins, L., & Fauconnier, M.-L. (2019). New insights into the biosynthesis of esterified oxylipins and their involvement in plant defense and developmental mechanisms. *Phytochemistry Reviews*, *18*, 343–358.
- González-Pérez, A. B., Grechkin, A., & de Lera, Á. R. (2017). Rearrangement of vinyl allene oxide geometric isomers to cyclopentenones. Further computational insights with biologically relevant model systems. *Organic & Biomolecular Chemistry*, *15*, 2846–2855.
- Hisamatsu, Y., Goto, N., Hasegawa, K., & Shigemori, H. (2003). Arabidopsides A and B, two new oxylipins from *Arabidopsis thaliana*. *Tetrahedron Letters*, *44*, 5553–5556.
- Hisamatsu, Y., Goto, N., Sekiguchi, M., Hasegawa, K., & Shigemori, H. (2005). Oxylipins arabidopsides C and D from *Arabidopsis thaliana*. *Journal of Natural Products*, *68*, 600–603.
- Hofmann, E., Zerbe, P., & Schaller, F. (2006). The crystal structure of *Arabidopsis thaliana* allene oxide cyclase: Insights into the oxylipin cyclization reaction. *The Plant Cell*, *18*, 3201–3217.
- Kourtchenko, O., Andersson, M. X., Hamberg, M., Brunnström, A., Göbel, C., McPhail, K. L., Gerwick, W. H., Feussner, I., & Ellerström, M. (2007). Oxo-phytodienoic acid-containing galactolipids in *Arabidopsis*: Jasmonate signaling dependence. *Plant Physiology*, *145*, 1658–1669.
- Laudert, D., Pfannschmidt, U., Lottspeich, F., Holländer-Czytko, H., Weiler, E. W. (1996). Cloning, molecular and functional characterization of *Arabidopsis thaliana* allene oxide

- synthase (CYP 74), the first enzyme of the octadecanoid pathway to jasmonates. *Plant Mol Biol.*, 31, 323-335.
- Nilsson, A. K., Fahlberg, P., Ellerström, M., & Andersson, M. X. (2012). Oxo-phytodienoic acid (OPDA) is formed on fatty acids esterified to galactolipids after tissue disruption in *Arabidopsis thaliana*. *FEBS Letters*, 586, 2483–2487.
- Nilsson, A. K., Fahlberg, P., Johansson, O. N., Hamberg, M., Andersson, M. X., & Ellerström, M. (2016). The activity of HYDROPEROXIDE LYASE 1 regulates accumulation of galactolipids containing 12-oxo-phytodienoic acid in *Arabidopsis*. *Journal of Experimental Botany*, 67, 5133–5144.
- Otto, M., Naumann, C., Brandt, W., Wasternack, C., & Hause, B. (2016). Activity Regulation by Heteromerization of *Arabidopsis* Allene Oxide Cyclase Family Members. *Plants (Basel, Switzerland)*, 5, E3.
- Pollmann, S., Springer, A., Rustgi, S., von Wettstein, D., Kang, C., Reinbothe, C., & Reinbothe, S. (2019). Substrate channeling in oxylipin biosynthesis through a protein complex in the plastid envelope of *Arabidopsis thaliana*. *Journal of Experimental Botany*, 70, 1483–1495.
- Schaller, F., Zerbe, P., Reinbothe, S., Reinbothe, C., Hofmann, E., & Pollmann, S. (2008). The allene oxide cyclase family of *Arabidopsis thaliana*: Localization and cyclization. *The FEBS Journal*, 275, 2428–2441.
- Shiva, S., Enniful, R., Roth, M. R., Tamura, P., Jagadish, K., & Welti, R. (2018). An efficient modified method for plant leaf lipid extraction results in improved recovery of phosphatidic acid. *Plant Methods*, 14, 14.
- Stelmach, B. A., Müller, A., Hennig, P., Gebhardt, S., Schubert-Zsilavecz, M., & Weiler, E. W. (2001). A novel class of oxylipins, sn1-O-(12-oxophytodienoyl)-sn2-O-(hexadecatrienoyl)-monogalactosyl Diglyceride, from *Arabidopsis thaliana*. *The Journal of Biological Chemistry*, 276, 12832–12838.
- Stenzel, I., Hause, B., Miersch, O., Kurz, T., Maucher, H., Weichert, H., Ziegler, J., Feussner, I., & Wasternack, C. (2003). Jasmonate biosynthesis and the allene oxide cyclase family of *Arabidopsis thaliana*. *Plant Molecular Biology*, 51, 895–911.
- Stenzel, I., Otto, M., Delker, C., Kirmse, N., Schmidt, D., Miersch, O., Hause, B., & Wasternack, C. (2012). ALLENE OXIDE CYCLASE (AOC) gene family members of *Arabidopsis thaliana*: Tissue- and organ-specific promoter activities and in vivo heteromerization. *Journal of Experimental Botany*, 63, 6125–6138.
- Wasternack, C., & Hause, B. (2013). Jasmonates: Biosynthesis, perception, signal transduction and action in plant stress response, growth and development. An update to the 2007 review in *Annals of Botany*. *Annals of Botany*, 111, 1021–1058.

Wasternack, Claus, & Feussner, I. (2018). The Oxylin Pathways: Biochemistry and Function. *Annual Review of Plant Biology*, 69, 363–386.

Chapter 6 - Conclusions and future directions

Conclusions

Chapter 2 describes a modified lipidomic approach to identify stress-induced changes in leaf lipid profile of Arabidopsis. In this work, the lipidomic approach is modified from previous methods (Shiva et al., 2018, 2013; Vu et al., 2014a; Vu et al., 2014b) and establishes an excellent platform for high-throughput analysis of various lipid phenotypes in plant leaf tissues. The lipidomics approach includes an optimized lipid extraction method for plant leaf tissues, direct-infusion MRM scanning operated in SCIEX Triple Quad 6500+, and data processing and normalization using MultiQuant 3.0 and LipidomeDB DCE. Lipidomics study of leaf tissues in Arabidopsis accession Col-0 showed that cold and mechanical wounding stresses resulted in distinct patterns of stress-induced lipid composition and revealed possible roles for specific lipids and their biosynthetic pathways in plant stress responses.

The most prominent change under cold stress is the large accumulation of storage lipids (TAG and DAG). The increase of TAG content was not uniformly distributed among different species; highly unsaturated 54C-TAG species such as TAG(18:2/36:4), TAG(18:1/36:6), TAG(18:2/36:5), TAG(18:3/36:5), and TAG(18:3/36:6) showed different patterns from less unsaturated 50C- and 52C-TAGs such as TAG(16:0/34:3), TAG(18:2/34:1), and TAG(18:3/34:2) at different cold temperatures. We hypothesize that the accumulated TAGs during cold acclimation derive from the *de novo* biosynthetic pathway catalyzed by DGAT1 (Tan et al., 2018), while the accumulation of highly unsaturated 54C-TAGs after -2 °C treatment might be derived from 36C-DAG through an alternative pathway which is catalyzed by PDAT1 (Demski et al., 2020). The accumulation of TAG under cold can help Arabidopsis maintain membrane stability and reduce damage by sequestering toxic free FA (Chen et al., 2015; Fan et

al., 2013; Lippold et al., 2012). Another remarkable change in cold is the elongation of fatty acyl chains in major phospholipids. The levels of 40C-PC, 38C-, 40C-, and 42C-PE species containing one VLCFA were significantly increased. The increased acyl chain length and acyl chain desaturation level of major phospholipids in plasma membrane and chloroplast membrane contribute to the ability of Arabidopsis to adjust membrane fluidity in response to low temperature.

Upon mechanical wounding, the major change in leaf lipid profile in Col-0 is the large production of plastidic lipids containing OPDA or dnOPDA. Esterified OPDA or dnOPDA have indirect or direct functions in plant wounding response. They might act as a pool of free OPDA or dnOPDA that could be released when necessary, the released OPDA could be used as a substrate for JA production, which is an essential hormone in defense mechanisms (Chini et al., 2007; Santner & Estelle, 2007). Some esterified OPDA such as Arabidopsides A, E, G show antifungal and antibacterial activities (Andersson et al., 2006; Kourtchenko et al., 2007; Pedras & To, 2017), helping Arabidopsis prevent microbial infection at the wounding site.

Chapter 3 describes a comparative analysis of leaf lipidomes among 679 natural Arabidopsis accessions. After a “super-cold” treatment (cold acclimation + -2°C treatment), most of the investigated lipid species were significantly changed, with the most obvious inductions being in triacylglycerols (TAGs) and very long chain fatty acid (VLCFA)-containing membrane lipids. GWAS on individual lipid species suggested that lipid remodeling under cold stress is in part controlled by natural sequence variants in specific lipid-related genes, including *FAD2*, *FAD7*, *LOH2*, *KCS9*, *FAB1*, and *GGPPS11*. The relative abundance of several lipid species in cold was significantly correlated with the freezing tolerance of the measured accessions, providing evidence for the role of specific lipid species and genes in plant freezing

tolerance. Some molecular species of polar membrane lipids containing 18:2 or 18:3 FA (e.g. MGDG(18:2/18:3), MGDG(18:3/16:2), MGDG(20:2/18:3), PC(18:2/18:2), PE(18:2/18:2), PG(18:3/16:0)) showed positive correlations with measured freezing tolerance, latitude and negative correlations with local temperature variables like minimum temperature of coldest month, implying that they are indicators for higher freezing tolerance. In contrast, some lipid species such as Sitosterol-Glc(16:0), GlcCer(34:1)-2, GlcCer(34:1)-2, PC(16:0/18:3), PC(18:1/18:3), PE(16:0/18:3) were negatively correlated with freezing tolerance, indicating that they are potential markers for lower freezing tolerance.

FAD2 and FAD7 are fatty acid desaturases which are mainly responsible for biosynthesis of unsaturated FA in major membrane lipids in ER and chloroplast, respectively. Plants can increase the fatty acyl unsaturation level in membrane lipids to enhance membrane fluidity and stabilization in cold (Chen & Thelen, 2013; Harayama & Riezman, 2018; Hugly & Somerville, 1992; Matos et al., 2007; Miquel et al., 1993). Arabidopsis natural accessions with higher proportions of 18:2 in major phospholipids and 18:3 in major galactolipids tend to better maintain their membrane fluidity and have higher freezing tolerance. LOH2 is a ceramide synthase essential for production of C16-GlcCer (Markham et al., 2011); KCS9 is involved in biosynthesis of VLCFA, which can affect biosynthesis of VLCFA-GlcCer. The relative levels of GlcCer(34:1)-2 and GlcCer(40:1)-3 were negatively correlated with freezing tolerance and latitude, indicating lower levels of specific GlcCer species lead to better performance of Arabidopsis in response to low temperature. Sphingolipids are essential components of plasma membrane, and the decrease of GlcCer is hypothesized to contribute to a greater hydration of the plasma membrane that could, in turn, increase membrane stability during cold stress. In conclusion, correlations between genome variation, lipidome variation, and variation in freezing

tolerance among natural accessions revealed the roles of specific lipids and candidate genes in plant freezing tolerance.

Chapter 4 describes a comparative analysis of leaf lipidomes among 360 natural *Arabidopsis* accessions and characterizes the response of the leaf lipidome to mechanical wounding. Upon wounding, there was large production of esterified oxylipins in most investigated accessions, and great variation existed in oxidized lipidomes among the accessions. GWAS on individual lipid species suggested that production of most esterified OPDA and esterified dnOPDA species after wounding was in part controlled by natural sequence variants in two genomic regions containing *AOC1/2/3* and *HPL1* respectively. Free and esterified OPDA and dnOPDA are produced directly from polyunsaturated FAs and polyunsaturated membrane lipids in reactions catalyzed by LOX2, AOS, and AOCs through the AOS pathway (Hofmann, Zerbe, & Schaller, 2006; Pollmann et al., 2019; Schaller et al., 2008; Stenzel et al., 2012). *HPL1* is a negative regulator because it competes with AOS for the same substrate (Duan et al., 2005; Matsui, 2006; Nakashima et al., 2013; Nilsson et al., 2016). Haplotype analysis showed that the relative abundances of oxylipins and oxylipin-containing lipids were correlated with sequence variation in non-coding regions in or near *AOC1/2/3* and upstream region of *HPL1*. Analysis of gene expression showed that sequence variant in upstream region significantly influenced *HPL1* level and *HPL1* inhibited esterified (dn)OPDA production upon wounding in *Arabidopsis*. Specific genomic variants in *AOC1/2/3* and *HPL1* in natural accessions improve the ability of *Arabidopsis* to generate esterified OPDA or dnOPDA, resulting in better performance after wounding damage.

Chapter 5 describes the functional characterization of *AOC1/2/3* in the biosynthesis of esterified (dn)OPDA under mechanical wounding stress. There was positive correlation between

AOC2 expression and the relative contents of esterified (dn)OPDA in WT and T1 overexpression lines of *AOC2* demonstrating that *AOC2* can promote esterified (dn)OPDA production upon wounding. Comparative analysis of leaf lipidomes between WT and T-DNA insertion lines *aoc1* and *aoc3* showed that *AOC1* is indispensable for the biosynthesis of esterified (dn)OPDA and knockout of *AOC3* led to a partial loss of the ability to generate esterified (dn)OPDA under wounding. There is a fine-tuning mechanism for free OPDA and JA biosynthesis in *Arabidopsis* depending on the physical interactions between *LOX2*, *AOS*, and *AOC* as well as the heteromerization of 4 *AOCs* (Otto et al., 2016; Pollmann et al., 2019; Stenzel et al., 2012). The heteromerization between *AOC1/2/3* might also regulate the level of esterified OPDA or dnOPDA under wounding stress.

Future directions

Arabidopsis accessions in the 1001 Genomes Project showed massive variability in lipid profile under stressed or unstressed conditions. Analysis of recombinant inbred lines produced from accessions with extreme lipid-level phenotypes has potential to identify novel quantitative trait loci that were not detected using GWAS.

Chapter 2 and Chapter 3 showed cold treatment at different temperatures (4 °C or -2 °C) induced distinct patterns of TAG accumulation in *Arabidopsis Col-0* and other natural accessions. It seems that accumulation of less-unsaturated TAG species during cold acclimation is enhanced by *DGAT1*, while the mechanism of large accumulation of highly unsaturated TAG species during mild-freezing (super-cold) period is elusive. *DGAT1* and *PDAT1* have been characterized to play important roles in plant cold/freezing tolerance (Demski et al., 2020; Tan et

al., 2018). Our future work will investigate the mechanism of TAG accumulation and its role in plant freezing tolerance by measuring *DGATI*, *PDATI* transcript abundance, lipid profiles, and freezing tolerance of Arabidopsis wild-type (Col-0), *dgat1*, and *pdatt1* mutants at different cold temperatures.

GWAS in Chapter 3 and Chapter 4 identified a list of candidate genes showing strong associations with lipid-level phenotypes, some genes, such as *FAD4* and *AAD3*, have not been well characterized in Arabidopsis in terms of their physiological functions (Bryant et al., 2016; Gao et al., 2009; Horn et al., 2020; Kachroo et al., 2007); more work need to be done to uncover their functions. Some SNPs identified from GWAS are strongly associated with lipid-level phenotypes especially SNPs located in non-coding regions of genes, e.g. SNP (Chr4_8834169), which is associated with both *HPLI* level and Arabidopside level. The potentially causative relationships between these candidate SNPs and gene expression or protein activity need to be verified by site-directed mutagenesis or other biochemical approaches.

From our discoveries in Chapter 4 and Chapter 5, the functions of AOC1/2/3 in esterified OPDA and dnOPDA production under wounding stress are not redundant, and each of them may play unique and essential roles in the biosynthetic pathway. Up to now, we only acquired data from T1 generation of overexpression lines. After genetic and phenotypic characterization on T2 and T3 generation of transgenic lines, the exact molecular function of AOC1/2/3 in OPDA and dnOPDA production will be better elucidated in the future.

References

- Andersson, M. X., Hamberg, M., Kourtchenko, O., Brunnström, A., McPhail, K. L., Gerwick, W. H., Göbel, C., Feussner, I., & Ellerström, M. (2006). Oxylipin profiling of the hypersensitive response in *Arabidopsis thaliana*. Formation of a novel oxo-phytodienoic acid-containing galactolipid, arabidopside E. *The Journal of Biological Chemistry*, *281*, 31528–31537.
- Bryant, F. M., Munoz-Azcarate, O., Kelly, A. A., Beaudoin, F., Kurup, S., & Eastmond, P. J. (2016). ACYL-ACYL CARRIER PROTEIN DESATURASE2 and 3 Are Responsible for Making Omega-7 Fatty Acids in the Arabidopsis Aleurone. *Plant Physiology*, *172*, 154–162.
- Chen, Q.-F., Xu, L., Tan, W.-J., Chen, L., Qi, H., Xie, L.-J., Chen, M.-X., Liu, B.-Y., Yu, L.-J., Yao, N., Zhang, J.-H., Shu, W., & Xiao, S. (2015). Disruption of the Arabidopsis Defense Regulator Genes SAG101, EDS1, and PAD4 Confers Enhanced Freezing Tolerance. *Molecular Plant*, *8*, 1536–1549.
- Chen, M., & Thelen, J. J. (2013). ACYL-LIPID DESATURASE2 Is Required for Chilling and Freezing Tolerance in Arabidopsis. *The Plant Cell*, *25*, 1430–1444.
- Chini, A., Fonseca, S., Fernández, G., Adie, B., Chico, J. M., Lorenzo, O., García-Casado, G., López-Vidriero, I., Lozano, F. M., Ponce, M. R., Micol, J. L., & Solano, R. (2007). The JAZ family of repressors is the missing link in jasmonate signalling. *Nature*, *448*, 666–671.
- Demski, K., Łosiewska, A., Jasieniecka-Gazarkiewicz, K., Klińska, S., & Banaś, A. (2020). Phospholipid:Diacylglycerol Acyltransferase1 Overexpression Delays Senescence and Enhances Post-heat and Cold Exposure Fitness. *Frontiers in Plant Science*, *11*, 611897.
- Duan, H., Huang, M.-Y., Palacio, K., & Schuler, M. A. (2005). Variations in CYP74B2 (hydroperoxide lyase) gene expression differentially affect hexenal signaling in the Columbia and Landsberg erecta ecotypes of Arabidopsis. *Plant Physiology*, *139*, 1529–1544.
- Fan, J., Yan, C., & Xu, C. (2013). Phospholipid:diacylglycerol acyltransferase-mediated triacylglycerol biosynthesis is crucial for protection against fatty acid-induced cell death in growing tissues of Arabidopsis. *The Plant Journal*, *76*, 930–942.
- Gao, J., Ajjawi, I., Manoli, A., Sawin, A., Xu, C., Froehlich, J. E., Last, R. L., & Benning, C. (2009). FATTY ACID DESATURASE4 of Arabidopsis encodes a protein distinct from characterized fatty acid desaturases: FATTY ACID DESATURASE4 of Arabidopsis encodes a distinct protein. *The Plant Journal*, *60*, 832–839.
- Harayama, T., & Riezman, H. (2018). Understanding the diversity of membrane lipid composition. *Nature Reviews. Molecular Cell Biology*, *19*, 281–296.

- Hofmann, E., Zerbe, P., & Schaller, F. (2006). The crystal structure of *Arabidopsis thaliana* allene oxide cyclase: Insights into the oxylipin cyclization reaction. *The Plant Cell*, *18*, 3201–3217.
- Horn, P. J., Smith, M. D., Clark, T. R., Froehlich, J. E., & Benning, C. (2020). PEROXIREDOXIN Q stimulates the activity of the chloroplast 16:1^{A3trans} FATTY ACID DESATURASE4. *The Plant Journal*, *102*, 718–729.
- Hugly, S., & Somerville, C. (1992). A role for membrane lipid polyunsaturation in chloroplast biogenesis at low temperature. *Plant Physiology*, *99*, 197–202.
- Kachroo, A., Shanklin, J., Whittle, E., Lapchyk, L., Hildebrand, D., & Kachroo, P. (2007). The *Arabidopsis* stearyl-acyl carrier protein-desaturase family and the contribution of leaf isoforms to oleic acid synthesis. *Plant Molecular Biology*, *63*, 257–271.
- Kourtchenko, O., Andersson, M. X., Hamberg, M., Brunnström, A., Göbel, C., McPhail, K. L., Gerwick, W. H., Feussner, I., & Ellerström, M. (2007). Oxo-phytodienoic acid-containing galactolipids in *Arabidopsis*: Jasmonate signaling dependence. *Plant Physiology*, *145*, 1658–1669.
- Lippold, F., vom Dorp, K., Abraham, M., Hölzl, G., Wewer, V., Yilmaz, J. L., Lager, I., Montandon, C., Besagni, C., Kessler, F., Stymne, S., & Dörmann, P. (2012). Fatty acid phytyl ester synthesis in chloroplasts of *Arabidopsis*. *The Plant Cell*, *24*, 2001–2014.
- Matos, A. R., Hourton-Cabassa, C., Çiçek, D., Rezé, N., Arrabaça, J. D., Zachowski, A., & Moreau, F. (2007). Alternative oxidase involvement in cold stress response of *Arabidopsis thaliana* fad2 and FAD3+ cell suspensions altered in membrane lipid composition. *Plant & Cell Physiology*, *48*, 856–865.
- Matsui, K. (2006). Green leaf volatiles: Hydroperoxide lyase pathway of oxylipin metabolism. *Current Opinion in Plant Biology*, *9*, 274–280.
- Miquel, M., James, D., Dooner, H., & Browse, J. (1993). *Arabidopsis* requires polyunsaturated lipids for low-temperature survival. *Proceedings of the National Academy of Sciences of the United States of America*, *90*, 6208–6212.
- Nakashima, A., von Reuss, S. H., Tasaka, H., Nomura, M., Mochizuki, S., Iijima, Y., Aoki, K., Shibata, D., Boland, W., Takabayashi, J., & Matsui, K. (2013). Traumatins- and dinortraumatins-containing galactolipids in *Arabidopsis*: Their formation in tissue-disrupted leaves as counterparts of green leaf volatiles. *The Journal of Biological Chemistry*, *288*, 26078–26088.
- Nilsson, A. K., Fahlberg, P., Johansson, O. N., Hamberg, M., Andersson, M. X., & Ellerström, M. (2016). The activity of HYDROPEROXIDE LYASE 1 regulates accumulation of galactolipids containing 12-oxo-phytodienoic acid in *Arabidopsis*. *Journal of Experimental Botany*, *67*, 5133–5144.

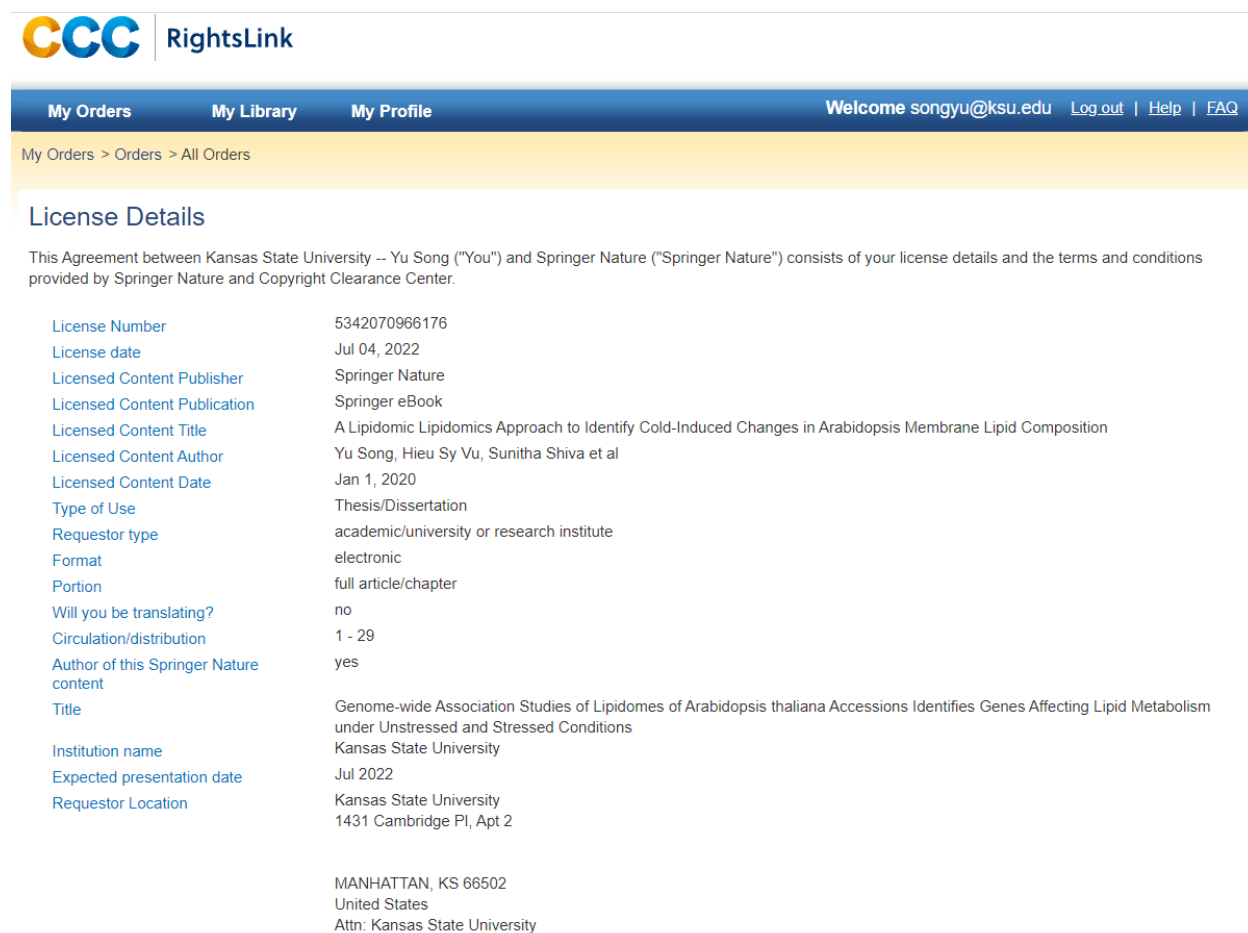
- Otto, M., Naumann, C., Brandt, W., Wasternack, C., & Hause, B. (2016). Activity Regulation by Heteromerization of Arabidopsis Allene Oxide Cyclase Family Members. *Plants (Basel, Switzerland)*, 5, E3.
- Pedras, M. S. C., & To, Q. H. (2017). Defense and signalling metabolites of the crucifer *Erucastrum canariense*: Synchronized abiotic induction of phytoalexins and galactoxylipins. *Phytochemistry*, 139, 18–24.
- Pollmann, S., Springer, A., Rustgi, S., von Wettstein, D., Kang, C., Reinbothe, C., & Reinbothe, S. (2019). Substrate channeling in oxylipin biosynthesis through a protein complex in the plastid envelope of *Arabidopsis thaliana*. *Journal of Experimental Botany*, 70, 1483–1495.
- Santner, A., & Estelle, M. (2007). The JAZ proteins link jasmonate perception with transcriptional changes. *The Plant Cell*, 19, 3839–3842.
- Schaller, F., Zerbe, P., Reinbothe, S., Reinbothe, C., Hofmann, E., & Pollmann, S. (2008). The allene oxide cyclase family of *Arabidopsis thaliana* - localization and cyclization: Oxylipin cyclization. *FEBS Journal*, 275, 2428–2441.
- Shiva, S., Enniful, R., Roth, M. R., Tamura, P., Jagadish, K., & Welti, R. (2018). An efficient modified method for plant leaf lipid extraction results in improved recovery of phosphatidic acid. *Plant Methods*, 14, 14.
- Shiva, S., Vu, H. S., Roth, M. R., Zhou, Z., Marepally, S. R., Nune, D. S., Lushington, G. H., Visvanathan, M., & Welti, R. (2013). Lipidomic analysis of plant membrane lipids by direct infusion tandem mass spectrometry. *Methods in Molecular Biology (Clifton, N.J.)*, 1009, 79–91.
- Stenzel, I., Otto, M., Delker, C., Kirmse, N., Schmidt, D., Miersch, O., ... Wasternack, C. (2012). ALLENE OXIDE CYCLASE (AOC) gene family members of *Arabidopsis thaliana*: Tissue- and organ-specific promoter activities and in vivo heteromerization. *Journal of Experimental Botany*, 63, 6125–6138.
- Tan, W.-J., Yang, Y.-C., Zhou, Y., Huang, L.-P., Xu, L., Chen, Q.-F., Yu, L.-J., & Xiao, S. (2018). DIACYLGLYCEROL ACYLTRANSFERASE and DIACYLGLYCEROL KINASE Modulate Triacylglycerol and Phosphatidic Acid Production in the Plant Response to Freezing Stress. *Plant Physiology*, 177, 1303–1318.
- Vu, H. S., Shiva, S., Hall, A. S., & Welti, R. (2014a). A lipidomic approach to identify cold-induced changes in *Arabidopsis* membrane lipid composition. *Methods in Molecular Biology (Clifton, N.J.)*, 1166, 199–215.
- Vu, H. S., Shiva, S., Roth, M. R., Tamura, P., Zheng, L., Li, M., Sarowar, S., Honey, S., McElhiney, D., Hinkes, P., Seib, L., Williams, T. D., Gadbury, G., Wang, X., Shah, J., & Welti, R. (2014b). Lipid changes after leaf wounding in *Arabidopsis thaliana*: Expanded lipidomic data form the basis for lipid co-occurrence analysis. *The Plant Journal: For Cell and Molecular Biology*, 80, 728–743.

Appendix A - Copyright Permissions

Published work – part of Chapter 2 (Song et al., 2020)

Springer Nature Copyright Policy: Authors have the right to reuse their article's Version of Record, in whole or in part, in their own thesis. Additionally, they may reproduce and make available their thesis, including Springer Nature content, as required by their awarding academic institution.

The agreement between the author and Springer Nature is attached as below:



CCC RightsLink

My Orders My Library My Profile Welcome songyu@ksu.edu Log out | Help | FAQ

My Orders > Orders > All Orders

License Details

This Agreement between Kansas State University -- Yu Song ("You") and Springer Nature ("Springer Nature") consists of your license details and the terms and conditions provided by Springer Nature and Copyright Clearance Center.

License Number	5342070966176
License date	Jul 04, 2022
Licensed Content Publisher	Springer Nature
Licensed Content Publication	Springer eBook
Licensed Content Title	A Lipidomic Lipidomics Approach to Identify Cold-Induced Changes in Arabidopsis Membrane Lipid Composition
Licensed Content Author	Yu Song, Hieu Sy Vu, Sunitha Shiva et al
Licensed Content Date	Jan 1, 2020
Type of Use	Thesis/Dissertation
Requestor type	academic/university or research institute
Format	electronic
Portion	full article/chapter
Will you be translating?	no
Circulation/distribution	1 - 29
Author of this Springer Nature content	yes
Title	Genome-wide Association Studies of Lipidomes of Arabidopsis thaliana Accessions Identifies Genes Affecting Lipid Metabolism under Unstressed and Stressed Conditions
Institution name	Kansas State University
Expected presentation date	Jul 2022
Requestor Location	Kansas State University 1431 Cambridge Pl, Apt 2 MANHATTAN, KS 66502 United States Attn: Kansas State University

Appendix B - Chapter 3 Supplemental Figures

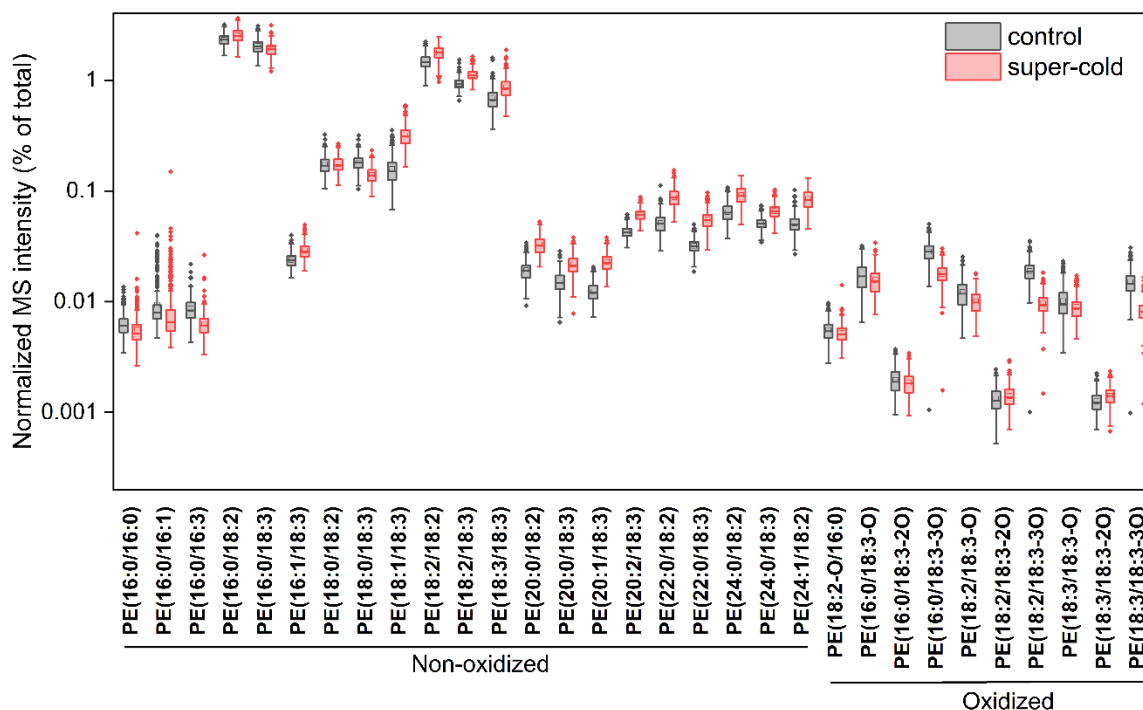


Figure B-1. Changes in the relative contents of 31 PE species in leaf tissues among the 360 investigated *Arabidopsis* accessions in unstressed and super-cold treated group

Changes in the leaf relative contents (% of total) of 31 PE species in the 360 investigated *Arabidopsis* accessions in unstressed (grey boxes) and super-cold (red boxes) group. Standard box plots are shown with horizontal bars in the boxes representing the median, bottom and top of the box indicate the 25th and 75th percentiles (lower and upper quartiles). Whiskers indicate 1.5-fold interquartile range, diamonds represent potential outliers. Note that the y-axis was log₁₀ scaled, due to the large differences in the relative contents of various lipids.

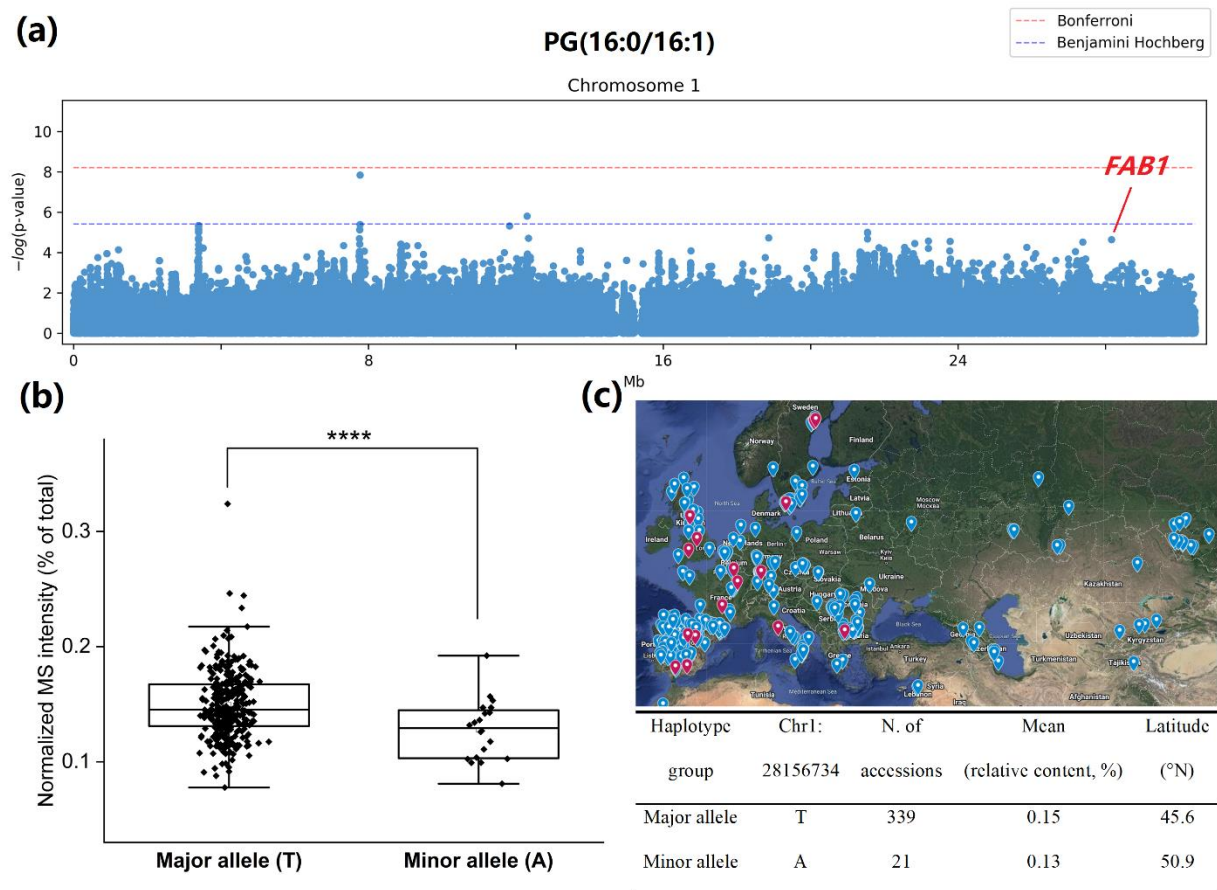


Figure B-2. The relative level of PG(16:0/16:1) is associated with the SNP in upstream region of *FAB1*

(a) Manhattan plot of genome-wide association study (GWAS) of relative level (%) of PG(16:0/16:1). (b) Haplotype analysis of relative level of PG(16:0/16:1) in 360 natural accessions based on the SNP (Chr1_28156734) and geographic distribution of the two haplotype groups in the world. Diamond plots showing the distribution of relative level of PG(16:0/16:1) in two haplotype groups. Error bars represent SD. Asterisks above the bars indicate significant difference between groups (Student's t-test, $P < 0.0001$). Blue pins represent accessions in major allele group, red pins represent accessions in minor allele group.

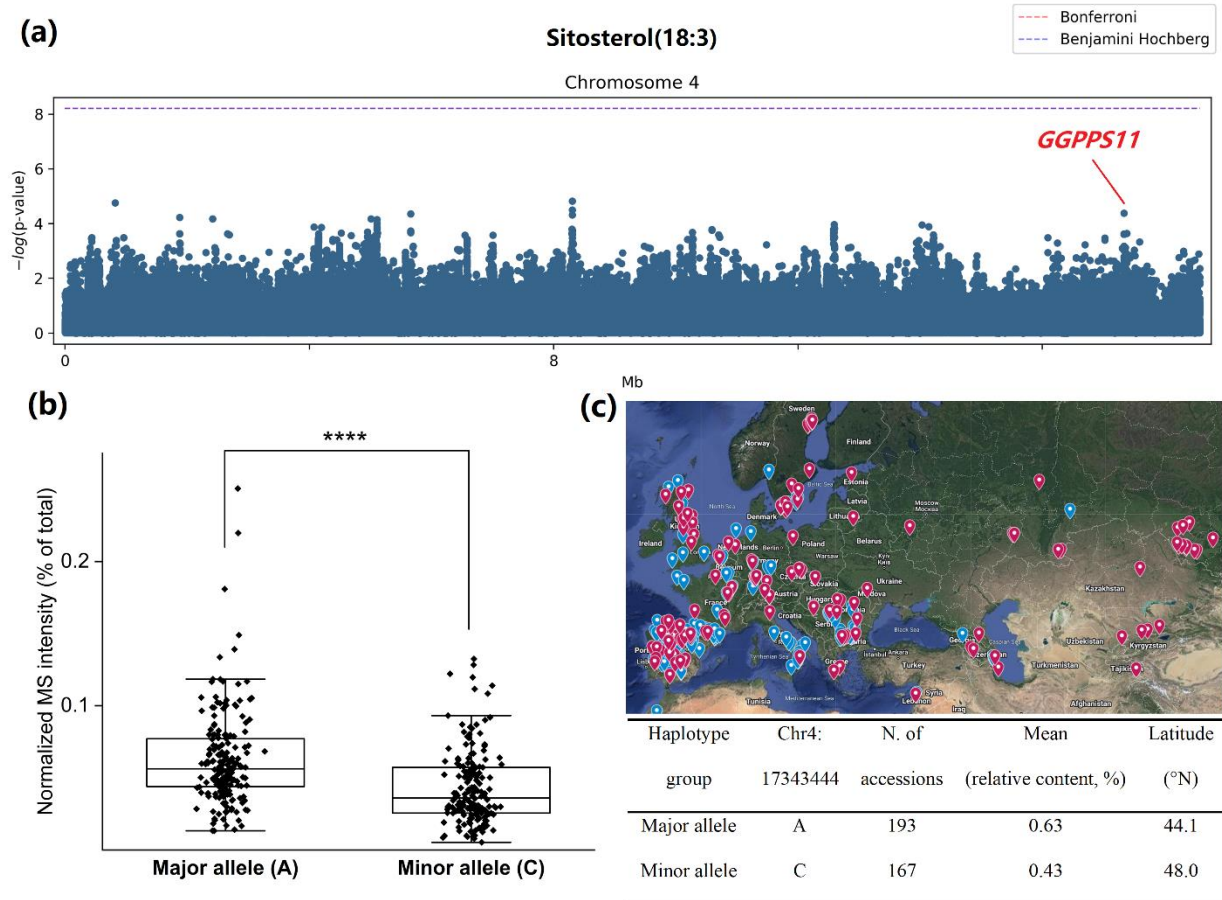


Figure B-3. The relative level of sitosterol(18:3) is associated with the SNP in 5' UTR of *GGPPS11*

(a) Manhattan plot of genome-wide association study (GWAS) of relative level (%) of sitosterol(18:3). (b) Haplotype analysis of relative level of sitosterol(18:3) in 360 natural accessions based on the SNP (Chr4_17343444) and geographic distribution of the two haplotype groups in the world. Diamond plots showing the distribution of relative level of sitosterol(18:3) in two haplotype groups. Error bars represent SD. Asterisks above the bars indicate significant difference between groups (Student's t-test, $P < 0.0001$). Blue pins represent accessions in major allele group, red pins represent accessions in minor allele group.

Appendix C - Chapter 4 Supplemental Figures

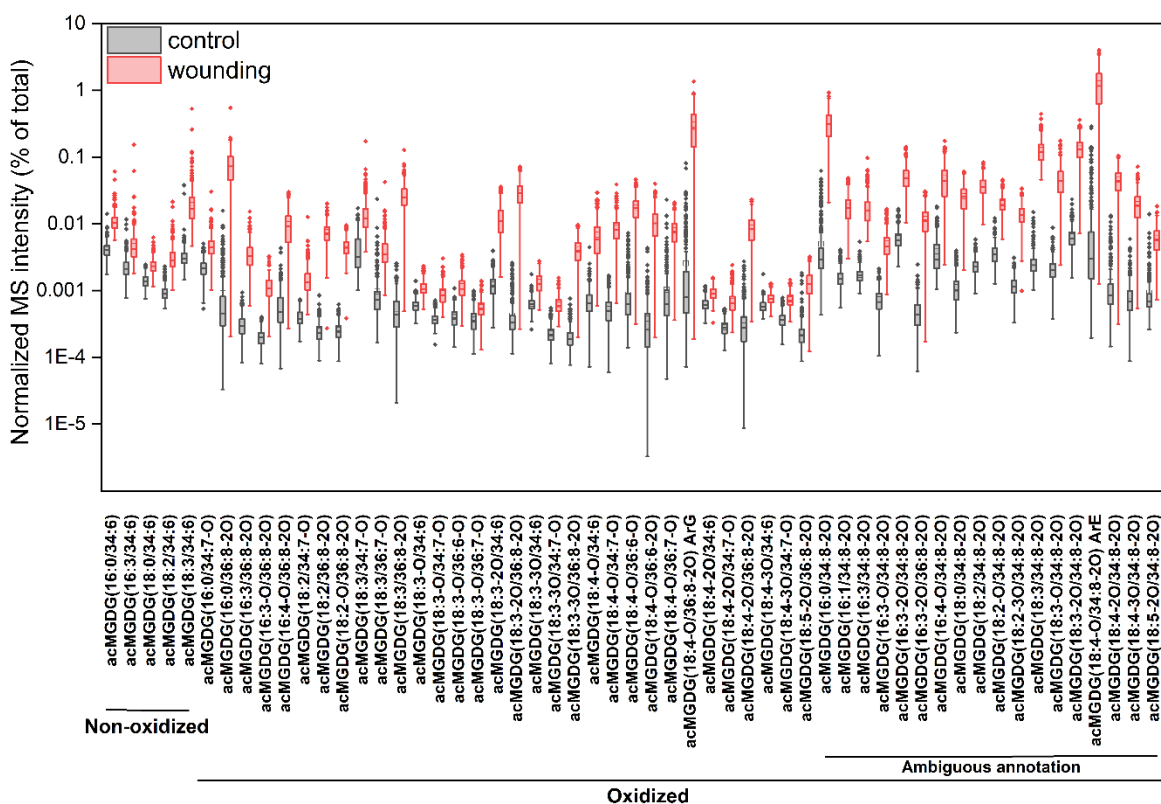


Figure C-1. Changes in the relative contents of 55 acMGDG species in leaf tissues in the 360 investigated Arabidopsis accessions before (control group) and 45 min after wounding treatment (wounding group)

Changes in the leaf relative contents (% of total) of 55 acMGDG species in the 360 investigated Arabidopsis accessions before (grey boxes) and after (red boxes) wounding treatment. Standard box plots are shown with horizontal bars in the boxes representing the median, bottom and top of the box indicate the 25th and 75th percentiles (lower and upper quartiles). Whiskers indicate 1.5-fold interquartile range, diamonds represent potential outliers. Note that the y-axis was log₁₀ scaled, due to the large differences in the contents of the lipid classes.

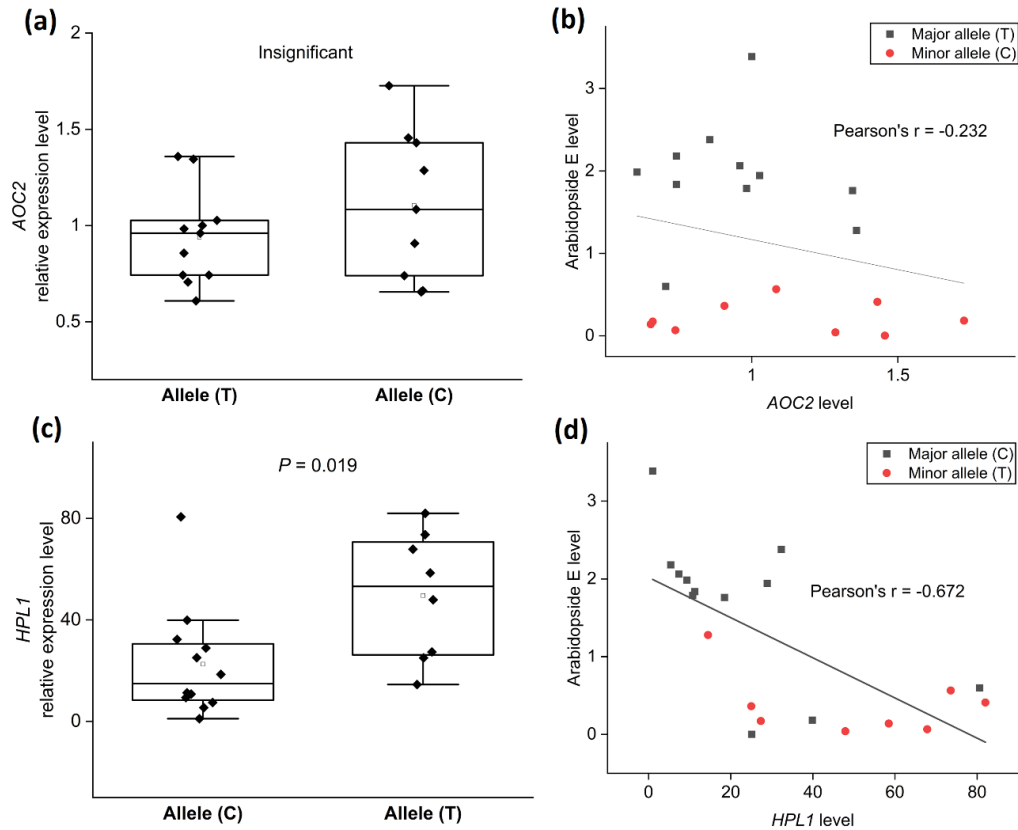


Figure C-2. Association between SNPs, gene expression level, and Arabidopside E level in subset-2 of 20 accessions

The distribution of *AOC2* and *HPL1* expression level and arabisidopside E content among a different subset of 20 accessions (subset-2). Haplotype analysis of *AOC2* (a) and *HPL1* (c) expression level based on SNP (Chr3:9406789) and SNP (Chr4:8834169). Relationship between the relative level of *AOC2* and relative content of Arabidopside E (b) and relationship between *HPL1* and Arabidopside E (d). Symbols indicate the distribution of *AOC2* and *HPL1* levels in two haplotype groups of accessions (black squares represent major allele group, red dots represent minor allele group). The horizontal lines within the boxes represent the medians, the boxes indicate the 25th and 75th percentiles, and the Error bars represent \pm SD. Exact *P*-values (Student's *t*-test) are shown above. Pearson correlation coefficient (Pearson's *r*) is shown above the trend line indicating the linear correlation between gene expression and lipid level.